Analysis of novel Steroidogenic Factor-1 targets in the human adrenal gland

Bruno Ferraz de Souza

UCL Institute of Child Health

University College London

Thesis submitted for the degree of Doctor of Philosophy (Ph.D.)

2011

Declaration

I, Bruno Ferraz de Souza, confirm that the work presented in this thesis is my own. Where information has been derived from other sources, I confirm that this has been indicated in the thesis.

Signed ……. Date …….

Abstract

Steroidogenic Factor-1 (SF-1, *NR5A1*) is a nuclear receptor transcription factor that plays a central role in adrenal and reproductive biology. In humans, SF-1 regulates adrenal development and disruption of SF-1 or its known targets is associated with impaired adrenal function. Therefore, the identification of novel SF-1 targets could reveal important new mechanisms in adrenal development and disease. This thesis describes three approaches to identifying SF-1 targets in NCI-H295R human adrenocortical cells.

SF-1-dependent regulation of *CITED2* and *PBX1* was investigated since these factors regulate adrenal development in mice through pathways shared with Sf-1. Expression of *CITED2* and *PBX1* was confirmed in the developing human adrenal, and SF-1 was found to bind to and activate the *CITED2* promoter and to cooperate with DAX1 to activate the *PBX1* promoter.

SF-1 binding was investigated using chromatin immunoprecipitation microarrays (ChIP-on-chip). These studies revealed that SF-1 binds to the extended promoter of 445 genes, including factors involved in angiogenesis. Angiopoietin 2 (*ANGPT2*) emerged as a key novel SF-1 target, confirmed by transactivational studies, suggesting that regulation of angiogenesis might be an important additional action of SF-1 during adrenal development and tumorigenesis.

Global gene expression analysis following SF-1 overexpression revealed differential expression of 1058 genes, many of which are involved in steroidogenesis, lipid metabolism and cell proliferation. Bidirectional manipulation of SF-1 revealed a subset of positively regulated genes, including the known targets *STAR* and *CYP11A1* and novel target *SOAT1*, a regulator of cholesterol esterification.

Considering that defects in several SF-1 targets have been associated with adrenal disorders, mutational analysis of *SOAT1* was performed in forty-three subjects with unexplained adrenal insufficiency but failed to reveal potentially disease-causing variants.

Taken together, manipulation of SF-1 in human adrenal cells has expanded our knowledge of the many potential actions of SF-1 in the human adrenal gland.

Acknowledgements

I would like to thank:

John Achermann, for his continuous support ever since the first e-mail exchanged in March 2004. I am truly inspired by his scientific insight, and, more than a mentor and a friend, I consider John a professional and personal role model. I am very grateful for his presence and solicitude. I am also very grateful to Mehul Dattani for dedicating time to guide and support me;

Lin Lin, for teaching me countless technical and practical aspects of research, and for her kindness and friendliness in doing so. I extend my gratitude to all past and present members of the Achermann lab, for maintaining such a stimulating and friendly atmosphere;

All collaborators that made this research project possible, especially: Rebecca Hudson-Davies; Rahul Parnaik; Mike Hubank, Nipurna Jina, and team at UCL Genomics; Jacky Pallas and Sonia Shah; Dianne Gerrelli and Patricia Cogram at the Human Developmental Biology Resource; and Ayad Eddaoudi and team at the Flow Cytometry Core Facility. I am also grateful to several colleagues throughout the Institute of Child Health who allowed use of equipment and shared their expertise;

Gudrun Moore and all members of the Clinical and Molecular Genetics Unit, for their encouragement, particularly during the past year;

Berenice Mendonça, for stimulating me to pursue a career as a clinician scientist and for opening the doors to the world for me and so many others from Brazil;

Coordenação de Aperfeiçoamento de Pessoal de Nível Superior (Capes/Brazil), for funding my studies at UCL, and my parents, Francisco Eno Viana de Souza and Ana Maria Ferraz de Souza, for supplementing the stipends, allowing me to focus on the research. I also thank The Wellcome Trust, for funding the exciting research conducted at the Achermann lab.

Rarely one is given the opportunity to acknowledge in print people who have contributed, in a variety of ways, towards the achievement of a milestone. Therefore,

I intend to exercise my *latinidad* and dedicate this final paragraph to much more personal notes. I am extremely grateful to my parents, who have given me every possible opportunity – many of which they did not have themselves – and paved the way for me to pursue my own interests in life. I am also thankful to my sister, her family, and our nuclear and extended family, for so much love and support. I consider myself exceptionally lucky to have many true friends, who, near or far, have constantly encouraged me. My gratitude goes to them altogether, in a slightly impersonal but very sincere blanket 'thank you'. During these wonderful years in London, Simon has filled my life with meaning, with love and with joy. I am very grateful for his daily doses of positivity and encouragement throughout this PhD. Without him, I would not have come this far.

For my parents

Aos meus pais, meus heróis

Table of Contents

List of Figures

List of Tables

Abbreviations

ACTH	adrenocorticotropic hormone
Ang2	angiopoietin 2, encoded by *ANGPT2*
bp	base pair
BSA	bovine serum albumin
cAMP	cyclic adenosine monophosphate
cDNA	complementary deoxyribonucleic acid
ChIP-on-chip	chromatin immunoprecipitation followed by microarray analysis
CITED2	Cbp/p300-interacting transactivator, with Glu/Asp-rich carboxy-terminal domain, 2
cRNA	complementary ribonucleic acid
CYP11A1	cytochrome P450, family 11, subfamily A, polypeptide 1; also known as cholesterol side chain cleavage enzyme (P450scc)
DAX1	dosage-sensitive sex reversal/adrenal hypoplasia congenita critical region on the X chromosome 1, encoded by *NR0B1*
DMSO	dimethyl sulfoxide
DNA	deoxyribonucleic acid
dNTPs	deoxyribonucleoside triphosphates
dUTP	2'-deoxyuridine-5'-triphosphate
EDTA	ethylenediaminetetraacetic acid
g	Earth's gravitational acceleration, used as a measure of relative centrifugal force (RCF)
GAPDH	glyceraldehyde-3-phosphate dehydrogenase
HE	haematoxylin and eosin
HGNC	Human Genome Organisation (HUGO) Gene Nomenclature Committee
HPA axis	hypothalamic-pituitary-adrenal axis
IMAGe	Intrauterine growth restriction, Metaphyseal dysplasia, Adrenal hypoplasia congenita and Genital anomalies
IPA	propan-2-ol, commonly referred to as isopropyl alcohol or isopropanol
IUGR	Intrauterine Growth Restriction
kb	kilobase
LB	lysogeny broth, also referred to as Luria-Bertani medium
LM-PCR	ligation-mediated PCR
LRH-1	liver receptor homologue-1, encoded by *NR5A2*
M	molar
MIM	Mendelian Inheritance in Man
min	minute

ml	millilitre
mM	millimolar
NCBI	National Center for Biotechnology Information
NCBIv36	National Center for Biotechnology Information human genome assembly version 36
ng	nanogram
NGFI-B	nerve growth factor IB, also known as Nur77, encoded by *NR4A1*
PBS	phosphate-buffered saline
PBX1	pre-B-cell leukemia homeobox 1
PCR	polymerase chain reaction
PMSF	phenylmethylsulphonyl fluoride
POMC	proopiomelanocortin
qPCR	quantitative PCR
qRT-PCR	quantitative reverse transcription PCR
RNA	ribonucleic acid
RNase	ribonuclease
rpm	revolutions per minute
RT-PCR	reverse transcription PCR
s	second
SDS	sodium dodecyl sulfate
SEM	standard error of the mean
SERKAL	46,XX Sex reversal and dysgenesis of Kidneys, Adrenals and Lungs
SF-1	steroidogenic factor-1, also termed Ad4BP, encoded by *NR5A1*
SOAT1	sterol O-acyltransferase 1
SOC medium	super optimal broth with catabolite repression
STAR	steroidogenic acute regulatory protein
TSS	transcriptional start site
V	volt
wpc	weeks post-conception
WT	wild type
µl	microlitre
µM	micromolar

CHAPTER 1

INTRODUCTION

1.1. The human adrenal gland

The left and right adrenal glands are pyramidal structures that lie immediately above the kidneys on their posteromedial surfaces. Each adult adrenal weighs approximately 4 g and is 2 cm wide, 5 cm long and 1 cm thick (Stewart, 2008). The adrenal gland is a major hormone-secreting organ composed of two functionally distinct compartments: the medulla, which occupies the central portion of the gland and accounts for 10% of its volume, and the cortex. Adrenomedullary chromaffin cells are derived from the neuroectoderm and synthesise catecholamines that are acutely secreted in response to stress through sympathetic stimulation (autonomous nervous system). Adrenocortical cells, on the other hand, are of mesodermal origin and synthesise steroid hormones that regulate body homeostasis and mediate chronic stress responses, as part of the endocrine hypothalamic-pituitary-adrenal (HPA) axis and renin-angiotensin system. Even though the adrenal cortex and medulla are engaged in a dynamic cross-talk throughout development and in relation to their function, these two compartments are largely studied separately. The present study focuses primarily on the human adrenal cortex.

1.1.1. Adrenocortical zonation

The adrenal cortex consists of three histologically recognisable concentric zones (Figure 1.1): the outer *zona glomerulosa*, lying immediately below the capsule and corresponding to approximately 15% of cortical volume, depending upon sodium intake; the middle *zona fasciculata*, corresponding to up to 75% of cortical volume; and the inner *zona reticularis* that lies next to the medulla (Miller et al., 2008). Glomerulosa cells are organised in rounded clusters around capillary coils or glomeruli; fasciculata cells are arranged in radial rows separated by trabeculae and

blood vessels; and reticularis cells are located within a uniform reticular net of connective tissue and blood vessels.

These three zones are not only histologically but also functionally distinct, secreting different classes of steroid hormones in response to individual regulatory mechanisms. Secretion of mineralocorticoids (aldosterone, deoxycorticosterone [DOC]) by glomerulosa cells is mainly regulated by the renin-angiotensin system and serum levels of potassium. Fasciculata cells secrete glucocorticoids (cortisol, corticosterone) in response to adrenocorticotropin hormone (ACTH), within the tightly regulated feedback system of the HPA axis. Reticularis cells synthesise the sex steroid precursors dihydroepiandrosterone (DHEA), dihydroepiandrosterone sulfate (DHEAS) and androstenedione, termed adrenal androgens because they have weak androgenic activity and can be peripherally converted to testosterone. Molar secretion of DHEAS exceeds that of cortisol throughout much of adult life, but the exact mechanisms driving reticularis steroidogenic output remain elusive (Miller, 2009). Remarkably, this functional zonation of the adrenal cortex is largely dependent on the zonal pattern of expression of specific enzymatic machinery required to produce these different classes of steroids.

1.1.2. Adrenocortical steroidogenesis

Steroid hormones are synthesised from cholesterol through a biosynthetic enzymatic pathway termed *steroidogenesis*, involving cytochrome P450 steroid hydroxylases and hydroxysteroid dehydrogenases. Steroidogenesis occurs mainly in the adrenal cortex, in theca and luteal cells in the ovary, and in Leydig cells in the testis. The variability in the relative expression of steroidogenic enzymes determines the types of steroids preferentially produced in each of these steroidogenic tissues. Besides

this tissue-specific expression of steroid hydroxylases, steroidogenesis is also regulated by cyclic AMP-dependent induction of such enzymes by tropic hormones, mainly ACTH for the adrenal cortex (Waterman, 1994).

Adrenocortical cells can synthesise cholesterol *de novo*, but most of their cholesterol supply comes from the uptake of plasma lipoproteins, largely low-density lipoproteins (LDL) in humans (Miller et al., 2008). Free cholesterol resulting from LDL metabolism can be readily used or esterified and stored in lipid droplets. For steroidogenesis, free cholesterol transport across mitochondrial membranes into the mitochondria is facilitated by the steroidogenic acute regulatory protein (STAR) (Figure 1.2). The initial and rate-limiting step in the pathway leading from cholesterol to steroid hormones is the cleavage of the side chain of cholesterol to yield pregnenolone. This step is catalysed by the inner mitochondrial membrane-bound cholesterol side chain cleavage enzyme (P450scc, CYP11A1), and involves three distinct chemical reactions: 20α-hydroxylation, 22-hydroxylation, and scission of the cholesterol side-chain to yield pregnenolone and isocaproic acid. In the adrenal, a series of conversions involving 3β-hydroxysteroid dehydrogenase 2 (HSD3B2), 17α-hydroxylase/17,20 lyase (CYP17), 21-hydroxylase (CYP21A2), 11β-hydroxylase (CYP11B1), and aldosterone synthase (CYP11B2) ensues to generate mineralocorticoids, glucocorticoids or androgenic precursors as shown in Figure 1.2.

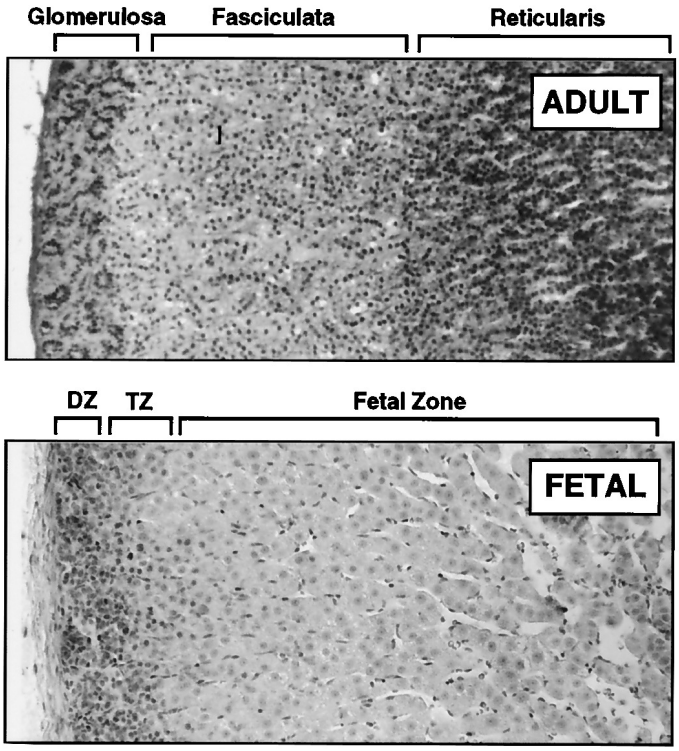

Figure 1.1. Morphology of the human adrenal cortex.

Upper panel, The three concentric zones of adult adrenal cortex are shown. The outer *zona glomerulosa* lies immediately below the capsule, followed by the middle *zona fasciculata* and the inner *zona reticularis*, which lies next to the medulla. Lower panel, Definitive (DZ), transitional (TZ) and fetal zones of mid-gestation fetal adrenal gland are shown. At this stage the fetal zone predominates, corresponding to approximately 90% of cortical volume. From Mesiano and Jaffe, 1997. Copyright 1997, The Endocrine Society.

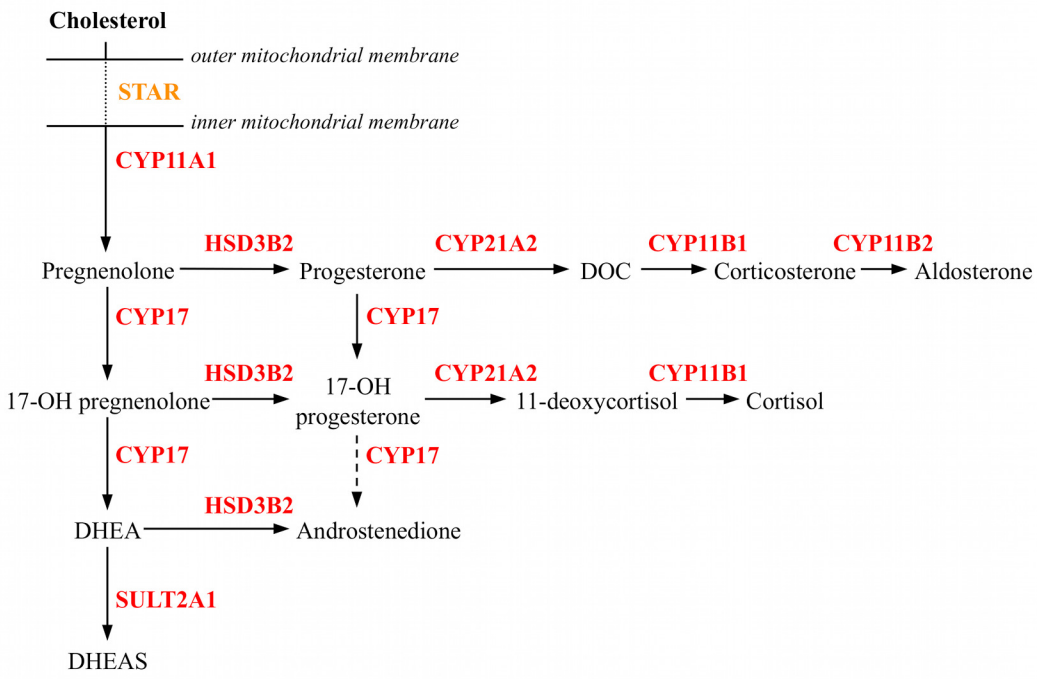

Figure 1.2. Main steroidogenic pathways in the human adrenal cortex.
Schematic representation with substrates and products printed in black, steroidogenic enzymes in red and STAR, which facilitates cholesterol transport through mitochondrial membranes, in orange.

1.2. Adrenal development in humans

Human adrenal development is a continuous process that initiates around the fourth week of gestation and extends into adult life. As early as 1968, seminal work by Sucheston and Cannon identified five landmarks in the development and zonal patterning of human adrenal glands from 3 to 4 weeks of gestation until 10 to 20 years of age (Sucheston and Cannon, 1968). Events unfolding during late embryonic and fetal stages of adrenal development are crucial for the formation of the organ and result in rapid growth of the gland, to a relative size many fold higher than that of the adult adrenal (Figure 1.3) (Mesiano and Jaffe, 1997). A brief outline of this complex process will be offered below, based on the comprehensive reviews by Mesiano and Jaffe in 1997 and Hammer, Parker and Schimmer in 2005. A timeline of major events is presented in Figure 1.4. In keeping with historical data, developmental stages will be mostly discussed in terms of weeks of gestation, i.e. counting from the first day of the last menstrual period. More recently, published reports on this field have embraced the concept of weeks post-conception (wpc), which roughly correspond to gestational age *minus* 2 weeks. This will be used where appropriate, in accordance with the data being quoted.

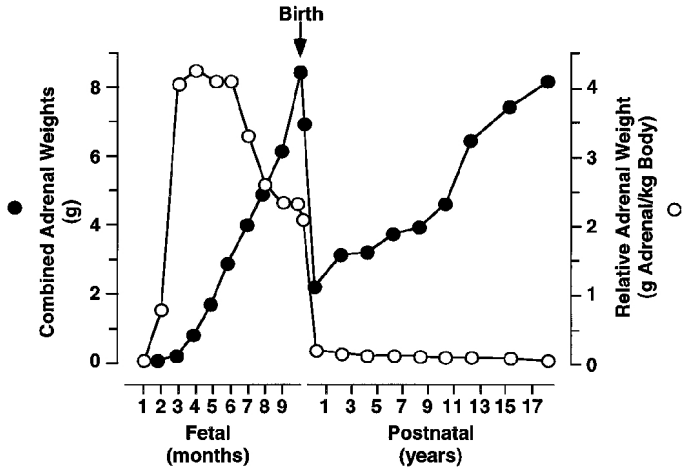

Figure 1.3. Evolution of adrenal weight throughout development.

Mean weight of the human adrenal glands (absolute; closed circles) and the ratio of adrenal weight to body weight (relative; open circles) during fetal and postnatal life are shown. After the second month of gestation, the fetal adrenals begin to grow rapidly due to hypertrophy of the fetal zone. Soon after birth, the fetal zone involutes and the weight of the glands rapidly decreases. The relative weight of the adrenals after birth markedly decreases and remains constant for the remainder of life. From Mesiano and Jaffe, 1997. Copyright 1997, The Endocrine Society.

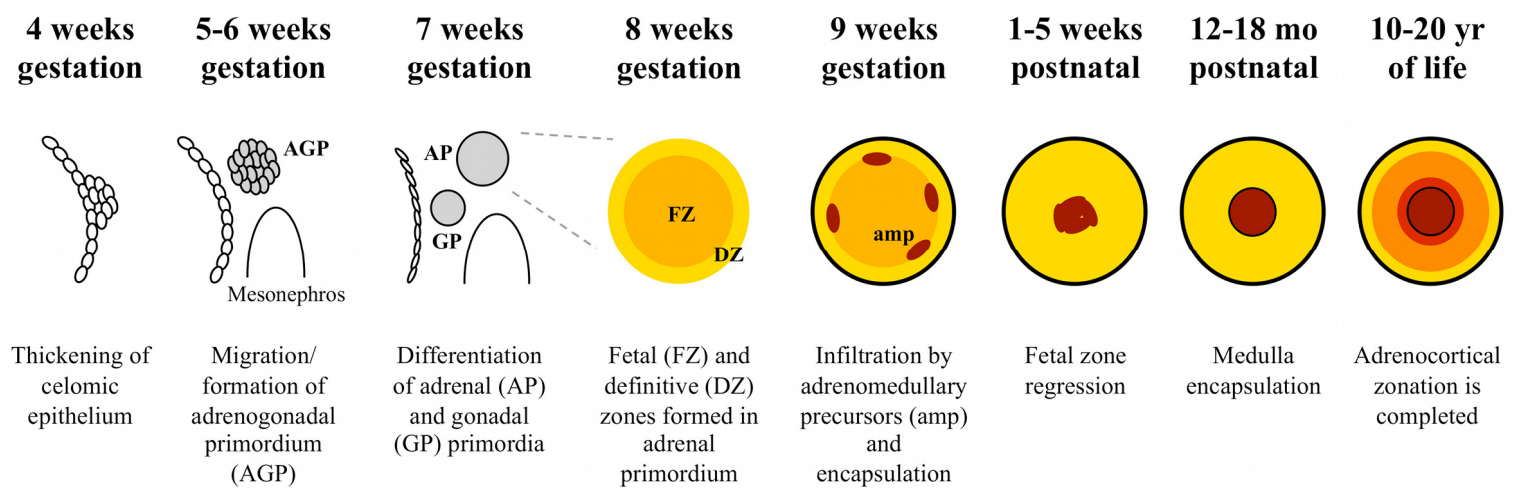

Figure 1.4. Cartoon representation of human adrenal development.

Major developmental events are shown, from the thickening of the celomic epithelium at approximately 4 weeks of gestation until the fully formed adult adrenal gland. The three concentric adult cortical zones are depicted in yellow (glomerulosa), orange (fasciculata) and red (reticularis), while adrenomedullary tissue is in brown. Based on Hammer et al., 2005 and Ferraz-de-Souza and Achermann, 2008.

1.2.1. Embryonic adrenal development

The adrenal cortex derives from a thickening of the celomic epithelium (and/or intermediate mesoderm) that appears between the urogenital ridge and the dorsal mesentery at around 4 weeks gestation in humans. This region contains adrenogonadal progenitor cells that give rise to the steroidogenic cells of the adrenal gland as well as those of the gonad (Mesiano and Jaffe, 1997; Hammer et al., 2005).

Cells destined to become adrenal tissue migrate dorsally towards the upper pole of the mesonephros from 5 to 7 weeks of gestation. At around eight weeks gestation the adrenal primordium is formed, consisting of an inner zone of large polyhedral eosinophilic cells, termed fetal zone, surrounded by a densely packed outer zone of basophilic cells, termed definitive zone. As will be discussed in detail later, cells of the adrenal primordium are capable of secreting cortisol and DHEAS from 8 weeks gestation (Goto et al., 2006; White, 2006).

At nine weeks gestation, the adrenal primordium is infiltrated by neural crest-derived cells that give rise to the adrenal medulla. These cells are thought to remain scattered in islands throughout the adrenal until birth, and differentiate into catecholamine-producing chromaffin cells under the influence of glucocorticoids. Encapsulation of the adrenal gland by specialised mesenchymal cells that migrate from the Bowman's capsule area occurs around nine weeks gestation, resulting in the formation of a distinct organ just above the developing kidney. Concomitantly, an extensive network of sinusoidal capillaries is formed, making the adrenal one of the most highly vascularised organs in the human fetus.

1.2.2. Fetal adrenal development

From 10-12 weeks gestation onwards, the morphology of the developing adrenal cortex does not change much. At mid-gestation (16 to 20 weeks), the fetal zone predominates and occupies 80 to 90% of cortical volume (Figure 1.1). Fetal zone cells are at that point large (20-50 μm), with typical steroid-secreting ultrastructural characteristics: large amounts of tubular smooth endoplasmic reticulum, mitochondria with tubulovesicular cristae, large Golgi complexes, and abundant lipid content.

The tightly packed cells of the mid-gestation definitive zone, on the other hand, have ultrastructural characteristics of cells in a proliferative state: small cytoplasmic volume containing free ribosomes, small dense mitochondria and scant lipid. Notably, definitive zone cells accumulate lipid and begin to resemble steroidogenic cells with increasing fetal age. Recent data has shown that they express steroidogenic enzymatic machinery from early embryonic stages (9 weeks), albeit to a much lower extent than fetal zone cells (Goto et al., 2006).

A putative transitional zone has been described between the definitive and fetal zones during later fetal development, containing cells with intermediate ultrastructural characteristics (Mesiano and Jaffe, 1997). This region was once proposed to contain stem cells that could differentiate into either definitive- or fetal-type tissue, although another hypothesis proposes that the main population of adrenal stem cells is located in the subcapsular region of the gland, and that cells mature through different stages of development as they migrate centripetally. The latter hypothesis seems to have been favoured recently (Kim et al., 2009).

1.2.3. Postnatal adrenal development

After birth, the fetal zone rapidly regresses by apoptosis so that it disappears completely by 3 months of life (Figure 1.3). Islands of chromaffin cells coalesce to form a rudimentary adrenal medulla by 4 weeks of age, which becomes fully encapsulated by 12-18 months postnatally (Figure 1.4).

The formation of definitive zone compartments starts around 30 weeks of gestation and lasts until puberty. The zonae glomerulosa and fasciculata are not fully differentiated until 3 years of age, and the reticularis may not be fully differentiated until about 15 years of age (Miller et al., 2008). The currently accepted model for zonal proliferation involves the existence of subcapsular progenitor cells that undergo centripetal migration and differentiation to form the three zones (Kim and Hammer, 2007; Kim et al., 2009). Glomerulosa-type cells, expressing CYP11B2, start producing aldosterone from the third trimester onwards. Fasciculata-type cells, expressing CYP11B1, produce cortisol steadily from mid-gestation but, recently, a brief 7 to 9 wpc (9 to 11 weeks gestation) window of cortisol production has been unveiled (Goto et al., 2006). It is tempting to believe that cells located at the interface of fetal and definitive zones, found to be responsible for this early cortisol surge, will give rise to the transitional zone and, eventually, to the zona fasciculata, but this has not been shown unequivocally. The timing of zona reticularis development is likewise obscure. Production of androgenic precursors DHEA and DHEAS decreases with fetal zone regression and rises again in the adrenarche, around 7 to 8 years of age. The mechanisms triggering adrenarche, a phenomenon unique to higher primates, are not completely understood.

1.2.4. Fetal adrenal steroidogenesis

Steroidogenesis in the fetal adrenal is essential for the maintenance of human pregnancy, and, at later stages, for fetal maturation. From 8 weeks gestation onwards, production of oestradiol by the maternal corpus luteum is taken over by the fetoplacental unit through a pathway that relies on the synthesis of DHEAS by the fetal adrenal cortex and its aromatisation to oestradiol in the placenta (White, 2006). The capacity of the fetal zone of the adrenal gland to produce large amounts of androgenic precursors (DHEA, DHEAS) is largely the result of a relative deficiency of HSD3B2 coupled with a relative abundance of the 17,20-lyase activity of CYP17 (Mesiano and Jaffe, 1997). The fetal adrenal also has significant expression of SULT2A1 sulfotransferase, which drives the conversion of DHEA to DHEAS and provides a substrate for conversion to circulating oestrogens by the placenta.

The understanding of steroidogenesis in the developing human adrenal gland has been greatly expanded by the robust immunohistochemical study of 121 fetal tissue samples by Goto and colleagues reported in 2006 (Figure 1.5) (Goto et al., 2006). Besides documenting the expression of the enzymatic machinery necessary for the generation of DHEAS as described above from as early as 7 wpc, the authors have shown expression of HSD3B2 and its potential regulator the orphan nuclear receptor NGFI-B (NR4A1), at 50-52 days post-conception (dpc). Expression of HSD3B2, stronger in a subpopulation of cells located in the transition of fetal to definitive zones, fades by 9.5 wpc and completely disappears by 14 wpc. This transient expression of HSD3B2 leads to detectable ACTH-responsive cortisol production at 8-9 wpc in male and female fetuses (Figure 1.6). It has been proposed that this early cortisol surge safeguards female sexual differentiation by down-regulating ACTH and consequently DHEA/DHEAS production at a time that placental aromatase

activity is not maximal and excess of DHEA/DHEAS could potentially virilise the female fetus (Goto et al., 2006; White, 2006).

Following this period of transient intact HPA axis activity, fetal adrenal glucocorticoid production is reduced as HSD3B2 activity declines. However, glucocorticoid production resumes in the third trimester so that the fetus is primed for postnatal existence, and development of the zona glomerulosa means that the adrenal is capable of responding to angiotensin II by producing mineralocorticoids after birth.

This figure has been removed from the electronic version of this thesis since copyright permission could not be obtained.

Figure 1.5. Expression patterns in the developing human adrenal gland.
From Goto et al., 2006.

This figure has been removed from the electronic version of this thesis since copyright permission could not be obtained.

Figure 1.6. Relative levels of cortisol and DHEAS secretion throughout development.
From White, 2006.

1.3. Regulation of adrenal development

Several factors have been identified that play potentially important roles in regulating adrenal development, zonation and growth (Table 1.1). Not surprisingly, most of these factors have been identified through studies in animal models, chiefly in transgenic mice (Hammer et al., 2005; Else and Hammer, 2005; Val and Swain, 2010). Marked differences exist between mouse and human adrenal development, especially with regard to the dynamics of the establishment and involution of the adrenocortical fetal zone (Hammer et al., 2005). The existence of a fetal zone in the mouse adrenal cortex has only recently been demonstrated (Zubair et al., 2006) and its function is still the subject of debate. The murine fetal zone is not as prominent as the human counterpart, and does not produce androgen precursors for placental conversion, a phenomenon restricted to higher primates (Zubair et al., 2008; Mesiano and Jaffe, 1997). Mice also have an "X zone", which corresponds to the accumulation of fetal zone cells at the juxtamedullary region. This X zone becomes distinguishable postnatally from 10-21 days and regresses at puberty in males or following the first pregnancy in females. There is no known parallel structure to the X zone in humans (Hammer et al., 2005). Therefore, the relative significance and interaction of developmental transcriptional regulators identified in mice remains largely to be determined in humans.

Despite this, in some cases molecular defects identified in patients with disorders of adrenal development have confirmed observations in mice. This is true for steroidogenic factor-1 (SF-1), proopiomelanocortin (POMC)-derived peptides and, possibly, Gli-Kruppel family member 3 (GLI3). However, for the majority of factors

implicated in mouse adrenal development, evidence of their direct role in *human* adrenal development is still lacking.

Key emerging concepts in adrenal development will be discussed in the following sections with a focus on several of the factors and mechanisms relevant to the work of this thesis, namely: hedgehog signalling/GLI3; regulation of steroidogenic factor-1 dosage; and DAX1 and ACTH signalling. A more comprehensive list of factors and mediators implicated in adrenal development through phenotypic analysis of human or mouse mutants is presented in Table 1.1.

1.3.1. Overview

Early stages of adrenal development appear to be regulated by a number of transcription factors (e.g. Osr1, Wt1, Sall1, Foxd2, Pbx1, SF-1, DAX1), co-regulators (e.g. Cited2), signalling factors (e.g., hedgehog/GLI3, Wnt3/WNT4/Wnt11, Mdk), matrix proteins (e.g. Sparc) and regulators of telomerase activity (e.g. Acd) (Else and Hammer, 2005; Hammer et al., 2005; Val and Swain, 2010). Subsequently, fetal adrenal growth depends upon the tropic effects of POMC-derived peptides, primarily ACTH, released from the anterior pituitary. The mechanisms by which ACTH stimulates adrenal growth and maturation may involve signalling pathways such as basic fibroblast growth factor (bFGF), epidermal growth factor (EGF) and insulin-like growth factor II (IGFII).

Table 1.1. Factors implicated in adrenal gland development through phenotypic analysis of humans or mice with gene disruptions.

Factor	Function	Disruption in mouse	Disruption in human	Adrenal phenotype in human
Direct involvement in adrenal development (presumed or defined)				
ACD	Telomere cap protein	Acd mouse (spontaneous) with *adrenal dysplasia*, infertility and hydronephrosis	Not reported (Investigated by Hutz et al., 2006, and Keegan et al., 2007)	Not found
CBX2 (M33)	Polycomb protein	HMZ lethal (postnatal), male-to-female sex reversal, *small adrenals*	XY gonadal dysgenesis (602770)	Normal
CITED2	Transcription co-factor	HMZ lethal (pre/perinatal), *adrenal agenesis*, cardiac and CNS defects	Cardiac septal defects (602937)	Not reported
DAX1 (NR0B1)	Transcription factor	Reproductive anomalies in males, ranging from infertility to XY sex reversal; *normal adrenal glands with X zone retention*	X-linked adrenal hypoplasia congenita, hypogonadotropic hypogonadism, spermatogenic defect (300200)	*Adrenal hypoplasia*
FOXD2	Transcription factor	Low penetrance kidney hypoplasia, *small adrenals*	Not reported	n/a
OSR1 (ODD1)	Putative transcription factor	HMZ lethal E11.5, cardiac defects; *absent adrenal glands*, kidneys and gonads	Not reported	n/a
PBX1	Transcription factor	HMZ lethal E15, *absent adrenal glands* and gonads, hypoplastic kidney and pancreas	Not reported	n/a
SF-1 (NR5A1)	Transcription factor	HMZ lethal (perinatal), *adrenal and gonadal aplasia*, VMH dysgenesis	XY gonadal dysgenesis, *adrenal hypoplasia*, primary ovarian insufficiency, spermatogenic defects (184757)	*Adrenal hypoplasia in a few cases*
WNT4	Secreted glycoprotein	HMZ lethal (perinatal), kidney and gonadal anomalies; *altered adrenocortical function with reduced aldosterone production*	Mullerian aplasia and hyperandrogenism (158330)	Normal
			SERKAL syndrome (611812): 46,XX sex reversal with dysgenesis of kidneys, *adrenals* and lungs	*Small or absent adrenals*

Factor	Function	Disruption in mouse	Disruption in human	Adrenal phenotype in human
WT1	Transcription factor	HMZ lethal E16.5, failure of gonad and kidney development, *adrenal aplasia or hypoplasia*	WAGR syndrome (194072)	Normal
			Denys-Drash syndrome (194080)	Normal
			Frasier syndrome (136680)	Normal
Direct and/or indirect involvement in adrenal development				
GLI3	Transcription factor	HMZ lethal (perinatal), polydactyly, GI defects, abnormal kidneys, *absent adrenal, no hypothalamic or pituitary defect reported*	Pallister-Hall syndrome (146510): hypothalamic hamartoma, *pituitary dysfunction*, central polydactyly and visceral malformations	*Absent or small adrenals in rare cases*
SALL1	Transcription factor	HMZ lethal, kidney agenesis, exencephaly, limb and anal deformities; *absent adrenal glands*	Townes-Brocks syndrome (107480)	Normal
SHH	Signalling factor	HMZ lethal, short limbs, dwarfism, cyclopia, midline defects, *adrenal hypoplasia*	Holoprosencephaly 3, microphthalmia, solitary median maxillary incisor (600725)	Not reported
Indirect involvement in adrenal development via ACTH signalling				
TPIT	Transcription factor	*Decreased corticotropes, hypopigmentation, 2^{ary} adrenal hypoplasia*	Isolated ACTH deficiency, *2^{ary} adrenal insufficiency* (604614)	*2^{ary} adrenal hypoplasia*
POMC	Peptide hormone precursor	Obesity, altered pigmentation, *2^{ary} adrenal hypoplasia*	Red hair, early onset obesity, *2^{ary} adrenal insufficiency* (176830)	*2^{ary} adrenal hypoplasia*
PCSK1 (PC-1)	Pro-protein convertase	Severe growth impairment, GH deficiency, *ACTH deficiency but normal corticosterone*, perinatal lethality	Obesity, hypogonadotropic hypogonadism, hypoglycaemia, *2^{ary} adrenal insufficiency* (600955)	*2^{ary} adrenal insufficiency in few cases*
MC2R	G-protein-coupled receptor	Neonatal lethality, adrenal hypoplasia, adrenal insufficiency including mild mineralocorticoid deficiency	*Familial glucocorticoid deficiency type 1* (202200)	*Adrenal hypoplasia (ACTH resistance)*
MRAP	GPCR accessory protein	n/a	*Familial glucocorticoid deficiency type 2* (607398)	*Adrenal hypoplasia (ACTH resistance)*

Factor	Function	Disruption in mouse	Disruption in human	Adrenal phenotype in human
AAAS	WD40-protein	Female infertility, behavioural changes, *normal adrenal glands*	Triple-A syndrome (231550): Achalasia, *adrenal insufficiency*, alacrima	*Adrenal hypoplasia (ACTH resistance)*

Abbreviations: HMZ, homozygous; n/a, not available; WAGR, Wilms tumour, aniridia, genitourinary anomalies and mental retardation; GI, gastrointestinal; CNS, central nervous system; VMH, ventromedial hypothalamus; GH, growth hormone; GPCR, G-protein-coupled receptor. In the 'Disruption in humans' column, the number between brackets corresponds to the Medelian Inheritance in Man (MIM) annotation. Based on Else and Hammer, 2005, and Val and Swain, 2010.

1.3.2. Hedgehog signalling/GLI3

The hedgehog signalling network is involved in several developmental processes (Ingham and McMahon, 2001). The three mammalian hedgehog ligands – sonic hedgehog (SHH), indian hedgehog (IHH) and desert hedgehog (DHH) – are capable of independently regulating distinct biological processes through the activation of a complex signalling cascade that culminates with modulation of GLI transcription factor activity (King et al., 2008). With respect to adrenocortical development, sonic hedgehog (Shh) has emerged as an important factor based on its expression pattern in the fetal adrenal and distinct abnormalities in adrenocortical development in mouse (King et al., 2008; King et al., 2009; Ching and Vilain, 2009). Several mutations in human SHH have now been identified in association with holoprosencephaly, a condition that is often accompanied by secondary adrenal insufficiency (Ching and Vilain, 2009). Nevertheless, primary hypoadrenalism itself has not been reported in individuals harbouring SHH mutations.

The downstream hedgehog signalling effector Gli-Kruppel family member 3 (GLI3; MIM 165240) was implicated in human adrenal development after the identification of frameshift mutations in *GLI3* in patients with Pallister-Hall syndrome (PHS; MIM 146510) (Kang et al., 1997). PHS is a pleiotropic autosomal dominant disorder characterised by hypothalamic hamartomas, pituitary dysfunction, postaxial polydactyly and a variety of visceral malformations including adrenal hypoplasia (Hall et al., 1980). Mutations in *GLI3* have also been associated with several malformation syndromes, including Greig cephalopolysyndactyly syndrome (GCPS; MIM 175700), which do not include an adrenal phenotype. Recently, a robust genotype-phenotype correlation has been established for truncating mutations in *GLI3* and these two phenotypes (Johnston et al., 2005). Truncating mutations in the

middle third of the gene generally cause PHS, whereas large deletions or truncating mutations elsewhere in the gene (amino-terminal or carboxy-terminal thirds of the gene) cause GCPS. It has been proposed that truncations in the middle third of the protein, but not in amino- or carboxy-terminal regions, would generate a constitutive repressor protein that skews the balance of activator and repressor forms of GLI3, determining the phenotypic variability (Johnston et al., 2010).

Notably, the occurrence of panhypopituitarism in PHS patients with adrenal hypoplasia precluded the analysis of direct GLI3 activity in the human adrenal. However, mutations similar to those found in PHS patients when introduced into mice led to a complete lack of adrenal glands without obvious hypothalamic or pituitary defects, therefore suggesting a direct role of Gli3 in adrenal development (Bose et al., 2002). Taken together with the observations of abnormal adrenal development following disruption of Shh in mice (King et al., 2008; Ching and Vilain, 2009), a key role for hedgehog signalling at early stages of adrenal development is becoming apparent.

1.3.3. Regulation of SF-1 dosage

The nuclear receptor transcription factor steroidogenic factor-1 (SF-1, encoded by *NR5A1*) is a master regulator of adrenal and gonadal development, and will be discussed at length in section 1.4. SF-1 is essential for adrenocortical development in mice and humans, as shown by numerous *in vivo* and *in vitro* expression and functional studies (Kim et al., 2009; Schimmer and White, 2010). Notably, homozygous disruption of *Nr5a1* in mice leads to adrenal agenesis by programmed cell death at around embryonic day E11.5/12.5, after the adrenal primordium is formed (Luo et al., 1994; Sadovsky et al., 1995). Therefore, while Sf-1 does not

trigger the formation of the adrenal primordium, its sustained activity is essential for organogenesis and function. Furthermore, studies of *Nr5a1* haploinsufficient mice have shown that full dosage of Sf-1 is essential early during adrenal development but not in the adult adrenal, by which stage compensatory mechanisms are able to restore near normal function (Bland et al., 2004). Therefore, the mechanisms leading to Sf-1 expression at early adrenal developmental stages have been increasingly investigated.

Recently, reports have focussed on the transcriptional regulation of Sf-1 dosage by Wt1, Cited2 and Pbx1 triggering adrenal cortex differentiation in mice (Figure 1.7). These mechanisms will be discussed in detail in the following sections. Other factors that have been shown to modulate Sf-1 dosage, including the polycomb protein Cbx2 (M33) (Katoh-Fukui et al., 2005) and the transcription factor Pod1 (Tamura et al., 2001) may also be important.

1.3.3.1. Wt1

Wilms' tumor 1 (WT1, MIM 607102) is a tumour suppressor zinc-finger transcription factor, isolated by positional cloning in familial embryonic kidney tumours (reviewed by Lee and Haber, 2001). Human mutations in *WT1* are associated with a variety of genitourinary malformations, including 46,XY disorders of sex development (DSD), but not with adrenal insufficiency. Studies in mice, however, have revealed that *Wt1* deficiency leads to adrenal agenesis (Kreidberg et al., 1993). Subsequent studies showed that Wt1 is expressed in the mouse urogenital ridge as early as E9.5 and that Sf-1 expression is abrogated in $Wt1^{-/-}$ mice (Wilhelm and Englert, 2002). Furthermore, one Wt1 isoform is capable of binding to and activating the Sf-1 promoter. Taken together, these data suggest that Wt1 acts

upstream of Sf-1 in the mouse adrenal developmental cascade, a concept that has been expanded by the study of its interaction with Cited2 (Val et al., 2007).

1.3.3.2. Cited2

Cbp/p300-interacting transactivator, with Glu/Asp-rich carboxy-terminal domain, 2 (Cited2) is a transcription cofactor expressed at high levels in the mouse adrenogonadal primordium and adrenal anlage (Val et al., 2007). From initial observations of adrenal absence in Cited2$^{-/-}$ mice (Bamforth et al., 2001), Cited2 has subsequently been shown to physically and functionally interact with Wt1 in the adrenogonadal primordium to up-regulate Sf-1 expression (Figure 1.7). Wt1/Cited2 regulation of Sf-1 dosage has emerged as an important mechanism for triggering adrenal differentiation in mice: complete absence of Cited2 (*Cited2*$^{-/-}$) resulted in 36% Sf-1 dosage and no adrenal development, while partial Cited2 or Wt1 deficiency (*Cited2*$^{+/-}$ or *Wt1*$^{+/-}$) resulted in 45% Sf-1 dosage and formation of small adrenal glands (Val et al., 2007).

1.3.3.3. FAdE: Pbx1

In 2006, Zubair and colleagues identified a 600-bp enhancer fragment in the fourth intron of *Nr5a1* that drives Sf-1 expression in the adrenal primordium as early as E10.5. This region was termed “fetal adrenal enhancer” (FAdE) (Zubair et al., 2006) and harbours conserved transcription factor-binding sites for Sf-1 itself and for Pbx/Prep and Pbx/Hox. It was shown that the transcription factor Pre-B-cell leukemia homeobox 1 (Pbx1) was required to initiate Sf-1 enhancer activity in the fetal adrenal and that this activity is maintained at later stages by Sf-1 itself. These findings are in accordance with the observed lack of adrenal glands in the *Pbx1*$^{-/-}$ mouse (Schnabel et al., 2003).

1.3.3.4. Model of Sf-1 dosage regulation

In light of all these findings, a model has been proposed for the control of Sf-1 expression during early adrenal development in mouse (Val and Swain, 2010) (Figure 1.7), involving: *i)* Wt1-induced Sf-1 expression in the adrenogonadal primordium, *ii)* increased Sf-1 expression by interaction of Cited2 with Wt1, *iii)* activation of FAdE in fetal adrenal cortex through Pbx1/Prep1/Hox, enhancing Sf-1 expression and *iv)* maintenance of FAdE by Sf-1 itself. It remains elusive, however, whether these mechanisms are relevant for human adrenal development.

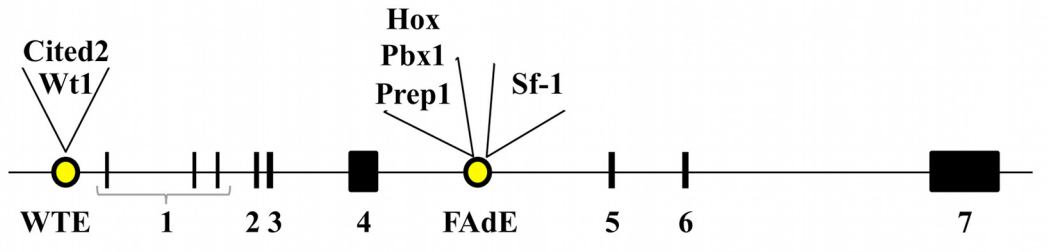

Figure 1.7. Cartoon representation of murine *Nr5a1* and its regulatory elements. Elements proposed to regulate Sf-1 dosage in early murine adrenal development are represented by yellow circles. *Nr5a1* is located on chromosome 2 and comprises 7 exons, numbered 1 to 7 (exon 1 has three alternative forms). Upstream of the first exon, Wt1-responsive elements (WTE) are bound and activated by Wt1, initiating Sf-1 expression in the adrenogonadal primordium. Dosage is increased by Cited2 interaction with Wt1. Sf-1 expression is further enhanced by Pbx1/Prep1/Hox binding to the fetal adrenal enhancer (FAdE) located in intron 4-5. Sf-1 itself is capable of sustaining FAdE activation at later stages. Based on the model proposed by Val and Swain, 2010.

1.3.4. DAX1 (NR0B1)

The involvement of Dosage-sensitive sex reversal-Adrenal hypoplasia congenita critical region on the X chromosome gene 1 (DAX1, *NR0B1*) in human adrenal biology resulted from the observation and study of an X-linked "cytomegalic" form of adrenal hypoplasia congenita (AHC). X-linked AHC is characterised by a dysfunctional adrenal cortex, with large vacuolated cells resembling cells from the fetal zone but lacking the definitive zone and postnatal zonation, and is associated with hypogonadotropic hypogonadism (Iyer and McCabe, 2004).

The description of rare cases of X-linked AHC as part of a contiguous gene deletion syndrome with glycerol kinase deficiency and Duchenne muscular dystrophy helped to map the *AHC* locus to Xp21 (Walker et al., 1992), leading to the subsequent identification of the gene *DAX1* (*NR0B1*) (Zanaria et al., 1994). Deletions or mutations in this gene cause AHC and hypogonadotropic hypogonadism (Muscatelli et al., 1994), whereas duplication of this region causes dosage sensitive "male-to-female sex reversal" (46,XY DSD/testicular dysgenesis) in XY individuals with intact *SRY* (Bardoni et al., 1994). DAX1 is expressed in humans throughout the hypothalamic-pituitary-adrenal-gonadal axis, consistent with the phenotype arising from its defects (Guo et al., 1995).

DAX1 is a very unusual orphan member of the nuclear receptor family of transcription factors as it lacks the highly conserved DNA binding domain (DBD) in its amino-terminal region (Figure 1.8) (Iyer and McCabe, 2004). Instead, the DAX1 amino-terminal domain has an unusual structure consisting of three and a half alanine/glycine-rich repeats of 65-70 amino acids, containing three leucine-rich receptor-binding LXXLL motifs involved in nuclear receptor interaction (Zhang et

al., 2000). The carboxy-terminal domain of DAX1 resembles a nuclear receptor ligand-binding domain (LBD), rendering its classification as a nuclear receptor.

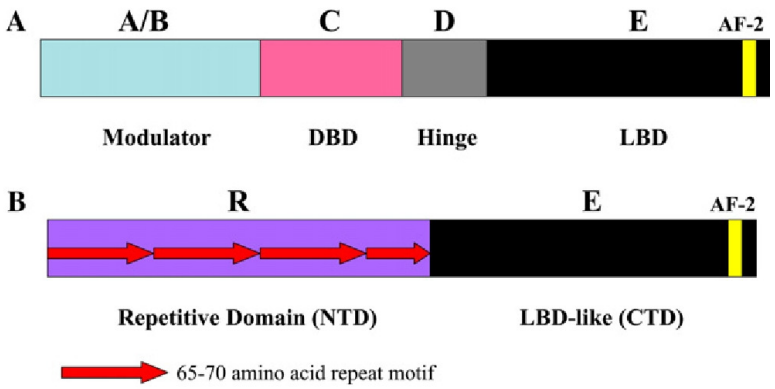

Figure 1.8. Functional domain structure of DAX1.

A, Structure of a typical nuclear receptor. Members of the nuclear receptor superfamily usually have characteristic domains (sub-regions A–E). Region A/B varies in size among family members and is considered a modulator domain. Region C is typically the most highly conserved and represents the DNA-binding domain (DBD) containing two zinc fingers that allow nuclear receptors to recognise and bind hormone response elements in the promoters of target genes. Region D serves as a hinge between the DBD and the ligand-binding domain (LBD, region E), which contains an AF-2 (Activating Function-2) hormone-dependent transactivation domain. B, DAX1 lacks a DBD and, instead, has an unusual structure (R) with 3.5 repeat motifs in its amino-terminal region (NTD). The carboxy-terminal region (CTD) of DAX-1 resembles that of a nuclear receptor (E), although a natural ligand has not yet been identified. From Iyer and McCabe, 2004. Copyright 2004, with permission from Elsevier.

Most *in vitro* studies have shown DAX1 to function primarily as a transcriptional repressor. DAX1 has been proposed to inhibit the expression of *STAR* by binding to DNA hairpin structures in its promoter (Zazopoulos et al., 1997), and, most notably, to repress SF-1-dependent transcriptional activation on several targets (Lalli and Sassone-Corsi, 2003). Moreover, DAX1 also represses the action of other nuclear receptors such as the androgen (AR, *NR3C4*), oestrogen (ER, *NR3A1-2*) and progesterone (PR, *NR3C3*) receptors and the liver receptor homolog-1 (LRH-1, *NR5A2*). Proposed mechanisms of DAX1 repression include: *i)* direct protein-protein interaction via binding through LXXLL elements present in the amino-terminal domain and impairing the recruitment of co-activators; *ii)* sequestering of NRs in the cytoplasm, preventing their translocation to the nucleus; *iii)* interfering with functional dimerisation of NRs; or *iv)* direct binding to DNA hairpin elements in promoters of target genes (Suzuki et al., 2003; Iyer and McCabe, 2004; Niakan and McCabe, 2005).

DAX1 is expressed throughout adrenocortical development (Hanley et al., 2001), but its function in adrenal development is poorly understood. In view of all the evidence implicating DAX1 as a repressor of steroidogenesis, it is paradoxical that DAX1 defects with reduced repressive capability *in vitro* should result in adrenal insufficiency *in vivo*. The generation of *Dax1*$^{-/Y}$ mice did not help to elucidate this puzzle since the resulting phenotype is quite different to that observed in AHC patients: these mice have fully developed adrenal glands, with functional zonation and normal hormonal output (Yu et al., 1998a). The only observed adrenal phenotype in these animals is lack of X zone regression at puberty. Dax1 is likely to have a critical role in early embryonic development, however, since complete deletion of *Dax1* in embryonic stem cells is lethal.

Overall, it is believed that DAX1 is involved in adrenocortical growth mainly through antagonistic interaction with SF-1 during development. Other hypotheses propose that DAX1 may regulate adrenal progenitor cell development and maturation (Lalli and Sassone-Corsi, 2003). Nevertheless, it is altogether possible that DAX1 has an as yet undiscovered function, since so many questions remain unanswered (Iyer and McCabe, 2004).

1.3.5. ACTH signalling

ACTH is the main trophic regulator of the adrenal cortex postnatally, and, not surprisingly, plays a central role in regulating fetal adrenal growth. Disruption of hypothalamic-pituitary function in human fetuses (for example in anencephalics or associated with maternal glucocorticoid treatment) results in normal fetal zone development until 15 weeks gestation, when it stalls and does not develop further, indicating that ACTH maintains tropic fetal zone growth after this time (Mesiano and Jaffe, 1997). Several defects in POMC-peptide signalling have now also been associated with disorders of adrenal development, and will be discussed in section 1.5.1.

ACTH binds to the G protein-coupled receptor melanocortin 2 receptor (MC2R) and activates several intracellular signalling pathways, the most widely studied of which is the cyclic AMP (cAMP) signalling cascade (Sewer et al., 2007). ACTH binding to MC2R results in the activation of adenylyate cyclase, increasing intracellular cAMP and activating the cAMP-dependent protein kinase (PKA). PKA phosphorylates downstream targets that increase the transcription of steroidogenic genes, the availability of free cholesterol, and/or the activity of steroidogenic enzymes. Besides intracellular targets of cAMP signalling, the tropic actions of ACTH in the fetal

adrenal cortex are likely mediated by local paracrine/autocrine growth factors (Mesiano and Jaffe, 1997). Signalling pathways involving basic fibroblast growth factor (bFGF), epidermal growth factor (EGF) and insulin-like growth factor II (IGFII) have been suggested to be involved. Indeed, such signalling pathways may play important roles on their own right in early adrenal developmental stages, independent of ACTH stimulation, as indicated by the observation of smaller adrenals in mice with conditional deletion of FGF-receptor type II (Fgfr2) at E15.5 (Kim et al., 2007; Val and Swain, 2010).

1.4. Steroidogenic Factor-1

Steroidogenic factor-1 (SF-1, NR5A1) is a member of the nuclear receptor superfamily that is expressed widely throughout the adrenal and reproductive axes during development and plays a central role in the function of these endocrine systems in postnatal and adult life (Parker and Schimmer, 1997; de-Souza et al., 2006; Schimmer and White, 2010; Hoivik et al., 2010). Much has been learned about the role of this transcription factor since its initial cloning in 1992, largely through studies of knockout mouse models, *in vitro* studies of nuclear receptor function and, more recently, following identification and characterisation of patients with naturally occurring SF-1 mutations (Figure 1.9).

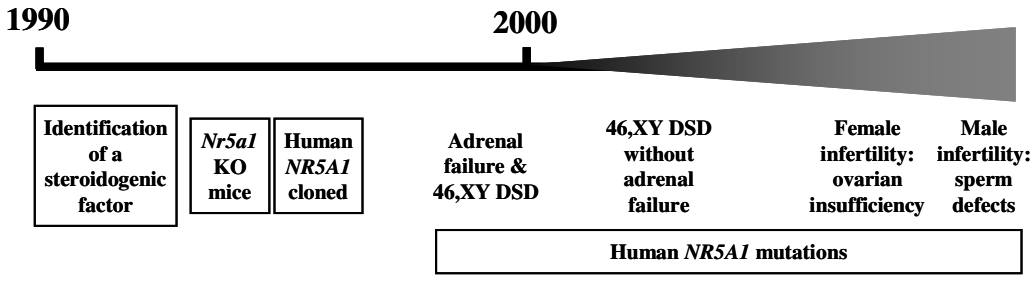

Figure 1.9. Timeline of major events in the history of SF-1/*NR5A1*.
KO, knockout; DSD, disorder of sex development.

1.4.1. Identification of a putative "steroidogenic factor"

The concept of a 'steroidogenic factor'- i.e. a single protein directly involved in the activation and regulation of various steps of steroidogenesis – was first proposed in the early 1990s following the recognition of a number of similar regulatory elements in the 5'-flanking region of steroidogenic genes by two independent groups (Rice et

al., 1991; Morohashi et al., 1992). These elements contained variations on an 5'-AGGTCA-3' DNA sequence motif, either 5'-PyCAAGGPyC- 3' or 5'-PuPuAGGTCA- 3' (where Py represents a pyrimidine [C/T] and Pu represents a purine [A/G]), which interacted only with a protein found in steroidogenic cells. This protein was termed steroidogenic factor-1 (SF-1) (Rice et al., 1991) or adrenal 4-binding protein (Ad4BP) based on its interaction with the Ad4 element in the bovine *CYP11B1* promoter (Morohashi et al., 1992).

Noting that these binding elements were similar to nuclear receptor binding sites, Lala and colleagues first cloned the murine Sf-1 in 1992 through an adrenal cDNA library screening using a probe comprising the DNA-binding domain (DBD) of the retinoid X receptor RXRβ (Lala et al., 1992). Independently, the bovine homologue was identified from an adrenal cDNA library using the partial sequence of a protein purified from bovine adrenal extracts (Honda et al., 1993). Both the murine and bovine proteins encoded by these cDNAs were shown to be able to increase the promoter activity of the steroid hydroxylases, and, thus, likely represented the proposed steroidogenic factor. Furthermore, analysis of both murine and bovine cDNAs revealed conserved regions similar to those of members of the nuclear receptor superfamily and high homology to the *Drosophila melanogaster* orphan nuclear receptor *fushi tarazu* factor 1 (FTZ-F1).

Using these cDNAs as probes, human SF-1 cDNA was subsequently isolated. The gene encoding human steroidogenic factor-1 was initially termed *FTZF1*, became widely known as *SF-1* (or *SF1*) and is now formally designated *NR5A1* for nuclear receptor subfamily 5 group A member 1. It is located at chromosome 9q33, spans 30 kb of genomic DNA and contains 7 exons, the first of which is not translated (Taketo et al., 1995; Oba et al., 1996; Wong et al., 1996). In keeping with customary usage in

the field, the gene will be referred to by *NR5A1* and the protein and mRNA by SF-1 hereafter (and, accordingly, *Nr5a1*/Sf-1 for mouse equivalents).

1.4.2. SF-1 is a nuclear receptor

Human SF-1 is a 461 amino acid protein that shares structural similarities with members of the nuclear receptor superfamily, and is highly conserved among different mammalian species (Figure 1.10). Critical structural domains of SF-1 include a two zinc finger DBD, an A box (or fushi tarazu factor 1 [FTZ-F1] box), a hinge region, and a carboxy-terminal ligand-like binding domain (LBD) bearing an activation function-2 (AF-2) domain (Figure 1.11) (Evans, 1988; Schimmer and White, 2010).

1.4.2.1. DNA-binding domain: SF-1 binds as a monomer

The DNA-binding domain of SF-1 is absolutely conserved among human, cow, rat and mouse orthologs (Figure 1.10) (Parker and Schimmer, 1997). In most nuclear receptors, the first zinc finger contains a proximal (P) box, which determines the DNA sequence recognition of half-sites of hormone-responsive elements, whereas a distal (D) box in the second zinc finger forms a dimerisation interface that determines appropriate spacing of half-sites as NRs commonly bind as homo- or heterodimers (Umesono and Evans, 1989). SF-1, however, is unusual amongst the nuclear receptor subfamily as it belongs to a small group of receptors thought to bind to DNA monomerically. This subgroup includes the nerve growth factor IB (NGFI-B, Nur77, NR4A1), the oestrogen-related receptors α and β (ERRα-β, NR3B1-2) and SF-1's closest mammalian relative, the liver receptor homologue-1 (LRH-1, NR5A2) (Parker and Schimmer, 1997). A key feature of these receptors is the presence of an A box, a 30-amino acid extension of the DBD adjacent to the second zinc finger

motif that recognises additional bases 5' to the consensus sequence. Indeed, it has been shown that SF-1's P box recognises and binds to variations of the 5'-AGGTCA-3' consensus hexamer in the major groove of the DNA helix and that monomeric binding is stabilised by A box interaction with specific 5' nucleotide sequences in the minor groove of DNA, resulting in a 9-bp high-affinity 5'-PyCAAGGPyCPu-3' SF-1 target sequence (Ueda et al., 1992; Wilson et al., 1993) (Figure 1.12). However, it is notable that the target sequence can be quite variable and transcriptional complexes involving co-activators and other DNA-bound factors may also be important in stabilising SF-1 binding (Little et al., 2006).

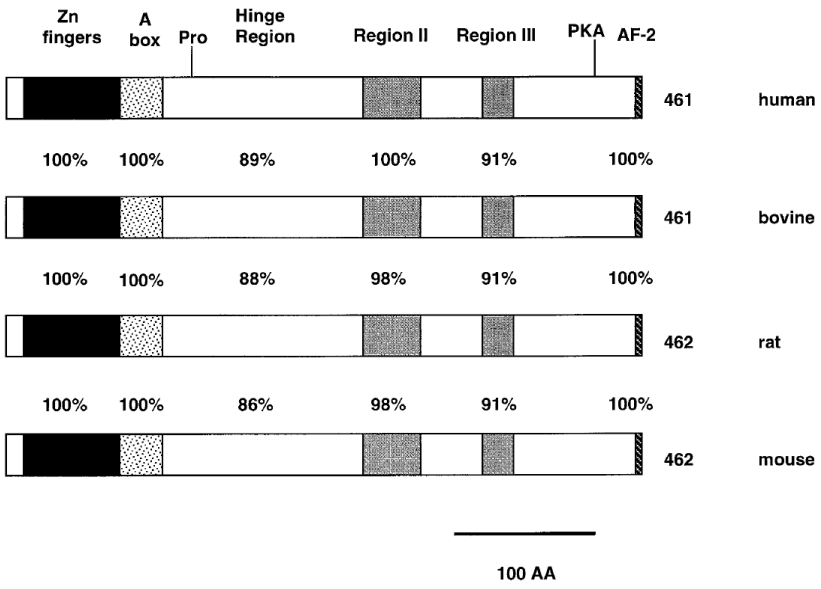

Figure 1.10. Conservation of SF-1 functional domain structure among species.
The percentage of identity of each region to human SF-1 is shown, as well as protein size. Pro, proline-rich sequence; PKA, cAMP-dependent protein kinase phosphorylation consensus motif. From Parker and Schimmer, 1997. Copyright 1997, The Endocrine Society.

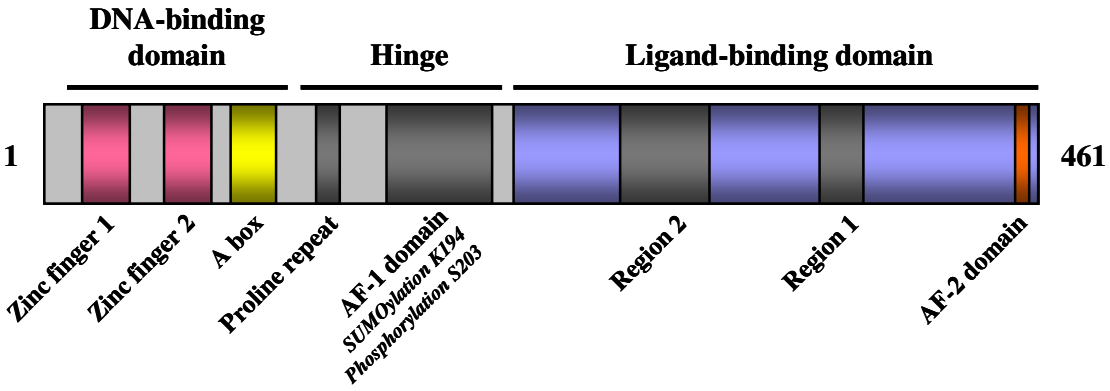

Figure 1.11. Functional domain structure of human SF-1.

The DNA-binding domain lies in the amino-terminal region, bearing two zinc fingers and the A box. The hinge region contains a conserved proline-rich region and the activation function (AF)-1 domain. Within the AF-1 domain, two amino acid residues susceptible to post-translational modification, lysine 194 and serine 203, are shown. The carboxy-terminal ligand-binding domain bears two conserved regions (1 and 2) and the AF-2 domain, which mediates interaction with co-factors. Based on Schimmer and White, 2010.

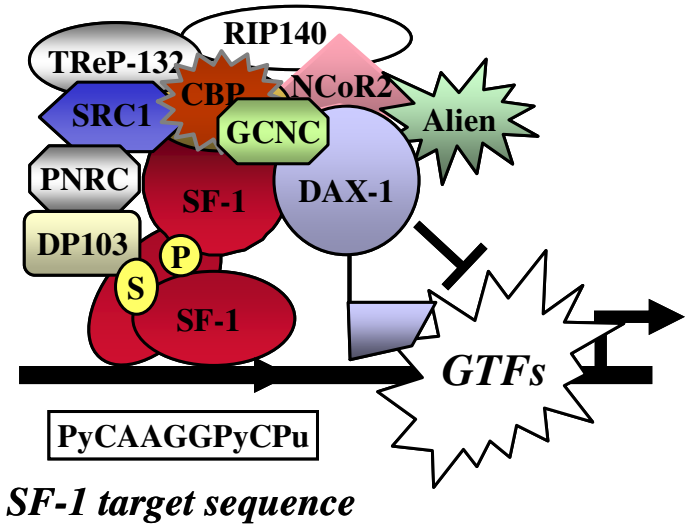

Figure 1.12. Interaction of SF-1 with target DNA-binding sites and selected co-factors.

Simplified cartoon representation of SF-1 binding to DNA to regulate transcription. SF-1 binds to DNA as a monomer, with the main DNA-binding interface occurring between the P-box of the zinc fingers of SF-1 and the major groove of DNA (variations on AGGPyCPu). The interaction between the A box and the minor groove region (PyCA) is proposed to stabilise monomeric binding. SF-1 undergoes post-translational modification (P, phosphorylation; S, SUMOylation) and interacts with a host of co-activators (e.g., CBP, SRC-1) and repressors (e.g., DP103). Interactions with DAX1 may represent a further tissue-specific means of modulating SF-1 function, although the majority of data reported to date suggest that DAX1 acts mainly as a repressor of SF-1 function. Py, pyrimidine (T or C); Pu, purine (A or G); GTF, general transcription factors. Modified from de-Souza et al., 2006. Copyright 2006, with permission of Y.S. Medical Media Ltd.

1.4.2.2. Ligand-binding domain: co-factors and phospholipid ligands

In addition to conserved regions that mediate DNA binding, three highly conserved regions exist in the carboxy-terminus of SF-1 – regions II, III and the AF-2 transactivation domain – that resemble a ligand-binding domain (LBD) of nuclear receptors (Figure 1.10). Structurally, the LBD of SF-1 forms 12 alpha helices, a typical feature of nuclear receptors. The AF-2 domain is found at the carboxy-terminus of many ligand-inducible nuclear receptors, forming an amphipathic helix involved in co-factor recruitment and essential for transcriptional activation (Parker and Schimmer, 1997). In SF-1, the conserved AF-2 domain (residues LLIEML) has indeed been shown to be essential for transactivation and to interact with co-activators such as CBP/p300 (CREBBP/EP300), SRC-1 (NCOA1), TReP-132 (TRERF1), PRNC1 and GRIP1, and co-repressors such as RIP140 (NRIP1), SMRT (NCOR2), and EID-1 (Figure 1.12) (Ito et al., 1998; Hammer et al., 1999; Mellgren et al., 2003; Park et al., 2007; Schimmer and White, 2010).

SF-1 has long been considered an orphan nuclear receptor as a high-affinity hormone-like ligand, regulating SF-1-mediated transcription, could not be identified. Many attempts have been made to discover a specific ligand for SF-1, and it remains debated whether SF-1 is indeed a true orphan or not. Several studies suggested 25-hydroxycholesterol as a possible ligand for SF-1 (Lala et al., 1997; Christenson et al., 1998), but subsequent investigations failed to demonstrate substantial enhancement of SF-1 transcriptional activation by this compound (Mellon and Bair, 1998). Thereafter, SF-1 was felt to be able to function independently of ligand activation, given its expression pattern, monomeric binding, stable helical structure and large hinge region, which is subject to post-translational modification.

More recently, though, the crystal structure of the SF-1 LBD bound to co-factor has been solved and its ligand-binding pocket was shown to be very large, very hydrophobic, and occupied by phospholipids (Krylova et al., 2005; Li et al., 2005; Sablin et al., 2009). These lipids are capable of up-regulating SF-1 function *in vitro* and may represent an interface between signalling pathways and SF-1 activation. However, the true physiologic role of phospholipid ligands *in vivo* remains to be clarified, and it seems unlikely they will represent a high-affinity specific ligand in the "classic" endocrine nuclear receptor sense. Finally, pharmacological ligands have recently been developed to increase or suppress (inverse agonists) SF-1 activity *in vitro*, and could represent promising pharmacological tools (Whitby et al., 2006; Del Tredici et al., 2008).

1.4.2.3. Hinge region: post-translational modifications

The hinge region between the DNA- and ligand-binding domains is important for the transcriptional capacity of SF-1 as its residues are subject to post-translation modification (Figure 1.11). In the amino-terminal portion of the hinge region, adjacent to the DBD, lies a proline-rich domain of approximately 100 amino acids containing a highly-conserved stretch of consecutive prolines that is unique amongst nuclear receptors and of yet undetermined function (Parker and Schimmer, 1997). The carboxy-terminal portion of the hinge region harbours the activation factor helix 1 domain (AF-1), which contains the single identified phosphorylation site within SF-1, serine 203 (S203).

SF-1 is phosphorylated at S203 via two signalling pathways, one involving the mitogen-activated protein kinases (MAPK) 1 and 3 (ERK2 and ERK1, respectively) and the other through cyclin-dependent kinase 7 (CDK7) (Hammer et al., 1999;

Lewis et al., 2008). Phosphorylation of SF-1 at S203 does not affect its half-life, subcellular localisation or binding to DNA, however it does enhance its ability to interact with co-activators and to sustain activation at certain promoters (Hammer et al., 1999; Schimmer and White, 2010). Indeed, it has been suggested that controlled cyclic phosphorylation/dephosphorylation of S203 could be an important mechanism of temporal coordination of SF-1-dependent activation of target genes (Sewer and Waterman, 2003; Winnay and Hammer, 2006).

The hinge region is also the site of SF-1 modification by small ubiquitin-like modifier (SUMO) conjugation, resulting in *repressed* SF-1 function. Two lysine (K) residues have been identified as SUMO-targets within SF-1: K119 in the DBD and K194 in the hinge region (Chen et al., 2004; Komatsu et al., 2004). The latter is considered to be the primary site of SF-1 SUMOylation, determining repression of SF-1-dependent transactivation of several target promoters *in vitro*. SUMOylation does not affect the stability or cellular localisation of SF-1, or its ability to bind to canonical response elements, but it does inhibit its phosphorylation by CDK7 at S203 (Yang et al., 2009). Another form of post-translational modification of lysine residues, acetylation, was found to enhance SF-1 activity and seems to be confined to residues in the DBD (Jacob et al., 2001; Chen et al., 2005). Overall, the dynamics and importance of SUMOylation or acetylation as mechanisms of regulation of SF-1 *in vivo* are still poorly understood as only a small fraction of SF-1 *in vivo* seems to be subject to such modifications (Schimmer and White, 2010).

Finally, within the amino-terminal portion of the hinge region lies a repression domain, located from residues 193 to 201 (Ou et al., 2001). Interaction of the DEAD (Asp-Glu-Ala-Asp) box protein DP103 (DDX20) with this domain results in repression of SF-1 transactivation activity. Taken together with preferential

expression of DP103 in steroidogenic tissues in the mouse, this could indicate a DP103-dependent mechanism of repression of SF-1 activity resulting in down-regulation of SF-1 target genes during development and function of steroidogenic tissues.

1.4.3. SF-1 is a developmental regulator: lessons from animal models

The physiological role of SF-1 was clearly established in the mid 1990s following the generation of *Nr5a1* knockout mice by three independent groups (Luo et al., 1994; Shinoda et al., 1995; Sadovsky et al., 1995). Despite using different targeting strategies (Luo et al. and Sadovsky et al. disrupted the DBD, while Shinoda et al. disrupted the LBD), strikingly similar phenotypic features were seen. Mice homozygous for the gene deletion (-/-) had adrenal and gonadal agenesis, male-to-female "sex reversal", and persistence of Müllerian structures in males (Figure 1.13). Whilst some evidence of early adrenogonadal primordium formation was seen in *Nr5a1* knockout embryos by E10.5, the progenitor cells rapidly regressed through apoptosis by E11.5-12). Sf-1 was shown to be obligatory, therefore, for both adrenal and gonadal development. These homozygous animals were alive at birth, indicating that Sf-1 is not critical for survival *in utero*, but died shortly after birth from adrenocortical insufficiency. Because gonadal progenitors regress prior to male sexual differentiation, the internal and external urogenital tracts of null mice are phenotypically female, irrespective of chromosomal sex.

Nr5a1$^{-/-}$ mice also exhibit impaired gonadotropin release and near absence of the ventromedial hypothalamus (VMH), a hypothalamic region linked to feeding and appetite regulation and female reproductive behaviour (Shinoda et al., 1995). Since gonadotrope function can be restored by GnRH treatment it was suggested that Sf-1

deficiency did not result in a complete loss of gonadotrope cell function. Furthermore, late-onset obesity seems to be a feature of null mice that are rescued by adrenal transplantation, possibly reflecting dysregulated metabolic function as a result of VMH abnormalities (Madjic et al., 2002). Finally, although the functional consequences remain unclear, *Nr5a1*$^{-/-}$ mice have reduced spleen size (Morohashi et al., 1999).

The generation of *Nr5a1* haploinsufficient mice has demonstrated the importance of full Sf-1 dosage for endocrine development. Heterozygous (+/-) *Nr5a1* knockout animals were originally thought to be normal, but more detailed studies have revealed small adrenals with abnormal architecture and vasculature, impaired corticosterone production in response to stress, and decreased gonadal size (Figure 1.14) (Bland et al., 2000; Bland et al., 2004). Of note, differences in adrenal development between heterozygous *Nr5a1*$^{+/-}$ animals and their wild type littermates were more pronounced during embryonic development than after birth, leading the authors to posit that up-regulation of related nuclear receptors (such as NGFIB [NR4A1]) in heterozygous animals could compensate for Sf-1 haploinsufficiency and partly rescue adrenal function by the time the animals were born (Bland et al., 2004). Nevertheless, full Sf-1 dosage seems to be essential for the ability of adult adrenocortical cells to proliferate, as no compensatory growth was evident in *Nr5a1*$^{+/-}$ animals following unilateral adrenalectomy (Beuschlein et al., 2002).

Mechanisms regulating Sf-1 dosage in early murine adrenal development have been the subject of much interest in recent years, as discussed in section 1.3.3. Full Sf-1 dosage also seems essential for the proliferative capacity of subcapsular progenitor cells, proposed to replenish the adrenal cortex by centripetal migration and differentiation (Kim et al., 2009).

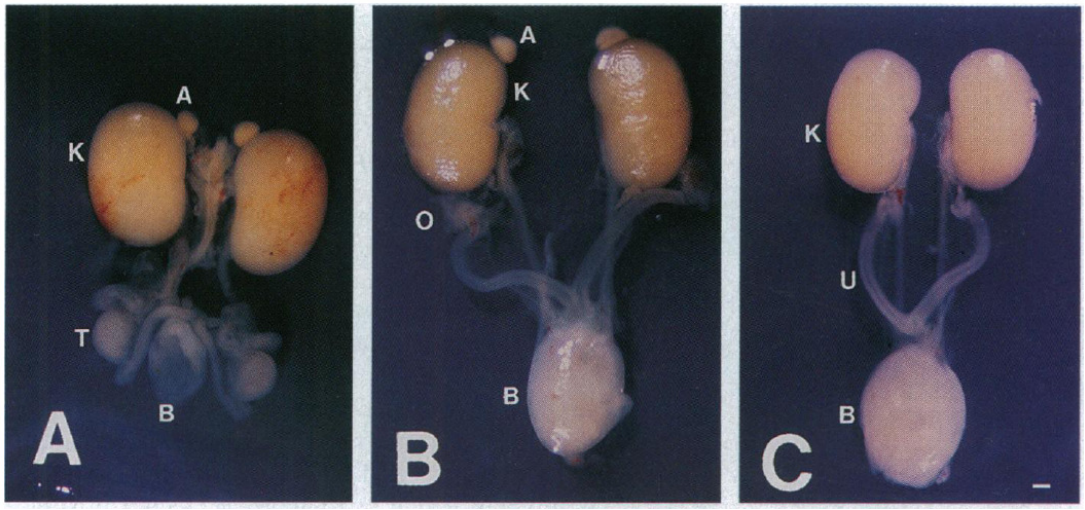

Figure 1.13. Adrenal and gonadal phenotype of *Nr5a1*$^{-/-}$ newborn mice.

A, Wild type male; B, Wild type female; and C, *Nr5a1*$^{-/-}$ male newborn mice. The adrenal glands (A) can be easily identified lying on top of the kidneys (K) in wild type male and female newborn mice, whereas they are absent in the *Nr5a1* null animal. Furthermore, the *Nr5a1*$^{-/-}$ male newborn lacks testes (T) and retains Mullerian structures (U, uterus). B, bladder; O, ovary. Bar = 500 µm. From Sadovsky et al., 1995. Copyright © by the National Academy of Sciences.

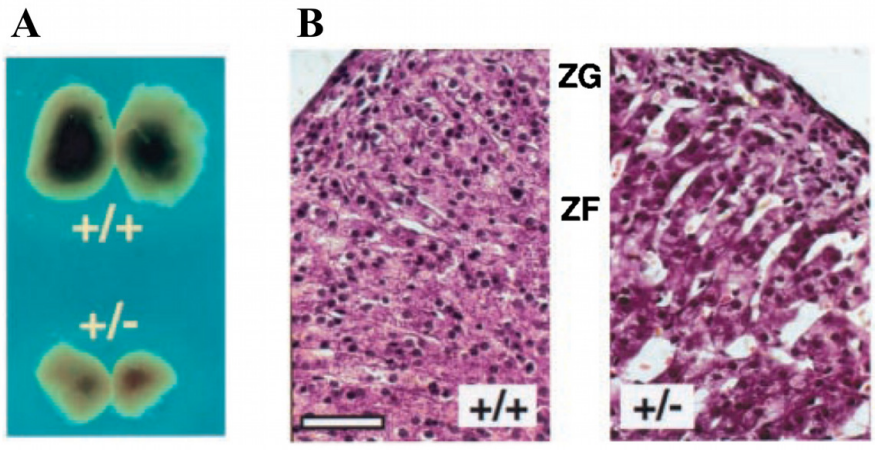

Figure 1.14. Adrenal phenotype of *Nr5a1*$^{+/-}$ haploinsufficient mice.

A, Adult Nr5a1$^{+/+}$ adrenals are significantly larger than Nr5a1$^{+/-}$ adrenals, despite equivalent body weight. B, Histological analysis of Nr5a1$^{+/+}$ and Nr5a1$^{+/-}$ adrenals. Nr5a1$^{+/-}$ adrenals display cortical cell hypertrophy, dilated adrenocortical sinusoids, and a hypoplastic zona fasciculata (ZF) adjacent to the zona glomerulosa (ZG). Bar = 50 µm. From Bland et al., 2000. Copyright © by the National Academy of Sciences.

1.4.4. SF-1 expression and target genes

The expression pattern of SF-1, in rodents and humans, is consistent with its critical role in adrenal development, steroidogenesis, gonadal differentiation and hypothalamo-pituitary reproductive function (Ikeda et al., 1994; Ramayya et al., 1997; Hanley et al., 1999). SF-1 is expressed in the early stages of human adrenal development – as early as 33 days post-conception – and gonadal development, where it plays a key role in determining cell fate (Hanley et al., 1999; Hanley et al., 2001). SF-1 is also expressed in the developing ventromedial hypothalamus (VMH), pituitary gonadotropes and spleen. Its expression persists in all these structures in postnatal and adult life, where it regulates transcription of an array of target genes involved in adrenal and gonadal function, steroidogenesis, puberty and metabolism (Table 1.2).

In general, SF-1 target genes have been identified through transient transfection assays using stretches of regulatory DNA, based on teleological associations. In the adrenal gland, for example, SF-1 was shown to up-regulate multiple targets involved in cholesterol metabolism and *all* the enzymes required for the biosynthesis of cortisol and corticosterone (Schimmer and White, 2010). Facilitating steroidogenesis, SF-1 increases the expression of factors involved in intracellular cholesterol transport such as the scavenger receptor B1 (SCARB1), sterol carrier protein 2 (SCP2), Niemann Pick C1 protein (NPC1) and STAR (Cao et al., 1997; Lopez et al., 2001; Gevry et al., 2003; Sugawara et al., 1996). Additionally, SF-1 also facilitates *de novo* cholesterol biosynthesis in adrenocortical cells by up-regulation of cytosolic HMG-CoA synthase (HMGCS1), and cholesterol metabolism, by activating the murine aldo-keto reductase 1 B7 (Akr1b7), which

detoxifies the by-product of cholesterol side chain cleavage (Mascaro et al., 2000; Aigueperse et al., 2001).

Importantly, SF-1 up-regulates the adrenocorticotropin receptor (MC2R), priming adrenocortical cells for ACTH-dependent activation of steroid biosynthesis (Naville et al., 1999). SF-1 also up-regulates DAX1 (Yu et al., 1998b; Vilain et al., 1997), and, indeed it has been proposed that, in mice, Dax1 activation by Sf-1 could constitute an intra-adrenal negative feedback loop, considering the role of Dax1 as a Sf-1 repressor (Gummow et al., 2006). SF-1-dependent activation of MC2R and DAX1 may represent mechanisms through which SF-1 regulates adrenal differentiation and development.

Consistent with the central role of SF-1 in steroidogenic tissue differentiation observed in transgenic mouse models, forced SF-1 expression in cultured SF-1 negative cell types such as murine embryonic stem cells or human bone marrow-derived mesenchymal cells induces their differentiation to a steroidogenic fate (Crawford et al., 1997; Tanaka et al., 2007). Moreover, it is striking that disruption of several SF-1 targets has been associated with disorders of adrenal development and steroidogenesis, such as: secondary adrenal hypoplasia and *MC2R* mutations (MIM 202200); congenital adrenal insufficiency and mutations in *CYP11A1* (MIM 118485); congenital lipoid adrenal hyperplasia and mutations in *STAR* (MIM 201710); congenital adrenal hyperplasia and *HSD3B2* mutations (MIM 201810); and aldosterone deficiency and *CYP11B2* mutations (MIM 124080) (Table 1.2).

Similarly broad ranges of SF-1 target genes are also found in the gonad and pituitary, indicating that SF-1 is a master-regulator of many aspects of adrenal, gonadal and reproductive development and function. Therefore, relatively small changes in SF-1 activity could have clinically significant effects on these different endocrine systems.

Table 1.2. SF-1 sites of action and selected target genes

Site of action	Target genes
Ventromedial hypothalamus	*NMDAR1, BDNF, A2BP1, AMIGO2, CDH4, NPTX2, SEMA3A, SLIT3, NETRIN3, FEZF1, NKX2-2*
Gonadotropes	*CGA, LHB, FSHB, GNRHR, NOS1*
Adrenal cortex	*STAR*, CYP11A1*, CYP17*, CYP21A2*, CYP11B1*, CYP11B2*, HSD3B2*, MC2R*, SCARB1, SCP2, NPC1, HMGCS1, AKR1B7, NR0B1 (DAX1)*, NR0B2 (SHP), SULT2A1, ADCY4, NOV, FATE1*
Gonads	*STAR, CYP11A1, CYP17, CYP19, LHR, FSHR , PRLR, AMH, AMHR2, INSL3, INHA, INHB, SRY, SOX9, VNN1, MAMLD1, OXT*

Compiled from Schimmer and White, 2010, Hoivik et al., 2010, and Kohler and Achermann, 2010. The asterisk denotes SF-1 targets in the adrenal cortex that have been associated with human adrenal disorders when disrupted.

1.4.5. SF-1 and human disease

The mouse *Nr5a1* knockout phenotype prompted studies of humans with combined adrenal and gonadal defects for possible mutations in *NR5A1*. To date, nearly 50 patients harbouring SF-1 mutations have been reported (MIM 184757) (Ferraz-de-Souza et al., 2010a). The phenotypic spectrum associated with these mutations is providing fascinating insight into the role of SF-1 in human endocrine development and function.

1.4.5.1. Mutations of SF-1

In 1999, the first human SF-1 mutation was described in a patient with phenotypic features similar to the null mouse: primary adrenal failure, XY sex reversal and persistent Müllerian structures (Achermann et al., 1999). Whereas the *Nr5a1*$^{-/-}$ mouse has complete agenesis of the adrenal gland and gonads, this patient had decompensated primary adrenal failure after birth and streak-like gonads removed in early adolescence, containing immature seminiferous tubules. Thus, the patient's phenotype was milder than that observed in the knockout mouse. Mutational analysis revealed a *de novo* heterozygous mutation G35E in the primary DNA-binding domain (P box) of SF-1, which impairs the ability of SF-1 to act as a transcriptional activator of target genes (Figure 1.15).

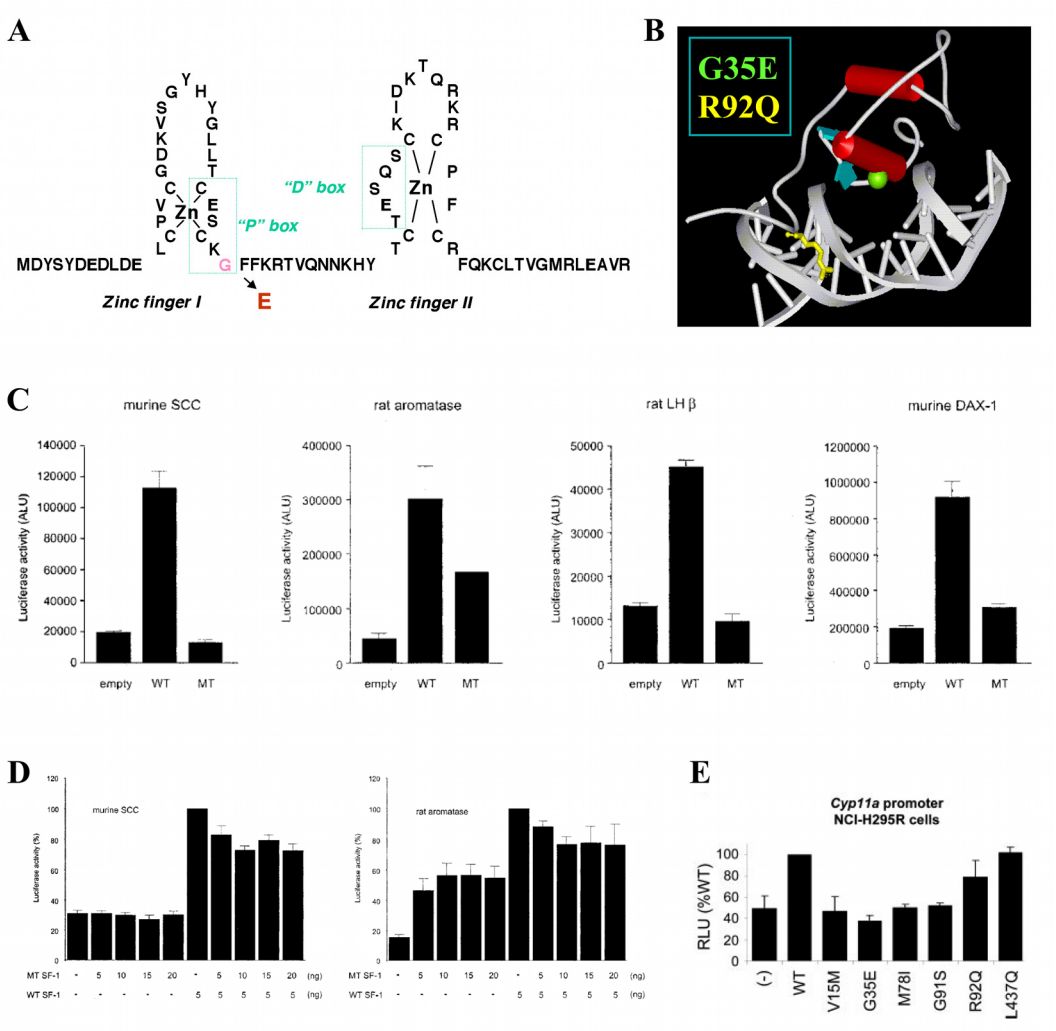

Figure 1.15. SF-1 mutations associated with adrenal failure and 46,XY DSD.

A, Amino acid structure of the zinc fingers of the DNA-binding domain of SF-1 showing the glycine residue altered by the G35E mutation. B, Model of the SF-1 DBD bound to DNA based on the crystal structure of NGFI-B. The glycine at amino acid 35 (green) of the P box forms the primary DNA-binding interface with the major groove of DNA and heterozygous disruption of this residue led to a severe phenotype. In contrast, the arginine at amino acid 92 (yellow) lies within the stabilising A box. Homozygous disruption of this residue (R92Q) led to the severe adrenogonadal phenotype. C, Effect of the G35E mutant on SF-1-responsive promoters, studied in tsA201 cells. Activation of the minimal promoters of murine cholesterol side-chain cleavage enzyme (SCC, *Cyp11a1*), rat *LHβ* and murine *DAX-1* (*Nr0b1*) was lost when the G35E mutant (MT) was tested. However, G35E SF-1 could partially activate the rat aromatase (*Cyp19*) promoter. D, A clear dominant negative effect of the G35E mutant was not seen on the activation of *Cyp11a1* and *Cyp19* promoter constructs by WT SF-1, but some partial reduction in overall transactivation was seen (tsA201 cells). E, The G35E mutant also failed to activate the *Cyp11a1* promoter in NCI-H295R adrenocortical cells, while partial activation by R92Q was seen. RLU, relative luciferase activity. From Achermann et al., 1999 (A), reprinted by permission from Macmillan Publishers Ltd.; Achermann et al., 2002 (B), copyright 2002, The Endocrine Society; Ito et al., 2000 (C and D), © the American Society for Biochemistry and Molecular Biology; and Lin et al., 2007 (E), copyright 2007, The Endocrine Society.

Understanding the exact biological effect of this mutation has proved challenging. Most *in vitro* studies have shown dramatically impaired DNA-binding and gene transactivation, leading to near complete failure to activate target promoter sequences (Figure 1.15) (Achermann et al., 1999; Ito et al., 2000; Lin et al., 2007). Nevertheless, these effects are to some degree variable as the G35E mutant SF-1 binds to and partly activates (50% of wild type) promoters containing 5'-CCAAGGTCA-3' sequences (for example, rat aromatase) (Ito et al., 2000). Although no clear dominant-negative function could be demonstrated (as might be expected given monomeric binding by SF-1), the G35E mutation likely has some competitive effect on wild type receptor activity (possibly by squelching co-factors), thus producing a dosage-dependent reduction of wild type SF-1-mediated transactivation (Figure 1.15) (Ito et al., 2000). In addition, some dominant negative effects have been seen in *in vitro* systems involving SF-1 synergistic activation with other transcription factors such as GATA binding protein 4 (GATA4) (Tremblay and Viger, 2003). Both these mechanisms would reduce the functional effects of the wild type allele. Therefore, the phenotype may be the result of reduced SF-1 transactivation on multiple targets throughout the genome and at different stages of development.

The concept of dose-dependent action of SF-1 was reinforced by the second report of a SF-1 mutation in a 46,XY individual in 2002 (Achermann et al., 2002). A 46,XY female with adrenal insufficiency was found to have a milder loss-of-function homozygous mutation (R92Q) in the A box region of SF-1 (Figure 1.15). As described above, the A box is involved in stabilising binding by monomeric nuclear receptors. Functional studies showed that this mutant only partially reduced SF-1 activity to about 40%, although variable activation of different promoters was seen.

Since this region is a secondary DNA-binding domain, it was believed that a homozygous change affecting both alleles was necessary for the full expression of the phenotype observed in this patient. Of note, three heterozygous relatives (both parents and a sibling) were clinically normal, with no evidence of adrenal insufficiency or reproductive dysfunction.

The only other report of a SF-1 mutation associated with an adrenal insufficiency phenotype came in 2000: a 2-yr old 46,XX girl who presented with primary adrenal failure but apparently normal ovarian function harboured a heterozygous mutation (R255L) in exon 4 of *NR5A1* (Biason-Lauber and Schoenle, 2000). It remains to be seen whether this patient will have sufficient ovarian function for normal pubertal development and folliculogenesis, since SF-1 expression and activity normally increases at puberty.

In contrast to the relatively small number of SF-1 mutations reported in association with adrenal failure, heterozygous SF-1 mutations have emerged as a relatively frequent finding in individuals with 46,XY disorders of sex development (DSD) *without* adrenal insufficiency (Figure 1.16) (Correa et al., 2004; Mallet et al., 2004; Hasegawa et al., 2004; Lin et al., 2007; Coutant et al., 2007; Reuter et al., 2007; Kohler et al., 2008). The majority of these cases presented with ambiguous genitalia at birth, a urogenital sinus, small inguinal testes and absent or rudimentary Mullerian structures, however less severe cases of 46,XY patients with hypospadias and small testes have also been reported (Lin et al., 2007; Kohler et al., 2009). Additionally, a link has been suggested between the common SF-1 polymorphism G146A with micropenis and cryptorchidism (Wada et al., 2005; Wada et al., 2006).

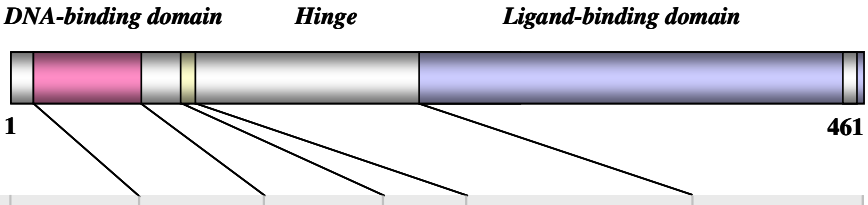

46,XY DSD with AI		**G35E**		**R92Q**		
46,XX with AI						**R255L**
46,XY DSD	**M1I** **M1V** **c.18delC**	**V15M** **C16X** **C33S** ***R39P*** **V41G** **c.151delG**	**M78I** **R84H** **R84H***	**G91S**	**c.369insC** **c.390delG** **Y138X** **c.424_427dup CCCA*** **c.536delC** **Y183X** **c.666delC**	**W279X** **c.1058_1065 AGCTGGTG** ***D380Y*** **c.1277dupT**
Severe penoscrotal hypospadias with cryptorchidism	**E11X** **c.103-3C>A**				**Q107X** **Y183X**	**W279X** **L437Q**
Bilateral anorchia with microphallus						**V355M**
Male factor infertility					**G123A + P129L** **P131L** **R191C** **G212S** **D238N**	
46, XX POI	**M1I**				**c.390delG** **Y183X** **c.666delC** **c.691_699del CTGCAGCTG**	**D293N**

Figure 1.16. Overview of reported changes in SF-1/*NR5A1* in humans.

The approximate location of the change within the predicted structure of SF-1 is shown. Yellow shaded areas represent changes found in 46,XX girls or women. Grey and white areas represent changes in individuals with a 46,XY karyotype. Underlined changes were detected in a homozygous state. All other changes were present in a heterozygous state. An asterisk denotes cases where the p.G146A polymorphism was also detected. The missense mutation shown in italics is predicted to disrupt function, but data from functional assays have not been reported. In addition, deletion of *NR5A1* on one allele has been reported as part of a contiguous gene deletion syndrome. AI, adrenal insufficiency; DSD, disorder of sex development, POI, primary ovarian insufficiency. From Ferraz-de-Souza et al., 2010a. Copyright 2010, with permission from Elsevier.

More recently, the spectrum of phenotypes associated with changes in SF-1 has considerably broadened. In 2009, SF-1 mutations impairing transcriptional activity were reported in 46,XX women with premature ovarian insufficiency (POI), either sporadic or within kindreds with a history of both 46,XY DSD and 46,XX POI (Lourenco et al., 2009). In 2010, mutations in SF-1 were reported in 4% of otherwise healthy infertile men with severe spermatogenic failure where the underlying cause was not found, suggesting that some forms of male infertility could indicate mild testicular dysgenesis (Bashamboo et al., 2010). While these findings need to be replicated in other settings, it is tempting to speculate that changes in SF-1 may have broad population implications in gonadal function and fertility.

The first three reported SF-1 mutations (Achermann et al., 1999; Biason-Lauber and Schoenle, 2000; Achermann et al., 2002) are important because they confirm that impaired SF-1 activity can result in adrenal failure in humans. Nevertheless, subsequent identification of individuals bearing SF-1 mutations has shown that adrenal involvement is not a common phenotypic feature, suggesting that, in humans, gonadal development and function are more sensitive to SF-1 dosage than the adrenal. This is in contrast with observations in mice, in which adrenal development seems to be more sensitive to insufficient Sf-1 dosage than gonadal development as shown by rescue of gonadal but not adrenal development by forced transgenic expression of Sf-1 in Sf-1-deficient mice (Fatchiyah et al., 2006; Val and Swain, 2010). Overall, substantial *in vivo* and *in vitro* data have shown that SF-1 is an essential regulator of the human adrenal gland. It can be hypothesised, therefore, that other factors – perhaps SF-1 targets themselves, as developmental regulatory systems can often be redundant – could compensate for SF-1 haploinsufficiency in the human adrenal gland.

1.4.5.2. Overactivity of SF-1

Given the critical role of SF-1 in regulating multiple stages of endocrine function, it could be conceived that small changes resulting in overexpression or overactivity of SF-1 could have important clinical effects. SF-1 *overexpression* could result from 1) genomic duplications of the chromosomal locus containing *NR5A1* resulting in biologically significant copy number variation (CNV), or from 2) up-regulation of *NR5A1* gene transcription due to increased promoter/enhancer activity or following decreased promoter methylation. Alternatively, *overactivity* of SF-1 could result from 1) increased protein stabilisation or reduced degradation, 2) loss of SUMOylation-dependent repression of transcriptional activity, or 3) specific changes in the structure of SF-1 that result in increased basal activity or increased affinity for native and/or alternative ligands (Ferraz-de-Souza et al., 2010a). Although no genomic activating changes in SF-1 have been described yet, several of these mechanisms are now being seen as potential causes or modifiers of human disease (Schimmer and White, 2010).

1.4.5.2.1. Adrenal tumorigenesis

Somatic duplications of 9q33 including *NR5A1* were originally described in 2005 in a cohort of children with adrenocortical tumours (ACTs) from Southern Brazil (Figueiredo et al., 2005). These changes occurred largely on the background of loss of heterozygosity for the tumour suppressor gene p53 (TP53). Increased *NR5A1* expression was subsequently confirmed in an independent study of ACTs, with a higher number of paediatric tumours showing *NR5A1* overexpression compared to adult tumours (Almeida et al., 2010). Notably, increased nuclear SF-1 protein expression was seen in many cases, sometimes independently of detectable *NR5A1*

gene expression. This finding has been supported by recent data from analysis of a large cohort of adult ACTs, which has shown a correlation between higher SF-1 protein levels and worse prognosis (Sbiera et al., 2010).

A role for SF-1 in human adrenocortical tumorigenesis is largely supported by studies in mice and in adrenal cell lines. SF-1 overexpression increases proliferation and decreases apoptosis of human adrenocortical cells, and can induce adrenocortical tumours in transgenic mice (Doghman et al., 2007). Furthermore, SF-1 inverse agonists have been shown to inhibit adrenocortical carcinoma cell proliferation *in vitro* (Doghman et al., 2009). Not much is known about specific molecular mechanisms through which SF-1 may promote cell proliferation and tumorigenesis. The fetal and adult testis expressed 1 protein (FATE1), which has been implicated in hepatocellular carcinoma and other tumours, was shown to be a target of SF-1 in adrenocortical carcinoma cells and may be part of a specific subset of pro-tumourigenic SF-1 targets (Doghman et al., 2007).

1.4.5.2.2. Endometriosis

Finally, SF-1 has been implicated in the pathogenesis of endometriosis (Bulun et al., 2009). SF-1 has been shown to be expressed in endometriotic cells whereas it is not usually detected in normal endometrium (Xue et al., 2007). Part of this aberrant expression may be the result of hypomethylation of a CpG-rich region in its proximal promoter region with subsequent activation by upstream stimulatory factor 2 (USF2) (Xue et al., 2007; Utsunomiya et al., 2008). Alternatively, SF-1 activity in endometriotic tissue may be increased following stimulation of the GPR30 oestrogen receptor (Lin et al., 2009). Increased SF-1 expression or activity in endometriotic tissue could result in increased activity of STAR and aromatase, resulting in

increased local oestrogen synthesis, a key pathological feature of this condition (Utsunomiya et al., 2008).

1.5. Disorders of adrenal development

Disorders of adrenal development generally result in small, poorly functioning glands, a clinical condition termed “adrenal hypoplasia” (Lin and Achermann, 2004; Else and Hammer, 2005). These conditions are clinically important as they are hard to diagnose and are associated with considerable morbidity and mortality unless treated promptly. Furthermore, milder forms can present more insidiously in childhood or even in young adulthood where they can result in malaise or even death if not appropriately recognised (Guclu et al., 2010).

Several single gene disorders have been identified in recent years that can affect the hypothalamic-pituitary-adrenal (HPA) axis at different levels, and a genetic cause is found in approximately 50% of all individuals with congenital forms of adrenal hypoplasia. These conditions can be subdivided into: 1) *secondary adrenal hypoplasia* due to defects in ACTH synthesis, processing and release; 2) *ACTH resistance syndromes*; and 3) *primary adrenal hypoplasia* due to defects in the development of the adrenal gland itself (Figure 1.17, Table 1.3).

Of note, several other congenital conditions can also result in adrenal insufficiency, including relatively common steroidogenic defects causing congenital adrenal *hyperplasia* (e.g., 21-hydroxylase deficiency due to mutations in CYP21A2) and rarer degenerative metabolic (e.g., adrenoleukodystrophy, Smith-Lemli-Opitz syndrome) or immune disorders affecting the adrenals. These will not be discussed here as they do not represent adrenal hypoplasia *per se*.

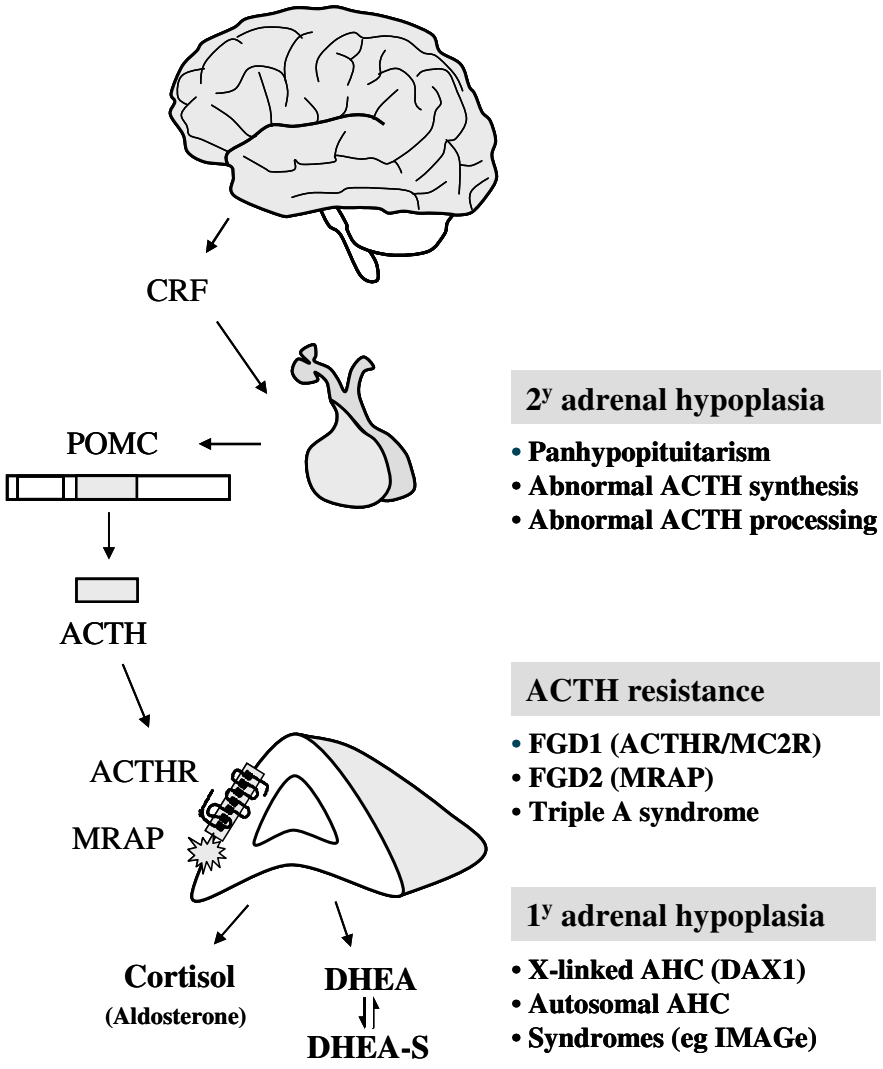

Figure 1.17. Overview of the hypothalamic-pituitary-adrenal (HPA) axis and different types of adrenal hypoplasia.

POMC, pro-opiomelanocortin; ACTH, adrenocorticotropin; DHEA, dehydroepiandrosterone; FGD, familial glucocorticoid deficiency; AHC, adrenal hypoplasia congenita. From Ferraz-de-Souza and Achermann, 2008. Reproduced with permission from S. Karger AG Basel.

Table 1.3. Overview of more common genetic causes of adrenal hypoplasia

Condition	Gene	ACTH	Cortisol	Aldo	Features
CPHD	*HESX1*	↓	↓	N	CPHD +/- SOD
	SOX3				CPHD
	LHX3				CPHD, skeletal[#], deafness
	LHX4				CPHD, cerebellar
	OTX2				CPHD, microphthalmia
	GLI2				CPHD, holoprosencephaly
	PROP1				CPHD
ACTH regulation	*TPIT*	↓	↓	N	-
	POMC				Obesity, red hair
	PC1				Obesity, hypoglyc, HH
FGD1	*MC2R*	↑	↓	N*	? Tall stature
FGD2	*MRAP*	↑	↓	N	?
Triple A	*AAAS*	↑	↓	N*	Achalasia, Alacrima Neurological
X-linked AHC	*NR0B1*	↑	↓	↓	HH, spermatogenesis
Autosomal	*NR5A1*	↑	↓	↓	46XY female, uterus
SERKAL	*WNT4*				46XX male, lung & kidney
IMAGe	nk	↑	↓	↓	IUGR, Metaphyseal dyspl., Genital hypoplasia

Aldo, aldosterone; CPHD, combined pituitary hormone deficiency; SOD, septo-optic dysplasia; ACTH, adrenocorticotropin; hypoglyc, hypoglycemia; HH, hypogonadotropic hypogonadism; N, within the normal range; FGD, familial glucocorticoid deficiency; AHC, adrenal hypoplasia congenita; nk, not known; IUGR, intrauterine growth restriction. [#]skeletal abnormalities associated with LHX3 mutations include short stiff neck, vertebral abnormalities, spinal stenosis, hyperextensible joints, and skeletal dysplasia; *mineralocorticoid insufficiency can occur in a number of cases of Triple A syndrome, and apparent hyponatraemia is seen rarely in FGD1. Updated from Ferraz-de-Souza and Achermann, 2008, with permission from S. Karger AG Basel.

1.5.1. Secondary Adrenal Hypoplasia

As discussed in section 1.3.5, ACTH is an important tropic stimulus to the adrenal gland during development. The mature ACTH peptide is cleaved from the larger precursor molecule, proopiomelanocortin (POMC), together with other small peptides such as β-endorphin and α- and β-melanocyte stimulating hormone (MSH) (Figures 1.17 and 1.18). Defects in ACTH synthesis, processing and/or release can result in secondary hypoplasia of the adrenal glands. Most children with these conditions present with signs and symptoms of glucocorticoid insufficiency (e.g. hypoglycaemia, prolonged jaundice, collapse). Salt-loss is extremely unusual as the main drive to adrenal aldosterone production, angiotensin II, is unaffected. Low serum concentrations of ACTH, the absence of hyperpigmentation and the presence of associated features (Table 1.3) can all help to point to the diagnosis of secondary adrenal hypoplasia rather than to ACTH resistance or a primary adrenal defect.

1.5.1.1. Combined pituitary hormone deficiencies (CPHD)

Several disorders of hypothalamo-pituitary development (e.g. septo-optic dysplasia, pituitary hypoplasia) or brain development (e.g. anencephaly) may be associated with impaired ACTH production as part of a combined pituitary hormone deficiency (CPHD) (Table 1.3). In most situations, growth hormone, thyroid stimulating hormone and gonadotropin (LH, FSH) release will also be affected, so that the child may have pronounced hypoglycaemia, signs of congenital hypogonadotropic hypogonadism (micropenis, undescended testes) or postnatal growth failure. Other neurodevelopmental defects such as absent septum pellucidum or optic nerve hypoplasia may be present.

A number of single gene disorders causing congenital hypopituitarism (CPHD) have been reported (Kelberman and Dattani, 2006; Kelberman et al., 2009). In brief, deletions, mutations or copy-number changes in the transcription factors HESX1 (MIM 601802), SOX3 (MIM 313430), LHX3 (MIM 600577), LHX4 (MIM 602146), OTX2 (MIM 600037), GLI2 (MIM 165230) and PROP1 (MIM 601538) can all cause ACTH insufficiency as part of a defect in pituitary development. In some cases, and with special regard to mutations in PROP1, ACTH insufficiency may not be present at the original time of diagnosis but may develop progressively with time. Additional features may be present which can help to focus the molecular diagnosis (Table 1.3).

1.5.1.2. Isolated ACTH deficiency

Isolated ACTH insufficiency is a rare condition that can be caused by recessively-inherited mutations in the T-box factor TPIT (TBX19, MIM 604614) (Lamolet et al., 2001, Pulichino et al., 2003). TPIT regulates the transcription of *POMC* specifically in corticotropes (Figure 1.18). Impaired TPIT function in these cells results in impaired synthesis of POMC and ACTH in the pituitary, whereas regulation of POMC synthesis in other cells (e.g. skin, hypothalamus) is unaffected. Thus, patients with *TPIT* mutations usually present with severe, early-onset isolated ACTH insufficiency. Hypoglycaemia and prolonged jaundice are common, and sudden neonatal death is reported (Vallette-Kasic et al., 2005).

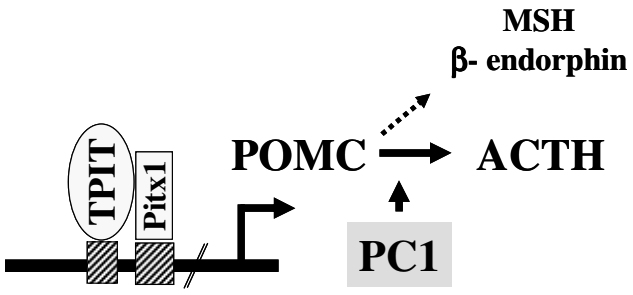

Figure 1.18. POMC synthesis and cleavage in the corticotrope.
Major events are shown. POMC, pro-opiomelanocortin; PC1, prohormone convertase 1. From Ferraz-de-Souza and Achermann, 2008. Reproduced with permission from S. Karger AG Basel.

1.5.1.3. Disorders in POMC synthesis and release

As shown in Figure 1.18, the mature ACTH peptide is cleaved from POMC together with other small peptides such as melanocyte stimulating hormone (MSH) and β-endorphin. These peptides play a crucial role in appetite regulation and weight, as well as pigmentation of the skin and hair. Therefore, mutations in POMC (MIM 176830) have more widespread consequences and are associated with pale skin, red hair and obesity in addition to ACTH deficiency (Krude et al., 1998). These cutaneous features may be less marked in individuals with dark hair, and may diminish with age (Krude et al., 2003).

Finally, processing of POMC into the mature ACTH peptide requires the actions of the cleavage enzyme prohormone convertase-1 (PC1, *PCSK1*, MIM 162150). Abnormalities in ACTH processing due to defects in PC1 can cause secondary adrenal failure in rare cases (Jackson et al., 1997). As the processing of several other peptide hormones is disrupted, associated features include obesity, hypogonadism, hypoglycaemia and persistent malabsorptive diarrhoea (Jackson et al., 2003).

1.5.2. ACTH resistance syndromes

ACTH tropic effect on adrenal development is mediated via the melanocortin 2 receptor (MC2R, ACTH receptor) and subsequent downstream signalling pathways. Abnormalities in these signalling processes result in adrenal hypoplasia due to ACTH resistance.

1.5.2.1. Triple-A syndrome

Triple-A syndrome (Achalasia-Addisonianism-Alacrima syndrome, Allgrove syndrome, MIM 231550) is a rare autosomal recessive disorder characterised by ACTH-resistant adrenal failure, alacrima, achalasia of the oesophageal cardia and progressive central, peripheral and autonomic neurological defects (Clark and Weber, 1998). Isolated glucocorticoid deficiency is seen in 80% of the cases, while additional mineralocorticoid deficiency is reported in 15%. Histologically, the adrenal glands have preserved zona glomerulosa with atrophic zonae fasciculata and reticularis. Following the mapping of the disease locus to 12q13, mutations in the gene *AAAS* (MIM 605378) have been identified in individuals with triple-A syndrome (Tullio-Pelet et al., 2000), and seem to occur in 82% of patients (Storr et al., 2009). The protein encoded by AAAS was termed ALADIN and contains a WD repeat domain, indicating that it may be involved in protein-protein interactions and/or associated with the assembly of nuclear pore complexes. Recently, the ferritin heavy chain protein was reported to interact with ALADIN, suggesting a role in protection from oxidative damage (Storr et al., 2009). Nevertheless, the exact function of ALADIN and the mechanisms of this heterogeneous disorder, especially with regard to the ACTH-resistant adrenal phenotype, remain largely unknown.

1.5.2.2. Familial glucocorticoid deficiency

Familial glucocorticoid deficiency (FGD) is a rare autosomal recessive disorder characterised by early onset severe cortisol deficiency, high plasma ACTH and, typically, normal mineralocorticoid levels (Clark and Weber, 1998). Symptoms of glucocorticoid deficiency such as hypoglycaemia and failure to thrive usually appear in the neonatal period or early childhood. Hyperpigmentation, due to ACTH stimulation of MC1R in the skin, usually develops by 6 weeks of life.

Following the cloning of *MC2R* (MIM 607397) in the early 1990s, more than 35 mutations in this gene have been identified in patients with FGD (Clark et al., 1993; Cooray et al., 2008). Identified mutations are scattered throughout the protein, affecting ligand binding, the transmembrane domain or signal transduction. Nevertheless, mutations in *MC2R* were only found in approximately 25% of patients with FGD, implying that this was a genetically heterogeneous disorder. Therefore, cases of FGD with MC2R defects were categorised as FGD type 1. Notably, the clinical presentation of patients with or without *MC2R* mutations did not differ, except for the observation of tall stature in those with MC2R defects (Clark and Weber, 1998)

With the advent of high throughput techniques in 2000s, another molecular defect was identified in FGD cases without MC2R defects. SNP-array genotyping of a family with three affected siblings revealed a candidate region at 21q22.1, and only one out of 30 known or predicted genes in the region was expressed in the human adrenal (Metherell et al., 2005). This gene encoded a novel single transmembrane domain protein termed melanocortin 2 receptor accessory protein (MRAP, MIM 609196), involved with trafficking MC2R from the endoplasmic reticulum to the cell

membrane. In the original study, mutations in *MRAP* were found in 25 out of 100 investigated FGD cases, leading to their categorisation as FGD type 2.

Taken together, a molecular etiology can currently be determined to approximately 45% of cases of FGD. It has recently been proposed that a subgroup of the remaining unexplained cases could be due to a nonclassic presentation of STAR defects masquerading as 'FGD type 3' (Baker et al., 2006; Metherell et al., 2009).

1.5.3. Primary adrenal hypoplasia

Adrenal hypoplasia congenita (AHC), also known as congenital adrenal hypoplasia, is a disorder of adrenal development resulting in primary adrenal insufficiency. Neonates usually present with hypoglycaemia or collapsed with a salt-losing crisis and unless the diagnosis is considered and appropriate treatment given, mortality and morbidity are high. This condition can also present in older children, more insidiously and is often precipitated by infection or stress. In all cases, steroid replacement is required for life and increased doses of steroids are required during stress to prevent adrenal crises.

The true incidence of AHC is not currently known. It is often quoted as being 1:12,500 births, following the 13-yr study of infant autopsies at the Royal Women's Hospital, Melbourne, Australia (1959 –1971) (Laverty et al., 1973). However, 7 out of the 11 cases identified in that series were anencephalic, precluding the assertion of primary adrenal hypoplasia. Considering only the remaining 4 cases (1 cytomegalic, 3 "miniature"), an incidence of around 1:37,000 births could be grossly estimated. Recently, Perry and colleagues reported a 20-year review of primary adrenal insufficiency in children (0-18 yr) presenting to Sainte-Justine Hospital, Montreal (1981–2001) (Perry et al., 2005). In that cohort, 7 out of 103 cases of primary

adrenal insufficiency identified could be interpreted as AHC (1 X-linked AHC, 6 unexplained cases of primary adrenal insufficiency). Congenital adrenal hyperplasia was diagnosed in 74 of 103 children and had an estimated populational incidence of 1:16,630, allowing an extrapolation that AHC might occur at approximately 1:176,000 children. However, it is likely that the incidence is underestimated as many children with this condition might die without the specific diagnosis being made.

Primary adrenal hypoplasia is classified into *i*) an X-linked form (due to mutations in DAX1), *ii*) a poorly understood autosomal form (occasionally due to mutations in SF-1), or *iii*) forms associated with syndromes, sometimes of unknown etiology. Recent data by Lin and colleagues on the analysis of DAX1 and SF-1 in 120 patients referred with adrenal hypoplasia show that currently a specific molecular diagnosis can only be reached in approximately 33% of cases (Lin et al., 2006).

1.5.3.1. X-linked adrenal hypoplasia

X-linked adrenal hypoplasia congenita (AHC) results from mutations in the nuclear receptor DAX1 (*NR0B1*), as discussed in section 1.3.4. This condition is the most common form of primary adrenal hypoplasia reported to date (Phelan and McCabe, 2001; Lin et al., 2006). X-linked AHC was probably first described in 1948 in an infant who died at 33 days of age with hyperpigmentation and small adrenal glands. The presence of some "cytomegalic" cells typical of fetal-zone adrenal tissue led to this condition being termed "cytomegalic adrenal hypoplasia". The X-linked pattern of inheritance of AHC became apparent in the 1960s and an association with hypogonadotropic hypogonadism was described as boys who received steroid

treatment did not progress through puberty. Details of the discovery of DAX1 and its function have been previously discussed (section 1.3.4).

X-linked AHC due to *DAX1* mutations is characterized by: 1) primary adrenal insufficiency; 2) hypogonadotropic hypogonadism; and 3) a likely primary defect in spermatogenesis. Boys tend to present with salt-losing adrenal failure in the first two months of life (60-70%) or more insidiously with adrenal failure throughout childhood (30-40%) (Reutens et al., 1999; Lin et al., 2006). Isolated mineralocorticoid deficiency may be the presenting feature in some cases and cortisol levels may appear normal initially; however, glucocorticoid deficiency usually develops with time (Wiltshire et al., 2001; Verrijn Stuart et al., 2007). Absent or arrested puberty due to a combined hypothalamic and pituitary defect typically occurs during adolescence. However, several reports of limited testicular enlargement or signs of premature sexual maturation in childhood have been published (Domenice et al., 2001; Ahmad et al., 2007). In a recent analysis of 64 boys with AHC, *DAX1* mutations were found in all individuals with primary adrenal failure, abnormal puberty and a family history of adrenal disease in males (8/8, 100%), but also in approximately 40% of a cohort of prepubertal boys with no family history of note, making mutations in *DAX1* the most commonly achieved molecular diagnosis in AHC (Lin et al., 2006).

Initial case reports of X-linked AHC were understandably biased to reporting individuals with contiguous gene deletion syndromes. Following the identification of *DAX1* as the gene responsible for this condition, more than 100 different *DAX1* mutations have been reported in more than 200 individuals and families with X-linked AHC. An analysis of 37 cases of X-linked AHC from a single centre accumulated during a 10 yr-period has shown isolated DAX1 gene deletions in 8

(22%) cases, contiguous gene deletions in 2 (5%) cases, and point mutations in the rest (nonsense, 7 [19%]; frameshift, 12 [32%]; missense, 8 [22%]) (Figure 1.19) (Lin et al., 2006). Missense mutations tend to cluster within certain regions of the ligand-like binding domain, but rare amino-terminal missense mutations have been described (Figure 1.19) (Verrijn Stuart et al., 2007). These point changes may interfere with nuclear localisation as well as affecting protein-protein interaction (Lehmann et al., 2003). Nonsense and frameshift mutations are located throughout the gene and loss of the carboxy-terminal region of the protein (containing the AF-2 domain) is sufficient for complete loss of protein function in most cases (Figure 1.19).

In addition to the phenotypes described above, atypical phenotypes have now been described in association with *DAX1* mutations. A delayed-onset form of X-linked AHC has been described in men who presented between 20-30 years of age with mild primary adrenal insufficiency or partial hypogonadism (Guclu et al., 2010). Some of these patients harbour missense mutations (I439S, Y380D) that have limited DAX1 function (Figure 1.19) (Tabarin et al., 2000; Mantovani et al., 2002). Finally, skewed X-inactivation may result in delayed puberty or even primary adrenal failure in girls or women who have heterozygous DAX1 changes (Shaikh et al., 2008).

Despite the significant number of DAX1 mutations described, the exact molecular pathogenesis of X-linked AHC remains unclear, as discussed in section 1.3.4.

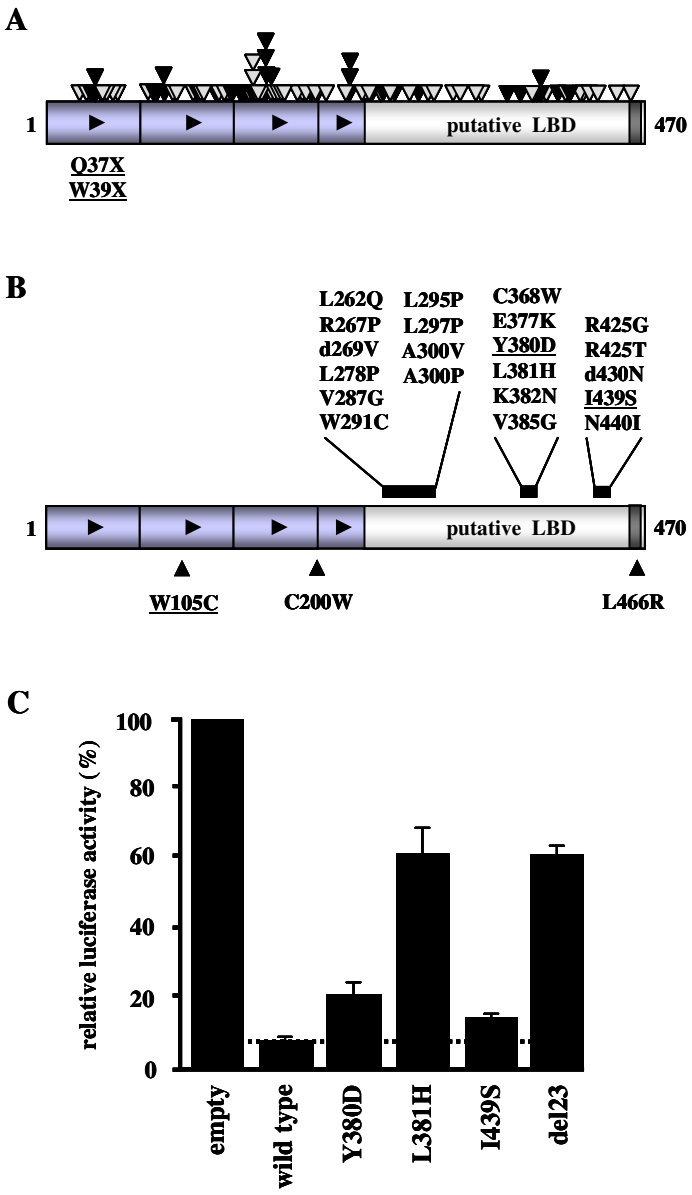

Figure 1.19. Overview of human mutations in DAX1/*NR0B1*.

A, Selected frameshift (grey arrowheads) and nonsense (black arrowheads) mutations found in individuals with X-linked adrenal hypoplasia congenita. B, Missense mutations in DAX1 tend to cluster within certain regions of the carboxyl terminus of DAX1 (black bars). Those changes associated with variant or late-onset phenotypes are underlined. C, Functional assay of DAX1 as a repressor of gene transcription. Wild type (WT) DAX1 represses luciferase activity in this *in vitro* assay compared to empty vector. Point mutations associated with a classic X-linked AHC phenotype (L381H, del23 amino acids from the carboxyl terminus) cause loss of function, whereas those changes associated with a delayed-onset adrenal failure (Y380D, I439S) have partial loss of function. From Ferraz-de-Souza and Achermann, 2008. Reproduced with permission from S. Karger AG Basel.

1.5.3.2. Autosomal adrenal hypoplasia

The molecular basis of autosomal forms of adrenal hypoplasia remains poorly understood. Rare heterozygous or homozygous mutations in SF-1 (*NR5A1*) have been reported in 46,XY phenotypic females with either spontaneous or recessively inherited primary adrenal failure, and a heterozygous SF-1 mutation has been described in a 46,XX girl with adrenal dysfunction (section 1.4.5.1). However, SF-1 mutations have not been found in phenotypic males with adrenal hypoplasia (Lin et al., 2006).

Although most steroidogenic defects present with adrenal hyperplasia, some forms have been described presenting with adrenal insufficiency due to hypoplastic glands. For example, mutations in *CYP11A1* were initially described in association with congenital lipoid adrenal hyperplasia (Tajima et al., 2001), but have been subsequently identified in a few patients without identifiable adrenal glands on imaging (Kim et al., 2008). Additionally, as discussed above, a subgroup of patients with STAR defects may have a nonclassic presentation mimicking ACTH resistance. Although mutations in *STAR* are classically associated with large lipid-filled glands (congenital lipoid adrenal hyperplasia), normal sized or even small glands have been reported (Baker et al., 2006; Metherell et al., 2009). Despite this progress, it is likely that other autosomal genes are responsible for rare recessive forms of adrenal hypoplasia as a substantial proportion of cases of AHC remain without a molecular diagnosis.

1.5.4. Syndromic forms of adrenal hypoplasia

Adrenal hypoplasia has been rarely described in association with congenital syndromes and, in most cases, the discrimination between primary *versus* secondary hypoplasia is challenging.

As discussed in section 1.3.2, adrenal absence is a rare feature of Pallister-Hall syndrome (PHS) caused by mutations in *GLI3*. Indeed, in the largest PHS cohort reported to date, only 2 out of 27 patients with extended PHS phenotypes had adrenal hypoplasia (Johnston et al., 2010). Concomitant absence of pituitary and adrenal glands in these patients precluded the identification of a direct action of GLI3 in human adrenal development. Therefore, the role of GLI3 in human adrenal development remains obscure, and the occurrence of adrenal hypoplasia as a feature of PHS seems to be very rare.

A few syndromes with unknown or poorly characterised gene defects have also been associated with adrenal hypoplasia or hypofunction, frequently in association with CNS defects (Else and Hammer, 2005). For example, two cases of Pena-Shokeir type I syndrome (Feta akinesia deformation sequence, FADS, MIM 208150) have been reported with miniature adrenal glands and grossly normal brain and pituitary (Moerman et al., 1983). However, considering that adrenal hypoplasia was not seen in several other cases and in view of the prominent neurological phenotype, the authors themselves hypothesised that the adrenal hypoplasia could be secondary to undetected CNS defects. Similarly, adrenal hypoplasia has been reported in rare cases of Galloway-Mowat syndrome (MIM 251300), Meckel syndrome (MIM 249000), hydrolethalus syndrome (MIM 236680), and pseudo-trisomy 13

(holoprosencephaly-polydactyly with normal karyotype, MIM 264480), all of which include CNS defects amongst phenotypic features (Else and Hammer, 2005).

Recently, the autosomal recessive SERKAL syndrome was described based on the analysis of four individuals belonging to a consanguineous kindred of Arab Muslim origin, presenting with 46,XX sex reversal and dysgenesis of kidneys, adrenals and lungs (Mandel et al., 2008). Within affected individuals, the adrenal glands were either not identified or exceedingly small but with apparently normal morphology. A causative homozygous null mutation was identified in the developmental regulator WNT4, a member of the wingless-type MMTV integration site family of secreted glycoproteins (MIM 603490). Notably, mutations in *WNT4* have been more frequently associated with mullerian aplasia and hyperandrogenism in females (Biason-Lauber et al., 2004). No further cases of SERKAL syndrome have yet been described, and although Wnt/β-catenin signalling has been implicated in adrenal development from studies in mice, the role of WNT4 in human adrenal development remains unclear.

The most well-defined syndromic association of primary adrenal hypoplasia is the IMAGe syndrome (Intrauterine growth retardation [IUGR], Metaphyseal dysplasia, Adrenal hypoplasia congenita and Genital anomalies, MIM 300290). This syndrome was described in 1999 by Vilain and colleagues based on the observation of three boys with primary adrenal hypoplasia and similar additional features (Vilain et al., 1999). These patients presented shortly after birth with growth retardation and severe adrenocortical insufficiency accompanied by metaphyseal dysplasia, with or without epiphyseal dysplasia and associated soft tissue calcifications, and genital abnormalities such as bilateral cryptorchidism and small phallus. High resolution karyotypes were normal, and mutations of DAX1 or SF-1 were excluded. In 2005,

Bergada and colleagues reported four cases (three male, one female) from a five-generation pedigree in Argentina that suggested inheritance through the maternal line, leading to the hypothesis that genomic imprinting of an autosomal gene might underlie the molecular basis of IMAGe syndrome (Bergada et al., 2005). The main feature in these cases was IUGR, with a seemingly variable degree of adrenal insufficiency. Indeed, another reported IMAGe patient presented with late-onset adrenal insufficiency at 4.6 years of age (Pedreira et al., 2004), suggesting that, albeit a constant feature of the syndrome, adrenal hypoplasia may present to variable degrees. Post-mortem findings in a reported female IMAGe patient included tiny adrenals, with histological features resembling cytomegalic adrenal hypoplasia due to DAX1 mutations, and a small anterior pituitary (Tan et al., 2006). Interestingly, an affected sibling of this patient presented with hypocortisolemia and very high ACTH at the first day of life, suggesting a primary adrenal defect. The underlying aetiology of this condition remains unknown.

1.6. Hypothesis and Aims

Despite recent advances and studies in the mouse, many aspects of human adrenal development are still poorly understood. Indeed, a better understanding of human adrenal development might provide more candidate genes for unexplained cases of primary adrenal hypoplasia. Steroidogenic factor-1 is a master regulator of adrenal and reproductive biology, expressed early in human adrenal development and associated with impaired adrenal function if disrupted. SF-1 regulates transcription of several genes involved in adrenal development and steroidogenesis, and defects in many of these genes have been associated with disorders of adrenal development and function.

Hypothesis:

Identification of novel SF-1 targets in the human adrenal could unravel important mechanisms in adrenal development and disease.

Aim I

Characterisation of candidate targets from animal models, *CITED2* and *PBX1*, in a human cell-based assay system;

Aim II

Genome-wide identification of SF-1-binding sites through chromatin immunoprecipitation microarrays (ChIP-on-chip) in human adrenal cells;

Aim III

Analysis of global gene expression induced by SF-1 overexpression in adrenal cells aiming to identify novel targets likely to be involved in human adrenal disorders.

CHAPTER 2

MATERIALS AND METHODS

2.1. Materials

2.1.1. Laboratory equipment and reagents

Laboratory equipment used is detailed in Appendix 1. Glassware was obtained from Schott Glass, UK, plasticware from VWR International, UK, and general reagents were obtained from Sigma-Aldrich, UK, or Thermo Fisher Scientific, UK.

Full project risk assessments were undertaken and approved by the Institute Safety Officer.

2.1.2. Laboratory water

Unless otherwise stated, grade 1 water (British Standards Institution, 1995) was used throughout, obtained from a Milli-Q Academic water purification system with Q-Gard 1 purification pack and Quantum EX cartridge filter (all from Millipore UK Ltd., UK). Grade 3 water, obtained from a RiOs 16 system (Millipore), was used for feeding the Milli-Q ultrapure system and waterbaths, and for glassware rinsing.

Nuclease-free water (Thermo Fisher Scientific) was used in all experiments involving RNA samples.

2.1.3. Biological samples

2.1.3.1. Human embryonic tissue samples

Human embryonic tissue samples (anonymised) were provided by the Medical Research Council/Wellcome Trust-funded Human Developmental Biology Resource (HDBR, www.hdbr.org) with Research Ethics Committee approval and informed consent.

2.1.3.2. DNA samples

Patient DNA samples were collected by Dr John Achermann with informed consent and ethical approval, and stored at -20°C. Samples were pseudo-anonymised and encoded. Genomic DNA samples were either obtained by extraction from blood samples at the Regional Molecular Genetics Laboratory, Great Ormond Street Hospital for Children NHS Trust, or sent by collaborators.

Control DNA panels were acquired from the Health Protection Agency Culture Collections (www.hpacultures.org.uk). The Human Random Control DNA panel set consists of DNA samples from a control population of 480 randomly selected, non-related UK Caucasian blood donors, collected in Oxford and Birmingham. Peripheral blood lymphocytes from donors were Epstein Barr Virus-transformed to generate lymphoblastoid cell lines from which DNA is extracted and made available in 2 μg aliquots in five 96-well plates.

2.1.4. Plasmid vectors

Available maps of vector backbones are provided in Appendix 2. All vectors, bacteria and cells used were registered with the UCL Institute of Child Health Genetic Modification Safety Committee and their used in these studies was approved.

2.1.4.1. pCMX expression vector

The pCMX expression vector was constructed at the Evans laboratory at the Salk Institute for Biological Studies, California, USA, by modifying and fusing pCDM8 (Seed, 1987) and pUC19, so that a multiple cloning site lies downstream of the CMV/T7 promoter and the ampicillin resistance gene from pUC19 is retained

(Umesono et al., 1991). This was used with permission of Dr. Ronald M. Evans. pCMX constructs bearing the entire coding region of human SF-1 (Wong et al., 1996) and DAX1 (Ito et al., 1997) were generated at the Jameson laboratory at Northwestern University Medical School, Illinois, USA. The G35E mutation in SF-1 (Achermann et al., 1999) and the R267P, A300P and I439S mutations in DAX1 (Tabarin et al., 2000) were introduced by site-directed mutagenesis also at the Jameson laboratory. All pCMX constructs were kindly provided by Dr J. Larry Jameson.

2.1.4.2. pGL4.10[*luc2*] luciferase reporter vector

The pGL4.10[*luc2*] luciferase reporter vector, bearing the synthetic firefly *luc2* (from *Photinus pyralis*) and *bla* (β-lactamase for ampicillin resistance) genes, was acquired from Promega, UK. This is a basic reporter vector lacking eukaryotic promoter and enhancer sequences, and, therefore, firefly luciferase expression is dependent on the functionality of DNA fragments inserted into the multiple cloning region. The protocol used for cloning promoter regions into this vector will be detailed in section 2.2.18.

2.1.4.3. pRL-SV40 *Renilla* luciferase reporter vector

The pRL-SV40 *Renilla* luciferase reporter vector (Promega), bearing the simian virus 40 (SV40) enhancer and early promoter elements providing high-level expression of *Renilla* (*Renilla reniformis*, also known as sea pansy) luciferase in co-transfected cells, was used as an internal control reporter. This vector confers ampicillin resistance to transformed bacterial cells.

2.1.4.4. pIRES2-AcGFP1-Nuc bicistronic expression vector

The pIRES2 AcGFP1-Nuc vector was obtained from Clontech-Takara Bio Europe, France. In this vector, the multiple cloning site (MCS) lies downstream of the immediate early promoter of human cytomegalovirus ($P_{CMV\ IE}$) and upstream of the internal ribosome entry site (IRES) element of the encephalomyocarditis virus (ECMV) (Jang et al., 1988; Jackson et al., 1990). Immediately downstream of the IRES lies the coding sequence of *Aequorea coerulescens* green fluorescent protein (AcGFP1) fused to three copies of the nuclear localisation signal of the SV40 large T-antigen, directing AcGFP1 into the nucleus of mammalian cells. The IRES sequence permits both the gene of interest, cloned into the MCS, and the AcGFP1-Nuc gene to be translated from a single bicistronic mRNA. This plasmid confers kanamycin resistance to *E. coli* hosts. Constructs generated from pIRES2-AcGFP1-Nuc were used for SF-1 overexpression experiments (Chapter 5).

2.2. Methods

2.2.1. Cell culture

All procedures involving cell culture were performed in aseptic conditions in a Class II biological safety cabinet. Cells were maintained at 37°C in a humidified atmosphere of 95% air, 5% carbon dioxide, and biological material was treated with Virkon (DuPont, UK) prior to disposal.

2.2.1.1. Cell lines

2.2.1.1.1. tsA201 transformed human embryonic kidney cells

Human embryonic kidney cells (HEK 293) (Graham et al., 1977) transformed to stably express an SV40 temperature-sensitive T antigen (known as tsA201) were obtained from the European Collection of Cell Cultures (ECACC; Health Protection Agency Culture Collections). These cells are highly transfectable and were used for the standardisation of luciferase assays.

2.2.1.1.2. NCI-H295R human adrenocortical carcinoma cells

In 1990, Gazdar and colleagues reported establishing the NCI-H295 cell line from an invasive primary adrenocortical carcinoma (Gazdar et al., 1990). The tumour had been excised from a 48-year-old African-American female patient presenting with a large invasive right adrenal mass (14 x 13 x 11 cm) and clinical and biochemical features of hypersecretion of corticosteroids, mineralocorticoids and adrenal androgens. Malignancy was confirmed by a plethora of histological features and by tumour recurrence with pulmonary metastases. After 7 to 10 years in culture, cultured cells retained steroidogenic capacity and secreted a broad spectrum of steroid products, from all three classes of adrenal steroids, suggesting pluripotency with regard to adrenocortical differentiation (Rainey et al., 1994).

Since H295 cells grow in suspension or in loosely attached patches and have long population doubling time, substrains with better substrate attachment and shorter cell cycle were sought through the manipulation of cell medium. Initially obtained through supplementation with a bovine derived serum substitute to increase cell growth rate, the substrain NCI-H295R grows in a monolayer, attached to the culture dish, and retains full steroidogenic capability (Rainey et al., 1994, Rainey et al.,

2004). This substrain is available from the American Type Culture Collection (ATCC) and has been extensively used as an adrenocortical model system. NCI-H295R cells express all genes involved in adrenal steroidogenesis and produce, in basal conditions, mineralocorticoids, glucocorticoids and adrenal androgens in a pattern that closely resembles parental H295 cells (Samandari et al., 2007).

NCI-H295R cells were, therefore, selected as an appropriate immortalised steroidogenic adrenal cell model for performing SF-1 ChIP-on-chip, analysis of gene expression following SF-1 overexpression and luciferase assays, and were obtained from the ATCC (catalogue number CRL-2128, deposited by Dr. William E. Rainey).

2.2.1.2. Media, supplements and reagents

- DMEM: Dulbecco's Modified Eagle's Medium with L-glutamine, 4500 mg/l D-glucose and 110 mg/l sodium pyruvate (GIBCO/Invitrogen, UK);
- DMEM:F12: 1:1 mixture of DMEM and Ham's F12 nutrient (GIBCO/Invitrogen);
- RPMI 1640: Roswell Park Memorial Institute medium 1640 (GIBCO/Invitrogen);
- FBS: Fetal bovine serum (Sigma-Aldrich);
- P/S: Stabilized solution of penicillin (10,000 U/ml) and streptomycin (10 mg/ml) (Sigma-Aldrich);
- ITS+ Premix: Supplement of human recombinant insulin (12.5 mg), human transferrin (12.5 mg), selenous acid (12.5 μg), bovine serum albumin (2.5 g), and linoleic acid (10.7 mg) (BD Biosciences, UK);
- Nu-Serum: Low-protein serum replacement (BD Biosciences);

- PBS: Phosphate-buffered saline pH 7.4 (GIBCO/Invitrogen);
- Trypsin-EDTA: Trypsin, 0.05%, with 0.2 g/l EDTA tetrasodium salt in Hanks' balanced salt solution (GIBCO/Invitrogen).

Complete media, PBS and 12-ml aliquots of trypsin-EDTA were stored at 4°C and warmed to 37°C prior to use.

2.2.1.3. Cell maintenance

Cells were used for experiments between five to twenty passages, at most. Additionally, thawed cells were sub-cultured three to four times before use.

tsA201 cells were maintained in 75 cm^2 tissue culture flasks with 15 ml of DMEM supplemented with 10% FBS and 1% P/S. Upon 80-90% confluency (usually every 3 to 5 days), cells were detached from the flask with 10 ml full medium and replated at 1:10 dilution.

NCI-H295R cells were maintained in 75 cm^2 tissue culture flasks with 15 ml of DMEM:F12 supplemented with 2.5% Nu-Serum, 1% ITS+ Premix and 1% P/S. Upon 80-90% confluency (usually every 4 to 6 days), cells were washed with 5 ml PBS and detached from flask through incubation with 3 ml trypsin-EDTA at 37°C for 3 min. Trypsin was inactivated by the addition of 7 ml full medium and resuspended cells were replated at 1:10 dilution.

2.2.1.4. Estimating cell number

Whenever necessary, cells were counted using a Neubauer haemocytometer (0.1 mm depth). In general, resuspended cells were diluted 1:10 and applied to coverslipped chambers. The numbers of cells in 5 out of the 9 main squares of both chambers

were counted under the microscope and added. The total count of 10 squares multiplied by 10^4 corresponded to number of cells per ml of original suspension.

2.2.2. Quantitation of nucleic acids

The concentration of nucleic acids in a solution was determined by the spectrophotometric measurement of the amount of ultraviolet irradiation absorbed at 260 nm wavelength (optical density, OD_{260}), where 1 OD_{260} unit corresponds to approximately 50 ng/µl double-stranded DNA or 38 ng/µl RNA. The ratio of absorbance at 260 nm and 280 nm provided an estimate of purity, with pure preparations having OD_{260}:OD_{280} values of 1.8 (for DNA) or 2.0 (for RNA). Absorption spectroscopy was measured using a NanoDrop 1000 spectrophotometer (Thermo Fisher Scientific), following manufacturer's instructions.

2.2.3. Amplification of whole genomic DNA

When limited amounts of DNA were available and re-sampling was not possible, whole genomic DNA was amplified using the GenomiPhi V2 DNA Amplification Kit (GE Healthcare, UK). This method utilises Phi29 DNA polymerase (from the *Bacillus subtilis* bacteriophage Φ29) and random-sequence hexamer primers to representatively amplify whole genomic DNA in an isothermal process. Accurate DNA replication is obtained due to the proofreading 3' to 5' exonuclease activity of the enzyme.

Briefly, 10-20 ng of template DNA were denatured at 95°C for 3 min in presence of random hexamer primers and subsequently cooled down to 4°C to allow non-specific annealing of hexamers. Phi29 polymerase and dNTPs were added and amplification was carried out at 30°C for 90 min, after which the reaction was incubated at 65°C

for 10 min to inactive the exonuclease activity of the DNA polymerase. Amplified DNA (usual yield around 15 µg) was diluted to approximately 200 ng/µl and stored at -20°C.

2.2.4. Polymerase Chain Reaction (PCR)

DNA amplification by the polymerase chain reaction technique consists of repeated cycles of strand separation at 95°C (denaturation), hybridisation of target-specific primers at 50-60°C (or, formally, 3-5°C lower than the calculated melting temperature of primers; annealing) and DNA synthesis by a thermostable DNA polymerase at 72°C (extension).

Primers were either designed using the software Primer3Plus available at http://www.bioinformatics.nl/cgi-bin/primer3plus/primer3plus.cgi, with standard settings (Untergasser et al., 2007), or manually designed according to concepts of optimal primer design (Sambrook and Russell, 2001).

In general, PCRs were performed in thin-walled 96-well plates or 0.5 ml tubes using MegaMix (Microzone Ltd., UK), a ready-to-use PCR mix containing *Taq* DNA polymerase, equimolar amounts of all four deoxyribonucleoside triphosphates (dNTPs), reaction buffer and stabilisers (the full formulation is proprietary information). Reactions were set up with 40 to 200 ng of DNA template and 12.5 pmol of forward and reverse primers in 20 µl total volume, taking appropriate precautions to avoid exogenous DNA contamination. Unless otherwise stated, the following thermal cycling conditions were used: initial denaturation at 95°C for 2 min; 35 cycles of denaturation at 95°C for 30 s, annealing at 55°C for 30 s and extension at 72°C for 1 min; and final extension at 72°C for 10 min.

2.2.5. Agarose gel electrophoresis of DNA

Amplification products were separated by electrophoresis on 0.8-2% (w/v) agarose gels made in 1x TAE buffer (40 mM Tris-acetate and 1mM EDTA at pH 8.3, Invitrogen/Life Technologies UK) with 0.2 μg/ml ethidium bromide. In general, 3 to 5 μl samples were mixed with loading dye (30% v/v glycerol, 0.2% w/v Orange G) at a 1:10 ratio and loaded onto gel wells, alongside DNA size markers (0.3 or 0.5 μg in 10% v/v loading dye, New England Biolabs [NEB] UK Ltd., or Invitrogen). Electrophoresis was carried out at room temperature in TAE buffer at 80-110 V until appropriate separation was obtained. Bands were visualised under 302 nm ultraviolet transillumination in a ChemiDoc system and images processed using the software Quantity One v4.4.1 (all from Bio-Rad Laboratories, UK).

2.2.6. Purification of DNA

2.2.6.1. DNA immobilised in agarose

Bands corresponding to DNA of interest were excised from agarose gels with the aid of an ultraviolet transilluminator and individually placed in 1.5 ml tubes. The QIAquick Gel Extraction Kit (Qiagen Ltd., UK), a silica-membrane-based spin-column system, was used according to manufacturer's instructions, and, at the last step of the protocol, DNA was eluted from silica membranes with 20 to 50 μl of water, depending on downstream application.

2.2.6.2. DNA in solution

As part of the DNA sequencing protocol, aliquots of PCR amplification products were purified prior to the sequencing reaction using microCLEAN (Microzone), a proprietary formulation that allows preferential precipitation of double-stranded

DNA. In general, 0.5 to 2 µl of amplification product was transferred to 96-well plates and equivalent amounts of microCLEAN (per well) was added. Following homogenisation and incubation at room temperature for 5 min, plates were centrifuged for 40 min at 4,000 rpm in a benchtop centrifuge. Plates were subsequently placed upside down onto tissue paper in the centrifuge holder, and centrifuged for 1 min at 600 rpm to eliminate supernatant. Purified DNA pellets were resuspended in 10 µl of water and directly submitted to sequencing reaction or stored at -20°C.

As part of cloning and ligation protocols (including ligation-mediated PCR), DNA was purified from enzymatic reactions using the QIAquick PCR Purification Kit (Qiagen), following manufacturer's instructions. Specific elution conditions varied according to the downstream application and will be detailed where appropriate.

2.2.7. DNA sequencing

Automated DNA sequencing was performed using a dye-terminator system (BigDye Terminator v1.1 Cycle Sequencing kit, Applied Biosystems/Life Technologies, UK) and 96-capillary electrophoresis for fluorescence detection (MegaBACE 1000 DNA Sequencing System, Molecular Dynamics, UK). The dye-terminator technique evolved from the dideoxy-mediated chain-termination sequencing method (Sanger sequencing; Sanger et al., 1977) by attaching a fluorescent dye to dideoxynucleotide terminators. Fluorescently labelled fragments of increasing sizes are separated by capillary electrophoresis and, once excited by lasers, emit fluorescent light that can be detected and converted into electrical current to produce an electropherogram.

2.2.7.1. Sequencing reaction

PCR products were purified as described, in 96-well plates. Sequencing reactions were performed with 2 µl of BigDye v1.1 mix and 5 pmol of appropriate primer in 15 µl total volume under the following thermal cycling conditions: initial denaturation at 95°C for 2 min, followed by 40 cycles of denaturation at 95°C for 20 s, annealing at 50°C for 10 s and extension at 60°C for 3 min.

2.2.7.2. Purification for capillary electrophoresis

Sequencing reaction products were purified by gel filtration under centrifugation to remove oligonucleotides, unincorporated dye terminators and salt. Columns were prepared in 96-well 0.45 µm hydrophilic polyvinylidene fluoride (PVDF) filter plates (MultiScreen-HV, Millipore) with 45 mm^3 of gel matrix Sephadex G-50 (Sigma-Aldrich) and 300 µl of water per well, incubated overnight at room temperature to allow resin swelling. Before use, filter plates were centrifuged at 910*g* for 5 min to remove excessive water from gel columns. Sequencing products were applied to gel columns and DNA filtrated by centrifugation at 910*g* for 5 min, then collected in clean 96-well plates. Samples were immediately submitted to capillary electrophoresis or stored at -20°C.

2.2.7.3. Operating the MegaBACE 1000 Sequencing System

Instructions were followed to fill capillaries with linear polyacrylamide (MegaBACE Long Read Matrix, GE Healthcare) under high pressure. Samples were injected into capillaries at 3 kV for 60 s, and electrophoresis run at 9 kV for 100 min in 1x running buffer. Once electrophoresis was finished, the instrument automatically generates one electropherogram per capillary/well. Retrieved electropherograms

were analysed using the DNA sequencing assembly software Sequencher 4.6 (Gene Codes Corp., USA).

2.2.8. Extraction of total RNA from tissues and cells

The TRIzol reagent (Invitrogen), a solution of phenol and guanidine isothiocyanate, was used for total RNA isolation from tissue samples and cells according to the single-step method (Chomczynski and Sacchi, 1987). Guanidine isothiocyanate is a strong denaturing agent capable of solubilising cellular compartments and denaturing endogenous RNases, while phenol, once combined to chloroform, allows phase separation and isolation of RNA. In order to minimise RNA degradation, nuclease-free plasticware and a set of pipettes specific for RNA handling were used.

Tissue samples were stored in RNA*later* (Ambion/Applied Biosystems, proprietary formulation) at -20°C to preserve cellular RNA until extraction, whereas cells pooled from culture vessels or collected by sorting were stored at -80°C in TRIzol, directly. For extraction, tissue samples and cell pellets were homogenised in 1 ml TRIzol using a Pellet Pestle micro-grinder (Kontes/Kimble Chase, USA) and instructions were followed. In brief, 0.2 ml chloroform was added to allow phase separation, and RNA precipitated from aqueous phase by the addition of 0.5 ml isopropyl alcohol (IPA). The RNA pellet was washed with 1 ml ice-cold 75% ethanol and air-dried for 10 min before resuspension in nuclease-free water.

2.2.9. Reverse Transcription PCR (RT-PCR)

For qualitative analysis of gene expression, RT-PCR was performed using the AccessQuick RT-PCR System (Promega). This system allows the generation of first-strand cDNA and subsequent DNA amplification to be performed in a single tube

from RNA template by combining the Avian Myeloblastosis Virus (AMV) reverse transcriptase and the thermostable *Tfl* DNA polymerase from *Thermus flavus*.

Reactions were performed in sterile nuclease-free tubes using 200 ng RNA and 1 µM forward and reverse primers in 30 µl total volume, following manufacturer's instructions. Reverse transcription was carried out at 45°C for 45 minutes in a thermal cycler and followed by PCR amplification: initial denaturation at 95°C for 2 min; 35 cycles of denaturation at 95°C for 30 s, annealing at 55°C for 30 s and extension at 72°C for 1 min; and final extension at 72°C for 10 min.

2.2.10. Quantitative Reverse Transcription PCR (qRT-PCR)

2.2.10.1. First-strand cDNA synthesis (reverse transcription)

Samples containing similar amounts of total RNA (from 200 to 800 ng, in general) were prepared in 8 µl total volume with nuclease-free water. Negative reverse transcription control samples containing similar amounts of RNA and water control samples were concomitantly prepared. In order to eliminate potential contamination by DNA prior to reverse transcription, samples were incubated with 1 U of amplification grade deoxyribonuclease I (DNase I, Amp Grade, Invitrogen) in appropriate buffer for 15 min at room temperature. DNase I was inactivated by incubation at 65°C with 2.2 mM EDTA for 10 min.

SuperScript II reverse transcriptase (Invitrogen) was used for first-strand cDNA synthesis, following manufacturer's instructions. This enzyme is an engineered version of the Moloney murine leukemia virus reverse transcriptase with reduced ribonuclease H activity and increased thermal stability. Samples were incubated with 100 ng of random hexamers (Thermo Scientific ABgene, UK) and nuclease-free dNTP (final concentration 0.5 mM) at 65°C for 5 min, chilled on ice, and

subsequently incubated in the reaction buffer supplied with dithiothreitol (final concentration 10 mM) and 40 U of RNasin ribonuclease inhibitor (Promega) at 25°C for 2 min. SuperScript II RT (200 U) was added to all samples but not to the negative reverse transcription control. Samples were incubated at 25°C for 10 min, 42°C for 50 min and 70°C for 15 min in a thermal cycler to generate first-strand cDNA, and stored at -20°C if not immediately used for quantitative real-time analysis.

2.2.10.2. Quantitative PCR

2.2.10.2.1. SYBR green chemistry

The cyanine compound SYBR Green I is a nucleic acid stain that preferentially binds to double-stranded DNA, generating fluorescence upon binding. Therefore, it can be used as a reporter of the amount of DNA generated at each cycle of PCR amplification when using fluorescence-detecting thermal cyclers. The comparison of the amounts of DNA amplified from different templates during the exponential phase of the PCR, when none of the components of the reaction are limiting, allows relative quantitation of initial concentration of target sequences. Of note, SYBR dyes bind to any DNA generated during PCR-amplification, therefore nonspecific amplification or the formation of primer-dimers can result in errors in quantitation.

RT^2 qPCR Primer Assays (SABiosciences, Qiagen) were used for gene expression analysis by SYBR Green-based quantitative RT-PCR. These assays are experimentally validated to amplify a single amplicon of the correct size with uniform PCR efficiency, according to the manufacturer. Optimisation experiments were performed and included: i) determination of primer pair efficiency through standard curves in order to ensure that amplification efficiencies for different targets were equivalent; ii) thermal denaturation curves of amplified DNA at the final stage

of thermal cycling (melting curves, 65 to 95°C in 0.3°C increments), and iii) electrophoretic separation of amplicons in agarose gels, both in order to confirm correct and specific amplification of target sequences.

Reactions were set up using 12.5 µl of RT^2 SYBR Green qPCR Master Mix (SABiosciences), 1 µl of gene-specific 10 µM RT^2 primer pair stock, 1µl of cDNA template and water to a final volume of 25 µl. Quantitative PCR was carried out using a DNA Engine Opticon 2 System (MJ Research, Bio-Rad) and the following thermal cycling parameters: initial denaturation at 95°C for 10 min followed by 40 cycles of denaturation at 95°C for 15 s, annealing at 55°C for 30 s and extension at 72°C for 30 s. Raw amplification data was analysed using Opticon Monitor software v3.1.

2.2.10.2.2. TaqMan Gene Expression Assays

The TaqMan method of quantitative PCR relies on the use of labelled oligonucleotides that anneal to internal sequences within amplified DNA fragments. These oligonucleotides are labelled with fluorescent groups (usually FAM) at the 5' end and with a quencher (TAMRA or MGB) at the 3' end. Due to the 5' to 3' exonuclease activity of *Taq* polymerase, the fluorophore is cleaved from the probe during the extension phase of PCR, and – being far from the quencher group – begins to fluoresce. Fluorescence is therefore proportional to the amount of amplicon generated, with increased specificity to the target sequence.

TaqMan Gene Expression Assays and Endogenous Control assays were obtained from Applied Biosystems. Only validated and inventoried assays were used. Reactions were set up according to manufacturer's instructions using 10µl of TaqMan Gene Expression Master Mix, 1 µl of gene-specific TaqMan assay, 1 µl of

cDNA template and water up to 20 µl final volume. Quantitative PCR was carried out using a StepOnePlus Real-Time PCR System (Applied Biosystems) and the following thermal cycling parameters: hold at 50°C for 2 min followed by denaturation at 95°C for 10 min, and 40 cycles of denaturation at 95°C for 15 s and annealing/extension at 60°C for 1 min. Raw amplification data was analysed using StepOne software v2.1.

2.2.10.2.3. Gene expression analysis

Relative quantification by the $2^{-\Delta\Delta Ct}$ method (Livak and Schmittgen, 2001) was used to determine differences in gene expression according to experimental settings. Quantitative PCR experiments were designed to include one or more endogenous controls (usually glyceraldehyde-3-phosphate dehydrogenase [GAPDH] or beta-2-microglobulin [B2M]) in order to normalise the PCR for the amount of RNA added to reverse transcription reactions. All experiments were performed in triplicate, and were repeated at least three times. Mean relative quantitation values were calculated and displayed in bar charts, with error bars representing minimum and maximum relative quantitation at 95% confidence (Livak and Schmittgen, 2001).

2.2.11. *In situ* hybridisation

In situ hybridisation analysis of gene expression in human fetal tissue was performed by Drs Patricia Cogram and Dianne Gerrelli at the in-house Gene Expression service at the Medical Research Council/Wellcome Trust funded Human Developmental Biology Resource. Briefly, seven-micrometre paraffin sections of paraformaldehyde-fixed fetal tissue were analysed. *In situ* hybridisation was performed using digoxigenin-11-UTP-labelled cRNA probes generated from cDNA sequences of interest cloned into RNA transcription vectors bearing SP6 or T7 RNA polymerase

promoters. An anti-digoxigenin antibody conjugated with alkaline phosphatase was used and enzymatically detected. Sense riboprobes were tested on adjacent sections, and showed no staining above background levels.

2.2.12. Extraction of protein from cells

Protein was extracted from cells by using the Cell Extraction Buffer (Invitrogen), a variation of the radio immunoprecipitation assay (RIPA) buffer, according to manufacturer's instructions. Incubation with the several detergent agents present in this buffer (1% Triton X-100, 0.1% SDS, 0.5% deoxycholate) leads to cell lysis and release of whole-cell protein into solution.

Immediately prior to use, aliquots of cell extraction buffer were supplemented with PMSF (final concentration 1 mM) and protease inhibitor cocktail (50 µl/ml). Cell pellets were incubated with buffer (1 ml per 10^8 or less cells) on ice for 30 min, with vigorous homogenisation every 10 min. Samples were subsequently centrifuged at 13,000 rpm for 10 min at 4°C, and the clear protein-containing lysate separated for immediate analysis or stored at -80°C.

2.2.13. Quantitation of protein

The concentration of solubilised protein was determined using the Bradford assay, a spectrophotometric quantitation assay. This method is based on an absorbance shift of the dye Coomassie Brilliant Blue G-250 in the presence of protein in a solution. The binding of the dye to protein results in a change in colour and in a shift in the absorbance maximum from 465 to 595 nm (Bradford, 1976). Measurement of absorbance at 595 nm and comparison to a standard curve provides a relative measurement of protein concentration in that solution.

The Bio-Rad Protein Assay (Bio-Rad) was used and manufacturer's instructions were followed. Five dilutions of bovine serum albumin (BSA, Sigma-Aldrich) were prepared for the generation of a standard curve: 100 µg/ml, 250 µg/ml, 500 µg/ml, 750 µg/ml and 1 mg/ml. Aliquots of 20 µl of each standard dilution or samples were placed in semi-micro cuvettes. Dye reagent concentrate was diluted (1:4) in water and added to cuvettes (1 ml per cuvette). Reactions were incubated at room temperature for 5 min and absorbance at 595 nm was determined using an Eppendorf BioPhotometer (Eppendorf AG, Germany).

2.2.14. SDS-polyacrylamide gel electrophoresis (SDS-PAGE)

Proteins were separated according to their electrophoretic mobility under denaturing conditions in SDS-polyacrylamide gels. Treatment of protein samples with SDS results in loss of secondary and tertiary structures and saturation with negative charges from peptide-bound SDS, which is proportional to the polypeptide chain length. Concomitant separation of markers of known molecular weight allowed the estimation of the molecular weight of polypeptides of interest. The Mini-PROTEAN II cell vertical electrophoresis system (Bio-Rad) was used.

Resolving polyacrylamide gels were prepared to allow linear separation of proteins of interest. In general, 10% acrylamide resolving gels were prepared using a 30% (w/v) acrylamide/methylene bisacrylamide stock solution (37.5:1 ratio) (ProtoGel, National Diagnostics, USA) with 375 mM Tris base (pH 8.8) and 0.1% (w/v) SDS. Polymerisation was induced by 0.1% (w/v) ammonium persulfate and accelerated by 0.04% (v/v) N,N,N',N'-tetramethylethylenediamine (TEMED). Samples were prepared in 50 mM Tris-HCl (pH 6.8), 10% (v/v) glycerol, 2% (w/v) SDS, 0.1% bromophenol blue and 100 mM dithiothreitol (DTT), denatured at 100°C for 5 min

and loaded onto the gel. Electrophoresis was carried out in Tris-glycine buffer (25 mM Tris base, 250 mM glycine and 0.1% SDS) at 100/150 volts until the bromophenol blue reached the end of the resolving gel.

2.2.15. Immunoblotting

After separation by SDS-PAGE, proteins were immobilised in a solid membrane and reacted with specific polyclonal or monoclonal antibodies (primary antibodies). Antigen-antibody complexes were located by a chemiluminescent reaction involving an enzyme-conjugated antibody (secondary antibody) that recognises common features of the primary antibody.

Proteins were transferred from SDS-polyacrylamide gels to polyvinylidene fluoride (PVDF) membranes (Immobilon-P, Millipore) by immersion electrophoresis, using the Mini Trans-Blot electrophoretic cell system (Bio-Rad). Manufacturers' instructions were followed, and a chilled 48 mM Tris base, 39 mM glycine, 0.0375% (w/v) SDS, 20% (v/v) methanol transfer buffer was used. Transfer cassettes were assembled in a way that membranes were placed on the anode-facing side of gels, and electrophoresis carried out at 100 V for 1 hour.

Following transfer, membranes were washed in 0.1% (v/v) Tween 20 in Tris-buffered saline (TBS-T, pH 7.6) and blocked by incubation in 5% low-fat dried milk in TBS-T for 3 h at room temperature, under orbital rotation. Incubation with primary antibody was performed overnight at 4°C in 50-ml tubes with recommended amounts of antibody in 10 ml of 5% BSA in TBS-T. On the following day, membranes were washed three times in TBS-T and incubated with horseradish peroxidase (HRP)-labelled secondary antibody in 10 ml of 5% low-fat dried milk in

TBS-T for 1 hour at room temperature. Membranes were washed three times in TBS-T following incubation with secondary antibody.

The Amersham ECL Plus Western blotting detection system (GE Healthcare) was used for chemiluminescent detection of immobilised protein conjugated to HRP-labelled antibody. This system is based on proprietary technology that relies on HRP/peroxide-catalysed oxidation of the Lumigen PS-3 Acridan susbstrate to generate an acridinium ester that produces intense light emission of long duration. Manufacturer's instructions were followed, and membranes were incubated with Revelation Solution for 1 min at room temperature. Emitted light was detected by autoradiography using Amersham Hyperfilm ECL (GE Healthcare) with approximately 30-s exposure. Films were developed using a Compact X4 automatic X-ray film processor (Xograph Healthcare Imaging Systems, UK) and subsequently analysed using a GS-800 calibrated densitometer and Quantity One software v4.4.1 (both from Bio-Rad).

2.2.16. Immunohistochemistry

Immunofluorescent detection of protein in tissue samples was performed by Dr Rahul Parnaik in our group. In brief, samples were embedded in optimal cutting temperature compound (O. C. T., VWR International), rapidly frozen, and 14-µm sections obtained using an OTF5000 cryostat (Bright lnstrument Co Ltd., UK). Unfixed sections were air-dried for 2 h, immersed in ethanol (-20°C) for 10 min and stored at -20°C. For immunostaining, slides were thawed to room temperature and fixed for 3 min in 4% paraformaldehyde in PBS to preserve tissue integrity with minimal increase in aldehyde-induced autofluorescence. Samples were washed in 1% Tween 20 in TBS (TBS-T) then blocked by 1 h incubation in 10% lamb serum in

TBS-T and incubated overnight at 4°C with primary antibodies. On the following day, slides were washed and incubated overnight at 4°C in 10% lamb serum in TBS-T with 4',6-diamidino-2-phenylindole (DAPI, 1 µg/ml) and secondary antibodies. DAPI is a fluorescent stain that binds strongly to DNA, widely used in fluorescence microscopy to stain cell nuclei. After washing, slides were mounted in Vectashield (Vector Labs, UK). Images were acquired using a LSM 710 confocal microscope (Carl Zeiss Ltd., UK).

2.2.17. Plasmid DNA propagation

Closed circular plasmid DNA can be greatly amplified by transformation of competent *E. coli*, and subsequent isolation and purification of plasmid DNA. The following protocol, relying on selection of bacteria expressing plasmid-encoded antibiotic resistance under selective growth conditions, was used to propagate plasmid constructs generated by ligation or site-directed mutagenesis, and for obtaining sufficient amounts of plasmids for transfection.

2.2.17.1. Preparation of medium, antibiotic stock solutions and plates

2% (w/v) lysogeny broth (LB) was prepared by resuspension of LB powder in water, sterilised by autoclaving and stored at 4°C. Antibiotic was added immediately prior to use.

Stock solutions of ampicillin and kanamycin were prepared at 50 mg/ml, aliquoted and stored at -20°C, prior to use at 1 µl per ml of broth/agar (final concentration 50 µg/ml).

For the preparation of selective LB agar plates, a solution of 2% (w/v) LB and 1.5% (w/v) bacteriological agar in water was autoclaved and cooled down to 50-60°C

before addition of antibiotic. 25 ml of mixture was poured per 9-cm plastic Petri dish, left to set at room temperature and stored inverted at 4°C.

2.2.17.2. Transformation of competent cells

Subcloning Efficiency DH5α Competent Cells (Invitrogen) were used, following manufacturer's instructions. Briefly, 50 µl aliquots of thawed cells with 10 to 100 ng of plasmid were incubated on ice for 30 min before 20-s incubation at 42°C (heat shock). Following a 2-min incubation on ice, 950 µl of SOC medium (Invitrogen) were added and cells cultured at 37°C, in orbital shaking, for 1 hour. In general, 100 µl of culture was spread onto pre-warmed selective LB agar plates, and incubated overnight, inverted, at 37°C. Plates were removed from 37°C incubation on the following day and stored at 4°C.

2.2.17.3. Mini- and maxi-preparation of plasmid DNA

Plasmid DNA was prepared using Qiagen's QIAprep Miniprep and Plasmid Maxi kits, for mini- and maxi-preparation, respectively. Both systems rely on plasmid DNA extraction from bacterial cells by alkaline lysis with SDS, but while the mini kit uses a silica membrane for DNA purification in a spin-column format, the maxi kit relies on DNA binding to an anion-exchange resin followed by high-salt elution and IPA precipitation.

For mini-preparation, single transformed colonies were picked from agar plates using sterile pipette tips and cultured overnight in 3 ml of selective LB at 37°C, in orbital shaking. On the following day, bacterial cells were pooled in 1.5 ml tubes by centrifugation, and instructions followed for lysis and DNA purification. Usually, DNA was eluted from column membrane with 35 µl of provided elution buffer (10 mM Tris·Cl, pH 8.5) rendering approximately 10-15 µg of purified plasmid.

For maxi-preparation, 2-ml selective LB starter cultures were inoculated with single transformed colonies and incubated at 37°C, shaking, for 8 hours. Usually, 200 µl of starter culture was used to inoculate 100 ml of selective LB (1/500 dilution) and left to grow overnight at 37°C in orbital shaking. The kit's protocol was followed, and the final air-dried DNA pellet was resuspended in 200 µl of elution buffer, resulting in approximately 600-800 µg of purified plasmid.

Plasmid DNA was analysed by absorption spectroscopy as described previously, then aliquoted and stored at -20°C.

2.2.17.4. Long-term storage of plasmids/bacterial strains

Single transformed colonies were picked from agar plates using sterile pipette tips and cultured overnight in 2 ml of selective LB at 37°C, in orbital shaking. On the following day, bacterial cells were precipitated by centrifugation (13,000 rpm for 1 min, at room temperature), resuspended in 7% (v/v) DMSO (Sigma-Aldrich) and stored at -80°C. Once necessary, bacteria were recovered by scrapping the frozen surface of the culture with a sterile loop and immediate inoculation of an appropriate selective LB agar plate. Plates were incubated overnight at 37°C to allow bacterial growth.

2.2.18. Cloning extended promoter regions into reporter constructs

The following protocol was used for the directional cloning of fragments of the promoters of genes of interest into a pGL4.10[*luc2*] luciferase reporter vector (Promega), a basic reporter vector lacking eukaryotic promoter and enhancer sequences. Luciferase expression is, therefore, dependent on the functionality of inserted promoter sequences, allowing for *in vitro* analysis of promoter activation through luciferase assays.

2.2.18.1. *In silico* analysis of promoter regions

Nucleotide sequences corresponding to the 5.0 kilobases 5' upstream of transcriptional start sites (TSS) of genes of interest were obtained from Ensembl (www.ensembl.org) and analysed with the software MatInspector available at www.genomatix.de, using standard settings. MatInspector identifies transcription factor binding sites in nucleotide sequences using a large curated and updated library of weight matrices and dedicated algorithms (Cartharius et al., 2005).

The location of predicted binding sites within the 'vertebrate steroidogenic factor' matrix family, which includes binding sites for SF-1 and the related NR5A nuclear receptor LRH-1 (liver receptor homologue-1, encoded by *NR5A2*), was recorded and determined the length of promoter fragments to be cloned.

2.2.18.2. PCR-amplification from genomic DNA: Long range PCR protocol

A long range PCR protocol was used to amplify promoter fragments from control genomic DNA. In order to avoid incorporation of incorrect bases, which can hinder the amplification of long segments of DNA, this protocol combines two thermostable DNA polymerases: the highly efficient but potentially error-prone HotStarTaq (Qiagen) and, in smaller amounts, the high-fidelity Platinum *Pfx* (Invitrogen) with proofreading 3' to 5' exonuclease activity.

Primers were manually designed, and, ideally, the reverse primer hybridised DNA within the untranslated region of the first exon of the gene of interest, avoiding the insertion of an additional start codon once the promoter was cloned into the reporter vector.

Long range PCR was set up as follows:

DNA template (300 ng/µl)	1.0 µl
HotStarTaq 10x buffer	2.5 µl
HotStarTaq Buffer Q (HotStar)	5.0 µl
25 mM solution of dNTP	3.5 µl
100 µM forward primer	1.0 µl
100 µM reverse primer	1.0 µl
1:10 diluted Platinum *Pfx* polymerase*	0.5 µl
HotStarTaq polymerase	0.5 µl
Water to a final volume of	25 µl

*diluted in 1x *Pfx* amplification buffer

Amplification was carried out with initial denaturation at 95°C for 15 min; 40 cycles of denaturation at 95°C for 20 s, annealing at 55°C for 30 s and extension at 68°C for X min (X being 1 min per kb of amplicon); and final extension at 68°C for 10 min.

Reaction products were separated in 1% agarose gel to confirm specific amplification of desired promoter fragments.

2.2.18.3. Cloning PCR products into T vectors (TA cloning)

Amplified promoter fragments were cloned into T vectors to allow subsequent directional subcloning into pGL4 reporter vectors. TA cloning relies on the single deoxyadenosine (A) added to 3' ends of PCR products by *Taq* polymerases, which permits efficient cloning into linearised vectors harbouring complementary unpaired 3' deoxythymidine (T) residues.

As many fragments were longer than 1.0 kb, the TOPO XL PCR cloning kit (Invitrogen) was used, following the manufacturer's instructions. Notably, this kit's protocol relies on UV-free gel-purification of DNA to increase cloning efficiency, avoiding potential DNA damage by UV exposure. In brief, PCR products were separated in 0.8% agarose gels made with 0.8 µg/ml crystal violet and bands of interest excised upon direct visualisation. DNA was purified from gel fragments using the provided spin-column system (S.N.A.P. UV-Free Gel Purification Kit, Invitrogen), and cloning reactions performed with 4 µl of purified PCR inserts and 1 µl of linearised pCR-XL-TOPO vector at room temperature for 5 min. 2 µl of cloning reaction was subsequently used for transformation of One Shot TOP10 chemically competent cells. Approximately 6 colonies per transformation were picked and cultured overnight for plasmid DNA isolation, as described. Constructs were analysed through combined restriction strategies, individually designed in light of specific restriction sites within inserts, to confirm the presence and correct orientation of the insert. If a suitable strategy could not be devised, primers were designed within the insert to be used in combination with supplied M13 primers (M13 priming sites present in the vector backbone) allowing confirmation of insert directionality through PCR amplification followed by agarose gel separation.

2.2.18.4. Subcloning inserts from pCR-XL-TOPO into pGL4.10[*luc2*] vectors

Given the position of restriction sites within the multiple cloning regions of pCR-XL-TOPO and pGL4.10[*luc2*] (vector maps available in Appendix 2), the restriction endonucleases *Kpn*I and *Xho*I were used for subcloning promoter inserts in the correct direction.

10 µg of pGL4.10[*luc2*] was digested overnight at 37°C with 20 U of *Xho*I (NEB) in 50 µl reaction volume. On the following day, the now linearised vector was purified using the QIAquick PCR purification kit and subsequently digested with 20 U of *Kpn*I at 37°C for at least 4 hours. At the same time, inserts were excised from pCR-XL-TOPO constructs (3 µg) through double digestion with 20 U *Xho*I and 20 U *Kpn*I in 20 µl reaction volume (NEB Buffer 1 supplemented with BSA, at 37°C for 4 hours). Digested pGL4 and promoter inserts were gel-purified using the crystal violet method as described above, and purified DNA was eluted from columns using 20 µl of water to increase concentration of product used for ligation. DNA was quantified by absorption spectroscopy.

Ligation was performed at 16°C overnight, in 0.5 ml tubes, with:

Digested pGL4.10[*luc2*]	1.0 µl
Digested insert	7.0 µl
10x T4 DNA Ligase buffer (NEB)	1.0 µl
T4 DNA Ligase (400,000 U/ml; NEB)	1.0 µl

Using this reaction set-up, the molar ratio of insert to vector varied from 2:1 to 6:1, according to insert length.

On the following day, the whole ligation reaction volume (10 µl) was used for transformation of DH5α cells, as described above, and the whole 1 ml transformation resulting from this was spread onto pre-warmed LB/ampicillin agar plates for overnight incubation at 37°C. Plasmid DNA was prepared from transformed colonies as described, and constructs were screened through restriction analysis. Finally, constructs were sequenced to confirm that promoter fragments were cloned in the correct orientation using the RVprimer3 priming site present in the pGL4 backbone.

Once the desired construct was obtained and confirmed, insert sequences were fully verified by direct sequencing and plasmids propagated as described previously.

2.2.19. Site-directed mutagenesis

Site-directed mutagenesis of plasmid DNA was performed using the QuikChange XL Site-Directed Mutagenesis Kit (Stratagene, now part of Agilent Technologies, UK), which consists of *in vitro* oligonucleotide-directed mutagenesis using a double-stranded DNA template and selection of mutants with the restriction enzyme *Dpn*I (circular mutagenesis). In this method, DNA sequence changes are introduced through linear amplification in a thermal cycler using oligonucleotide primers complementary to opposite strands of the vector, both containing the desired mutation, and high-fidelity *PfuTurbo* DNA polymerase. Subsequent treatment of the amplification reaction with *Dpn*I allows enrichment for mutated plasmids since this enzyme digests methylated template DNA (bacterially propagated) but not unmethylated mutagenised plasmid DNA (*in vitro* synthesised).

Oligonucleotide primers were designed using the online QuikChange Primer Design tool (www.genomics.agilent.com/qcpd), observing the manufacturer's recommendations. In general, these were between 25 and 45 bases in length, had a melting temperature greater than or equal to 78°C, and bore the desired mutation in the middle with at least 12 bases of correct sequence on each side. Amplification reactions were performed following manufacturer's instructions with 20 ng of plasmid DNA template and 125 ng of each primer in 50 µl total volume. Of note, thermal cycling parameters were adjusted to allow 1 minute of extension at 68°C per kilobase of plasmid length at every cycle. Digestion with 10 U of *Dpn*I was performed at 37°C for 1 hour, and 2 µl of *Dpn*I-treated DNA was used for

transformation of XL10-Gold ultracompetent cells, according to the manufacturer's instructions. Transformed colonies were screened using individually-tailored restriction digest strategies, and successfully mutagenised plasmids were sequenced in their entirety.

2.2.20. Reporter gene assays

Reporter gene assays were used to study the regulation of gene expression by transcription factor-dependent promoter transactivation *in vitro*. The set up involved the transient co-transfection of tsA201 human embryonic kidney or NCI-H295R human adrenocortical cells with:

- An 'expression vector', constitutively expressing the transcription factor of interest (wild type or mutant pCMX-SF1 or pCMX-DAX1);
- A 'reporter vector' bearing the promoter fragment of interest upstream of the reporter firefly luciferase *luc2* gene (pGL4.10[*luc2*] constructs); and
- An internal control reporter vector (pRL-SV40 plasmid expressing *Renilla* luciferase).

Luciferase activity was assayed 24-48 h after transfection and reflected the degree of promoter transactivation. Assayed *Renilla* luciferase activity was used to adjust for variability in cell number or viability or in transfection efficiency.

2.2.20.1. Transient transfection in 96-well format (lipofection)

Experiments were performed in triplicate (i.e. three wells for each experimental condition) and repeated at least 3 times on separate occasions. All steps involving manipulation of living cells were performed in aseptic conditions. Unless otherwise stated, 96-well plates (TPP Techno Plastic Products AG, Switzerland) were used.

2.2.20.1.1. Plating cells

Twenty-four hours before transfection, cells were harvested from 90% confluent 75cm^2 tissue culture flasks in 10 ml, as described, and further diluted 1:8 in full culture medium so that 150 µl of dilution distributed per well contained approximately 10^4 cells. Plates were incubated at 37°C in a humidified atmosphere of 5% carbon dioxide to obtain 70% confluent cells at the time of transfection.

2.2.20.1.2. Preparing DNA aliquots

Aliquots of DNA to be delivered to each triplicate of wells were prepared in 15 µl volume. In general, a maximum of 200 ng of DNA per well was used and total DNA amount was kept constant amongst all triplicates within the same experiment. Relative amounts of expression and reporter vectors varied between experiments and will be detailed opportunely. In every experiment the initial mastermix contained the internal control pRL-SV40 reporter, at a concentration of 7.5 ng per well.

2.2.20.1.3. Delivering DNA to cells: lipofection

The transfection reagent Lipofectamine 2000 (Invitrogen) was used. This proprietary formulation uses cationic lipids to create vesicles of nucleic acid (liposomes) capable of adhering to and fusing with membranes, thereby delivering the nucleic acid to the interior of the cell.

Lipofectamine 2000 (1.5 µl/triplicate) was diluted with pre-warmed Opti-MEM Reduced Serum Medium (75 µl/triplicate; Invitrogen) and incubated at room temperature for 5 min. Aliquoted DNA was diluted in 75 µl of Opti-MEM plus 76.5 µl of Opti-MEM/lipofectamine mixture, and incubated at room temperature for 20 min. Fifty microlitres of DNA/lipofectamine dilution was distributed per well, and plates were re-incubated at usual culture conditions.

2.2.20.2. Luciferase assays

The Dual-Luciferase Reporter Assay System (Promega) was used to sequentially measure the activities of firefly and *Renilla* luciferases in a single sample. Both enzymes are monomeric proteins that do not require post-translational processing for enzymatic activity and can, therefore, act as genetic reporters immediately upon translation (Wood et al., 1984; Matthews et al., 1977). Nevertheless, these two luciferases are structurally different and have different substrate requirements (luciferin for firefly luciferase, coelenterazine for *Renilla* luciferase), hence their individual ability to generate bioluminescence can be discriminated. Firefly luciferase was assayed first by adding Luciferase Assay Reagent II to generate a luminescent signal. Once firefly luminescence was quantified, this reaction was quenched and the *Renilla* luciferase reaction was simultaneously initiated by adding Stop & Glo Reagent. *Renilla* luminescence was subsequently quantified.

2.2.20.2.1. Cell lysis

Twenty-four hours after transfection, media were removed from wells and 25 µl 1x Passive Lysis buffer (provided as part of the Dual-Luciferase Reporter Assay System) was added per well. Plates were incubated in a vibrating platform shaker at 900 rpm for 20 min at room temperature. To ensure complete lysis, plates were stored at -20°C and thawed once lysates were frozen in all wells. Twenty microlitres of thawed lysates were transferred to opaque 96-well plates (Corning Costar, USA) for analysis.

2.2.20.2.2. Luciferase assays

The FLUOstar OPTIMA luminescence plate reader (BMG Labtech Ltd., UK), equipped with two built-in reagent injectors, was set to perform eight luminescence

measurements over 7.0 s (basal measurement and then every second until 7.0 s) and to inject 50 µl of Luciferase Assay Reagent II at 2.0 s and 50 µl of Stop & Glo Reagent at 5.0 s. Plates were kept at room temperature with 1 mm-wide orbital shaking (600 rpm) throughout. Each experiment was fully assayed in one instance, using a single batch of reconstituted reagents and uniform settings.

This luminescence reader allows for adjustment of gain (sensitivity of the photo reader) so that measurements are kept within the linear reading range of the instrument (0-1,000,000 luminescence units). Gain was therefore individually adjusted for each experiment based on the reading for a biological replicate of the experimental intervention expected to generate the highest levels of luminescence, which was obtained just prior to the full assay.

2.2.20.2.3. Data analysis

Raw luminescence readings were analysed using Microsoft Office Excel. Given the injection times of substrates, luminescence readings between 2.0 and 5.0 s corresponded to firefly luciferase activity whereas readings between 5.0 and 7.0 s corresponded to *Renilla* luciferase activity. For the purposes of analysis, maximal readings at 3.0 to 4.0 s for wells representing a biological triplicate were averaged and normalised by the corresponding average of maximal readings at 6.0 to 7.0 s (relative luciferase activity; firefly luciferase activity/*Renilla* luciferase activity).

Within each experiment, a baseline was defined, usually corresponding to co-transfection of the promoter construct being studied with 'empty' pCMX (backbone). Relative luciferase activity values for specific experimental interventions (for example, increasing doses of pCMX-SF1/DAX1 or mutagenised pCMX) were normalised by the baseline and thus expressed as fold activation.

Experiments were repeated in full on at least three separate occasions and mean fold activation (±SEM) calculated. Results were displayed as bar charts. In order to determine statistical significance of observed results, one-way analysis of variance (ANOVA) followed by a Bonferroni Multiple Comparison Test was performed using GraphPad Prism software v5.04 (GraphPad Software Inc., USA). P-values less than 0.05 were considered significant.

2.2.21. Amaxa nucleofection

Nucleofection was used to transfect pIRES2-AcGFP1-Nuc constructs into NCI-H295R cells for studies of transient SF-1 overexpression (Chapter 5). This transfection method, developed by Amaxa Biosystems (now part of Lonza, Switzerland), is based on electroporation using the Nucleofector device, which delivers specifically developed electrical parameters, and Nucleofector kits that contain cell-specific optimised solutions. Details of the electrical parameters and transfection solutions are proprietary information. For transfection into NCI-H295R cells, use of Nucleofector device program T-020 and Nucleofector solution R had been previously reported and was recommended by the manufacturer (Casal et al., 2006; Romero et al., 2006; Romero et al., 2007). The number of cells and amount of plasmid DNA used per transfection had been previously optimised by Dr Rebecca Hudson-Davies in our group.

NCI-H295R cells were harvested from 90% confluent 75cm^2 tissue culture flasks in 10 ml final volume as described previously and counted using a haemocytometer (section 2.2.1.4). In general, approximately 25 x 10^6 cells were obtained per flask. Appropriate volumes of harvested cells in suspension were precipitated by centrifugation (90 *g* for 10 min at room temperature) and resuspended in

Nucleofector solution R to yield 5 x 10^6 cells per 100 µl of solution R. Aliquots of 10 µg of plasmid DNA mixed with 100 µl of resuspended cells were transferred into nucleofection cuvettes, which were placed into the Nucleofector II device and submitted to program T-020. After nucleofection, cells were washed from cuvettes with 500 µl of pre-warmed RPMI 1640 medium and transferred to 6-well plates containing 3 ml of usual growth media (DMEM:F12 supplemented with 2.5% Nu-Serum, 1% ITS+ Premix and 1% P/S) per well (one transfection per well). Plates were incubated at 37°C in a humidified atmosphere of 5% carbon dioxide for 48 h until harvesting for fluorescence-activated cell sorting.

2.2.22. Fluorescence-activated cell sorting (FACS)

Fluorescence-activated cell sorting (FACS) was used to select green fluorescent protein (GFP)-positive cells in studies of transient SF-1 overexpression in NCI-H295R cells (Chapter 5). Flow cytometry and sorting were performed at the UCL Institute of Child Health Flow Cytometry Core Facility. Preparation of cell samples for FACS required optimisation due to cell clumping, and will be detailed below.

2.2.22.1. Sample preparation

Preparation of adherent cells for flow cytometry is often complicated by cell clumping (Davies, 2007; Houtz et al., 2004; Garcia-Pineres et al., 2006). The main reasons for cell stickiness are the presence of free DNA (released by dead cells), and of protein and Ca^{+2} in the solution. To overcome this problem, the sample preparation protocol was optimised to include treatment with DNAse I and EDTA in a low-protein solution, and filtration through a 70-µm nylon mesh.

For harvesting, growth medium was removed from wells and the cell monolayer was washed two times (1 ml/well) with calcium- and magnesium-free PBS supplemented

with 1% (w/v) bovine serum albumin (BSA), 10 U/ml of recombinant DNAse I (Roche Applied Sciences, UK) and 5 mM EDTA. Cells were detached from the plate by incubation with trypsin-EDTA (0.6 ml/well) at 37°C for 2 min. Trypsin was inactivated by the addition of full medium (1.4 ml/well) and resuspended cells were transferred to 15-ml tubes. Cells were precipitated by centrifugation (90 *g* for 10 min at room temperature), resuspended in 0.5 ml of supplemented PBS and transferred to 5 ml polystyrene round-bottom tubes (BD Biosciences). Tubes were kept on ice and, immediately before flow cytometry, cell suspensions were filtered through 70-µm nylon cell strainers (BD Biosciences).

2.2.22.2. Flow cytometry and cell sorting

Flow cytometry consists of a process through which physical and chemical characteristics of single cells suspended in a fluid stream are measured by an electronic apparatus (Shapiro, 2003). Most commonly, it involves the emission of a beam of light of single wavelength (usually laser light) and detection of scattered and fluorescent light elicited when a single cell passes through the emitted beam. For fluorescence-activated cell sorting, flow cytometry is coupled to electrical or mechanical means to divert and collect cells based upon specific operator-selected fluorescent characteristics of each cell. This way, a heterogeneous mixture of biological cells can be sorted into two or more containers, one cell at a time, based upon their characteristics and fluorescence.

FACS was performed by Dr Ayad Eddaoudi and team at the UCL Institute of Child Health Flow Cytometry Core Facility using a MoFlo XDP cell sorter (Beckman Coulter, UK). Events with size and granularity compatible with viable cells were gated, and viability was confirmed by staining of mock samples with 7-

aminoactinomycin D (7-AAD) where lack of stain indicates live cells with intact membranes. Subsequent gating and sorting were based on detection of *Aequorea coerulescens* GFP fluorescence, excited by a 488 nm argon ion laser line with an emission around 530 to 540 nm. Cells were collected in PBS in 1.5-ml tubes.

2.2.23. Global gene expression microarray analysis

Global gene expression was analysed using GeneChip Human Gene 1.0 ST arrays (Affymetrix UK Ltd., UK) on the Affymetrix microarray platform. These arrays cover the whole human transcriptome through the representation of 28,869 genes based on the National Center for Biotechnology Information (NCBI) human genome assembly 36 (NCBIv36; equivalent to the University of California at Santa Cruz [UCSC] genome browser build hg18; released March 2006). Each gene is covered by approximately twenty-six 25-mer probes spread across the full length of the gene.

2.2.23.1. Sample processing and array hibridisation

Samples and arrays were processed by Dr Priya Panchal at UCL Genomics (University College London). The Affymetrix GeneChip platform was used, and all necessary reagents and equipments were obtained from Affymetrix UK Ltd, unless otherwise stated.

Quality control of RNA samples was performed using the 2100 Bioanalyzer and the RNA 6000 Pico Assay (Agilent). The 2100 Bioanalyzer consists of a microfluidics system that allows miniaturised gel electrophoresis in a chip platform, therefore allowing RNA quantification and quality control. The RNA 6000 Pico assay was used, and manufacturer's instructions were followed throughout. In brief, dye-supplemented gel matrix was injected into the RNA 6000 Pico chip and ladder and samples (1 μl) were added to individual wells. Samples were prepared by heating at

70ºC for 2 min. The loaded chip was run inside the Bioanalyzer. RNA quality was assessed through the patented RNA Integrity Number (RIN) (Schroeder et al., 2006).

Following quality control, samples were prepared for microarray hybridisation using the GeneChip Whole Transcript (WT) Sense Target Labeling Assay kit (Affymetrix), starting with 200 ng total RNA of each sample. This assay generates amplified and biotinylated sense-strand DNA targets from total RNA samples. Manufacturer's instructions were followed throughout. In brief, first-strand cDNA was synthesised from polyadenylated RNA using T7-$(N)_6$ primers and SuperScript II reverse transcriptase. Second-strand cDNA was subsequently synthesised using the first-strand as template and DNA polymerase I. Samples were subjected to *in vitro* translation overnight with proprietary reagents including unlabelled ribonucleotides to generate antisense RNA (cRNA). First-strand (sense) cDNA was subsequently generated from cRNA using random hexamers and a mixture of dNTP+dUTP. Following cRNA hydrolysis and purification, sense cDNA was fragmented by incubation at 37°C for 1 hour with uracil DNA glycosylase (UDG) and human apurinic/apyrimidinic (AP) endonuclease (APE1). UDG excises uracil residues incorporated during amplification and APE1 recognises the generated AP (apurinic/apyrimidinic) site and cleaves the backbone adjacent to the missing base. Resulting cDNA fragments were subsequently end-labelled with biotin allonamide triphosphate.

Labelled sense cDNA fragments were hybridised to GeneChip Human Gene 1.0 ST arrays for 16 hours at 45°C, in rotation. Arrays were subsequently washed and stained using the GeneChip Hybridization, Wash and Stain Kit and scanned in a GeneChip Scanner 3000 7G System. Raw data files (.CEL files) were retrieved from the scanner for analysis.

2.2.23.2. Microarray data analysis

Quality control of raw microarray data was performed using R/Bioconductor and the Partek Genomics Suite (PGS, Partek Inc., USA). Analysis of raw array data with PGS included plotting of three-dimensional Principal Component Analysis (PCA).

Analysis with R/Bioconductor was performed by Dr Sonia Shah at the Bloomsbury Centre for Bioinformatics. Differential gene expression analysis was performed using the limma package in R/Bioconductor. Multiple testing correction was applied according to the Benjamini and Hochberg False Discovery Rate method (Benjamini and Hochberg, 1995). A Benjamini-Hochberg-corrected P-value cut-off of 0.05 was used to select significant differentially expressed transcripts. Transcripts were identified based on information from Affymetrix (NetAffx analysis platform, available at www.affymetrix.com/analysis) and the Human Genome Organization (HUGO) Gene Nomenclature Committee (HGNC, www.genenames.org).

2.2.24. Chromatin immunoprecipitation

Chromatin immunoprecipitation assays were performed using the ChIP-IT Express kit (Active Motif, Belgium), following manufacturer's instructions. This kit relies on the use of protein G-coated magnetic beads that allow for high-capacity specific IgG binding due to the high affinity of streptococcal protein G for the Fc region of mammalian antibodies, while washing and elution are facilitated by magnetic separation.

2.2.24.1. Crosslinking and preparation of nuclei extract

NCI-H295R human adrenocortical tumour cells were grown to 80% confluency in three 15-cm plates (approximately 4.5 x 10^7 cells in total). Fixation was carried out

by replacing culture medium with 20 ml of 1% (v/v) formaldehyde in medium solution and incubating for 10 minutes at room temperature in an orbital shaking platform in order to crosslink bound proteins to DNA. Plates were subsequently washed with 10 ml of ice-cold PBS, and fixation stopped by incubation with 10 ml of 'glycine stop fix' solution for 5 min shaking at room temperature. Cells were scraped from plates in 2 ml of PBS supplemented with phenylmethylsulfonyl fluoride (PMSF, final concentration 0.5 mM) using 1.8-cm blade cell scrapers (BD Biosciences) and transferred into a single 15 ml conical tube. An aliquot of 10 µl of cell suspension was separated for cell counting as described, and remaining cells were pooled by centrifugation at 2,500 rpm for 10 min at 4°C.

In order to release the nuclei, pooled cells were resuspended in 1 ml of ice-cold 'lysis buffer' supplemented with protease inhibitor cocktail (PIC) and PMSF to preserve protein/DNA interactions, and incubated on ice for 30 min. To aid in nuclei release, cells were gently homogenised in an ice-cold dounce homogeniser. Nuclei were subsequently pooled by centrifugation at 5,000 rpm for 10 min at 4°C. For chromatin fragmentation by enzymatic digestion, the nuclei pellet was resuspended in 1.0 ml of 'digestion buffer', warmed to 37°C for 5 min and subdivided in 50 µl aliquots. For chromatin fragmentation by sonication, the nuclei pellet was resuspended in 1.0 ml of 'shearing buffer' and divided into three aliquots of approximately 350 µl each, following manufacturer's instructions.

2.2.24.2. Chromatin fragmentation by enzymatic digestion

Three 50-µl aliquots of nuclei extract were digested with 0.5 U of 'enzymatic shearing cocktail' (supplied with the ChIP-IT Express Enzymatic kit) by incubation at 37°C for 10, 15 or 20 minutes, respectively. Digestion was stopped by incubation

with 0.5 µmol EDTA on ice for 10 minutes. Samples were centrifuged at 13,000 rpm for 10 min at 4°C and chromatin-containing supernatants were collected.

2.2.24.3. Chromatin fragmentation by sonication

Aliquots of 350 µl of nuclei extract were sonicated on ice using a Sanyo Soniprep 150 sonicator (Sanyo Gallenkamp Plc, UK). For optimisation, the effects of eight 20-s cycles of sonication at 2 or 10 µm of amplitude were compared. For all subsequent experiments, samples were submitted to eight 20-s cycles of sonication at 2 µm of amplitude. Following sonication, samples were centrifuged at 13,000 rpm for 10 min at 4°C and chromatin-containing supernatant were collected.

2.2.24.4. Purification of DNA for quantitation and analysis of fragmentation range

During optimisation and for all chromatin immunoprecipitation experiments, aliquots of fragmented chromatin were separated in order to allow determination of DNA concentration and visualisation of fragmentation range by electrophoretic separation in agarose gels. Crosslinking was reversed by overnight incubation of 25-µl aliquots of fragmented chromatin in 0.2 M NaCl at 65°C. Aliquots were subsequently incubated with Proteinase K (0.025 µg/µl) at 42°C for 90 minutes, and DNA purified using the QIAquick PCR Purification kit (Qiagen). Purified DNA fragments were separated by electrophoresis on 1.5% (w/v) agarose gels for analysis of fragmentation range, and total DNA concentration determined using a NanoDrop 1000 spectrophotometer, as described.

2.2.24.5. Immunoprecipitation assay

Immunoprecipitation was carried out in aliquots of sheared chromatin from approximately 1 x 10^6 cells (around 6.0 µg of chromatin). Reactions were set up in 1.7-ml siliconized tubes with 25 µl of magnetic beads, 10 µl of '10x ChIP buffer 1', 1 µl of PIC and 3 µg of antibody in a total volume of 100 µl and incubated overnight at 4°C in a tube rotator (blood tube rotator SB1, Stuart Scientific/Bibby, UK). For SF-1 IP, the rabbit polyclonal anti-SF-1 antibody 07-618 from Upstate Millipore was used. For negative control IP, negative control IgG (ChIP-IT Control Kit - Human, Active Motif) was used.

On the following day, beads were washed with 800 µl of 'ChIP buffer 1' and '2', according to instructions and with the aid of a magnetic tube stand (Ambion/Applied Biosystems). Beads were resuspended in 50 µl of 'elution buffer AM2'and incubated for 15 min at room temperature shaking horizontally on a vibrating platform shaker (Titramax 100, Heidolph, Germany). 'Reverse cross-link buffer' (50 µl) was subsequently added, and chromatin-containing supernatant was quickly collected in a fresh tube.

2.2.24.6. Crosslink reversal and DNA purification

Previously separated 10-µl aliquots of input chromatin were eluted to 100 µl in 'ChIP buffer 2' supplemented with 10 µmol NaCl. Chromatin immunoprecipitation and input samples were incubated at 94°C for 15 min to reverse crosslinking and subsequently incubated with 1 µg of proteinase K at 37°C for 1 hour to digest proteins. Digestion with proteinase K was stopped by returning tubes to room temperature and adding 2 µl of 'proteinase K stop solution'. At this stage, samples

were ready for ChIP-PCR (below). For amplification and microarray analysis, samples were further purified using the QIAquick PCR Purification kit.

2.2.24.7. Confirmation of enrichment by PCR analysis (ChIP-PCR)

Enrichment of promoter regions of known SF-1 targets by chromatin immunoprecipitation was verified using PCR (ChIP-PCR). Primers and promoters investigated will be detailed in Chapter 4, section 4.2.4. PCR reactions were set up using 5 µl of template (SF-1 IP, IgG IP, 0.2% input DNA or H_2O), 12.5 pmol of forward and reverse primers and MegaMix in 30 µl total volume, and carried out for 35 cycles, with an annealing temperature of 55°C. Amplification products (7 µl) were separated by electrophoresis on 2% (w/v) agarose gels and visualised as described in section 2.2.5.

2.2.25. Chromatin immunoprecipitation microarray analysis (ChIP-on-chip)

In order to obtain sufficient amounts of DNA for microarray detection, aliquots of input and immunoprecipitated chromatin were amplified by ligation-mediated PCR (LM-PCR) (Ren and Dynlacht, 2004; Oberley et al., 2004). This method consists on blunt-ending of DNA fragments by the 3'-5'exonuclease activity of T4 DNA polymerase to allow ligation of a universal nucleotide linker and subsequent linear amplification by PCR. Additionally, a 1:4 mix of deoxyuridine triphosphate (dUTP) and deoxythymidine triphosphate (dTTP) is used in the amplification reaction, allowing for incorporation of deoxyuracil into amplified chromatin. Incorporated uracil residues are subsequently targeted for amplicon fragmentation prior to hybridisation to arrays.

2.2.25.1. Amplification by Ligation-Mediated PCR (LM-PCR)

SF-1-IP and respective input DNA samples were amplified by ligation-mediated PCR, following previously published protocols (Ren et al., 2000; Oberley et al., 2004; Lee et al., 2006). In brief, chromatin was blunt-ended by 1-hour incubation at 37°C with T4 DNA Polymerase (NEB) and 0.1 mM deoxyribonucleotide triphosphate mix (dNTP; Bioline, UK). Long (5'-GCG GTG ACC CGG GAG ATC TGA ATT C-3') and short (5'-GAA TTC AGA TC-3') unidirectional oligonucleotides were heated to 100°C in a 50 mM NaCl solution, and slowly cooled to room temperature to generate double-stranded linkers, which were ligated to blunted chromatin overnight at 16°C using T4 DNA ligase (NEB). Linker-ligated chromatin was linearly amplified by PCR using 0.1 U Taq polymerase, 3 μM long oligonucleotide, 1 M betaine, 2.5 mM $MgCl_2$ and 0.1 mM dNTP + dUTP mix (25% dATP, 25% dCTP, 25% dGTP, 20% dTTP and 5% dUTP, all obtained from Bioline) and the following thermal cycling parameters: 1 cycle of 55°C for 2 min, 72°C for 5 min and 95°C for 2 min, 15 cycles of 95°C for 30 s, 55°C for 30 s and 72°C for 5 min, followed by a 4-minute final extension at 72°C. After purification, the DNA concentration was determined and after two rounds of amplification samples of amplicons were separated by agarose gel electrophoresis to verify the preservation of fragmentation range.

2.2.25.2. Fragmentation, end-labelling and hybridisation to tiled microarrays

Final preparation of samples for hybridisation and microarray processing were performed by Dr Nipurna Jina at UCL Genomics (University College London). I was present throughout and was able to discuss the protocol with her. The Affymetrix

GeneChip platform was used, and all necessary reagents and equipment were obtained from Affymetrix UK Ltd., unless otherwise stated. Experiments were performed following manufacturer's instructions. In brief, amplicons were fragmented by incubation at 37°C for 1 hour with uracil DNA glycosylase (UDG) and human apurinic/apyrimidinic (AP) endonuclease (APE1). Fragmentation was verified using the 2100 Bioanalyzer (Agilent) and was successful in all samples, with most fragments being around 66 bp in length.

Fragments were subsequently end-labelled using the GeneChip WT Double-Stranded DNA Terminal Labelling Kit. Biotinylated 'DNA labelling reagent' (biotin allonamide triphosphate) was incorporated at 3' ends by incubation at 37°C for 1 hour with terminal deoxynucleotidyl transferase. Labelled DNA fragments were hybridised to GeneChip Human Promoter 1.0R arrays for 16 hours at 45°C, in rotation. Following hybridisation, arrays were washed and stained using the GeneChip Hybridization, Wash and Stain Kit and scanned in a GeneChip Scanner 3000 7G System. Raw data files (.CEL files) were retrieved from the scanner for analysis.

2.2.25.3. Microarray data analysis

Quality control of raw microarray data was performed by Dr Sonia Shah at the Bloomsbury Centre for Bioinformatics using Tiling Analysis Software (TAS, Affymetrix) and R/Bioconductor. Pairs of arrays (input and SF-1-IP) that met quality control standards were used for peak detection.

The ChIP-on-chip peak detection tool CisGenome (Ji et al., 2008) was used to define protein-binding regions. Quantile normalisation was applied prior to analysis, and a moving average (MA) statistic was computed for each probe based on a half-window

size of 300 bp or 5 probes (Ji and Wong, 2005; Ji et al., 2006). In order to increase stringency, probes with the MA statistic 3.5 S.D. away from the global mean were used to define protein-binding regions. Peaks were discarded if they contained less than five probes or were less than 100 base pairs in width. Peaks that were separated by less than 300 base pairs or 5 probes were merged. Peaks that had a left-tail false discovery rate greater than 5% were discounted (Ji et al., 2008). The genomic coordinates of all regions were converted into coordinates based on the NCBI human genome assembly 36 (NCBIv36) and mapped to neighbouring transcriptional start sites (TSS). Identified peaks were visualised using the Integrated Genome Browser (IGB, Affymetrix) (Nicol et al., 2009).

2.2.26. Bioinformatics

Genes and proteins were characterised based on information from the National Center for Biotechnology Information (NCBI, USA) Entrez Gene portal (www.ncbi.nlm.nih.gov/gene), GeneCards (www.genecards.org) and UniProt (www.uniprot.org). Information on gene DNA and protein sequences and genomic annotation were obtained from the Ensembl Genome Browser (www.ensembl.org) and the UCSC Genome Browser (www.genome.ucsc.edu).

The BioMart Central Portal (www.biomart.org) was used for *in silico* characterisation of genes. BioMart is a query-oriented data management system, suitable for complex descriptive data. Patterns of gene expression in human tissues and organs investigated through BioMart were derived from two publicly available data sets, eGenetics (Kelso et al., 2003) and GNF (Su et al., 2002). Gene ontology information was obtained from BioMart and from AmiGO (Gene Ontology Consortium, www.geneontology.org) (Carbon et al., 2009).

Functional annotation enrichment analysis for subsets of genes was performed using the Database for Annotation, Visualization and Integrated Discovery (DAVID) v6.7 (http://david.abcc.ncifcrf.gov/) (Dennis et al., 2003; Huang et al., 2009).

Information on human and mouse genetic phenotypes were obtained from the Online Mendelian Inheritance in Man portal (www.ncbi.nlm.nih.gov/omim) and from the Mouse Genome Informatics portal (The Jackson Laboratory, www.informatics.jax.org), respectively.

2.2.26.1. Functional annotation and network analysis using MetaCore

Gene functional annotation and potential network interactions were investigated using MetaCore software (GeneGo Inc., USA; www.genego.com). MetaCore is a software suite for pathway analysis of experimental data and gene lists, based on a proprietary curated integrated database of human protein-protein and protein-DNA interactions, transcription factors, and signalling and metabolic pathways. As of January 2009, the manually curated database contained information on approximately 19,000 human genes, 900 transcription factors, 270,000 protein-protein interactions, 570,000 DNA-protein interactions and 700 pathway maps built upon published experimental data.

Experimental gene lists were uploaded into GeneGo using unique 'Entrez Gene ID' identifiers (NCBI), and only genes annotated by the Human Genome Organization (HUGO) Gene Nomenclature Committee (HGNC, www.genenames.org) were included for analysis. To determine which functional categories and biological processes were enriched in the experimental list of genes the 'Compare Experiments' workflow in GeneGo was used. Experimental targets were mapped onto functional ontologies in MetaCore, in particular GeneGo Process Networks, a set of

approximately 110 cellular and molecular processes where content is defined and annotated by GeneGo. Gene interaction networks were constructed using the 'Analyze Networks' algorithm with default settings.

CHAPTER 3

ANALYSIS OF *CITED2* AND *PBX1* AS TARGETS OF SF-1

3.1. Introduction

During the past decades, several factors involved in human adrenal development and function have been identified through gene expression analysis, studies of regulatory regions and transgenic mouse models. Two candidate factors arising from mouse models that lack adrenal glands are CITED2 and PBX1. In mice, Cited2 and Pbx1 participate in adrenal development through pathways shared with Sf-1, leading to the hypothesis that these factors might also be involved in human adrenal development and under SF-1 regulation.

The transcriptional coactivator Cbp/p300-interacting transactivator, with Glu/Asp-rich carboxy-terminal domain, 2 (CITED2, MIM 602937) was identified in 1997 through an expressed sequence tag (EST) database screening for cDNA clones structurally similar to the melanocyte-specific gene 1 (*MSG1*, now termed *CITED1*) (Shioda et al., 1997; Sun et al., 1998). *CITED2* was cloned and mapped to 6q23.3 in humans in 1999, and shown to encode a nuclear protein capable of binding to the transcriptional coactivators/histone acetyltransferases EP300 and CREBBP (Leung et al., 1999; Bhattacharya et al., 1999). The generation of mice lacking Cited2 revealed its importance in adrenal development as *Cited2*$^{-/-}$ embryos died with adrenal agenesis, cardiac malformations, abnormal cranial ganglia and exencephaly (Figure 3.1) (Bamforth et al., 2001). Following studies proposed that Cited2-dependent regulation of Sf-1 dosage could be a mechanism to explain this phenotype, as discussed in section 1.3.3.2. Recently, expression of CITED2 in fetal (8 wpc) and adult human adrenal glands was reported, as well as *CITED2* up-regulation by fibroblast growth factor 2 (FGF2) *in vitro* (Haase et al., 2007).

However, many aspects of the regulation of *CITED2* expression in the human adrenal cortex remain obscure.

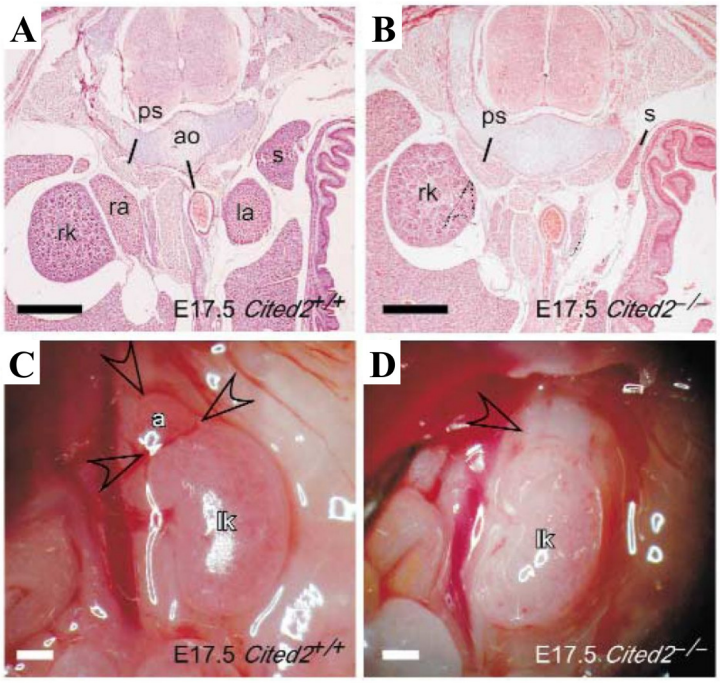

Figure 3.1. Adrenal agenesis in *Cited2*$^{-/-}$ mouse embryos.
A and B, HE-stained abdominal transverse sections from E17.5 mouse embryos. Normal right and left adrenal glands (ra and la) are identified in wild type embryo (A), but not seen in *Cited2*$^{-/-}$ embryo (B). C and D, Dissection of E17.5 mouse embryos. A normal left adrenal gland (C) is identified in the *Cited2*$^{+/+}$ embryo, but is absent in the *Cited2*$^{-/-}$ embryo (D). Rk, right kidney; ao, aorta; ps, psoas major muscle; s, spleen; lk, left kidney. From Bamforth et al., 2001. Reprinted by permission from Macmillan Publishers Ltd., copyright 2001.

Pre-B-cell leukemia homeobox 1 (PBX1, MIM 176310) is a non-Hox-homeodomain transcription factor that acts as a Hox cofactor throughout development (Moens and

Selleri, 2006). Initially identified as part of a chimeric t(1;19) translocation protein found in human pre-B-cell acute lymphoblastic leukaemia (Kamps et al., 1990; Nourse et al., 1990), PBX1 emerged as a steroidogenic regulator from studies of cAMP-dependent transcriptional regulation of bovine (Kagawa et al., 1994; Bischof et al., 1998) and human (Ogo et al., 1997) cytochrome P450c17 (*CYP17*). In 2003, studies of the embryonic lethal *Pbx1* null mice revealed complete lack of adrenal glands (Figure 3.2) and suggested that a Pbx1-dependent pathway regulated the expansion of SF-1 positive cells essential for adrenal formation and gonadal differentiation (Schnabel et al., 2003). This concept was expanded by the characterisation of an enhancer region in intron 4 of murine *Nr5a1* through which transcription of Sf-1 in the fetal adrenal was initiated by a Hox-Pbx1-Prep1 complex (Zubair et al., 2006). Nevertheless, subsequent studies of Pbx1 haploinsufficient mice confirmed the necessity of full *Pbx1* dosage for normal adrenal development and showed that Sf-1 directly activates the *Pbx1* promoter *in vitro* and *in vivo*, suggesting that an intricate relationship between these factors is essential for the development and maintenance of a functional adrenal cortex in mice (Lichtenauer et al., 2007).

Given these findings, and considering the key role of SF-1 in the developing human adrenal gland, it was hypothesised that CITED2 and PBX1 could be targets of SF-1 in the human adrenal gland. Therefore, the expression of these factors during critical stages of human adrenal development, and SF-1-dependent activation of the *CITED2* and *PBX1* promoters in human adrenocortical cells, were studied. Considering that the transactivational activity of SF-1 is repressed by the related orphan nuclear receptor DAX1 in many adrenal-based systems, the effects of DAX1 on regulation of these genes was also investigated.

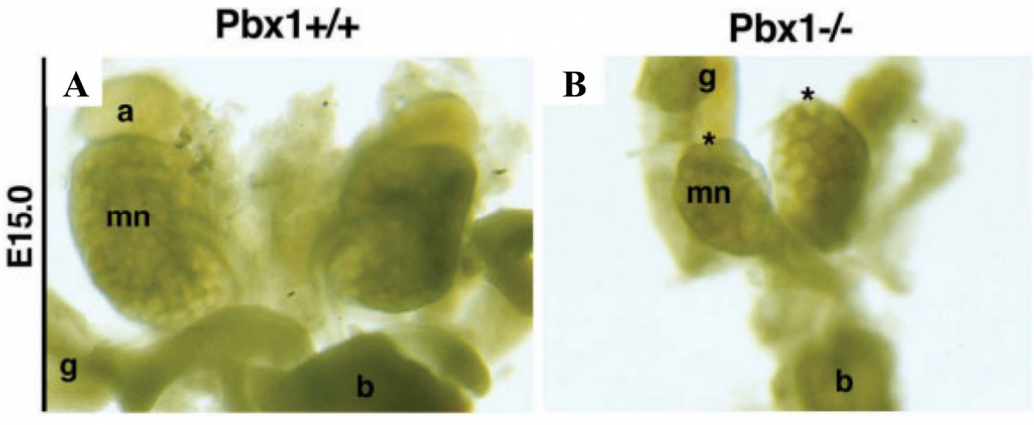

Figure 3.2. Adrenal absence in *Pbx1*$^{-/-}$ mouse embryos.

A and B, Whole mount preparation of E15.0 mouse embryos. Normal adrenal glands (a) are identified in wild type embryos (A), but are absent in Pbx1-/- littermates (B, expected position of glands marked with *). Mn, mesonephros; g, gonad; b, bladder. From Schnabel et al., 2003. Reprinted by permission from John Wiley & Sons, Inc.

3.2. Materials and Methods

3.2.1. Reverse Transcription Polymerase Chain Reaction (RT-PCR)

Qualitative RT-PCR, with visualisation of amplification products by electrophoretic separation in agarose gels, was performed to assess the expression of *CITED2* and *PBX1* in the developing human adrenal gland. Human fetal adrenal tissue from 7 and 10 weeks post-conception (wpc) was obtained from the Medical Research Council/Wellcome Trust-funded Human Developmental Biology Resource (www.hdbr.org). RNA was extracted as described in section 2.2.8, and 200 ng of extracted RNA was used for RT-PCR following the protocol described in section 2.2.9.

Specific intron-spanning primers were designed to avoid co-amplification of potential contaminating genomic DNA. Primers for *CITED2* were located within exon 1 (forward, 5'-CAGGAAGGTCCCCTCTATGTG-3') and within exon 2 (reverse, 5'-GCGCCGTAGTGTATGTGCTC-3'), and were predicted to generate a 275-bp amplicon. Primers for *PBX1* were located within exon 4 (forward, 5'-GTTCCCGATTTCTGGATGC-3') and within exon 6 (reverse, 5'-CATGGGCTGACACATTGGTA-3'). These primers were predicted to generate a 279-bp amplicon. Glyceraldehyde-3-phosphate dehydrogenase (GAPDH; forward primer, 5'-CCCTTCATTGACCTCAACTA-3', reverse primer 5'-CCAAAGTTGTCATGGATGAC-3', 399-bp amplicon) was used as a positive control. Amplification products were subsequently separated by 1.2 % agarose gel electrophoresis, as described in section 2.2.5.

3.2.2. *In situ* hybridisation

In situ hybridisation analysis of *CITED2* and *PBX1* expression in 7 wpc human embryonic tissue was performed by Dr Patricia Cogram and Dr Dianne Gerrelli at the Human Developmental Biology Resource, as summarised in section 2.2.11.

Digoxigenin-labelled riboprobes were generated from a pOTB7 vector containing the 1903-bp full cDNA sequence of *CITED2* and a pCR4-TOPO vector containing the 1388-bp full cDNA sequence of *PBX1*. Both plasmids were obtained from the Mammalian Gene Collection, National Institutes of Health, USA (IMAGE ids 3640855 and 8069084, respectively).

3.2.3. *In vitro* studies of *CITED2* and *PBX1* regulation by SF-1

Luciferase reporter gene assays were designed to investigate the activation of *CITED2* and *PBX1* promoter fragments by SF-1, following the protocol described in section 2.2.20. Activation by wild type SF-1 was compared to that induced by the naturally occurring G35E mutant SF-1, known to have impaired transactivational activity *in vivo* and *in vitro* (Achermann et al., 1999; Ito et al., 2000). Additionally, studies were designed to investigate potential inhibition of SF-1-dependent activation by DAX1 (*NR0B1*), which has been extensively documented *in vitro* (Lalli and Sassone-Corsi, 2003; Iyer and McCabe, 2004). The action of wild type DAX1 was compared to naturally occurring DAX1 mutants associated with severe (R267P, A300P) or mild (I439S) forms of X-linked adrenal hypoplasia (Muscatelli et al., 1994; Achermann et al., 2001; Tabarin et al., 2000), which have been shown to have impaired repressor activity.

The 5.0-kb upstream regions of *CITED2* (Ensembl transcript ENST00000367651, NCBIv36) and *PBX1* (Ensembl transcript ENST00000340699, NCBIv36) were

analysed *in silico* using MatInspector, as described in section 2.2.18.1. Based on the location of predicted SF-1 or LRH-1 (*NR5A2*) binding sites, pGL4.10[*luc2*] constructs bearing 600-bp, 900-bp and 3.3-kb fragments of the *CITED2* promoter and a 910-bp fragment of the *PBX1* promoter were generated. Strategies for co-transfection of reporter constructs and pCMX expression vectors containing SF-1 or DAX1 cDNAs will be detailed in the following paragraphs and in the figures and figure legends. In all studies, 7.5 ng/well of internal control pRL-SV40 reporter was co-transfected to allow firefly luciferase activity normalisation by *Renilla* luciferase in Dual-Luciferase reporter assays. Pilot studies using different amounts of expression and reporter vectors were performed to determine dose values near optimal but not supramaximal in each experimental scenario. Importantly, activation of an empty pGL4 reporter was also assessed to gauge the contribution of elements in the pGL4 vector backbone to luciferase expression and was always many fold smaller than when pGL4 contained cloned promoter fragments. Luciferase assays were performed and analysed as detailed in section 2.2.20.2.

3.2.3.1. *CITED2* promoter activation by SF-1

Studies of the degree of activation of the three *CITED2* promoter constructs by SF-1 were standardised in tsA201 human embryonic kidney cells using 50 ng/well of expression vector (empty pCMX, pCMX-WTSF1 or pCMX-G35ESF1) and molar equivalent amounts of reporter vector: 1.29 ng/well of pGL4-CITED2pro600bp (size 4913 bp), 1.36 ng/well of pGL4-CITED2pro900bp (size 5202 bp) or 2 ng/well of pGL4-CITED2pro3.3kb (size 7642 bp). The total amount of DNA transfected was kept constant at 100 ng/well by adding empty pCMX vector as necessary.

Similar studies were performed in NCI-H295R human adrenocortical cells using molar equivalent amounts of reporter (64 ng/well of pGL4-CITED2pro600bp, 68 ng/well of pGL4-CITED2pro900bp or 100 ng/well of pGL4-CITED2pro3.3kb) and 25 ng/well of expression vector, keeping total DNA constant at 140 ng/well.

SF-1-dependent activation of the construct containing the 3.3-kb *CITED2* promoter fragment was further studied in NCI-H295R cells using 100 ng/well of pGL4-CITED2pro3.3kb and increasing amounts (10, 20, 50 or 100 ng/well) of pCMX-WTSF1 or pCMX-G35ESF1, keeping total DNA constant at 207.5 ng/well.

3.2.3.2. *PBX1* promoter activation by SF-1

Activation of the *PBX1* promoter construct by SF-1 was tested in tsA201 cells using 100 ng/well of pGL4-PBX1pro910bp and increasing amounts (10, 20, 50 or 100 ng/well) of pCMX-WTSF1 or pCMX-G35ESF1. Studies were repeated in NCI-H295R cells using similar amounts of vectors, and keeping total DNA transfected constant at 207.5 ng/well.

3.2.3.3. Effects of DAX1 on SF-1-dependent activation of the *CITED2* promoter

Increasing amounts of pCMX-WTDAX1 (2, 5, 10, 20 or 50 ng/well) were co-transfected with 50 ng/well of pCMX-WTSF1 and 100 ng/well of pGL4-CITED2pro3.3kb (total DNA amount 210 ng/well) into NCI-H295R cells to study the effects of DAX1 on SF-1-dependent activation of the 3.3-kb *CITED2* promoter fragment.

3.2.3.4. Effects of DAX1 on SF-1-dependent activation of the *PBX1* promoter

The effects of DAX1 on SF-1-dependent activation of the 910-bp *PBX1* promoter were studied in NCI-H295R cells using increasing amounts of pCMX-WTDAX1 (2, 5, 10, 20 or 50 ng/well), 100 ng/well of pCMX-WTSF1 and 100 ng/well of pGL4-PBX1pro910bp to a total of 260 ng of DNA per well.

In order to compare the effects of wild type versus mutant DAX1, studies were performed in NCI-H295R cells using 100 ng/well of pGL4-PBX1pro910bp, 100 ng/well of either empty pCMX or pCMX-WTSF1 and 50 ng/well of DAX1-expressing vector (pCMX-WTDAX1, pCMX-R267PDAX1, pCMX-A300PDAX1 or pCMX-I439SDAX1) to a total amount of 260 ng/well of DNA.

3.3. Results

3.3.1. *CITED2* and *PBX1* are expressed in the human fetal adrenal gland

Analysis of *CITED2* and *PBX1* by RT-PCR showed abundant expression of these genes in RNA derived from 7 and 10-wpc human fetal adrenal glands (Figure 3.3A). Strong amplification was also seen for the housekeeping gene, *GAPDH*, but the water control was negative. Expression of *CITED2* and *PBX1* was confirmed by *in situ* hybridisation on human fetal adrenal tissue at Carnegie Stage 20 (7 wpc) (Figure 3.3B and C), which showed strong signal in the fetal adrenal gland comparing to surrounding structures.

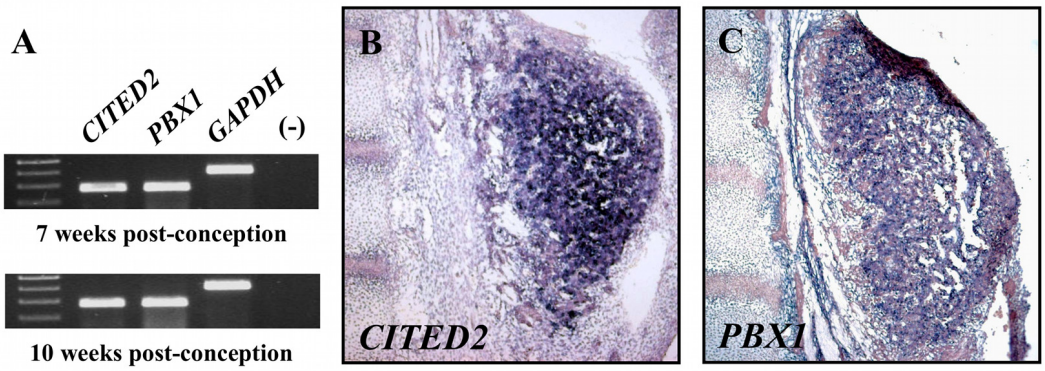

Figure 3.3. *CITED2* and *PBX1* are expressed in the human fetal adrenal.
A, RT-PCR of *CITED2* and *PBX1* at 7 and 10 weeks post-conception (wpc). (-), water control. B and C, In situ hybridisation of *CITED2* and *PBX1* in human fetal adrenal tissue at Carnegie Stage 20 (7 wpc). In situ hybridisation analysis was performed by Dr Patricia Cogram and Dr Dianne Gerrelli at the Human Developmental Biology Resource. From Ferraz-de-Souza et al., 2009. Copyright 2009, The Endocrine Society.

3.3.2. The *CITED2* promoter is activated by SF-1

Four putative SF-1-binding sites were identified in the *CITED2* 5.0-kb promoter, located 3,080 bp, 1,274 bp, 665 bp and 458 bp upstream of the transcription start site (Figure 3.4). Three reporter constructs were generated containing 600-bp, 900-bp or 3.3-kb fragments of the *CITED2* promoter, respectively, and their activation by SF-1 was studied in tsA201 and NCI-H295R cells. In both cell lines the shorter promoter fragments (600 and 900 bp) failed to be activated by wild type SF-1, whereas activation of the longer 3.3-kb promoter was observed (Figure 3.5, A and B). Further studies focussed on the steroidogenic NCI-H295R adrenocortical cell line. Using increasing doses of pCMX expression vector, the 3.3-kb *CITED2* promoter was activated by wild type SF-1 in a dose-dependent manner up to 6-fold above baseline (empty pCMX), but not by the functionally-impaired G35E mutant SF-1 (Figure 3.6A). Co-expression of DAX1 with SF-1 had no inhibitory or activating effects on the *CITED2* promoter (Figure 3.6B).

A

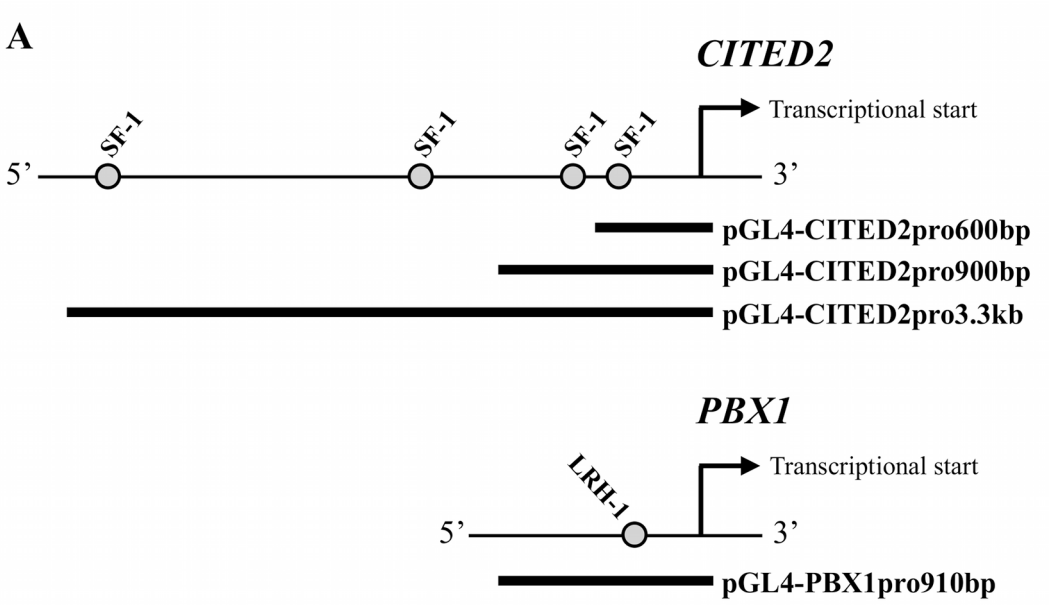

B

Promoter	Distance (bp) to transcriptional start	Putative site
CITED2	-3,080	GGTACAAGGCCAA
CITED2	-1,274	GAAGCAAGGTTAT
CITED2	-665	CTTTCAAGGACAG
CITED2	-458	GGCACAAGGGCAC
PBX1	-368	TTTGCAAGGCAGA

Figure 3.4. Putative binding sites in *CITED2* and *PBX1* upstream sequences.
A, Cartoon representation of putative 'vertebrate steroidogenic family' binding sites (grey circles) identified in the upstream sequences (5.0 kb) of *CITED2* and *PBX1* using MatInspector. Based on their location, pGL4.10[luc2] reporter constructs were generated bearing fragments of the promoters of these genes. The length of the promoter fragment represented in each individual reporter construct is shown. B, Details of MatInspector analysis. For each identified putative binding site, the distance in relation to the transcriptional start (-, upstream) and DNA nucleotide sequence are shown. Core sequence elements recognised by MatInspector are underlined. While the four sites in the *CITED2* promoter were characterised as primarily SF-1-binding sites, the site in the *PBX1* promoter was identified as a primarily LRH-1 (NR5A2)-binding site.

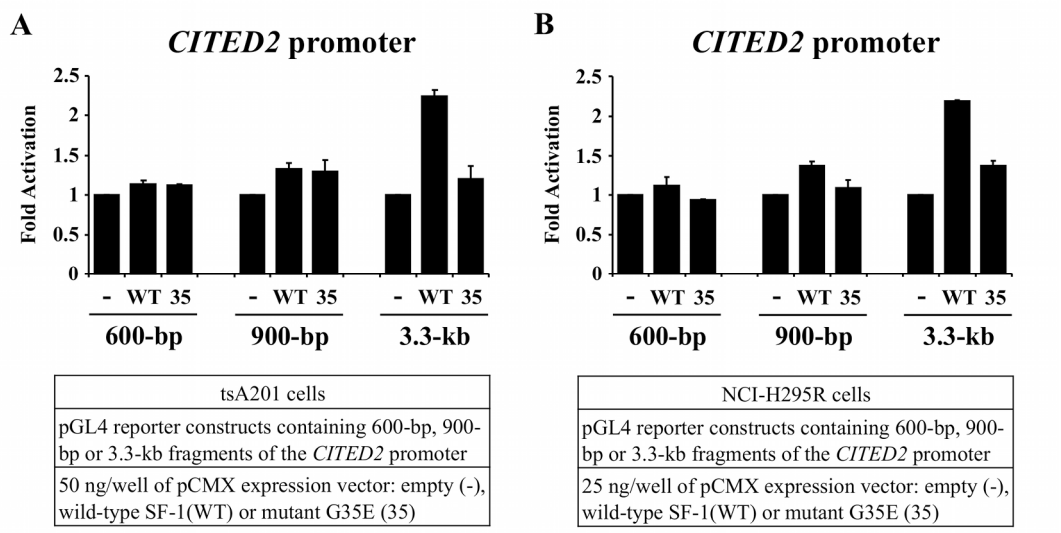

Figure 3.5. Studies of *CITED2* promoter activation by SF-1.

A, Comparison of the degree of SF-1-dependent activation of constructs bearing 600-bp, 900-bp or 3.3-kb fragments of the *CITED2* promoter in tsA201 cells. While the shorter promoter fragments failed to be activated by wild type SF-1, activation of the construct bearing the 3.3-kb *CITED2* promoter fragment was seen (3.3 WT > -, P<0.0001; 900 and 600 WT > -, not significant). B, A similar pattern of activation was observed when studies were performed in NCI-H295R human adrenocortical cells, with stronger activation of the 3.3-kb *CITED2* promoter construct by wild type SF-1 (3.3 WT > -, P<0.0001; 3.3 WT > 900 WT, P<0.001; 3.3 WT > 600 WT, P<0.0001). Data shown as mean ± SEM of at least three experiments each performed in triplicate. Fold activation is shown in relation to normalised luciferase signal elicited by co-transfection of the reporter of interest with empty expression vector (-).

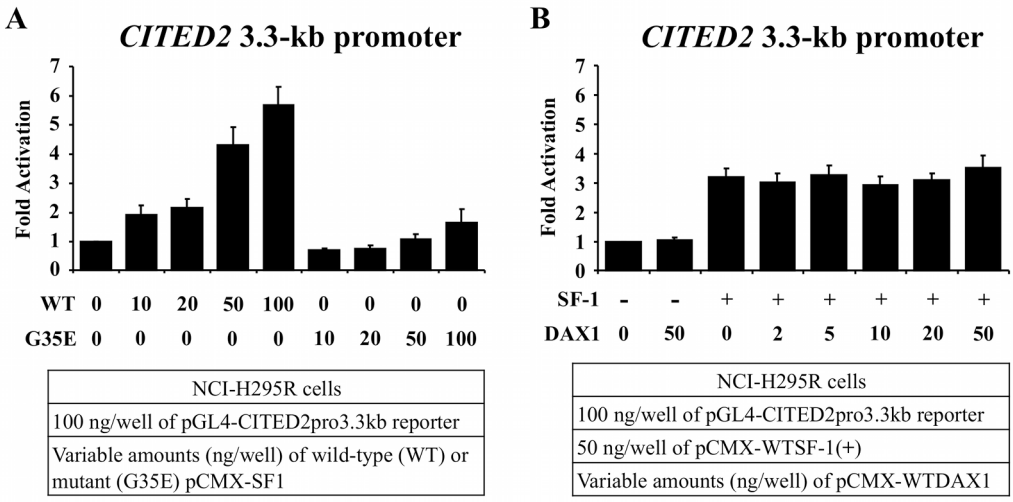

Figure 3.6. Studies of the 3.3-kb *CITED2* promoter activation by SF-1 and DAX1 in NCI-H295R cells.

A, Dose-dependent activation of the 3.3-kb *CITED2* promoter by wild type SF-1 was lost when the G35E mutant was used (WT 50 > 0, P<0.001; WT 100 > 0, P<0.0001; G35E 100 > 0, not significant). B, Increasing doses of wild type DAX1 had no effect on the SF-1-dependent activation of the 3.3-kb *CITED2* promoter (SF-1 + > - [DAX1 0 or 50], P<0.0001; 2, 5, 10, 20 or 50 DAX1 *vs* 0 DAX1 [SF-1 +], not significant). Data shown as mean ± SEM of at least three experiments each performed in triplicate. Fold activation is shown in relation to normalised luciferase signal elicited by co-transfection of the reporter of interest with empty expression vector (- or 0 ng).

3.3.3. The *PBX1* promoter is synergistically activated by SF-1 and DAX1

SF-1-binding sites were not identified in the 5.0-kb *PBX1* promoter, however a putative binding site for the related nuclear receptor LRH-1 (NR5A2) was identified 368 bp upstream of the transcriptional start (Figure 3.4). Whereas the 910-bp *PBX1* promoter was not activated by wild type SF-1 in tsA201 human embryonic kidney cells (Figure 3.7A), 2-fold activation was seen in NCI-H295R human adrenocortical cells (Figure 3.7B). Co-expression of increasing doses of DAX1 with SF-1 revealed synergistic activation of the 910-bp *PBX1* promoter, 4-fold higher than baseline (empty pCMX) and 2.3-fold greater than the activation resulting from SF-1 alone (Figure 3.8A). This increased activation was lost when DAX1 mutants associated with severe X-linked adrenal hypoplasia (R267P, A300P) were co-transfected instead of WT cDNA, and partially reduced when the I439S mutant associated with a milder, late-onset form of X-linked adrenal hypoplasia was studied (Figure 3.8B).

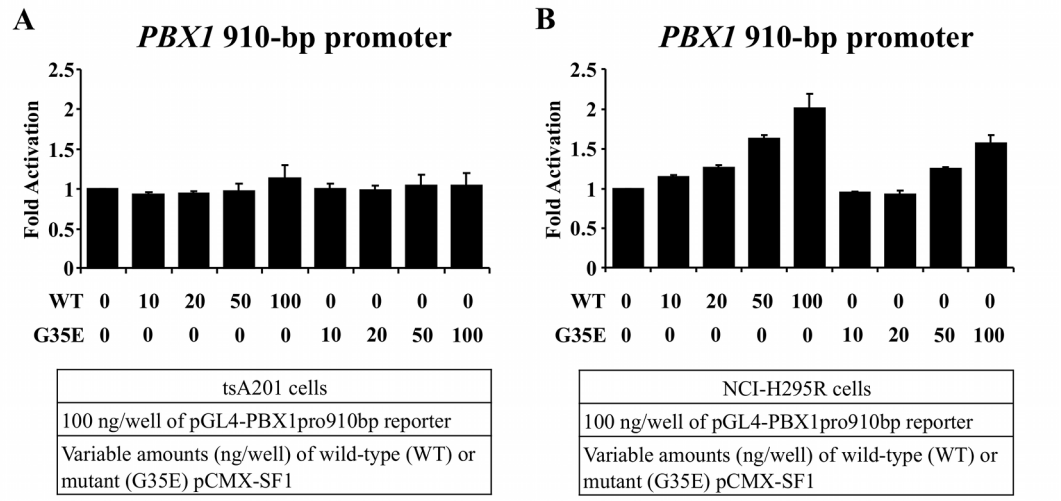

Figure 3.7. Studies of *PBX1* promoter activation by SF-1.

A, The 910-bp *PBX1* promoter construct was not activated by increasing doses of wild type or mutant G35E SF-1 in tsA201 cells (WT 100 > 0, not significant). B, When similar studies were performed in NCI-H295R human adrenocortical cells, dose-dependent activation of the *PBX1* promoter by wild type SF-1 was seen (WT 50 > 0, P<0.001; WT 100 > 0, P<0.0001). Data shown as mean ± SEM of at least three experiments each performed in triplicate. Fold activation is shown in relation to normalised luciferase signal elicited by co-transfection of the reporter of interest with empty expression vector (0 ng).

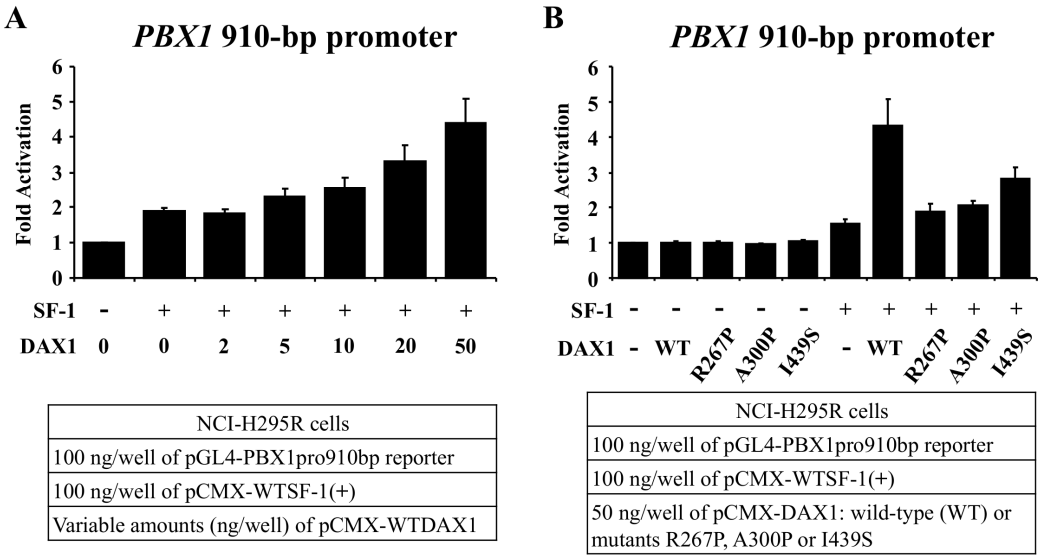

NCI-H295R cells
100 ng/well of pGL4-PBX1pro910bp reporter
100 ng/well of pCMX-WTSF-1(+)
Variable amounts (ng/well) of pCMX-WTDAX1

NCI-H295R cells
100 ng/well of pGL4-PBX1pro910bp reporter
100 ng/well of pCMX-WTSF-1(+)
50 ng/well of pCMX-DAX1: wild-type (WT) or mutants R267P, A300P or I439S

Figure 3.8. Studies of *PBX1* promoter activation by SF-1 and DAX1 in NCI-H295R cells.

A, Synergistic activation of the 910-bp *PBX1* promoter was seen when increasing doses of wild type DAX1 were co-transfected with wild type SF-1 (DAX1 50 > 0 [SF-1 +], P<0.01; DAX1 50 > 0 [SF-1 -], P<0.001). D, This synergistic activation was attenuated when naturally occurring DAX1 mutants associated with severe (R267P, A300P) or mild (I439S) forms of X-linked adrenal hypoplasia were studied (WT > R267P or A300P; P<0.001; WT > I439S; P<0.05). Data shown as mean ± SEM of at least three experiments each performed in triplicate. Fold activation is shown in relation to normalised luciferase signal elicited by co-transfection of the reporter of interest with empty expression vector (- or 0 ng).

3.4. Discussion

The transcriptional regulators CITED2 and PBX1 have recently been implicated in adrenal gland development mainly through observations of adrenal absence in transgenic mice lacking these factors. However, relatively little is known about the involvement of CITED2 and PBX1 in *human* adrenal development. The studies described here confirm that *CITED2* and *PBX1* are both expressed during the early stages of human fetal adrenal development at a time when the gland is undergoing significant morphological and functional differentiation (Hammer et al., 2005; Goto et al., 2006) and concordant with expression of SF-1 (Hanley et al., 1999).

SF-1 is an important regulator of many target genes involved in adrenal development and function, therefore it was plausible to hypothesise that SF-1-dependent regulation of *CITED2* and *PBX1* might occur in humans. Previous studies have shown that Sf-1 up-regulates *Pbx1* expression in mice (Lichtenauer et al., 2007), and that Pbx1 and Cited2 may in turn mediate *Sf-1* (*Nr5a1*) expression in *in vitro* and *in vivo* systems (Zubair et al., 2006; Val et al., 2007). By focusing on a human adrenal cell line, SF-1 is shown to strongly activate the human *CITED2* promoter when an extended 3.3-kb fragment of the promoter is studied, suggesting that elements located more than 1 kb upstream of the transcriptional start site may be necessary for SF-1-dependent regulation of *CITED2*.

Furthermore, while SF-1 appears to be a relatively weak activator of the minimal promoter of human *PBX1*, synergistic activation of this promoter by SF-1 and DAX1 is observed in adrenal cells. Interestingly, SF-1-dependent activation of the *PBX1* promoter was not seen in non-steroidogenic tsA201 human embryonic kidney cells, suggesting that cell-specific co-factors might be necessary for this effect.

Considering that DAX1 is expressed in NCI-H295R cells (Guo et al., 1995; Ehrlund et al., 2009), it is possible that native DAX1 expression is mediating SF-1-dependent activation in these cells.

Although mutations in both DAX1 and SF-1 can result in variable degrees of adrenal insufficiency, it remains enigmatic how these two transcription factors interact during adrenal development and function because most studies have shown that DAX1 acts as a repressor of SF-1-mediated transactivation (Ito et al., 1997; Zazopoulos et al., 1997; Babu et al., 2002; Iyer and McCabe, 2004). More recently, however, a limited number of reports are starting to emerge of synergistic SF-1/DAX1 regulation of genes potentially involved in adrenal development and function. For example, Verrijn Stuart and colleagues have shown activation of the human *CYP11B1* promoter by SF-1 and DAX1 in NCI-H295R cells (Verrijn Stuart et al., 2007) and Xu and colleagues observed synergistic activation of murine *Mc2r* by SF-1 and Dax1 in human choriocarcinoma JEG-3 cells, amplified by interaction with the steroid receptor RNA activator 1 (SRA1) (Xu et al., 2009). Furthermore, activation of the human *GNRH1* (encoding the gonadotropin-releasing hormone, GnRH) promoter by SF-1 and DAX1 has recently been described in studies performed in mouse GT1-7 immortalised hypothalamic cells (Li et al., 2010). Therefore, the present observation of synergistic activation of SF-1 and DAX1 on the *PBX1* promoter forms part of the growing evidence that DAX1 may also have an activating role during certain stages of development, on specific promoters, or together with cell-specific transcriptional complexes. This mechanism may contribute to the impaired definitive zone development in patients with X-linked AHC because the synergy of DAX1 was attenuated when naturally occurring severe and partial DAX1 mutants were studied.

Taken together, the findings of *CITED2* and *PBX1* expression in the developing human adrenal gland and their regulation *in vitro* by SF-1 and DAX1 suggest that these genes are likely to be important mediators of adrenal development and function in humans as well as in mice.

CHAPTER 4

GENOME-WIDE ANALYSIS OF SF-1-BINDING TARGETS

4.1. Introduction

As outlined in Chapter 1, SF-1 plays a central role in many aspects of adrenal and reproductive development and function. Indeed, disruption of SF-1 can lead to adrenal agenesis or hypoplasia in both mice and humans (Luo et al., 1994; Shinoda et al., 1995; Sadovsky et al., 1995; Achermann et al., 1999; Biason-Lauber and Schoenle, 2000; Achermann et al., 2002). Beyond its role as a regulator of development, SF-1 is also emerging as a potentially important regulator of adrenal tumorigenesis (Lalli, 2010). For example, somatic duplication of the locus 9q33 that contains *NR5A1* has been reported in a high proportion of paediatric adrenal tumours on a background of *TP53* loss of heterozygosity (Figueiredo et al., 2005); overexpression of SF-1 transcript levels has been reported in paediatric adrenal carcinomata (Almeida et al., 2010); and, more recently, SF-1 protein expression was found to be associated with poor clinical outcome in a large cohort of adult adrenocortical carcinomata (Sbiera et al., 2010). These data are further supported by observations of adrenocortical cell proliferation and adrenal tumorigenesis resulting from overexpression of Sf-1 in the mouse (Doghman et al., 2007).

Although many SF-1 target genes have already been identified through detailed characterisation of the promoter and enhancer regions of known key factors (Schimmer and White, 2010; Hoivik et al., 2010), it is likely that several other important SF-1 targets exist. We hypothesised that genome-wide identification of SF-1-binding sites through chromatin immunoprecipitation microarrays (ChIP-on-chip) in human adrenal cells could lead to the identification of novel SF-1 targets and unravel potentially important mechanisms in adrenal development and disease.

ChIP-on-chip is a powerful method for the identification of transcription factor-binding sites throughout the genome (Ren et al., 2000; Iyer et al., 2001; Weimann et al., 2002; Carroll et al., 2006). It relies on chromatin immunoprecipitation assays to selectively enrich for chromatin fragments bound by transcription factors following treatment of living cells with formaldehyde, a cross-linking agent that results in covalent and reversible linkage between genomic DNA and associated proteins (Oberley et al., 2004; Ren and Dynlacht, 2004). The immunoprecipitated chromatin fragments are subsequently identified through hybridisation to tiling microarrays, which can represent the whole genome or specific regions (Lee et al., 2006).

Fifteen reports were found in the literature of chromatin immunoprecipitation by SF-1 (Table 4.1). These experiments have focussed largely on known SF-1 targets and used PCR or quantitative PCR (qPCR) for post-ChIP analysis. Data for SF-1 ChIP coupled to microarray analysis or an equivalent high-throughput method of sequence identification have not yet been reported in full.

Table 4.1. Summary of previous reports of SF-1 chromatin immunoprecipitation (ChIP) assays

Reference	Species	Cells used for SF-1 ChIP	Anti-SF-1 antibody used	Post-ChIP analysis
Mouillet et al., 2004	Mouse	LβT2 gonadotrope cell line	Upstate (06-431)*	PCR
Hong et al., 2004	Rat	R2C Leydig cell carcinoma cell line	Morohashi**	PCR
Hiroi et al., 2004	Mouse	MA10 Leydig tumour cell line and primary granulosa cells	Morohashi	qPCR
Curtin et al., 2004	Mouse	LβT2	not reported	qPCR
Gu et al., 2005	Mouse	Embryonic stem cells and P19 embryonic carcinoma cell line	Upstate (06-431)	PCR
Baba et al., 2005	Mouse	Primary granulosa cells	Morohashi	PCR
Weck and Mayo, 2006	Mouse	GRMO2 granulosa cell line	Affinity (mouse)	PCR
Song et al., 2006	Rat	R2C	not reported	PCR
Parakh et al., 2006	Human	KGN granulosa tumour cell line	Upstate	PCR
Gummow et al., 2006	Mouse	Primary adrenocortical cells	Upstate	qPCR
Dammer et al., 2007	Human	NCI-H295R adrenocortical tumour cell line	Upstate (07-618)	qPCR
Fan et al., 2007	Human	NCI-H295R	Morohashi	qPCR
Li et al., 2007	Human	NCI-H295R	Upstate (07-618)	qPCR
Doghman et al., 2007	Human	NCI-H295R	Upstate (07-618)	PCR
Campbell et al., 2008	Human	HEK293 embryonic kidney cell line	Upstate (07-618)	qPCR

*Upstate Millipore antibody 06-431 was discontinued in 2006, **antibody developed by the Morohashi laboratory, not commercially available (Morohashi et al., 1993)

4.2. Materials and methods

4.2.1. Overview of experimental design

A protocol for SF-1 ChIP-on-chip was established in NCI-H295R human adrenocortical tumour cells using Upstate Millipore's anti-SF-1 antibody 07-618 and Affymetrix's GeneChip Human Promoter 1.0R arrays (Figure 4.1A).

Based on published reports and on commercial availability, the anti-SF-1 antibody 07-618 from Upstate Millipore was chosen for chromatin immunoprecipitation. This is a rabbit polyclonal antibody generated against murine SF-1 that has been shown to successfully recognise human SF-1 by several groups and has been previously used for SF-1 ChIP in four independent studies from different research groups, three of which used NCI-H295R cells (Table 4.1) (Dammer et al., 2007; Li et al., 2007; Doghman et al., 2007; Campbell et al., 2008).

GeneChip Human Promoter 1.0R arrays (Affymetrix, High Wycombe, UK) are single tiling arrays covering approximately 25,500 promoter regions through over 4.6 million probes. Probe sequences were selected from NCBI human genome assembly build 34 (NCBIv34), based on gene annotation from Ensembl (as of May 2004) and NCBI GenBank's Refseq and complete-CDS mRNAs (as of February 2004 and December 2003, respectively). Probes are tiled at an average resolution of 35 bp (25-mer oligonucleotide sequences 10-bp apart from each other) to cover from 7.5 to 10 kb upstream and 2.5 kb downstream of every transcriptional start site (Figure 4.1B).This array platform was chosen given its ability to interrogate a large number of promoter regions in a single array.

Considering that chromatin immunoprecipitation is an enrichment relative to a reference and not an absolute measurement, the choice of reference sample (hybridisation control) is an important element of experimental design and a matter of debate within the field (Lee et al., 2006). Whilst a few initial reports opted for using chromatin immunoprecipitated by non-specific IgG (Iyer et al., 2001), most reports have used unenriched, genomic DNA (input chromatin) as a reference for comparison with DNA immunoprecipitated by the antibody against the transcription factor of interest (Ren et al., 2000; Carroll et al., 2006; Johnson et al., 2008). Therefore, input DNA chromatin was separated and used as reference in the present study.

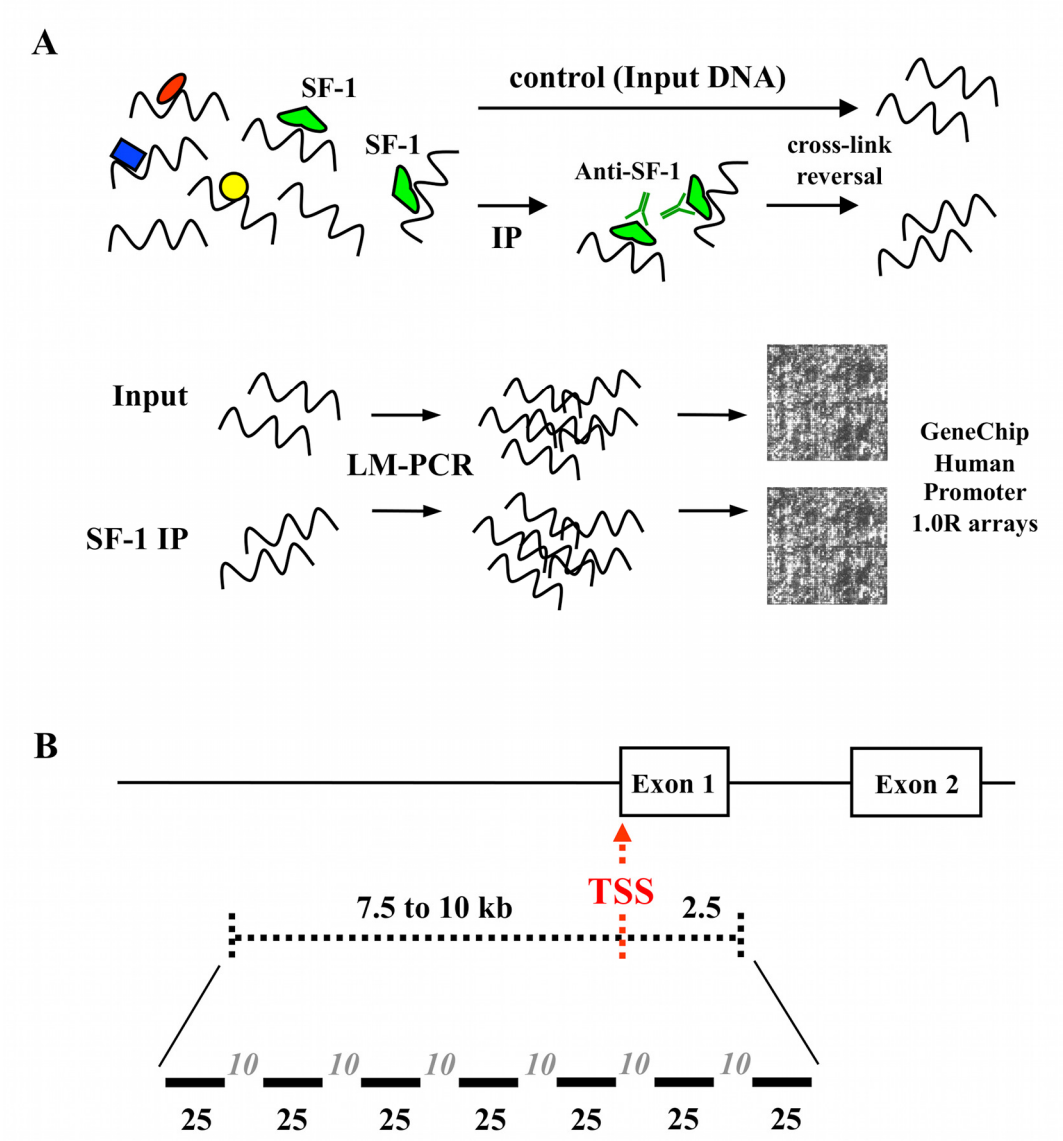

Figure 4.1. Overview of SF-1 ChIP-on-chip experimental design.

A, Schematic representation of SF-1 ChIP-on-chip protocol. NCI-H295R adrenocortical cells were fixed with formaldehyde to cross-link proteins to DNA, and chromatin extracted and fragmented by sonication. Fragments of chromatin to which SF-1 was bound were immunoprecipitated using a specific anti-SF-1-antibody, and the cross-link subsequently reversed, allowing purification of SF-1-IP and input DNA (control) samples. DNA samples were amplified by ligation-mediated PCR (LM-PCR) and hybridised to GeneChip Human Promoter 1.0R microarrays for identification of enrichment. B, Cartoon of promoter region coverage by GeneChip Human Promoter 1.0R arrays. In general, 7.5 to 10 kb upstream and 2.5 kb downstream of transcription start sites (TSS) are covered by 25-mer oligonucleotide sequences located 10 bp apart from each other. Approximately 25,500 promoter regions are interrogated per array, according to gene annotations based on the NCBI human genome assembly build 34 (March 2004).

4.2.2. Chromatin immunoprecipitation (ChIP)

Chromatin immunoprecipitation assays were performed using the ChIP-IT Express kit (Active Motif, Rixensart, Belgium) as described in section 2.2.24.

4.2.2.1. Optimisation of chromatin shearing

It was important to optimise chromatin fragmentation because long chromatin fragments are not as efficiently immunoprecipitated or detected on microarrays as are short fragments (Kim and Ren, 2006). It is generally recommended that chromatin fragments range from 200 to 1,000 bp in length, with the majority of fragments ideally being from 200 to 600-bp in length for efficient ChIP-on-chip (Lee et al., 2006).

Two methods of chromatin shearing were compared; sonication and enzymatic digestion. Sonication is a hydrodynamic shearing method and has been widely used for ChIP-on-chip (Ren and Dynlacht, 2004; Oberley et al., 2004). Notably, sonication protocols vary substantially according to cell type and equipment used. A literature review was undertaken to aid the design of sonication protocols appropriate to available equipment (Appendix 3), and sonication was performed as described in section 2.2.24.3. Enzymatic digestion of chromatin was recently introduced as an alternative to sonication, with potential advantages of being faster and less prone to operator-induced variability. Chromatin digestion was performed using a proprietary enzymatic cocktail from Active Motif (ChIP-IT Express Enzymatic), as described in section 2.2.24.2.

Optimal chromatin fragmentation was achieved by sonication at low amplitude, which resulted in a homogeneous smear with most fragments ranging from 200 to 600 bp in length (Figure 4.2, lane 6). Although easy to perform and effective,

enzymatic shearing resulted in a heterogeneous distribution of fragments, most of which were less than 200-bp long (Figure 4.2, lanes 2-4). Therefore, for all subsequent ChIP assays, chromatin shearing was obtained by sonication at low amplitude as described in section 2.2.24.3.

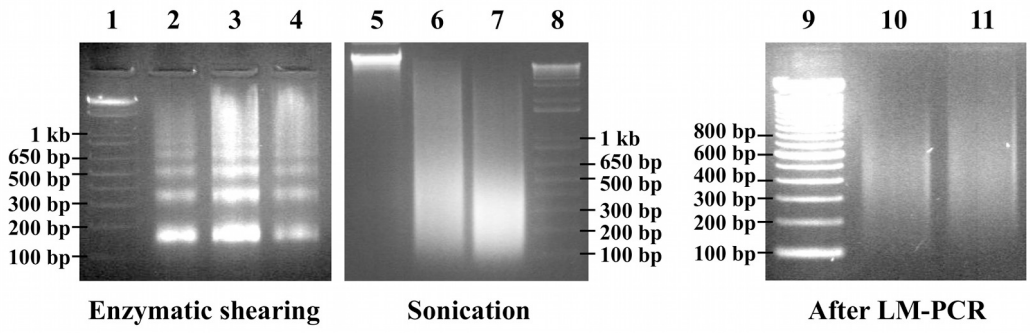

Figure 4.2. Verification of chromatin fragmentation.

Fragmentation was verified by electrophoretic separation of DNA on 1.5% (w/v) agarose gels. Lanes 2 to 4, chromatin fragmentation by enzymatic digestion for 10 min (lane 2), 15 min (lane 3) or 20 min (lane 4). Even though enzymatic shearing was effective, it resulted in a sequence-dependent heterogeneous distribution of fragments, not ideal for ChIP-on-chip. Lanes 6 and 7, chromatin fragmentation by sonication using low-amplitude (2µm, lane 6) or high-amplitude (10µm, lane 7) sonication protocols, in comparison to unfragmented chromatin (lane 5). The high-amplitude sonication protocol resulted in chromatin over-shearing, with most fragments ranging from 100 to 400 bp in length, whereas the low-amplitude protocol yielded a majority of 200 to 600-bp fragments and was selected for all experiments. Lanes 10 and 11, confirmation of adequate fragmentation range of input (lane 10) or SF1-IP (lane 11) DNA samples (300 ng) following two rounds of amplification by ligation-mediated PCR (LM-PCR). Lanes 1, 8 and 9, DNA size marker.

4.2.2.2. ChIP assays

ChIP assays were performed as described in section 2.2.24.5. Five independent SF-1 ChIP experiments were performed and are summarised in table 4.2. In each experiment, two SF-1 ChIP assays were performed in parallel to allow pooling of immunoprecipitated chromatin after purification.

Although it was possible to determine the DNA concentration of resulting SF-1-immunoprecipitated chromatin using NanoDrop 1000, measurements were commonly in low detection range (1-2 ng/µl) and, hence, might lack accuracy. Therefore, the yield shown in table 4.2 is likely to be an estimate.

In the first experiment, chromatin immunoprecipitation by non-specific IgG was performed in parallel to SF-1 ChIP to serve as a negative control for verification of enrichment for known SF-1 target promoters (ChIP-PCR, see below). Given the higher yield of immunoprecipitated chromatin, experiments 3, 4 and 5 were selected for subsequent microarray analysis. Samples from experiments 1 and 2 were not used further.

Table 4.2. Characteristics of the five SF-1 chromatin immunoprecipitation experiments performed

Exp	Cell culture passage	Cell count after fixation	Sheared chromatin DNA concentration	Sheared chromatin used for assay	Estimated SF-1 ChIP DNA yield
1	P4	5.7 x 10^7 cells	68.6 ng/µl	4.3 µg	50 ng
2	P4	8.5 x 10^7 cells	108 ng/µl	3.8 µg	45 ng
3	P4	10.8 x 10^7 cells	116 ng/µl	5.8 µg	70 ng *
4	P5	11 x 10^7 cells	120 ng/µl	6.0 µg	90 ng *
5	P5	7.8 x 10^7 cells	93.6 ng/µl	5.7 µg	85 ng *

Exp, experiment; P, passage number; Column 5 reflects the amount of chromatin used per ChIP assay while column 6 reflects an estimation (see below) of DNA yield of two SF-1 ChIP assays performed in parallel and pooled. *used for subsequent microarray analysis.

4.2.3. Chromatin immunoprecipitation microarray analysis (ChIP-on-chip)

It is well established that the DNA yield from ChIP assays is not sufficient for microarray detection (Johnson et al., 2008). Although initial reports relied on pooling several ChIP assays performed in parallel for microarray analysis (Weinmann et al., 2002), robust amplification methods have subsequently been developed allowing efficient generation of chromatin amplicons (Oberley et al., 2004). One such amplification method is ligation-mediated PCR (LM-PCR), which has been widely used in published reports (Ren et al., 2000; Carroll et al., 2005; Carroll et al., 2006).

SF-1-immunoprecipitated DNA from experiments 3, 4 and 5 and 50-ng aliquots of respective input DNA were amplified by LM-PCR as described in section 2.2.25.1 and shown in table 4.3. After two rounds of amplification by LM-PCR, aliquots of amplified DNA (input and SF-1-IP) were separated by electrophoresis in 1% (w/v) agarose gels and preservation of optimal fragmentation range was verified (Figure 4.2, lanes 10-11). Samples were stored at -20°C prior to hybridisation to microarrays.

All six samples (SF-1-IP 3, 4 and 5 and input DNA 3, 4 and 5) were prepared for and individually hybridised to six GeneChip Human Promoter 1.0R arrays by Dr Nipurna Jina at UCL Genomics as described in section 2.2.25.2. I was present throughout and was able to discuss the protocol with her.

Table 4.3. Amounts of DNA obtained after each of two complete rounds of amplification by LM-PCR

Exp	Input DNA		SF-1-IP DNA	
	After 1st round	After 2nd round	After 1st round	After 2nd round
3	1.16 µg	5.60 µg	1.99 µg	5.38 µg
4	0.89 µg	5.68 µg	0.27 µg	3.93 µg
5	1.37 µg	4.74 µg	1.43 µg	5.57 µg

Exp, experiment

4.2.3.1. Microarray data analysis

Quality control of raw microarray data (3 SF-1-IP arrays, 3 input DNA arrays) was performed by Dr Sonia Shah at the Bloomsbury Centre for Bioinformatics as described in section 2.2.25.3. Plotted histograms of the raw data intensity suggested that enrichment by SF-1 IP was suboptimal in experiment 4 (Appendix 4). Therefore, array data corresponding to SF-1-IP 4 and respective input were excluded from peak detection analysis.

The ChIP-on-chip peak detection tool CisGenome was used to define SF-1-binding regions according to the parameters detailed in section 2.2.25.3.

4.2.4. Confirmation of chromatin enrichment by PCR (ChIP-PCR)

In order to confirm chromatin enrichment by SF-1-immunoprecipitation, SF-1-IP, IgG-IP and input DNA samples were used as template for standard PCR-amplification (ChIP-PCR) of the promoters of known SF-1 targets, *CYP11A1* (Ito et al., 2000; Hu et al., 2001; Gizard et al., 2002; Guo et al., 2007) and *FATE1* (Doghman et al., 2007), and of the putative target *CITED2* (see Figure 4.3).

For amplification of the *CYP11A1* proximal promoter (100 bp upstream of the transcriptional start site [TSS]), forward and reverse primers were designed using

Primer3Plus: F, 5'-AGAAATTCCAGACTGAACCTTCATA-3' and R, 5'-CTGTGACTGTACCTGCTCCACTTC-3' (198-bp amplicon). For amplification of the proximal *FATE1* promoter (140 bp upstream of TSS), primers reported by Doghman et al. (2007) were used: F, 5'-TAGCAGAGGAGAAGGCCACT-3' and R, 5'-GCTATGGCTAAGGATGCACA-3' (202-bp amplicon). For amplification of the *CITED2* distal promoter (3.0 kb upstream of TSS), primers were designed using Primer3Plus: F, 5'-CGGGAAACCACCAAAAGC-3' and R, 5'-AAGCAATGGCGAAAACTGTAA-3' (200-bp amplicon). As a negative control for SF-1 binding, primers amplifying exon 2 of *PBX1* were used: F, 5'-TGTTTTCACCCTGTGCATTATC-3', R, 5'-AGATTTGTGACTGCTGGTTAAG-3' (223 bp long amplicon). PCR reactions were performed and amplification products visualised as described in section 2.2.24.7.

4.2.5. *In vitro* studies of promoter activation by SF-1

SF-1-responsiveness of ChIP-on-chip-identified targets, *CITED2* and *ANGPT2*, were studied through luciferase reporter gene assays. Activation of the promoters of these genes by wild type SF-1 was compared to that elicited by the naturally occurring G35E mutant SF-1, known to have impaired transactivational activity *in vivo* and *in vitro* (Achermann et al., 1999; Ito et al., 2000). The generation of *CITED2* promoter reporter constructs and details of luciferase assays involving these constructs have already been described in Chapter 3, section 3.2.3.

4.2.5.1. *ANGPT2* promoter constructs

The 5.0 kb 5'-upstream sequence of *ANGPT2* (transcript ENST00000325203, Ensembl release 54 [NCBIv36]) was analysed for putative SF-1 binding sites using MatInspector as described in section 2.2.18.1. Based on the position of predicted

sites, the 4.5-kb, 1.9-kb and 1.1-kb upstream sequences of the *ANGPT2* promoter were PCR-amplified and individually cloned into a pGL4.10[luc2] luciferase reporter vector following the protocols described in sections 2.2.18.2 to 2.2.18.4. Insert sequences were fully verified by direct sequencing.

4.2.5.2. Luciferase reporter gene assays

Co-transfection of reporter constructs and pCMX expression vectors containing SF-1 cDNA (wild type or mutant G35E) was performed according to the protocol described in section 2.2.20. In all studies, 7.5 ng/well of internal control pRL-SV40 reporter was co-transfected to allow firefly luciferase activity normalisation by *Renilla* luciferase in Dual-Luciferase reporter assays.

In order to analyse the effects of SF-1 on *ANGPT2* regulation according to promoter length, SF-1-dependent activation of the three *ANGPT2* promoter constructs was studied in NCI-H295R cells using 50 ng/well of expression vector (empty pCMX, pCMX-WTSF1 or pCMX-G35ESF1) and molar equivalent amounts of reporter vector: 61.9 ng/well of pGL4-ANGPT2pro1.1kb (size 5494 bp), 70.8 ng/well of pGL4-ANGPT2pro1.9kb (size 6284 bp), 100 ng/well of pGL4-ANGPT2pro4.5kb (size 8876 bp) or 47.8 ng/well of 'empty' pGL4.10[luc2] backbone (size 4242 bp; for background assessment). The total amount of DNA transfected was kept constant at 157.5 ng/well by adding empty pCMX vector as necessary.

Activation of the 4.5-kb *ANGPT2* promoter by SF-1 was studied further using increasing amounts of pCMX-SF1 (WT or G35E) expression vectors (10, 50 and 100 ng/well) and 100 ng/well of pGL4-ANGPT2pro4.5kb. Total DNA transfected was kept constant at 207.5 ng/well.

In all studies, cells were lysed 24 h after transfection and luciferase assays performed as described in section 2.2.20.2.

4.2.6. Assessment of gene function and network analysis

MetaCore software (GeneGo Inc.; www.genego.com) was used to investigate the functional annotations and potential network interactions of genes identified as putative novel SF-1 targets from the ChIP-on-chip analysis, as described in section 2.2.26.1. Genes were selected based on the criteria for protein-binding regions described in section 2.2.25.3 and where the identified site was within 10 kb upstream and 3 kb downstream of a recognised transcriptional start site.

4.2.7. Immunohistochemistry of SF-1 and Ang2

Fetal adrenal tissue (Fetal Stage 1, 8 weeks post-conception) was obtained from the Human Developmental Biology Resource (HDBR, www.hdbr.org) with Research Ethics Committee approval and informed consent. Immunofluorescent detection of SF-1 and Ang2 was performed by Dr Rahul Parnaik in our group, as described in section 2.2.16. Simultaneous overnight incubation was performed with the following primary antibodies: mouse anti-human SF-1 (434200, Invitrogen; 1:200 dilution) and rabbit anti-human angiopoietin-2 (ab65835, Abcam Plc., UK; 1:200 dilution). The secondary antibodies Alexa647 goat anti-mouse antibody (A21235, Invitrogen; 1:400 dilution) and Alexa555 goat anti-rabbit (A21429, Invitrogen; 1:400 dilution) were used for detection.

4.3. Results

4.3.1. Validation of chromatin enrichment

Chromatin enrichment by immunoprecipitation with the anti-SF-1 antibody was confirmed by PCR-amplification of the promoters of known SF-1 targets, *CYP11A1* and *FATE1* (ChIP-PCR, Figure 4.3). SF-1 regulation of *CYP11A1* is well-established (Ito et al., 2000; Hu et al., 2001; Gizard et al., 2002; Guo et al., 2007), and SF-1-binding in the *FATE1* promoter, determining transcriptional activation, has recently been shown in NCI-H295R cells (Doghman et al., 2007). Activation of the *CITED2* promoter by SF-1 was shown *in vitro* by the experiments described in Chapter 3, and binding of SF-1 to the *CITED2* promoter was confirmed by ChIP-PCR (Figure 4.3). Exon 2 of *PBX1*, which is located 3.4 kb downstream of the transcriptional start site and does not bear SF-1-binding sites, could not be amplified from SF-1-IP DNA, confirming specificity of chromatin enrichment by ChIP.

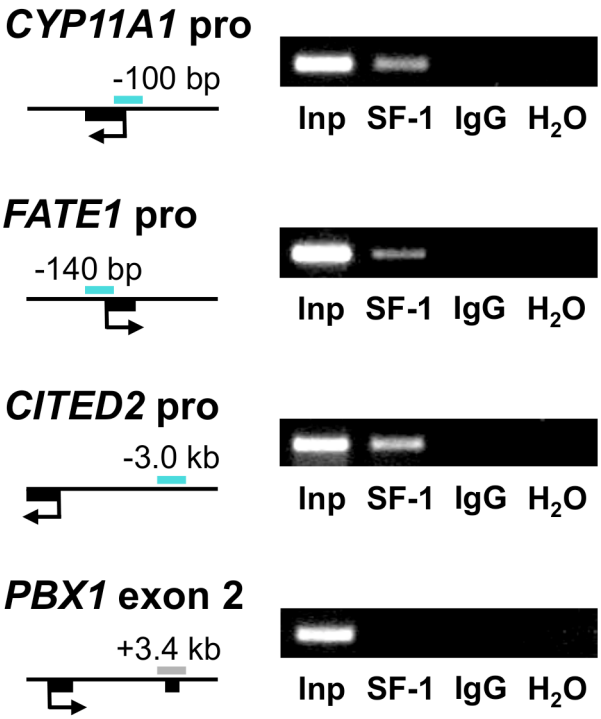

Figure 4.3. Validation of chromatin enrichment by ChIP-PCR.

Proximal promoters of known SF-1 targets *CYP11A1* and *FATE1* were amplified from anti-SF-1 immunoprecipitated DNA (SF-1) but not from anti-IgG immunoprecipitation (IgG). Furthermore, detection of the distal promoter of *CITED2* was also enriched by anti-SF-1 immunoprecipitation. Exon 2 of *PBX1*, which is not expected to bear SF-1-binding sites, was used as negative control for enrichment. Cartoons show the position of amplicons in relation to transcriptional start sites, which are represented by arrows indicating the start and direction of transcription (exons are represented by black bars). Inp, 0.2% input DNA. From Ferraz-de-Souza et al., 2010b. Copyright 2010, The Federation of American Societies for Experimental Biology.

4.3.2. Characterisation of SF-1-dependent regulation of *CITED2*

The ChIP-on-chip analysis identified a binding region in the *CITED2* promoter (Chr6:139,739,907-139,740,330; NCBIv36) peaking at approximately 2.9 kb upstream from the transcriptional start site (TSS; located at Chr6:139,737,478) with a moving average (MA) Z-score of 4.44, corresponding to 4.44 S.D. above the mean (Figure 4.4A). As described in section 3.3.2, *in silico* analysis of the 5.0 kb upstream sequence of *CITED2* with MatInspector software revealed four putative SF-1 binding sites at 3080, 1247, 665 and 458 bp upstream of the TSS (Figure 4.4B, upper panel). Three different length promoter reporter constructs were designed to investigate differential activation of the *CITED2* promoter by SF-1 in luciferase assays. Activation of a 3.3-kb *CITED2* promoter construct by SF-1 was greater than that of the 900- and 600-bp promoter constructs, consistent with the prediction from ChIP-on-chip analysis (Figure 4.4B, lower panel).

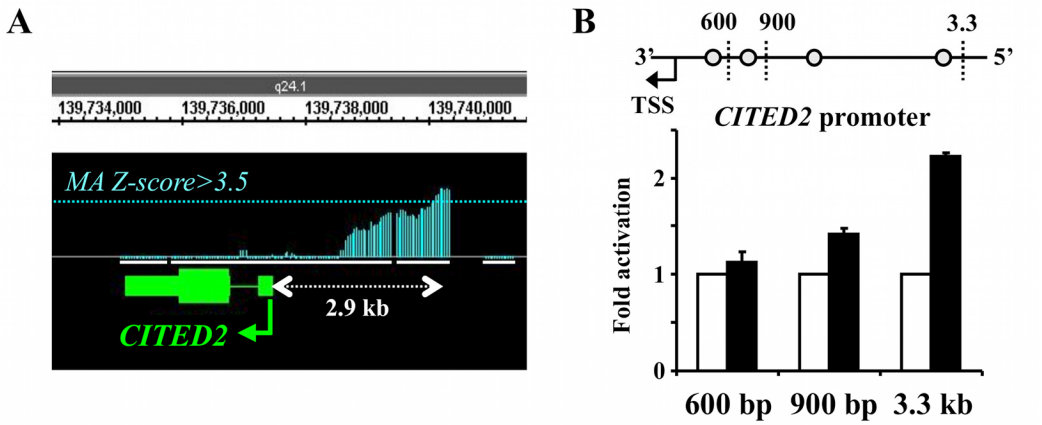

Figure 4.4. Characterisation of SF-1-dependent regulation of *CITED2*.

A, A SF-1-binding region was identified by ChIP-on-chip in the *CITED2* promoter, peaking at approximately 2.9 kb upstream from the transcriptional start (visualised using the Integrated Genome Browser). The blue dotted line represents the threshold for MA Z-score>3.5 and the white solid bar represents array coverage of the *CITED2* promoter. B, Upper panel, Cartoon representation of putative SF-1-binding sites (white circles) identified by MatInspector in the *CITED2* promoter and their relation to the different reporter constructs studied (600-bp, 900-bp and 3.3-kb in length); Lower panel, Activation of different length *CITED2* promoter constructs by SF-1 (25 ng) in luciferase assays. Consistent with the prediction from ChIP-on-chip analysis, SF-1-dependent activation (black bars) of the 3.3-kb construct was greater than that of the 900- and 600-bp constructs (3.3 kb > 900 bp, P<0.001; 3.3 kb > 600 bp, P<0.0001). White bars represent transfection with empty expression vector. Data are presented as mean ± SEM of at least three independent experiments, each performed in triplicate. From Ferraz-de-Souza et al., 2010b. Copyright 2010, The Federation of American Societies for Experimental Biology.

4.3.3. Identification of novel SF-1-binding sites by ChIP-on-chip

Analysis of ChIP-on-chip experiments with CisGenome identified 738 SF-1-binding regions that met criteria of an MA (moving average) score more than 3.5 mean ± S.D. and a false discovery rate of less than 5%. Subsequent analysis focussed on those regions that were located between 10 kb upstream and 3 kb downstream of the TSS of known genes (as defined by HGNC), in keeping with the design of the Human Promoter 1.0R arrays. Using this approach, binding regions were annotated to 445 gene loci (full data set shown in Appendix 5). The distribution of immunoprecipitated sequences revealed greater density of SF-1-binding sites around 2.5 kb upstream and 1.5 kb downstream of TSSs (Figure 4.5).

Binding regions surrounded the transcriptional start site of 397 unique genes. More than one SF-1-binding site was identified in the defined -10 kb < TSS < +3 kb region of 35 genes: of these, 27 genes had two binding sites, 4 genes had three, 3 genes had four and 1 gene had five SF-1-binding sites (Appendix 6). Top-ranking TSS-neighbouring binding sites (MA Z-score >5.0) are detailed in Table 4.4.

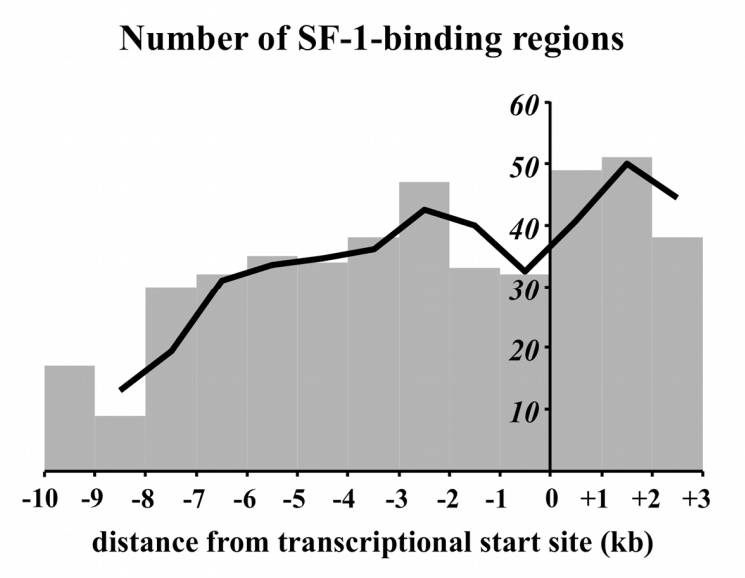

Figure 4.5. Distribution of SF-1-binding regions neighbouring transcriptional start sites (TSS).

A greater density of SF-1-binding sites is observed approximately 2.5 kilobases (kb) upstream (-) and 1.5 kb downstream (+) of transcriptional start sites, with peaks greater than +1 SD from the mean. The solid line represents a 2-point moving average for the data set. From Ferraz-de-Souza et al., 2010b. Copyright 2010, The Federation of American Societies for Experimental Biology.

Table 4.4. Top-ranking SF-1-binding regions located from 10 kilobases (kb) upstream to 3 kb downstream of a transcriptional start site

MA Z-score	Chr	Start	End	Region length	Distance to TSS	Gene	Gene Name	Selected GO Biological Process/*Molecular Function*
8.02	19	61052876	61053237	362	-2142	*NLRP4*	NLR family, pyrin domain containing 4	*ATP binding; nucleotide binding; protein binding*
7.26	4	606174	606996	823	-2787	*PDE6B*	phosphodiesterase 6B, cGMP-specific, rod, beta	detection of light stimulus; response to stimulus; signal transduction
7.22	3	8671294	8671558	265	-2690	*C3orf32*	chromosome 3 open reading frame 32	(Mouse: protein folding; *heat shock protein binding*)
7.14	13	113199316	113199973	658	-6621	*DCUN1D2*	DCN1, defective in cullin neddylation 1, domain containing 2 (S. cerevisiae)	
6.81	9	99502264	99502676	413	-3011	*XPA*	Xeroderma pigmentosum, complementation group A	DNA damage removal; signal transduction resulting in induction of apoptosis; response to oxidative stress
6.51	15	20377626	20377881	256	-7189	*TUBGCP5*	tubulin, gamma complex associated protein 5	microtubule cytoskeleton organization; microtubule nucleation
6.17	13	113367394	113368774	1381	-7583	*ATP4B*	ATPase, H+/K+ exchanging, beta polypeptide	ion transport; ATP biosynthetic process; response to lipopolysaccharide
					-1513	*GRK1*	G protein-coupled receptor kinase 1	positive regulation of phosphorylation; signal transduction; apoptosis
6.12	3	8672091	8672356	266	-3487	*C3orf32*	chromosome 3 open reading frame 32	(Mouse: protein folding; *heat shock protein binding*)
5.84	14	92455627	92456518	892	-3172	*CHGA*	chromogranin A (parathyroid secretory protein 1)	regulation of blood pressure; *protein binding*
5.78	19	3123496	3123904	409	-6065	*S1PR4*	sphingosine-1-phosphate receptor 4	G-protein coupled receptor protein signaling pathway; elevation of cytosolic calcium ion concentration
5.61	8	6411196	6412323	1128	-3588	*ANGPT2*	angiopoietin 2	angiogenesis; blood vessel morphogenesis; multicellular organismal development
5.49	13	113149179	113149920	742	1908	*ADPRHL1*	ADP-ribosylhydrolase like 1	protein amino acid de-ADP-ribosylation; *magnesium ion binding*
5.49	19	40729390	40729965	576	1293	*TMEM147*	transmembrane protein 147	*protein binding*
5.36	2	183644509	183645199	691	-6877	*DUSP19*	dual specificity phosphatase 19	protein amino acid dephosphorylation; inactivation of MAPK activity; JNK cascade

MA Z-score	Chr	Start	End	Region length	Distance to TSS	Gene	Gene Name	Selected GO Biological Process/*Molecular Function*
5.30	7	43878032	43878592	561	-2643	*MRPS24*	mitochondrial ribosomal protein S24	translation; *structural constituent of ribosome*
5.24	9	110664647	110665656	1010	-7121	*ACTL7B*	actin-like 7B	*protein binding; structural constituent of cytoskeleton*
					728	*ACTL7A*	actin-like 7A	*protein binding; structural constituent of cytoskeleton*
5.21	22	22563867	22564131	265	-2565	*MIF*	macrophage migration inhibitory factor (glycosylation-inhibiting factor)	positive regulation of ERK1 and ERK2 cascade; negative regulation of apoptosis
5.19	21	44030889	44031745	857	-2541	*RRP1*	ribosomal RNA processing 1 homolog (S. cerevisiae)	rRNA processing
5.14	9	130885372	130885644	273	2282	*DOLPP1*	dolichyl pyrophosphate phosphatase 1	protein amino acid N-linked glycosylation; *catalytic activity*
5.12	7	43881830	43882948	1119	-6720	*MRPS24*	mitochondrial ribosomal protein S24	translation; *structural constituent of ribosome*
5.08	2	121263371	121263617	247	-2832	*GLI2*	GLI family zinc finger 2	mammary gland development; positive regulation of transcription; developmental growth; *transcription factor activity*
5.08	3	12804229	12804769	541	-8671	*CAND2*	cullin-associated and neddylation-dissociated 2 (putative)	regulation of transcription; *transcription activator activity; TATA-binding protein binding*
5.07	3	48450915	48451316	402	-9370	*PLXNB1*	plexin B1	multicellular organismal development; intracellular signaling pathway
					-5574	*CCDC72*	coiled-coil domain containing 72	
5.07	9	139889204	139889711	508	-2604	*CACNA1B*	calcium channel, voltage-dependent, N type, alpha 1B subunit	calcium ion transport; transmembrane transport; *voltage-gated calcium channel activity*
5.06	15	38971991	38972237	247	-1805	*VPS18*	vacuolar protein sorting 18 homolog (S. cerevisiae)	protein transport; endosome organization
5.05	15	73417958	73418364	407	-8301	*NEIL1*	nei endonuclease VIII-like 1 (E. coli)	DNA repair; metabolic process; negative regulation of nuclease activity
					2735	*COMMD4*	COMM domain containing 4	*protein binding*
5.04	7	43924834	43926219	1386	-7045	*UBE2D4*	ubiquitin-conjugating enzyme E2D 4 (putative)	regulation of protein metabolic process; post-translational protein modification

Chromosomal coordinates (NCBIv36) and length (bp) of SF-1-binding regions meeting criteria of an MA Z-score higher than 5.0 are shown. For each region, distances (bp) to transcriptional start sites (TSS) of neighbouring genes are detailed (negative if upstream of TSS, positive if downstream of TSS). Selected gene ontology (GO) annotation, when available, is also provided. From Ferraz-de-Souza et al., 2010b. Copyright 2010, The Federation of American Societies for Experimental Biology.

4.3.4. Angiopoietin 2 (ANGPT2) as a target of SF-1

In order to identify potential networks of target genes being regulated by SF-1, the gene loci data set was analysed using the MetaCore platform of GeneGo systems biology software. Network analysis, based on GeneGo's curated integrated database of human protein-protein and protein-DNA interactions and drawn by MetaCore software around the experimental data set, revealed several potential gene interaction networks focussing on established nuclear receptor systems (Figure 4.6). Functional enrichment analysis revealed that experimental targets mapped to biological processes related to blood vessel morphogenesis (p=0.002) and regulation of angiogenesis (p=0.027) (Figure 4.7). ChIP-on-chip-identified SF-1 binding targets involved in such processes included *ADORA3*, *ANGPT2*, *CXCR4*, *GLI2*, *HTR1A*, *PLCD1*, *S100A7*, *SP1* and *SPARC*, among others.

Considering that ChIP-on-chip experiments were performed on an adrenocortical tumour cell line, and that SF-1 may play an important role in adrenal tumorigenesis, experimentally identified SF-1 targets were compared to published data sets of adrenocortical tumour gene expression in children (West et al., 2007) and adults (Giordano et al., 2009; Soon et al., 2009) (Table 4.5). Angiopoietin 2 (Ang2, encoded by *ANGPT2*) (MIM 601922) emerged as a common factor in all these data sets and within a GeneGo angiogenic process network.

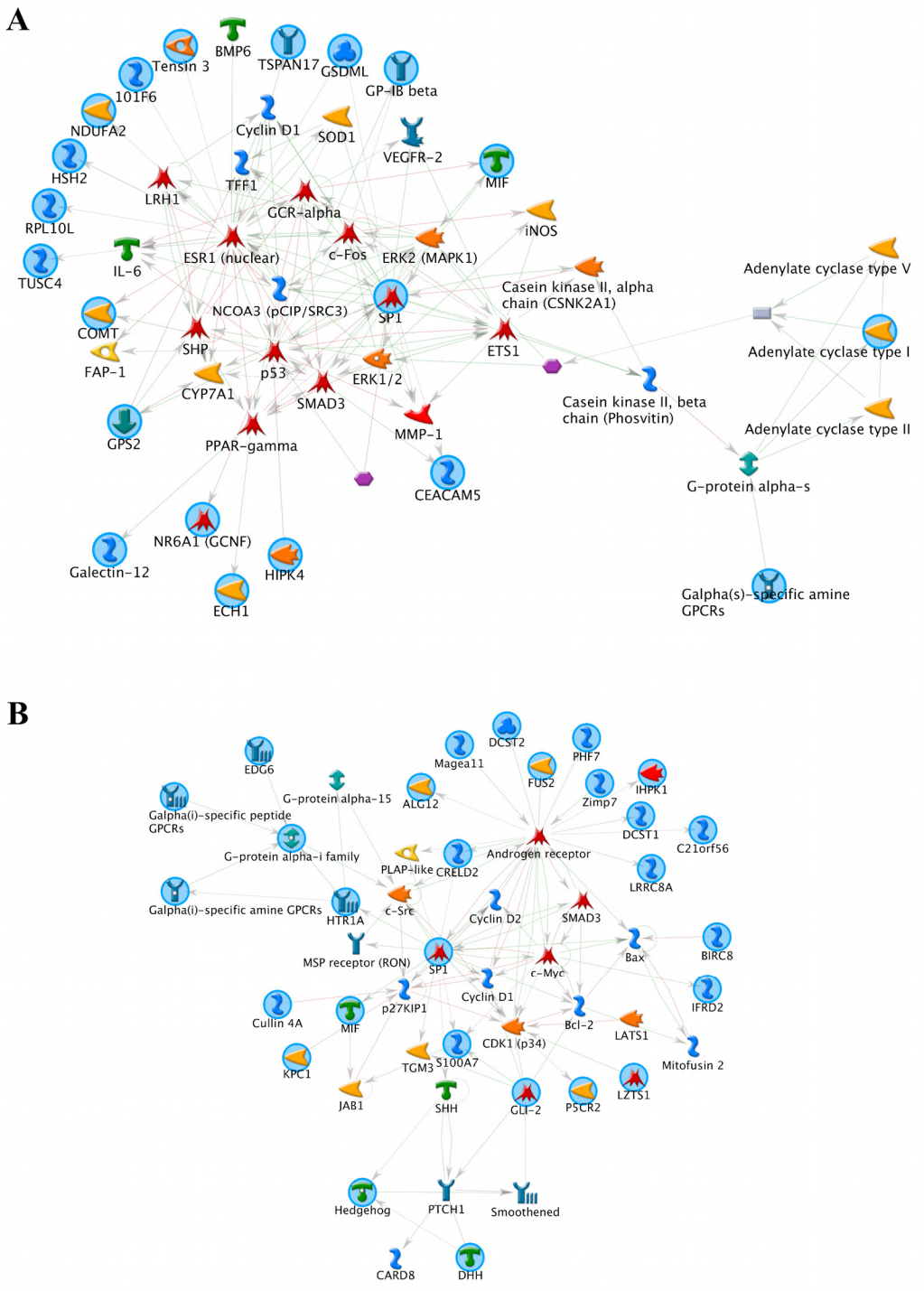

Figure 4.6. Network analysis of experimentally identified SF-1 targets.

A, Highest, and B, second-highest identified networks from 397 unique experimental SF-1 target genes. Blue circles indicate SF-1 targets identified by ChIP-on-chip. Potential gene interaction networks were investigated using Metacore software ('Analyze Networks (AN) algorithm').

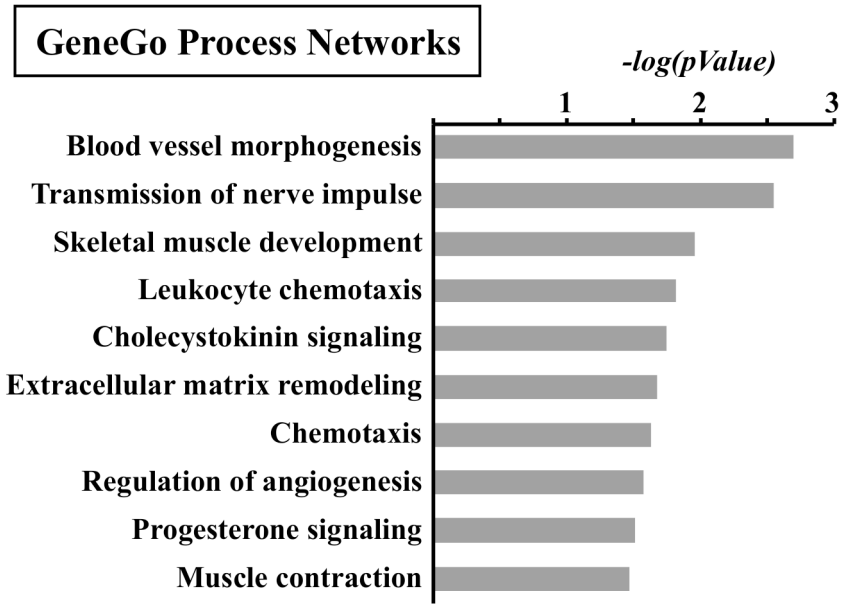

Figure 4.7. Functional annotation enrichment analysis of experimental data set. **The analysis was performed using MetaCore software at GeneGo; GeneGo Process Networks consist of approximately 110 cellular and molecular processes where content is defined and curated by GeneGo, representing a pre-set network of protein interactions characteristic for each process.**

Table 4.5. Comparison of experimental SF-1 targets to published adrenocortical tumour gene expression data sets

MA Z-score	SF-1 Target	Giordano et al., 2009	West et al., 2007	Soon et al., 2009
5.61	*ANGPT2*	+	+	+
4.79	*SHMT2*	+		
4.58 3.84	*YKT6*	+	+	
4.74	*TBRG4*	+		
4.18	*SLC31A2*		+	
4.07	*PCSK6*	+	+	
3.97	*SPARC*		+	
3.96	*RGS3*	+		
3.83	*KPNA4*	+		
3.76	*TSPAN17*	+		
3.73	*DOLK*		+	
3.70	*ATAD2*	+		
3.68	*CREB5*	+		
3.65	*LPCAT4*	+		
3.63	*NR6A1*	+		
3.55	*CDC20*	+		
3.54	*KIF3C*		+	

ChIP-identified SF-1 targets that have been found to be overexpressed in adrenocortical carcinomata in comparison to adenomas (Giordano et al., 2009, and Soon et al., 2009) and in paediatric adrenocortical tumours in general (West et al., 2007). Two independent SF-1 binding regions were identified at the *YKT6* gene loci. From Ferraz-de-Souza et al., 2010b.

4.3.5. Characterisation of *ANGPT2* regulation

The SF-1 binding region identified in the *ANGPT2* promoter by ChIP-on-chip spans 1.1 kilobases from Chr8:6,411,196 to Chr8:6,412,323 (NCBIv36) with an MA Z-score of 5.61 (Figure 4.8A). Since the transcriptional start site of *ANGPT2* is at Chr8:6,408,174 (in the reverse strand) in that genome assembly, ChIP-on-chip data predicted the binding region to be located from 3.0 to 4.1 kb upstream of the TSS. Analysis of the 5.0 kb upstream sequence of *ANGPT2* with MatInspector identified 20 putative SF-1 binding sites, 18 of which clustered in a highly-repetitive region between 3.1 to 4.1 kb upstream of the TSS, in accordance with the experimental data (Figure 4.8B). To confirm these findings, reporter vectors containing variable lengths of the *ANGPT2* promoter (1.1 kb, 1.9 kb and 4.5 kb) were constructed and activation by SF-1 in NCI-H295R human adrenal cells was assessed by luciferase assays. Shorter promoter fragments (1.1 and 1.9 kb) were not activated by wild type SF-1 (Figure 4.9A), whereas dose-dependent activation of the 4.5 kb *ANGPT2* promoter construct was seen (Figure 4.9B). This activation was lost when the functionally-impaired G35E mutant SF-1 construct was used.

A

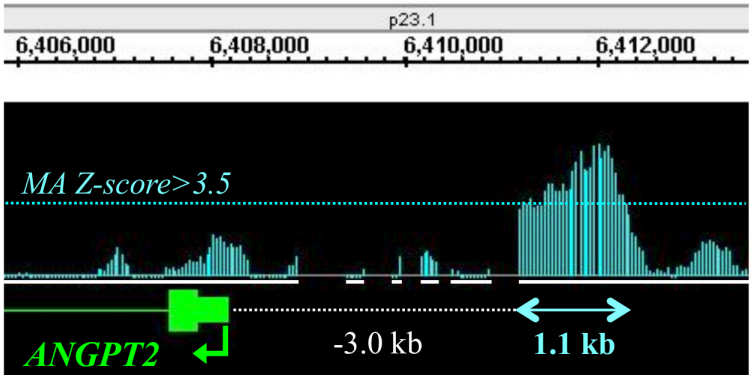

B

agttctgagatcccccctagtcaagcctcatttagagtgaaggggtcccagatgggtggcctcagacccccaggctgcatggtggtgttac
tggacacccacaactccaggctttgcacctaatgccttcaagggcctcccattggctccccgaggcttcctggtcagtggcctggcagac
catgtctccacttccctaggggccacagctgagcgcccatccatgcacacttgcatcccaggccacttcctggcccctctccccacctgg
catccttaattcacttcagtgtggcactttctctaagcacctattctatcccgttagtaagcccctgtaagcagccacacagaaggctga
gccgaggcaccagtcctcccctgttcacacggtggtcactgcaccgtgtgcactatccatggccttgccgatcaaacatggtcaccgcac
cgtgtgcactatccatgaccttgcggatcacacatggtcatcgcaccgtgtacactatccatgaccttgcggatcacacacggtcaccgc
actgcatgctctatcatggccttaccgatcacacacggtcaccgcaccacgtgcactatccatggccttgctgatcatacatggacacca
cgccacgggcactatccatggccttgccgatcacacacggtcaccgcaccgcgtgcactatccatggccttgccgatcacacacggtcac
cacaccgcgtgcactatccatggccttgccgatcacacatggtcaccgcaccgcgtgcactatctatggccttgccgatcacacacggtc
accgcaccgcgtgtactatccatggccttgccgatcacacacggtcaccgcaccgcgtgcactatccatggccttgccgatcacacatgg
tcaccgcaccgcgtgtactatccatggccttgctgatcacacatggtcaccgcaccgtgtgcactcactatccatggccttgcggatcac
acacggtcaccacaccataagcactgtcgatggtcatgccaatcacacatggtcaccgcaacacgtgcactatccatggccttgccgatc
acacacggtcaccgcaccacgttcactatccatggccttgccaatcacacagggtcaccgcaccacatgcactatccatggccttgccga
tcacacatggatacccacaccacgggcactatccacggccttgctgatcacacatggtcaccgtgctgtgtgccctgttaatggccatgcc
gaccacaggtggtcactgtactgtgtgcactctccatggccttgctgaccacacacggtcgctgcacggcgtacagtgtcaatagccttg
ctcgccacacacggttattgcactgtgtggactgtggatggccttgctgaccacacacggtggttgctgcactgtgtgtactgctgacag
ccttgccaaccacacacggtcaccacaccgcgtgcactgtggacggccttgcccagcacctcctacccccacagaccacctaggctctca
gaggccagcaagctacagtccaggcccggttctcaacagcctatgagctaagaatggttttaaacttttaaatgattgcagaaaatagca
atctttcatgatgtgaaaattacaagaaattcaaatttcagtatcacgaataaagctttattggagcccagcacgctcactcagttaatg
ctgtcccacagctgctttgcaccgcattacctttgagtggtggcgatggtggccgtatagcctgcagagccgaaaataattaccatctga
cactggacagagtttgccaactccggctctactagagcttcccctgactctctggttccgataatttccatttaggaatctacaaagagc
tgttccttccatgttcggaacttgagggaatttgaaaaggatggagtccatgccagctgcacatggcatattgtgcacccggaagcatca
ctgtctttctttgtgctccgactgctctctcttaccacatccaatttgtttatgggtctctccctctccatacactattagcttctctttag
gtcagacacccagttgccttaatctctatcccccagtgcatagcatggtgtctgcacacaaggctggtagacaaaaagtactgtggtgtgcc
ctctttctatttgttccttttaaactactctatttgcctggaagacaactgaatgacttttaaaaccatatatgcaggccaggtacagtg
gctcacacctgtgatcccagcactttgggaggccaagcaagaggatcattggatgccaggagttcaagaccagcctgggcaacaagagtg
agaccccgtctctacaaaaaatacttagaaaaaggtaaaaccacatatgtgatattaatacctacaatatgcttttcaaacaggaa
ataaaaaaaattgtaccctatgccactgccactgctttgcattcagagaatagcagagttatactatttgatggtggaagaactgatcccc
atttaatggagcatgcctgtaaagaaaaggaacaaatatttctaaacatacaattatatcttaatcctaaaaaccctacagagaaaaaat
gatctccatcttatgactagggagactgaggctccaagaatggaagcatttgctggaggtcacacagaagcagggttctaacacaggtct
catctttaagacctatatgcttttcttcgacggtgcactgtccggatgggtatagcatctttaattggttcccttagtggaaaccatgtcc
agaaccttggtggaatcatactacctcttctactaatgagatccttccagagcatgtcttccagcttttctgtgtgacagaaccctttgg
ttgtctggtgaagcctataaacacctttctcaaaagaagacacatgctactttattccaatgttcagtagcaagatctagggctgggttta
ataaaaatgtagttctgagtattgtggcagcaaataaaaagagctgatttctgaggatgagaaagtcacagatattcacactgttgttcg
ttaactattcattgataagggaaaggctgtctttcggttagagcttagtaaaaaataaagatcttttatgggtagatgtggtctgttaag
tcagtgtaccagctattcagcgctcactgggaataataaaccttgtaccttgagagataaaccgcagcaaaggcaggggtcttttccct
atgtacacttgggctgctgagttaacatattattaatctctgaagtattaagttttagttgttaaaggaagtgacttgcagaacttacag
agccataggattgaaggtgaaaaatcttgtgagtgcaccccttgaattgcacagatgaggacattagagcttaattaaaacagggaagtg
acttgcccgagtctaatacccaaggggactaatgtaattgatgaatgtgttacaaaatgctgagatgtcaacaaattctgacacaataaag
aagtttgtggccaggcatggtgactcacacctgtaatctcagcactttgggaggccaaaggcgagtcgatcacaaggtcatgagtttga
gaccagcctaacatggtgaaaccctgtctctactaaaaatacaaaaattagccgggtgtggtggcgtttgcctgtaatcccagctgctca
ggagcctgaggcaagagaatcacttgaacccggaaggcggaggttgcagtgagccaacattgccccactgcactctagcctggtcgacag
agcgagactccgtctcaaaaaaaaaaaaaaaaaaaaaaaaagtttgtattcctctttctacacaggcacttaaattctaatttctctattgt
aatgtaatgaacttaatcagtacagtgtatttttagagtgaatatccaagtggagttttttaaagaataaaggtcagagctcagaaact
gatgtttctaacgtgacttaataacagatctttctatccaactgttcggaaatgaaaatcttttgtaacttggctagtggttcaagaatc
aactaaaatcaatgaatctatttttccctctgaaaaggcacacgtttacaggagccaaacttcttcctctttatttgtaataacaaaaat
aaaccgaagtcctgacctatttgtaatatttttattcctaaaggaaaaaacaggaactttcattgtacttcaacattaaagttattacct
cagatattttgccagcttagcacggcaaaaatcagtttcagacaaaagagatcaactgctctctctaggaaatacttaattggggtggtg
cctaggaaatgcccaggggtcctgtaacagatcggttttcccagagggtttctgcagcatgggtcctggttggagggcaggcattctgc
tctgatttttcctgttgcctggctagtgacccccctacaggaagatcaccggctaagccaggagggcggagcagccccactacacatgtctgg
ctgctcttatcaacttatcatataaggaaaggaaagtgattgattcggat**ACTGACACTGTAGGATCTGGGGAGAGAGGAACAAAGGACC**
GTGAAAGCTGCTCTGTAAAAGCTGACACAGCCCTCCCAAGTGAGCAGGACTGTTCTTCCCACTGCAATCTGACAGTTTACTGCATGCCTG

Figure 4.8. SF-1-binding on the *ANGPT2* promoter.

A, ChIP-on-chip identified a 1.1-kb SF-1-binding region in the promoter region of *ANGPT2* located from 3.0 to 4.1 kb upstream of the transcriptional start. The blue dotted line represents the threshold for MA Z-score>3.5 and the white solid bar represents array coverage. B, Consistent with this, *in silico* analysis of the upstream sequence of *ANGPT2* with MatInspector identified 20 putative SF-1 binding sites (highlighted in grey), 18 of which clustered in a highly repetitive region between 3.1 to 4.1 kb upstream of the TSS (*ANGPT2* transcribed sequence shown in bold and underlined; transcript ENST00000325203, Ensembl release 54 [NCBIv36]). From Ferraz-de-Souza et al., 2010b. Copyright 2010, FASEB.

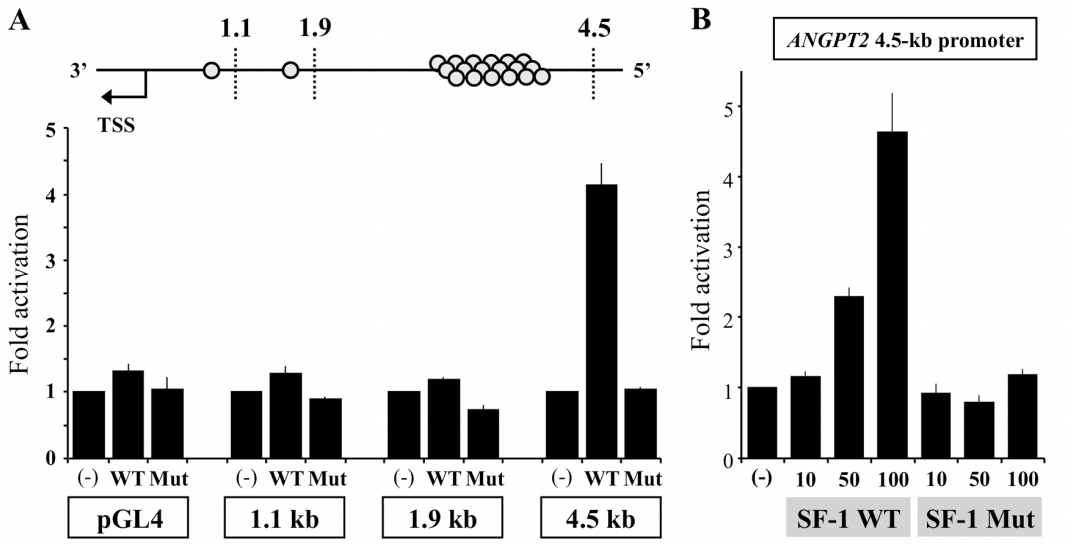

Figure 4.9. SF-1-dependent regulation of *ANGPT2*.

A, Upper panel, Cartoon representation of putative SF-1-binding sites (white circles) identified by MatInspector in the *ANGPT2* promoter in relation to the three different length reporter constructs studied (1.1 kb, 1.9 kb and 4.5 kb; TSS, transcriptional start site); Lower panel, pGL4 reporter vectors containing variable lengths of the *ANGPT2* promoter (or empty, for background assessment) were co-transfected into NCI-H295R human adrenal cells with either wild type SF-1 (WT), mutant G35E SF-1 (Mut) or empty (-) expression vectors 24 hours prior to luciferase assays. While shorter promoter fragments (1.1 and 1.9 kb) failed to be activated by SF-1, the 4.5 kb *ANGPT2* promoter construct was activated by the wild type protein (4.5 kb WT > [-], P<0.0001). B, Dose-dependent activation of the 4.5 kb *ANGPT2* by wild type SF-1 was seen (WT 50 > [-], P<0.05; WT 100 > [-], P<0.0001). This effect was not observed when the functionally-impaired G35E mutant SF-1 construct was used (Mut 100 > [-], not significant). All data represents mean ± SEM of at least three independent experiments, each performed in triplicate. From Ferraz-de-Souza et al., 2010b. Copyright 2010, The Federation of American Societies for Experimental Biology.

4.3.6. SF-1 and Ang2 expression during early human fetal adrenal development

To investigate the potential co-expression of SF-1 and Ang2 in a biologically relevant system, immunohistochemistry was performed using human fetal adrenal tissue (Fetal Stage 1, 8 weeks post-conception). This is a stage of rapid adrenal development and growth, as well as the onset of steroidogenesis (Goto et al., 2006). Strong nuclear expression of SF-1 was seen in the developing definitive zone with less intense staining of a subset of cells within the fetal cortex (Figure 4.10). Ang2 expression was observed in the cytoplasm of cells and extra-cellular space, predominantly in the definitive zone and subcapsular region and around areas of strong SF-1 expression.

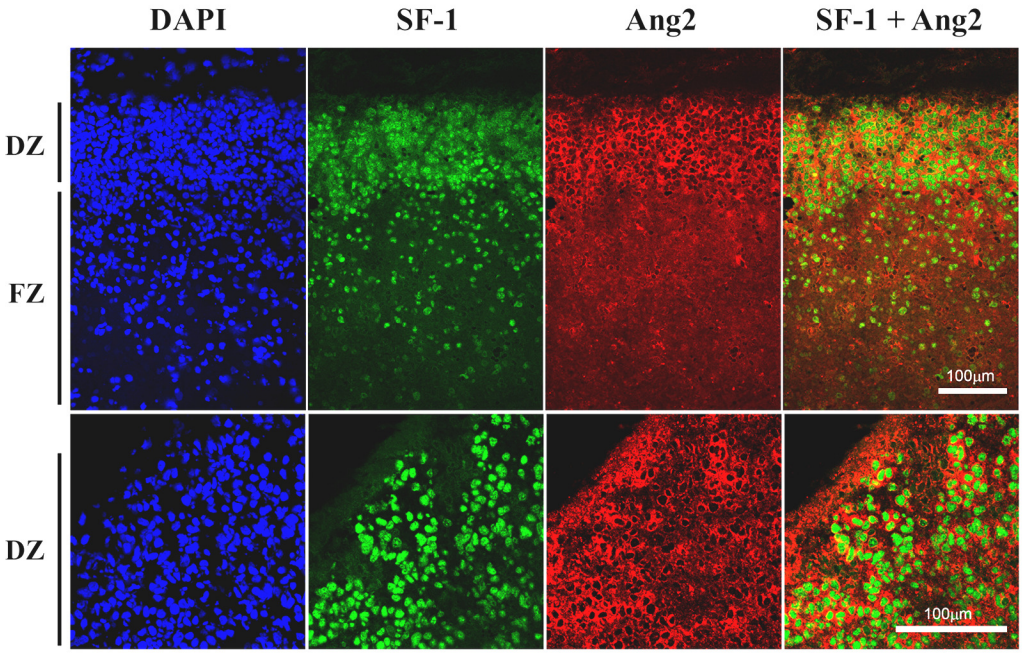

Figure 4.10. SF-1 and Ang2 expression during early human fetal adrenal development.

Upper panel, Immunofluorescent detection of SF-1 and Ang2 in the human fetal adrenal gland (Fetal Stage 1, 8 weeks post-conception) shows strongest expression of these factors in the developing definitive zone (DZ) (FZ, fetal zone). Nuclear staining is shown with DAPI. Lower panel, higher-power magnification shows co-expression of SF-1 and Ang2 in areas of the definitive zone. These studies were performed by Dr Rahul Parnaik in our group. From Ferraz-de-Souza et al., 2010b. Copyright 2010, The Federation of American Societies for Experimental Biology.

4.4. Discussion

The analysis of genome-wide SF-1-binding using ChIP-on-chip aimed to identify novel binding targets for this nuclear receptor in the human adrenal cortex. SF-1 is a key regulator of adrenal development and cancer, and angiogenesis is important in these processes, but until now a direct link between SF-1 and vascular remodelling has not been established. By using a combination of ChIP-on-chip, network analysis, expression data and functional genomic studies, angiopoietin 2 (Ang2, *ANGPT2*) was identified as a potentially important novel target of SF-1 in the adrenal gland.

Angiopoietins are secreted ligands for the tyrosine receptor kinase Tie2 that act in concert with vascular endothelial growth factor (VEGF, mainly VEGF-A) to regulate angiogenic remodelling (Yancopoulos et al., 2000). While Ang1, the first identified Tie2 ligand, acts towards stabilising vessel walls, Ang2 has a central role in destabilising vasculature so that regression (in the absence of VEGF) or angiogenic sprouting (in presence of VEGF) can occur. Ang2 is widely expressed in the endothelium during developmental stages and in sites of active vascular remodelling such as the placenta, ovaries and uterus (Yancopoulos et al., 2000). VEGF and Ang2 are key regulators in tumour angiogenesis, facilitating tumour growth and metastasis, and overexpression of Ang2 has been documented in many tumour types (for example, liver, renal, gastric, breast, colon, pancreas, lung) (Papetti and Herman, 2002; Bach et al., 2007). Consistent with this, a higher Ang2:Ang1 ratio correlates with worse prognosis for many cancers (Bach et al., 2007).

Angiogenesis and vascular remodelling are also important in the development of endocrine tissues, including the adrenal gland. Although these systems are not as well studied as tumorigenesis, recent work has shown a preponderance of

subcapsular angiogenesis during human fetal adrenal development and that adrenocorticotropin (ACTH)-driven zonal differential expression of Ang2 is an important part of this process (Ishimoto et al., 2006; Ishimoto et al., 2008). In those studies, it was proposed that local factors would mediate the angiogenic response to tropic stimuli during fetal adrenal development, and up-regulate *ANGPT2* in the definitive zone of the fetal gland. The experiments described here show a direct interaction of SF-1 in binding to and activating the *ANGPT2* promoter. Furthermore, immunohistochemical studies show that SF-1 and Ang2 are strongly co-expressed in the subcapsular region and developing definitive zone of the human fetal adrenal gland at a critical early stage of development, namely 8 weeks post-conception. Considering that the architectural arrangement of blood vessels in the adrenal cortex is such that nearly every adrenocortical cell is thought to lie adjacent to a vascular endothelial cell (Ehrhart-Bornstein et al., 1998), SF-1-dependent Ang2 expression in adrenocortical cells could be postulated to act in a paracrine way and coordinate vascular remodelling in the developing adrenal. This is supported by findings of abnormal adrenocortical vasculature in adult *Sf-1* haploinsufficient mice (Bland et al., 2000).

Even though a role for SF-1 in regulating angiogenesis has not yet been described, members of the related NR4A nuclear receptor sub-family have recently been recognised as important regulators of vascular gene expression, playing critical roles in many aspects of vascular biology (Zhao and Bruemmer, 2010). In particular, NR4A1 (Nur77, NGFI-B) has been shown to drive the transcription of the plasminogen activator inhibitor 1 (PAI-1) in human umbilical vein endothelial cells (Gruber et al., 2003) and to act as a transcriptional mediator for VEGF-A-induced angiogenesis, with distinct pro-angiogenic effects *in vivo* (Zeng et al., 2006).

Interestingly, up-regulation of NR4A1 was proposed by Bland and colleagues as a compensatory mechanism for maintaining transcriptional regulation of steroidogenesis in *Sf-1* haploinsufficient mice (Bland et al., 2004). Considering the crossover in the regulatory *spectra* of these related nuclear receptors, a role for SF-1 itself in the regulation of adrenal vascular biology is further supported.

It is tempting to speculate that SF-1 could regulate *ANGPT2* not only in adrenocortical cells, as shown here, but also in other cell types and tissues where it is expressed such as the spleen. SF-1 is expressed in the human adult spleen (Ramayya et al., 1997) and structural and functional abnormalities have been described in the spleen of *Nr5a1* knockout mice (Morohashi et al., 1999). In the study by Morohashi and co-workers, Sf-1 expression in precursors of the splenic vascular system was observed in normal mice but abrogated in the spleen of knockout animals, leading to a poor organisation of the vascular system. The exact function of Sf-1 expression in endothelial cells of the spleen has not yet been clarified, probably due to a lack of information on downstream genes regulated by Sf-1 in that system (Morohashi et al., 1999). Considering its key role in vascular remodelling and angiogenesis, angiopoietin 2 becomes a promising candidate effector of Sf-1 regulation during the construction of basic splenic architecture.

Although the analysis was focussed on the link between SF-1 and angiogenesis, several other potentially interesting SF-1 targets have also emerged from the data set (Table 4.4), including, for example, *CHGA* (encoding chromogranin A) and *GLI2* (encoding GLI family zinc finger 2). Furthermore, there are other considerations in relation to the data provided. Most notably, these studies are limited by the use of an immortalised adrenal cell line as a model of the human adrenal cortex. Although NCI-H295R adrenocortical tumour cells express SF-1 in basal conditions and retain

full steroidogenic capability (Rainey et al., 1994; Rainey et al., 2004; Samandari et al., 2007), SF-1-binding in these cells might not necessarily reflect that of developmental, physiological or pathological states *in vivo*.

ChIP-on-chip experiments reflect protein-DNA interactions happening at the moment of cross-link, and therefore have to be taken as a 'snapshot' of binding at very specific conditions. This could result in a bias for detection of genes that are basally activated by SF-1, rather than early or intermediate response genes that may be up-regulated by SF-1 in response to stress or stimulation. Nevertheless, it could be argued that such a subset of basally regulated genes may be more applicable to stable developmental or tumorigenic processes, perhaps explaining why angiogenic processes were so prominent in the functional annotation enrichment analysis.

Finally, another limitation of the experimental design employed here regards the restricted representation of genomic regions in the microarray platform used. ChIP-on-chip experiments using sets of tiling arrays covering the whole genome and, more recently, ChIP-Seq (ChIP coupled with next-generation sequencing techniques) have shown a majority of transcription factor-binding regions to be located far from the transcriptional start site, within intronic or non-coding regions (Carroll et al., 2005; Johnson et al., 2007; Jothi et al., 2008; Welboren et al., 2009), which were not analysed here. It is still uncertain how significant many of these distantly located binding sites are, although certain key upstream regulatory regions or intronic enhancers clearly exist (Zubair et al., 2006). Nevertheless, the studies described here have expanded our understanding of the many roles that a major developmental and physiological regulator such as SF-1 may play.

Taken together, the finding of SF-1 binding to and activating *ANGPT2*, and potentially other angiogenic factors, in adrenal cells provides novel insight into

additional mechanisms by which SF-1 may exert its pivotal actions during adrenal development and tumorigenesis, and supports previous findings of Ang2 as an important mediator of early human fetal adrenal development. Indeed, inverse agonists of SF-1 have been studied *in vitro* as a potential therapeutic option in the treatment of adrenal cancer (Doghman et al., 2009), and antibody-based therapy targeting a range of angiogenic factors is being investigated for the adjuvant treatment of many cancers (Ferrara and Kerbel, 2005), including ongoing phase 2 studies of Anti-Ang2 therapy (Mita et al., 2010). Although further evaluation is necessary, it could be speculated that targeted SF-1 antagonism combined with anti-angiogenic treatment may be a future option in the treatment of adrenal tumours.

CHAPTER 5

GENE EXPRESSION ANALYSIS FOLLOWING SF-1 OVEREXPRESSION

5.1. Introduction

Since the identification of SF-1 as a transcriptional regulator of genes involved in steroidogenesis in the early 1990s (Rice et al., 1991; Morohashi et al., 1992), a gamut of target genes have been shown to be regulated by this nuclear receptor at different developmental and physiological stages, as discussed in section 1.4.4 (Chapter 1). Most of these targets were identified based on hypothetic functional associations with SF-1 or similarity of expression patterns, and SF-1 activation was confirmed through transient transfection assays using stretches of regulatory DNA. Considering the role of SF-1 as a master-regulator of adrenal, gonadal and reproductive development and function, it is possible that many other targets exist and remain to be identified, and that these targets themselves could be important regulators of adrenal development and steroidogenesis. In addition to the ChIP-on-chip analysis presented in Chapter 4, other high-throughput technologies such as global gene expression analysis in microarrays provide an exciting methodological approach to exploring novel SF-1 targets *in vitro*. Such an approach could provide information about more acutely regulated SF-1 targets that are up- or down-regulated over a matter of hours or days following changes in SF-1 expression or activity.

In the human adrenal cortex, SF-1 up-regulates multiple target genes involved in cholesterol metabolism and *all* the enzymes required for steroidogenesis (Schimmer and White, 2010). Disruption of SF-1 itself and of several of these targets has been associated with disorders of adrenal development and steroidogenesis, such as secondary adrenal hypoplasia and *MC2R* mutations (MIM 202200); congenital adrenal insufficiency and mutations in *CYP11A1* (MIM 118485); congenital lipoid adrenal hyperplasia and mutations in *STAR* (MIM 201710); congenital adrenal

hyperplasia and *HSD3B2* mutations (MIM 201810); and aldosterone deficiency and *CYP11B2* mutations (MIM 124080). Considering that approximately 60% of cases of primary adrenal hypoplasia remain without a molecular diagnosis (Lin et al., 2006, discussed in section 1.5.3) and that the genetic basis of many forms of primary adrenal insufficiency or combined adrenogonadal failure remain unknown, we hypothesised that yet unidentified SF-1 target genes could contribute to the molecular basis of this heterogeneous group of disorders.

Using an experimental strategy based on global gene expression analysis following overexpression of SF-1 in a human adrenal cell line, a subset of positively regulated SF-1 targets was identified and the potential role of one of these genes as a cause of adrenal insufficiency in humans was investigated.

5.2. Materials and Methods

5.2.1. Overview of experimental design

In order to be able to analyse global gene expression in adrenal cells overexpressing SF-1, a strategy was devised to transiently co-express green fluorescent protein (GFP) and SF-1 (*NR5A1*) cDNA in NCI-H295R human adrenocortical cells, allowing enrichment for successfully transfected and viable cells through fluorescence-activated cell sorting (FACS) (Figure 5.1). Independent co-expression of SF-1 and GFP in cells was obtained using constructs generated from a pIRES2-AcGFP1-Nuc vector backbone. As discussed in section 2.1.4.4, the internal ribosome entry site (IRES) element in these constructs permits the translation from a single bicistronic mRNA of both SF-1 and nuclear localisation signal-tagged *Aequorea coerulescens* GFP (AcGFP1-Nuc). Constructs were transfected into NCI-H295R adrenocortical tumour cells using Amaxa nucleofection and FACS performed 48 hours later. RNA was extracted from viable GFP-expressing cells and global gene expression analysed using GeneChip Human Gene 1.0 ST microarrays.

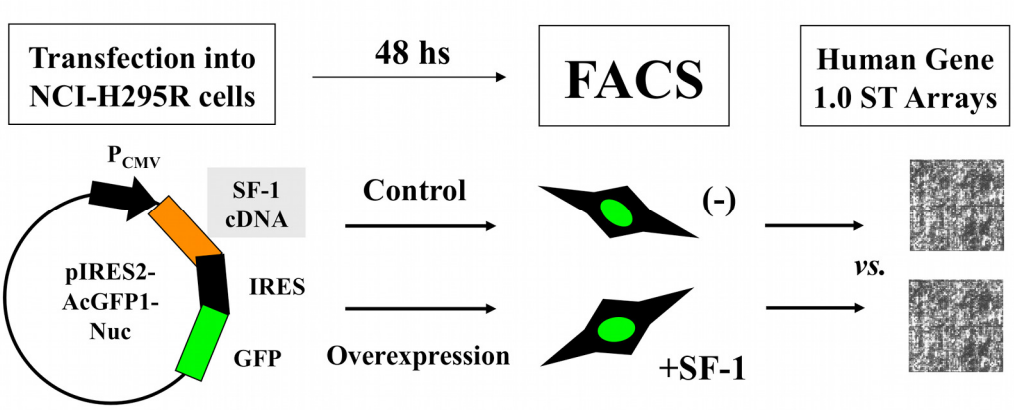

Figure 5.1. Overview of SF-1 overexpression experimental design.
pIRES-AcGFP1-Nuc constructs were transfected into NCI-H295R cells using Amaxa nucleofection, leading to co-expression of SF-1 cDNA and green fluorescent protein (GFP). Cells were submitted to fluorescence-activated cell sorting (FACS) 48 hours later and GFP-positive cells collected for RNA extraction and gene expression analysis with GeneChip Human Gene 1.0 ST arrays.

5.2.2. Generation of pIRES2-AcGFP1-Nuc constructs

5.2.2.1. pIRES2-AcGFP1-Nuc-WTSF1

A pIRES2 construct co-expressing wild type (WT) SF-1 and AcGFP1-Nuc had been generated by Dr Rebecca Hudson-Davies by digesting the entire coding sequence of human SF-1 from a pEGFP-C2 construct (Lin et al., 2007) and sub-cloning it into pIRES-AcGFP1-Nuc using the restriction sites for *Eco*RI and *Sma*I.

Surprisingly, pilot studies using this construct and 'empty' pIRES2-AcGFP1-Nuc backbone as a transfection control showed a markedly reduced number of GFP-positive cells in the control sample (Table 5.1). Failing to find an explanation for this phenomenon in published reports, the manufacturer of pIRES2-AcGFP1-Nuc (Clontech Laboratories, Takara Bio Europe) was contacted and it was established that the expression of the protein downstream of the IRES element (GFP) could be substantially reduced in the absence of a coding sequence upstream of the IRES element, for reasons not completely understood. Therefore, a mutant pIRES2AcGFP1-Nuc-SF1 construct, bearing the well-characterised G35E change that impairs SF-1 transactivational function *in vivo* (Achermann et al., 1999) and *in vitro* (Ito et al., 2000), was generated to be used as experimental control.

5.2.2.2. pIRES2-AcGFP1-Nuc-G35ESF1

Mutant pIRES2-AcGFP1-Nuc-G35ESF1 was generated by site-directed mutagenesis as described in section 2.2.19, using the wild type construct as template. In order to mimic the naturally occurring GGC to GAA change at nucleotides 104 and 105 of SF-1 cDNA that results in the glycine to glutamate substitution at position 35 of the protein (Achermann et al., 1999), the following 36-nucleotide primers were used:

forward, 5'- GTGTGAGAGCTGCAAGGAATTCTTCAAGCGCACGGT-3', and reverse, 5'- ACCGTGCGCTTGAAGAATTCCTTGCAGCTCTCACAC-3'. The entire SF-1 coding sequences of wild type and mutant constructs were verified by direct sequencing.

Pilot studies were repeated using the mutant construct as control and equivalent numbers of GFP-positive cells were retrieved from pIRES2-AcGFP1-Nuc-WTSF1 or pIRES2-AcGFP1-Nuc-G35ESF1 transfection (Table 5.1).

Table 5.1. Retrieval of GFP-expressing cells following transfection with different pIRES2-AcGFP1-Nuc constructs in pilot studies

Transfected plasmid	GFP+ cells (% of viable)
pIRES-AcGFP1-Nuc-WTSF1	21%
pIRES-AcGFP1-Nuc (empty)	7%
pIRES-AcGFP1-Nuc-G35ESF1	20%

Plasmids were transfected into NCI-H295R cells using nucleofection. 48 h later, cells were harvested, prepared and submitted to fluorescence-activated sorting. Numbers of GFP-positive cells retrieved in each experimental condition are expressed as percentage of events with characteristics of viable cells. Experimental procedures are detailed below.

5.2.3. Transfection into NCI-H295R adrenocortical tumour cells

Plasmids (10 μg per 5 x 10^6 cells) were transfected into NCI-H295R cells using Amaxa Nucleofector II (Lonza), Nucleofector kit R and program T-020, as described in section 2.2.21. Altogether, 4 experiments were performed to yield RNA for microarray gene expression analysis. In each experiment, 5 x 10^6 cells were used for each condition (wild type SF-1 or mutant control).

5.2.4. Fluorescence-activated cell sorting (FACS)

Forty-eight hours after transfection, cells were harvested and prepared for FACS as described in section 2.2.22.1. Flow cytometry and sorting were performed by Dr Ayad Eddaoudi and team at the UCL Institute of Child Health Flow Cytometry Core Facility using a MoFlo XDP cell sorter (described in section 2.2.22.2; examples of FACS reports are shown in Appendix 7). Sorted GFP-expressing cells were pooled by centrifugation at 1500 rpm for 10 min at 4°C and resuspended in TRIzol reagent for RNA extraction, which was performed as described in section 2.2.8. Table 5.2 summarises the characteristics of the four experiments subjected to microarray analysis. For protein analysis (validation studies), sorted cells were pooled by centrifugation and frozen to -80°C.

Table 5.2. Characteristics of the four SF-1 overexpression experiments performed in NCI-H295R cells for microarray analysis

Exp		GFP+ cells retrieved	RNA Integrity Number
1	**SF-1 WT**	53,000	8.6
	SF-1 G35E	66,000	9.1
2	**SF-1 WT**	51,000	7.8
	SF-1 G35E	45,000	5.7
3	**SF-1 WT**	57,000	9.6
	SF-1 G35E	65,000	9
4	**SF-1 WT**	60,000	9.6
	SF-1 G35E	72,000	7.9

Exp, experiment number; SF-1 WT corresponds to transfection of pIRES-AcGFP1-Nuc-WTSF1 and SF-1 G35E to transfection of pIRES-AcGFP1-Nuc-G35ESF1. Numbers of GFP-positive events with characteristics of viable cells are shown. RNA integrity number was determined by analysis with a 2100 Bioanalyzer (Schroeder et al., 2006).

5.2.5. Microarray analysis

Processing of RNA samples and hybridisation to microarrays were performed by Dr Priya Panchal at UCL Genomics, as described in section 2.2.23.1. Quality control of RNA samples was performed using the 2100 Bioanalyzer (Agilent Technologies, UK) (Table 5.2). Aliquots of 200 ng total RNA of each sample were used for gene expression microarray analysis with GeneChip Human Gene 1.0 ST arrays (Affymetrix), as described.

Microarray data was analysed by Dr Sonia Shah at the Bloomsbury Centre for Bioinformatics, as described in section 2.2.23.2. Quality control showed that array data corresponding to overexpression of mutant G35E SF-1 (control) in experiment 2 was suboptimal (Figure 5.2). This finding was in accordance with the poor RNA Integrity Number of that sample (Table 5.2). Therefore, arrays corresponding to experiment 2 (paired SF-1 WT and control) were excluded from gene expression analysis.

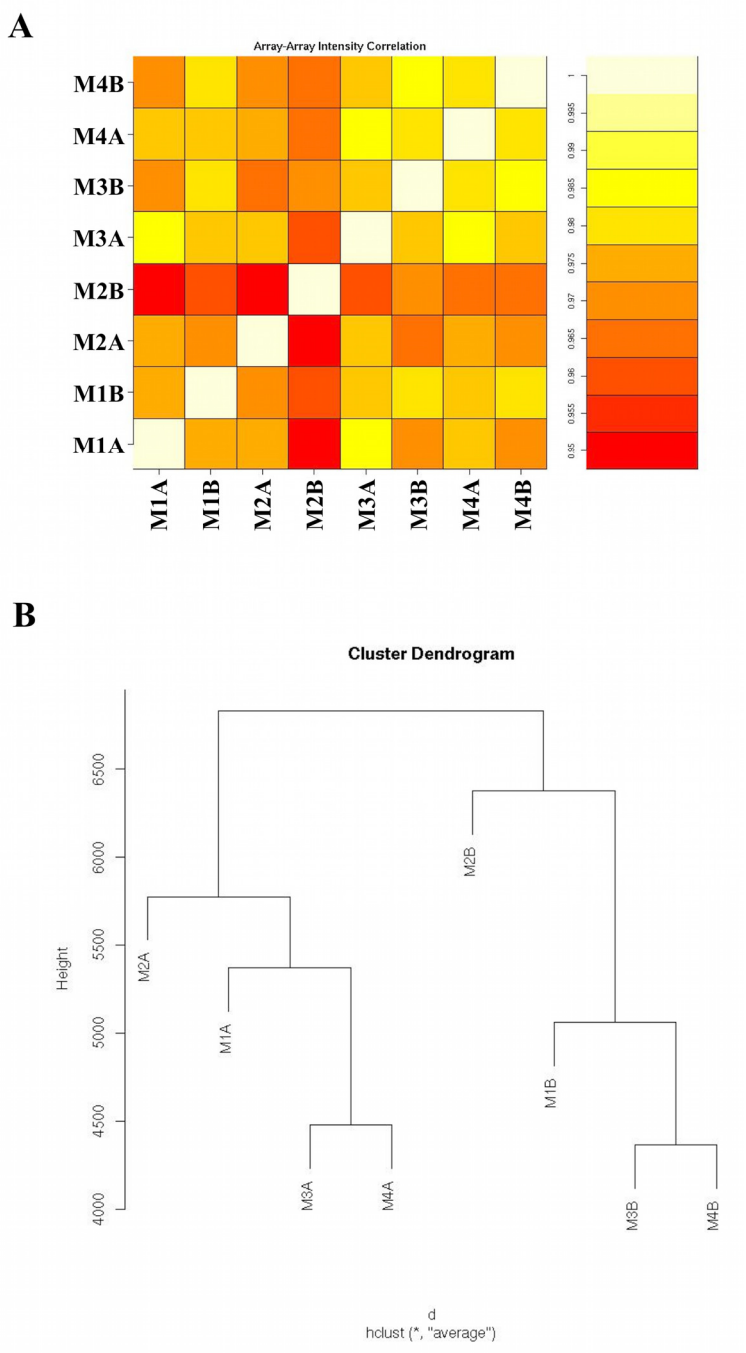

Figure 5.2. Quality control of microarray data.

Correlation plot (A) and cluster dendrogram (B) show that the control array corresponding to overexpression of G35E SF-1 in experiment 2 (M2B) was an outlier. Experiments 1 to 4 are labelled M1 to M4, followed by A if WT SF-1 or B if G35E SF-1 (control). Quality control of array data was performed by Dr Sonia Shah at the Bloomsbury Centre for Bioinformatics using R/Bioconductor.

5.2.6. Validation by immunoblotting and quantitative RT-PCR

5.2.6.1. Immunoblotting

SF-1 expression in transfected cells was assessed at 24 and 48 hours after transfection by immunoblotting, performed as described in section 2.2.15, and compared to basal (time 0 hours). It was not possible to assay protein amount in transfected cells due to small number of cells obtained, therefore cells were directly lysed in SDS-PAGE sample buffer and concomitant immunoblotting of β-actin (ACTB) was performed for signal normalisation. For immunoblotting, rabbit anti-SF-1 antibody (07-618, Upstate Millipore; dilution 1:1000) and mouse anti-β-actin antibody (AC-15, ab6276, Abcam; dilution 1:5000) were used. Anti-rabbit IgG and anti-mouse IgG horseradish peroxidase (HRP)-conjugated secondary antibodies were obtained from Promega and used at 1:2500 dilution. Optical densities of blots were quantified as described in section 2.2.15, normalised by β-actin expression and graphically represented in relation to basal.

5.2.6.2. Quantitative reverse transcription PCR

SF-1-dependent changes in transcript levels of target genes were assessed by qRT-PCR. First-strand cDNA was generated and quantitative PCR performed using SYBR Green chemistry as described in sections 2.2.10.1 and 2.2.10.2.1. RT² qPCR Primer Assays for *STAR* (PPH20960A), *CYP11A1* (PPH01275A), *SOAT1* (PPH21350E) and *B2M* (PPH01094E, endogenous control) were obtained from SABiosciences/Qiagen. Data were analysed using the $2^{-\Delta\Delta CT}$ method as described in section 2.2.10.2.3.

5.2.7. Bioinformatics

In silico analysis of the data set of genes differentially expressed following SF-1 overexpression was performed using the BioMart portal (www.biomart.org), the Database for Annotation, Visualization and Integrated Discovery (DAVID) v6.7, and additional online databases as described in section 2.2.26.

5.2.8. Identification of targets by bidirectional manipulation of SF-1

A data set of genes differentially expressed following SF-1 *knockdown* with small hairpin RNA (shRNA) was used to identify targets of bidirectional manipulation of SF-1 in NCI-H295R cells. Differential gene expression analysis following SF-1 knockdown was performed by Dr Rebecca Hudson-Davies in our group, following an experimental design similar to that of overexpression studies. Briefly, NCI-H295R cells were transfected with SureSilencing shRNA Plasmid for Human NR5A1 with GFP marker kit (KH05887G, SABiosciences), which includes a mismatch control, using Amaxa Nucleofection. Forty-eight hours after transfection, cells were FAC-sorted and RNA and protein obtained from GFP- and shRNA-expressing cells. Validation of SF-1 knockdown was obtained by immunoblotting of SF-1 protein and qRT-PCR of SF-1 targets, as described above. Gene expression analysis was performed using GeneChip Human Gene 1.0 ST arrays (5 SF-1 knockdown arrays, 4 mismatch control arrays), and microarray data was analysed as described.

5.2.9. *In vitro* studies of promoter activation by SF-1

SF-1-responsiveness of newly identified targets *VSNL1*, *SOAT1* and *MTSS1* were studied through luciferase reporter gene assays. Activation of the promoters of these

genes by wild type SF-1 was compared to that induced by the naturally occurring G35E mutant SF-1 (Achermann et al., 1999; Ito et al., 2000).

5.2.9.1. Generation of promoter reporter constructs

The 5.0 kb 5'-upstream sequence of *VSNL1* (transcript ENST00000295156, Ensembl GRCh37), *SOAT1* (ENST00000367619) and *MTSS1* (ENST00000325064) were analysed for putative SF-1 binding sites using MatInspector as described in section 2.2.18.1. Based on the position of predicted sites, the 1.0-kb, 4.8-kb and 1.7-kb upstream sequences of *VSNL1*, *SOAT1* and *MTSS1*, respectively, were PCR amplified and individually cloned into the pGL4.10[luc2] luciferase reporter as described in sections2.2.18.2 to 2.2.18.4.

5.2.9.2. Luciferase reporter gene assays

Co-transfection of reporter constructs (100 ng/well) and pCMX expression vectors containing SF-1 cDNA (wild type or mutant G35E, 50 or 100 ng/well) into NCI-H295R cells was performed according to the protocol described in section 2.2.20.1. In all studies, 7.5 ng/well of internal control pRL-SV40 reporter was co-transfected to allow firefly luciferase activity normalisation by *Renilla* luciferase in Dual-Luciferase reporter assays. Cells were lysed 24 h after transfection and luciferase assays performed as described in section 2.2.20.2.

5.2.10. Detection of SOAT1 in human fetal adrenal glands

5.2.10.1. Quantitative reverse-transcription PCR

Human fetal adrenal tissue from 6 to 9 weeks post-conception (wpc) and control tissue (heart; 8 wpc) were provided by the Human Developmental Biology Resource

(HDBR, www.hdbr.org) with Research Ethics Committee approval and informed consent. Expression of *SOAT1* transcript was assessed by qRT-PCR using TaqMan Gene Expression Assays as described in section 2.2.10.2.2. TaqMan Gene Expression Assays for human *SOAT1* (Hs00162077_m1) and human GAPDH as endogenous control (4333764T) were obtained from Applied Biosystems. Data were analysed using the $2^{-\Delta\Delta CT}$ method as described.

5.2.10.2. Immunohistochemistry

Immunofluorescent detection of SOAT1 in tissue samples was performed by Dr Rahul Parnaik in our group, as described in section 2.2.16. Mouse polyclonal anti-human SOAT1 antibody (H00006646-B01, Abnova, Taiwan; 1:400 dilution) and Alexa Fluor 555 anti-mouse IgG secondary antibody (Invitrogen; 1:400 dilution) were used for detection.

5.2.11. Mutational analysis

After institutional board approval and with informed consent, direct sequencing of the entire coding region of *SOAT1* (transcript ENST00000367619, Ensembl GRCh37) was undertaken in a cohort of 43 patients with adrenal insufficiency of unknown etiology, with or without associated features (Table 5.3). All patients had been previously screened for mutations in *NR5A1* (SF-1) and *NR0B1* (DAX1). The Human Random Control-1 British Caucasian DNA Panel (Health Protection Agency Culture Collections, UK) was used for the analysis of previously unreported non-synonymous changes. The potential effects of coding sequence changes in exonic splicing enhancer elements were investigated using RESCUE-ESE (http://genes.mit.edu/burgelab/rescue-ese) (Fairbrother et al., 2002).

PCR reactions were performed as described in section 2.2.4, using primers designed by Primer3Plus for the entire coding region of *SOAT1* (Table 5.4). Amplification products were verified by agarose gel electrophoresis as described in section 2.2.5 and purified for sequencing reaction as described in section 2.2.6.2. Direct sequencing was performed as described in section 2.2.7. Electropherograms were analysed using the DNA sequencing assembly software Sequencher v4.6 (Gene Codes).

Table 5.3. Associated features of the 43 studied patients with adrenal insufficiency of unknown etiology

	46,XY (n=40)	**46,XX** (n=3)
Gonadal abnormalities e.g., microphallus, mild hypospadias, ambiguous genitalia and complete underandrogenisation	15	-
Cardiac abnormalities	2	1
IUGR	8	-
Skeletal / IMAGe IUGR, Metaphyseal Dysplasia, Adrenal Hypoplasia Congenita and Genital Anomalies	3	-
Renal abnormalities	2	-

Other features: brain abnormalities (1) and short stature (1); IUGR, intrauterine growth restriction

Table 5.4. Forward and reverse primers used to PCR-amplify the coding sequence of *SOAT1*

Exon	Forward primer	Reverse primer
2	5'-ccatgcggaactgtgagac-3'	5'-aaggacttattgtctaattgctttg-3'
3	5'-tgcaccacagtttacgcagt-3'	5'-cagcaactgatgaatggctta-3'
4	5'-tgcttttactcctgcgaactc-3'	5'-accagggtgtgaactcaagc-3'
5	5'-tcctagtagtgaaaaggtcattgg-3'	5'-cagatacagaactcattacatgtcca-3'
6	5'-tgagatgtttttggagagtgga-3'	5'-cagggcaaaggaatatcacc-3'
7	5'-aaggttgaaagtttggtgtttga-3'	5'-tgaaaatttatccaagttaatacagc-3'
8	5'-tcaggattttctgactttactgg-3'	5'-gggtgaaatatccagccaat-3'
9	5'-attccggagatcaggaaaaa-3'	5'-ccatttgaggcttctcaggt-3'
10	5'-tgtgagggtctttattcaagttca-3'	5'-tgcataatgtcaacagaaagcat-3'
11	5'-aaatggaatacatatgcgaaca-3'	5'-tgcaaaagaggtcaagatgg-3'
12	5'-acaaaataatcccagctaaataaaat-3'	5'-ttgtgtgaaaggctggtgac-3'
13	5'-tctgtcaccagtgtatgaacca-3'	5'-tgagcaattaaatataacttcttccag-3'
14	5'-caataggtgcctttggcata-3'	5'-tcaaagtcaatattctgaccatctg-3'
15	5'-cgaacttctgacctctgataactgta-3'	5'-ccaactctcacaaacagagaataaac-3'
16	5'-tggtgggaggcattttagag-3'	5'-gcctggagtggtccaaataa-3'

5.3. Results

5.3.1. Validation of the experimental strategy

Overexpression of SF-1 resulted in increased SF-1 protein at 48 hours in comparison to basal (Figure 5.3A). Overexpressed mutant G35E SF-1 (experimental control) was also recognised by the anti-SF-1 antibody, and expression levels of both wild type and mutant SF-1 were equivalently increased at 24 and 48 h in comparison to basal.

The ability of overexpression of wild type SF-1 to identify known target genes was assessed prior to microarray analysis using the well-established SF-1-regulated genes steroidogenic acute regulatory protein (*STAR*) and *CYP11A1* (P450 side-chain cleavage enzyme) (RefSchimmer2010). Increased *STAR* and *CYP11A1* mRNA levels were seen in cells overexpressing wild type SF-1 in comparison to control (Figure 5.3B). Finally, principal component analysis showed distinct differences in the genomic profiles resultant from SF-1 overexpression compared to control samples (Figure 5.3C).

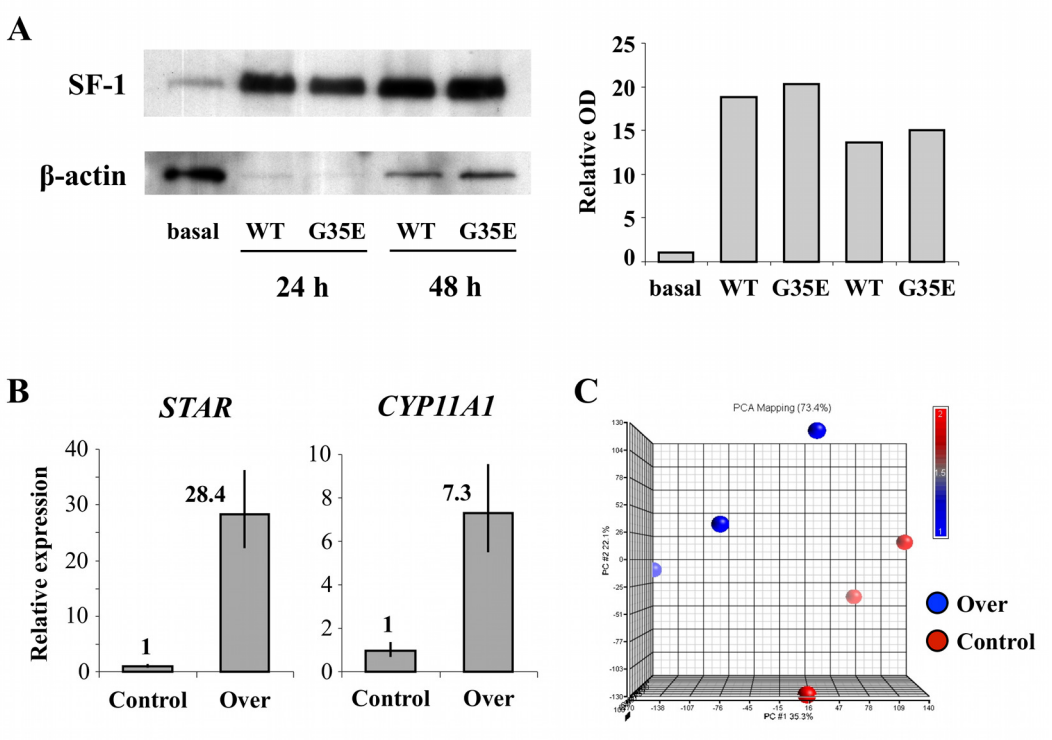

Figure 5.3. Validation of SF-1 overexpression experiments.

A, Immunoblotting analysis of SF-1 protein. Overexpression of wild type (WT) or mutant G35E SF-1 led to equivalently increased protein levels at 24 and 48 h after transfection in comparison to basal. Optical density (OD) of SF-1 bands were normalised by β-actin signal and expressed in relation to basal values (right panel). One representative experiment is shown. B, Quantitative reverse transcription-PCR expression analysis of well-established SF-1-target genes *STAR* and *CYP11A1* 48 h after transfection revealed markedly increased mRNA levels following overexpression of WT SF-1 (Over) in comparison to those elicited by overexpression of mutant G35E SF-1 (Control). Data were analysed according to the $2^{-\Delta\Delta Ct}$ method, and bars represent minimum and maximum relative quantification at 95% confidence. C, Global gene expression analysed using GeneChip Human Gene 1.0 ST arrays and principal component analysis (PCA) showed distinct differences in the genomic profiles resulting from overexpression of wild type SF-1 (Over) compared to G35E SF-1 (Control) (3 arrays each, PCA performed using Partek Genomics Suite).

5.3.2. Differential gene expression following SF-1 overexpression

Overexpression of SF-1 in NCI-H295R adrenocortical cells led to differential expression of 1058 genes ($P<0.05$, Benjamini-Hochberg correction for multiple comparisons) (Appendix 8). Expression of 570 genes was significantly increased by SF-1 overexpression, whereas expression of 488 genes was significantly decreased by SF-1 overexpression (top results shown in Tables 5.5 and 5.6).

In line with SF-1's key role in steroid biosynthesis, functional annotation analysis of genes up-regulated by transient SF-1 overexpression using DAVID revealed enrichment for the descriptors "steroidogenesis" ($P=0.0006$) and "cellular hormone metabolic process" ($P=0.0029$), and also "lipid biosynthetic process" ($P=0.003$) amongst others (Table 5.7). Notably, genes down-regulated by SF-1 overexpression were enriched for functional annotation terms "cytoskeletal protein binding" ($P=0.0001$), "regulation of apoptosis" ($P=0.0002$) and "catecholamine metabolic process" ($P=0.0004$) (Table 5.8).

Table 5.5. Genes up-regulated by transient SF-1 overexpression in NCI-H295R cells (top 40 results)

Transcript ID	FC	Adj.P-Val	Gene Symbol	Gene name	Selected GO Biological Process/*Molecular Function*
7972946	12.4	0.00000751	*RASA3*	RAS p21 protein activator 3	Intracellular signalling pathway; regulation of small GTPase-mediated signal transduction
7935116	12.3	0.00000751	*RBP4*	Retinol binding protein 4, plasma	Response to retinoic acid; male gonad development; glucose homeostasis
8039353	9	0.00000978	*TNNI3*	Troponin I type 3 (cardiac)	Cardiac muscle contraction; cellular calcium ion homeostasis; vasculogenesis
8071642	6.36	0.00000751	*IGLV6-57*	Immunoglobulin lambda variable 6-57	
8095110	6.15	0.000903	*KIT*	v-kit Hardy-Zuckerman 4 feline sarcoma viral oncogene homolog	Hemopoiesis; positive regulation of cell proliferation; spermatogenesis
8141737	5.35	0.0000978	*MYL10*	Myosin, light chain 10, regulatory	*Calcium ion binding*
8114249	5.17	0.000656	*CXCL14*	Chemokine (C-X-C motif) ligand 14	Chemotaxis; immune response
8056113	4.38	0.000128	*CD302 / LY75*	CD302 molecule / Lymphocyte antigen 75	Endocytosis; *sugar binding*; *receptor activity*
7920285	4.29	0.000402	*S100A2*	S100 calcium binding protein A2	Endothelial cell migration
8116653	4.06	0.000073	*BPHL*	Biphenyl hydrolase-like (serine hydrolase)	*Hydrolase activity*
8116649	4.06	0.000073	*TUBB2A / TUBB2B*	Tubulin, beta 2A / Tubulin, beta 2B	Mitosis; microtubule-based movement; neuron differentiation
8036079	3.61	0.0000974	*DMKN*	Dermokine	
7991323	3.61	0.000329	*PEX11A*	Peroxisomal biogenesis factor 11 alpha	Peroxisome organisation; signal transduction; brown fat cell differentiation
7934993	3.56	0.000903	*NUDT9P1*	Nudix (nucleoside diphosphate linked moiety X)-type motif 9 pseudogene 1	
8069508	3.53	0.0171	*C21orf81*	Chromosome 21 open reading frame 81	
8103951	3.51	0.00121	*ACSL1*	Acyl-CoA synthetase long-chain family member 1	Regulation of fatty acid oxidation; triglyceride biosynthetic process
8087691	3.51	0.000168	*CACNA2D2*	Calcium channel, voltage-dependent, alpha 2/delta subunit 2	Calcium ion transport; *voltage-gated ion channel activity*
7951662	3.41	0.000588	*CRYAB*	Crystallin, alpha B	Lens development; anti-apoptosis; negative regulation of gene expression; response to oestradiol stimulus

Transcript ID	FC	Adj.P-Val	Gene Symbol	Gene name	Selected GO Biological Process/*Molecular Function*
8066214	3.36	0.00028	*TGM2*	Transglutaminase 2 (C polypeptide, protein-glutamine-gamma-glutamyltransferase)	Induction of apoptosis; positive regulation of inflammatory response; blood vessel remodelling
8158671	3.29	0.00316	*ASS1*	Argininosuccinate synthase 1	Arginine biosynthetic process; kidney development; liver development
8104930	3.16	0.000888	*SLC1A3*	Solute carrier family 1 (glial high affinity glutamate transporter), member 3	Glutamate biosynthetic process; positive regulation of synaptic transmission
7920278	3.14	0.00278	*S100A3*	S100 calcium binding protein A3	*calcium ion binding*
8158995	3.03	0.0272	*LCN1*	Lipocalin 1 (tear prealbumin)	Proteolysis; sensory perception of taste
8101828	3.03	0.00354	*TSPAN5*	Tetraspanin 5	
8123407	3.01	0.000244	*MLLT4*	Myeloid/lymphoid or mixed-lineage leukemia (trithorax homolog, Drosophila); translocated to, 4	Cell adhesion; cell-cell signalling; signal transduction
8053741	2.97	0.000423	*ANKRD20A1 to 4 ANKRD20B*	Ankyrin repeat domain 20 family, members A1 to A4 / Ankyrin repeat domain 20B	
8080184	2.93	0.000306	*ALAS1*	Aminolevulinate, delta-, synthase 1	Heme biosynthetic pathway; tetrapyrrole biosynthetic process
8155591	2.89	0.00255	*CCDC29*	Coiled-coil domain containing 29	
8160531	2.69	0.00544	*C9orf72*	Chromosome 9 open reading frame 72	
8037053	2.69	0.000959	*CEACAM7*	Carcinoembryonic antigen-related cell adhesion molecule 7	
7942064	2.68	0.00917	*GAL*	Galanin prepropeptide	Neuropeptide signalling pathway; regulation of glucocorticoid metabolic process
8171653	2.66	0.000588	*MAP3K15 / PDHA1*	Mitogen-activated protein kinase kinase kinase 15 / Pyruvate dehydrogenase (lipoamide) alpha 1	Protein phosphorylation / Regulation of acetyl-CoA biosynthetic process from pyruvate; glycolysis
7904408	2.6	0.00808	*HSD3B2*	Hydroxy-delta-5-steroid dehydrogenase, 3 beta- and steroid delta-isomerase 2	Steroid biosynthetic process
8123246	2.58	0.00647	*SLC22A3*	Solute carrier family 22 (extraneuronal monoamine transporter), member 3	Organic cation transmembrane transporter activity
8058238	2.53	0.00171	*ALS2CR11*	Amyotrophic lateral sclerosis 2 (juvenile) chromosome region, candidate 11	
8172043	2.53	0.000423	*SRPX*	Sushi-repeat-containing protein, X-linked	Cell adhesion
8033233	2.5	0.00207	*TUBB4*	Tubulin, beta 4	Microtubule-based movement

Transcript ID	FC	Adj.P-Val	Gene Symbol	Gene name	Selected GO Biological Process/*Molecular Function*
7902883	2.48	0.000631	*LRRC8D*	Leucine rich repeat containing 8 family, member D	*Protein binding*
7990333	2.46	0.00598	*CYP11A1*	Cytochrome P450, family 11, subfamily A, polypeptide 1	C21-steroid hormone biosynthetic process
8079588	2.46	0.0249	*NDUFB1P1*	NADH dehydrogenase (ubiquinone) 1 beta subcomplex, 1 pseudogene 1	

HGNC-recognised genes are ordered by fold change (FC) in transcript levels. Selected gene ontology (GO) annotation, when available, is provided. Transcript ID, Affymetrix Human Gene 1.0 ST array Transcript Cluster ID; Adj.P-Val, Benjamini-Hochberg-corrected P-value.

Table 5.6. Genes <u>down-regulated</u> by transient SF-1 overexpression in NCI-H295R cells (top 40 results)

Transcript ID	FC	Adj.P-Val	Gene Symbol	Gene name	Selected GO Biological Process/*Molecular Function*
8091243	-7.36	0.0000265	*PCOLCE2*	Procollagen C-endopeptidase enhancer 2	*Heparin binding; protein binding*
8166593	-5.86	0.000128	*IL1RAPL1*	Interleukin 1 receptor accessory protein-like 1	Negative regulation of exocytosis; signal transduction
7909789	-5.82	0.0000265	*TGFB2*	Transforming growth factor, beta 2	Regulation of cell growth, proloferation and death; heart development; eye development
8163637	-5.54	0.0000325	*TNC*	Tenascin C	Cell adhesion; signal transduction; prostate gland epithelium morphogenesis
8092134	-4.53	0.000247	*PLD1*	Phospholipase D1, phosphatidylcholine-specific	Phospholipid biosynthetic/catabolic process; response to peptide hormone stimulus
8077270	-4.5	0.000631	*CHL1*	Cell adhesion molecule with homology to L1CAM (close homolog of L1)	Cell adhesion; cell differentiation; nervous system development
8105040	-4.44	0.000073	*OSMR*	Oncostatin M receptor	Positive regulation of cell proliferation; response to cytokyne stimulus
7957570	-4.32	0.000222	*PLXNC1*	Plexin C1	Signal transduction; *receptor activity*
7957966	-4.2	0.00387	*MYBPC1*	Myosin binding protein C, slow type	Cell adhesion; *actin binding*; *titin binding*
8055688	-4.17	0.00112	*RND3*	Rho family GTPase 3	Small GTPase mediated signal transduction
8122660	-3.97	0.000247	*UST*	Uronyl-2-sulfotransferase	Carbohydrate biosynthetic process; *sulfotransferase activity*
8121712	-3.94	0.000073	*SLC35F1*	Solute carrier family 35, member F1	Transport
8161884	-3.92	0.000903	*PRUNE2*	Prune homolog 2 (Drosophila)	Induction of apoptosis; G1 phase; *pyrophosphatase activity*
7920123	-3.92	0.00738	*S100A10*	S100 calcium binding protein A10	*Calcium ion binding*
7964834	-3.84	0.000413	*CPM*	Carboxypeptidase M	Proteolysis; *zinc ion binding*; *metallocarboxypeptidase activity*
7965322	-3.63	0.00205	*KITLG*	KIT ligand	Negative regulation of apoptosis; positive regulation of cell proliferation; ovarian follicle development
7910022	-3.61	0.00493	*CNIH3*	Cornichon homolog 3 (Drosophila)	Intracellular signalling pathway
8056257	-3.61	0.000888	*FAP*	Fibroblast activation protein, alpha	Endothelial cell migration; *serine-type endopeptidase activity*
8171297	-3.56	0.000311	*MID1*	Midline 1 (Opitz/BBB syndrome)	Negative regulation of microtubule depolymerisation; positive regulation of stress-activated MAPK cascade
7956759	-3.56	0.000222	*SRGAP1*	SLIT-ROBO Rho GTPase activating protein 1	Rho protein signal transduction; *GTPase activator activity*
7926545	-3.48	0.000247	*PLXDC2*	Plexin domain containing 2	

Transcript ID	FC	Adj.P-Val	Gene Symbol	Gene name	Selected GO Biological Process/*Molecular Function*
8168622	-3.39	0.00237	*KLHL4*	Kelch-like 4 (Drosophila)	*Actin binding*
8089011	-3.34	0.000247	*PROS1*	Protein S (alpha)	Blood coagulation; *calcium ion binding*
7922474	-3.27	0.000631	*KIAA0040*	KIAA0040	
8171624	-3.16	0.00587	*GPR64*	G protein-coupled receptor 64	Neuropeptide signalling pathway
7957140	-3.16	0.000888	*LGR5*	Leucine-rich repeat-containing G protein-coupled receptor 5	*Protein hormone receptor activity*
7956009	-3.16	0.000128	*METTL7B*	Methyltransferase like 7B	Metabolic process; *methyltransferase activity*
7902687	-3.14	0.000904	*CYR61*	Cysteine-rich, angiogenic inducer, 61	Intussusceptive angiogenesis; *heparin binding*; *insulin-like growth factor binding*
8088192	-3.14	0.000311	*ERC2*	ELKS/RAB6-interacting/CAST family member 2	*Protein binding*
8154491	-3.12	0.000253	*ADAMTSL1*	ADAMTS-like 1	*Metallopeptidase activity*; *zinc ion binding*
8037949	-3.12	0.00138	*SULT2A1*	Sulfotransferase family, cytosolic, 2A, dehydroepiandrosterone (DHEA)-preferring, member 1	Sulfation; steroid metabolic process; bile acid catabolic process
8122222	-3.1	0.000307	*PDE7B*	Phosphodiesterase 7B	Signal transduction; *hydrolase activity*
7961306	-3.1	0.000222	*PRB1/PRB2*	Proline-rich protein BstNI subfamily 1 and 2	
7961320	-3.07	0.000253	*PRB3*	Proline-rich protein BstNI subfamily 3	
8175492	-2.93	0.000378	*ATP11C*	ATPase, class VI, type 11C	ATP biosynthetic process; phospholipid transport
7933872	-2.91	0.00026	*EGR2*	Early growth response 2	Regulation of transcription, DNA-dependent; myelination; response to insulin stimulus
8105302	-2.89	0.00645	*FST*	Follistatin	BMP signalling pathway; female gonad development; negative regulation of cell differentiation
7917954	-2.87	0.0049	*FRRS1*	Ferric-chelate reductase 1	Electron transport chain; histidine catabolic process; *oxidoreductase activity*
8112220	-2.87	0.000631	*PDE4D*	Phosphodiesterase 4D, cAMP-specific	Signal transduction; *3',5'-cyclic-AMP phosphodiesterase activity*
7954559	-2.81	0.00163	*PPFIBP1*	PTPRF interacting protein, binding protein 1 (liprin beta 1)	*Protein binding*

HGNC-recognised genes are ordered by fold change (FC) in transcript levels. Selected gene ontology (GO) annotation, when available, is provided. Transcript ID, Affymetrix Human Gene 1.0 ST array Transcript Cluster ID; Adj.P-Val, Benjamini-Hochberg-corrected P-value.

Table 5.7. Functional annotation enrichment analysis of genes up-regulated by SF-1 overexpression (fold change > 1.5)

Category	Term	P-value	Genes
SP_PIR_KEYWORDS	Steroidogenesis	0.0006	*HSD3B2, CYP17A1, CYP11A1, STAR*
GOTERM_BP_FAT	Regulation of system process	0.0020	*TF, FLT1, TNNC2, EPAS1, STAR, STXBP1, KIT, TNNI3, PLCE1, TNNT1, SLC1A3, RASGRF1, PRKACA, SLC22A5*
GOTERM_BP_FAT	Cellular hormone metabolic process	0.0029	*RBP4, CYP17A1, CYP11A1, STAR, ALDH1A3, HSD17B6*
GOTERM_BP_FAT	Lipid biosynthetic process	0.0030	*HSD3B2, CHKA, CYP11A1, STAR, SCD, LSS, SGMS1, LPCAT3, PLCE1, CYP17A1, DGAT1, ELOVL3, FABP3, HSD17B6*
GOTERM_BP_FAT	Glutamine family amino acid biosynthetic process	0.0036	*SLC1A3, ASS1, GLUD2, GLUD1*
SP_PIR_KEYWORDS	Microtubule	0.0046	*HAUS3, CEP57, TUBB2B, TUBB2A, DYNLL2, MAP1A, KIF16B, SKA1, PTPN20B, DYNC1I2, PTPN20A, TUBB4*
SP_PIR_KEYWORDS	Transit peptide	0.0050	*GRPEL1, CYP11A1, STAR, GLUD2, GLUD1, CA5B, MOSC2, MOSC1, MIPEP, MTHFD1L, ISCA1, MUT, ALAS1, MRPS9, ALDH1B1, OXCT1, PDHA1*
GOTERM_MF_FAT	Molybdenum ion binding	0.0060	*MOCOS, MOSC2, MOSC1*
GOTERM_BP_FAT	Response to drug	0.0102	*SLC1A3, ACSL1, STAR, ALDH1A3, ATP1A3, FABP3, SLC22A5, GAL, DDIT3, ABCB4*
GOTERM_BP_FAT	Folic acid and derivative biosynthetic process	0.0113	*LOC286297, MTHFD1L, GCH1*
GOTERM_BP_FAT	Regulation of hormone levels	0.0132	*RBP4, CYP17A1, DGAT1, CYP11A1, STAR, ALDH1A3, HSD17B6, GAL*
GOTERM_BP_FAT	Steroid biosynthetic process	0.0136	*HSD3B2, CYP17A1, CYP11A1, STAR, HSD17B6, LSS*
SP_PIR_KEYWORDS	Cholesterol metabolism	0.0148	*SOAT1, MUT, CYP11A1, SORL1*

Top results are shown. Functional annotation enrichment analysis was performed using the Database for Annotation, Visualization and Integrated Discovery (DAVID) v6.7. P-values correspond to the EASE score, a modified Fisher's exact test to measure significance of gene enrichment in annotation terms. SP_PIR, Protein Information Resource; GOTERM_XX_FAT, Gene Ontology database term set curated by DAVID; BP, biological process; MF, molecular function.

Table 5.8. Functional annotation enrichment analysis of genes down-regulated by SF-1 overexpression (fold change < -1.5)

Category	Term	P-value	Genes
GOTERM_MF_FAT	Cytoskeletal protein binding	0.0001	*FMNL2, LIMA1, CAP2, MYH15, MYBPC1, UTRN, SNCA, IQGAP2, LMO7, ACTN1, FXYD5, KLHL4, CAPN2, TPM2, ARFGEF1, CORO1C, NCK2, SYNE1, NEB, CXCR4, FYN, MSN, CDC42EP3, SPTB*
GOTERM_MF_FAT	Actin binding	0.0001	*FMNL2, LIMA1, CAP2, MYH15, MYBPC1, UTRN, IQGAP2, LMO7, ACTN1, FXYD5, KLHL4, TPM2, CORO1C, SYNE1, NEB, CXCR4, MSN, SPTB*
GOTERM_BP_FAT	Regulation of apoptosis	0.0002	*SH3RF1, CADM1, MMP9, SNCA, STK17B, ASNS, ITM2B, TGFB2, PRUNE2, PEA15, BDNF, APOH, TNFRSF19, DYRK2, DDAH2, NQO1, NEFL, ADAM9, PRKCA, TXNIP, ARHGEF3, ANXA1, ACTN1, IFI16, SOD2, ATP7A, INHBA, AMIGO2, SERPINB2, APAF1, ACVR1*
GOTERM_BP_FAT	Catecholamine metabolic process	0.0004	*ATP7A, SNCAIP, SNCA, NPR1, MOXD1, TGFB2*
GOTERM_BP_FAT	Ion homeostasis	0.0006	*PRKCA, SCN1A, EGR2, SNCA, EDN1, SLC7A8, TAC1, NPR1, SOD2, ATP7A, CD55, SERINC5, CXCR4, MT2A, CLDN1, CAMK2D, STC1, PPP3CA, MT3*
GOTERM_BP_FAT	Regulation of locomotion	0.0009	*PRKCA, PLD1, CREB3, CXCR4, MMP9, SNCA, EDN1, APOH, TAC1, ADAM9, TRIB1, TGFB2*
GOTERM_BP_FAT	Response to toxin	0.0009	*PRKCA, ATP7A, SLC7A8, TRIM16, NQO1, NEFL, SLC7A11*
GOTERM_BP_FAT	Positive regulation of secretion	0.0009	*PRKCA, INHBA, CADM1, SNCA, EDN1, TAC1, TRIM16, ADAM9, TGFB2*
SP_PIR_KEYWORDS	Metal-thiolate cluster	0.0009	*MT2A, MT1G, MT1X, MT3*
GOTERM_MF_FAT	Cytokine binding	0.0010	*A2M, TNFRSF1B, CXCR4, OSMR, TNFRSF19, TRIM16, IL7R, GFRA2, ACVR1*

Top results are shown. Functional annotation enrichment analysis was performed using the Database for Annotation, Visualization and Integrated Discovery (DAVID) v6.7. P-values correspond to the EASE score, a modified Fisher's exact test to measure significance of gene enrichment in annotation terms. SP_PIR, Protein Information Resource; GOTERM_XX_FAT, Gene Ontology database term set curated by DAVID; BP, biological process; MF, molecular function.

5.3.3. Identification of targets by bidirectional manipulation of SF-1

In order to identify a subset of target genes regulated by bidirectional manipulation of SF-1 in this system, results from overexpression studies were compared to a data set of genes differentially expressed by SF-1 *knockdown* with small hairpin RNA. Studies of SF-1 knockdown were performed by Dr Rebecca Hudson-Davies in our group and resulted in decreased SF-1 protein, reduced *STAR* and *CYP11A1* mRNA and altered genomic profiles (Figure 5.4B). Microarray analysis identified 59 genes significantly up-regulated and 23 genes significantly down-regulated by SF-1 knockdown with shRNA ($P<0.05$, Benjamini-Hochberg correction). As expected, fewer genes reached statistical significance in these studies as the signal changes were smaller and variance greater than in the overexpression studies.

The overlap of overexpression and knockdown data sets identified seven positively regulated genes at six loci (*CYP11A1*, *VSNL1*, *STAR*, *ZIM2*/*PEG3*, *SOAT1* and *MTSS1*) (Figure 5.5A) as well as fifteen negatively regulated genes at fourteen loci (Table 5.9). The subset of positively regulated genes included the well-established SF-1 targets, *STAR* and *CYP11A1*, and five novel putative SF-1 target genes: visinin-like 1 (*VSNL1*); zinc finger, imprinted 2 (*ZIM2*); paternally expressed 3 (*PEG3*); sterol O-acyltransferase 1 (*SOAT1*, also known as acyl-Coenzyme A:cholesterol acyltransferase 1); and metastasis suppressor 1 (*MTSS1*). *ZIM2* (Entrez Gene ID 23619) and *PEG3* (Entrez Gene ID 5178) share the same genomic locus and are represented by the same transcript cluster in GeneChip Human Gene 1.0 ST arrays.

In order to confirm SF-1 responsiveness of *VSNL1*, *SOAT1* and *MTSS1*, the 5.0-kb upstream region of these genes was investigated *in silico* and putative SF-1-binding sites were found, located at -821 bp from the *VSNL1* transcriptional start; -4645 bp, -

4630 bp, -3293 bp and -2964 bp from the *SOAT1* transcriptional start; and -1506 bp from the *MTSS1* transcriptional start. Promoter reporter constructs were generated based on the location of these putative sites (*VSNL1* [1.0 kb], *SOAT1* [4.8 kb] and *MTSS1* [1.7 kb]) and SF-1-dependent activation of all these promoters was confirmed *in vitro* (Figure 5.5B). Studies of the *ZIM2*/*PEG3* locus could not be easily performed as it was not straightforward to clone a specific relevant promoter region.

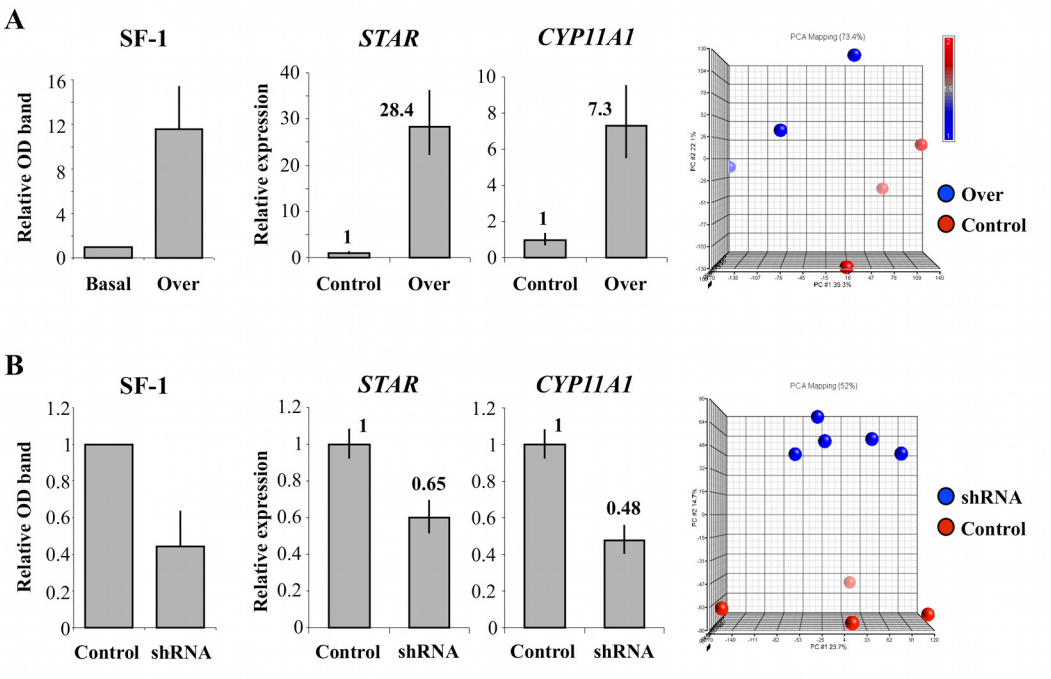

Figure 5.4. Validation of bidirectional manipulation of SF-1 in NCI-H295R adrenocortical cells.

A, <u>Overexpression</u>: transient overexpression of wild type SF-1 induced a 12-fold increase in SF-1 protein levels 48 hours after transfection in relation to basal (immunoblotting). Wild type SF-1 overexpression led to increased mRNA levels of well-established target genes *STAR* and *CYP11A1* in comparison to control (qRT-PCR), and principal component analysis showed distinct differences in the genomic profile resultant from wild type SF-1 overexpression compared to control samples (these results have been shown in Figure 5.3). B, <u>Knockdown</u>: conversely, transient knockdown of SF-1 using SF-1-specific small hairpin RNA (shRNA) resulted in approximately 55% decrease in SF-1 protein levels in comparison to mismatch shRNA control at 48 hours, reduced mRNA levels of *STAR* and *CYP11A1* and distinct array genomic profiles (5 SF-1-specific shRNA arrays, 4 mismatch controls; principal component analysis performed using Partek Genomics Suite). From Ferraz-de-Souza et al., 2011; Copyright 2011, The Endocrine Society.

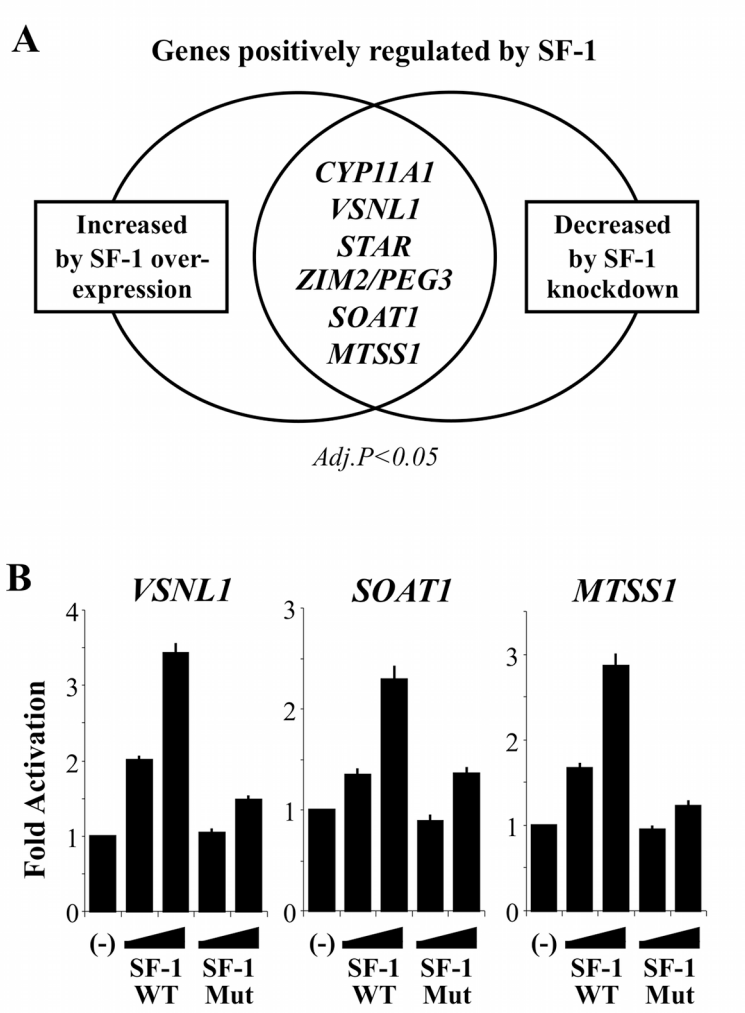

Figure 5.5. Target genes identified by bidirectional manipulation of SF-1 in NCI-H295R adrenocortical cells.

A, Combinatorial analysis of overexpression and knockdown data sets led to the identification of seven genes that were both significantly up-regulated by SF-1 overexpression and down-regulated by SF-1 knockdown (P<0.05, Benjamini-Hochberg correction for multiple comparisons). B, SF-1 responsiveness of *VSNL1*, *SOAT1* and *MTSS1* was confirmed by luciferase assays. Promoter constructs were generated based upon *in silico* identification of SF-1-binding sites within the promoters of these genes (*VSNL1* [1.0 kb], *SOAT1* [4.8 kb] and *MTSS1* [1.7 kb]). Dose-dependent activation of all three promoters by wild type SF-1 (WT) was seen (P<0.0001). This activation was diminished when the functionally-impaired G35E mutant SF-1 (Mut) was used (-, empty expression vector, followed by 50 and 100 ng/well of WT or Mut SF-1 expression vectors; data expressed as mean ± SEM of at least three independent experiments, each performed in triplicate). From Ferraz-de-Souza et al., 2011; Copyright 2011, The Endocrine Society.

Table 5.9. Genes differentially expressed following both SF-1 overexpression and knockdown in NCI-H295R adrenocortical cells

	Transcript Cluster ID	SF-1 Overexpression		SF-1 Knockdown		Gene Symbol	Gene Name
		FC	Adj.P	FC	Adj.P		
Positively regulated by SF-1	7990333	2.46	0.006	-1.36	0.0264	*CYP11A1*	cytochrome P450, family 11, subfamily A, polypeptide 1
	8040430	2.2	0.004	-1.37	0.0197	*VSNL1*	visinin-like 1
	8150253	2.03	0.0049	-1.49	0.0197	*STAR*	steroidogenic acute regulatory protein
	8039607	1.75	0.0045	-1.28	0.0121	*ZIM2*	zinc finger, imprinted 2
	8039607	1.75	0.0045	-1.28	0.0121	*PEG3*	paternally expressed 3
	7907702	1.61	0.0114	-1.35	0.047	*SOAT1*	sterol O-acyltransferase 1
	8152764	1.35	0.0362	-1.25	0.0264	*MTSS1*	metastasis suppressor 1
Negatively regulated by SF-1	7962000	-1.36	0.0498	1.43	0.0361	*PTHLH*	parathyroid hormone-like hormone
	8161701	-1.37	0.0299	1.26	0.0454	*TMEM2*	transmembrane protein 2
	8156610	-1.38	0.0382	1.28	0.0218	*HABP4*	hyaluronan binding protein 4
	8156610	-1.38	0.0382	1.28	0.0218	*CDC14B*	CDC14 cell division cycle 14 homolog B (S. cerevisiae)
	8102800	-1.56	0.0119	1.29	0.0124	*SLC7A11*	solute carrier family 7, (cationic amino acid transporter, y+ system) member 11
	7943760	-1.63	0.006	1.31	0.0437	*SIK2*	salt-inducible kinase 2
	7983527	-1.85	0.0024	1.32	0.0264	*SEMA6D*	sema domain, transmembrane domain (TM), and cytoplasmic domain, (semaphorin) 6D
	8102415	-1.86	0.0179	1.6	0.0075	*CAMK2D*	calcium/calmodulin-dependent protein kinase II delta
	8168472	-2	0.0041	1.25	0.0317	*ATP7A*	ATPase, Cu++ transporting, alpha polypeptide
	8122807	-2.01	0.0035	1.52	0.0357	*AKAP12*	A kinase (PRKA) anchor protein 12
	7968015	-2.1	0.0118	1.25	0.0405	*TNFRSF19*	tumor necrosis factor receptor superfamily, member 19
	8155849	-2.33	0.0061	1.3	0.0258	*ANXA1*	annexin A1
	8163637	-5.54	3E-05	1.47	0.0176	*TNC*	tenascin C
	7909789	-5.82	3E-05	1.54	0.0084	*TGFB2*	transforming growth factor, beta 2
	8166593	-5.86	0.0001	1.37	0.0218	*IL1RAPL1*	interleukin 1 receptor accessory protein-like 1

Transcript Cluster ID, Affymetrix Human Gene 1.0 ST array Transcript Cluster ID; Adj.P, Benjamini-Hochberg-corrected P-value. Gene symbols and names according to the HGNC.

5.3.4. Investigation of *SOAT1* as a novel SF-1 target in steroidogenesis

SF-1 regulation of *SOAT1* was studied further as this gene is involved in cholesterol metabolism and *Soat1* deficient mice have marked adrenocortical lipid depletion and variable abnormalities of cholesterol esterification and corticosterone synthesis (Meiner et al., 1996; Meiner et al., 1998; Taylor and Meier, 1975) (Table 5.10). Overexpression and knockdown of SF-1 resulted in up-regulation or down-regulation of *SOAT1*, respectively, by qRT-PCR as well as microarray analysis, in an independent set of validation experiments (Figure 5.6A).

As information on *SOAT1* expression in the human adrenal gland was not available from public databases, SOAT1 expression during fetal adrenal development was investigated using quantitative RT-PCR and immunohistochemical analysis. *SOAT1* transcript levels were higher in the fetal adrenal gland at a stage of active steroidogenesis compared to control tissues (Figure 5.6B) and immunofluorescence showed strong SOAT1 signal in the developing definitive zone of the fetal adrenal cortex (Figure 5.6C).

Table 5.10. Characteristics of genes positively regulated by SF-1

Gene Symbol	Human adrenal expression		Selected GO Biological Processes (evidence)	MIM: morbidity	Mouse model / Adrenal phenotype reported
	eGenetics (fetal/adult)	GNF (fetal)			
CYP11A1	Y	Y	C21-steroid hormone biosynthetic process (IDA)	Congenital Adrenal Insufficiency	**Y / Y**
VSNL1	Y	Y	*calcium-mediated signalling; central nervous system development (in rat; TAS)*		N
STAR	Y		Regulation of steroid biosynthetic process (IEA)	Lipoid Congenital Adrenal Hyperplasia	**Y / Y**
ZIM2	Y		DNA-dependent regulation of transcription (NAS)		N
PEG3	Y		DNA-dependent regulation of transcription (NAS)		Y / N
SOAT1			Cholesterol esterification, cholesterol metabolic process (IDA)		**Y / Y**
MTSS1	Y	Y	Actin cytoskeleton organization (TAS), cell adhesion (NAS), signal transduction (IEA)		Y / N

Human adrenal expression was investigated through BioMart using two data sets, eGenetics (Kelso et al., 2003) and GNF (Su et al., 2002). Evidence codes for gene ontology (GO) annotation: IDA, inferred from direct assay; TAS, traceable author statement; IEA, inferred from electronic annotation; NAS, non-traceable author statement. Human morbidity information from online Mendelian Inheritance in Man (MIM) and mouse information from Mouse Genomic Informatics. In cases where an adrenal phenotype was not reported in an available mouse model it is unknown whether physiological studies of adrenal function were actively investigated.

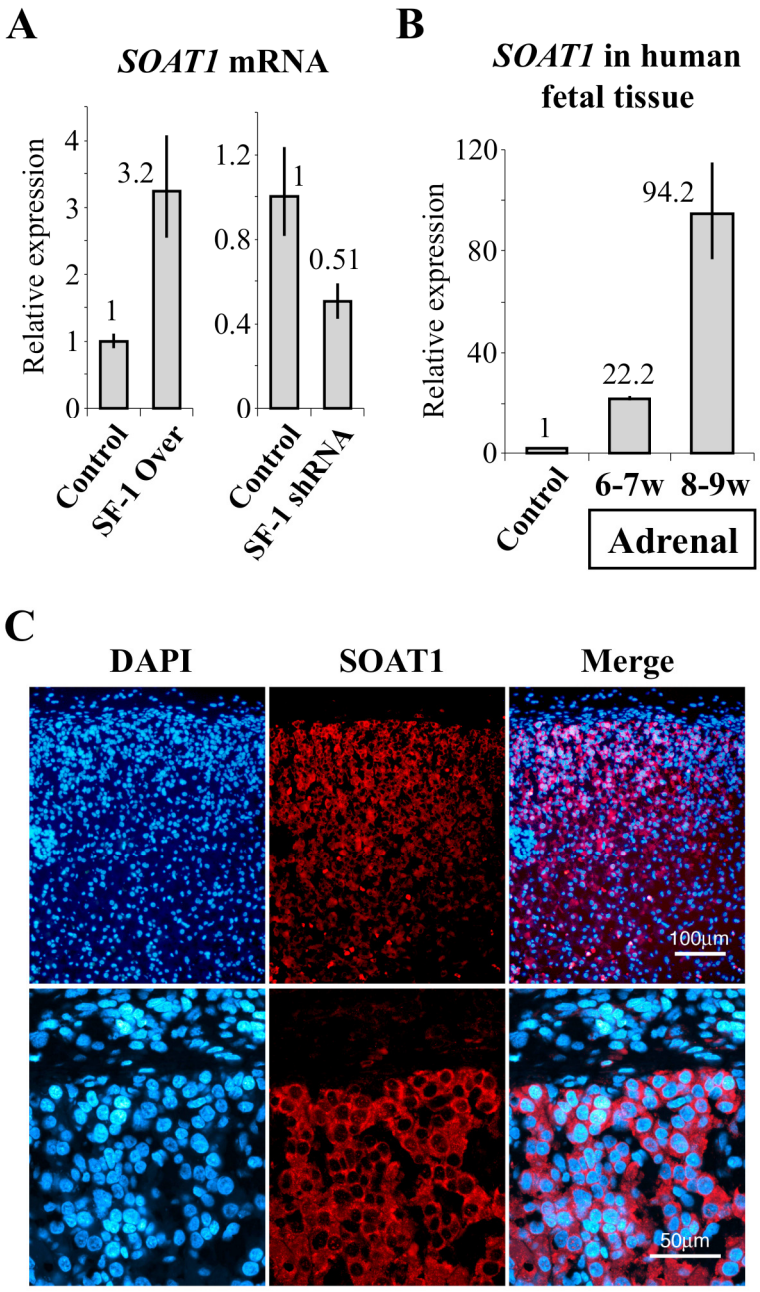

Figure 5.6. ***SOAT1*** **as a novel target of SF-1 in the human adrenal gland.**

A, Increased and decreased levels of ***SOAT1*** **mRNA 48 hours after SF-1 overexpression or knockdown, respectively, were confirmed by qRT-PCR (data expressed according to the** $2^{-\Delta\Delta CT}$ **method). B, A marked increase in** ***SOAT1*** **mRNA expression in human fetal adrenal tissue from 6-7 to 8-9 wpc was detected by qRT-PCR compared to control tissue (heart, 8 wpc), reflecting active steroidogenesis in the fetal adrenal cortex. C, Immunofluorescence confirmed strong expression of SOAT1 in the outer layers of the human fetal adrenal cortex at 8 wpc, but not in overlying non-steroidogenic capsule cells; DAPI was used to visualise nuclei. The omission of primary antibody resulted in no signal (data not shown). Immunohistochemical studies were performed by Dr Rahul Parnaik in our group. From Ferraz-de-Souza et al., 2011; Copyright 2011, The Endocrine Society.**

5.3.5. A role for SOAT1 in human steroidogenesis

Sterol O-Acyltransferase 1 (SOAT1, also known as acyl-Coenzyme A:cholesterol acyltransferase 1 and previously referred to as ACAT) is an important regulator of cholesteryl ester formation in the adrenal gland (Chang et al., 2009). These stored pools of esterified cholesterol can be readily liberated by the action of hormone-sensitive lipase following ACTH stimulation, and protect the adrenal cells from the potentially damaging effects of free cholesterol (Figure 5.7A) (Kraemer, 2007). Therefore, it was hypothesised that impaired SOAT1 activity could result in adrenal insufficiency in humans through reduced cholesteryl ester reserves or through toxic destruction of the adrenal cells during development (Figure 5.7B).

Mutational analysis of *SOAT1* was undertaken in a cohort of 43 patients with adrenal insufficiency of unknown etiology. Seven previously reported variants were identified in this cohort, with variable frequencies (Table 5.11). Two novel variants were identified, one of which resulted in a non-synonymous change in the protein sequence (Table 5.11 and Figure 5.8). *In silico* analysis with RESCUE-ESE failed to reveal any effect of the heterozygous synonymous c.1476T>C (p.D492D) variant in disrupting exonic splicing enhancer (ESE) elements. The novel heterozygous non-synonymous variant c.872T>C (p.I291T) in *SOAT1* was identified in four UK Caucasian patients who presented with isolated adrenal insufficiency (4/84 alleles, 4.8%). However, three out of 93 ancestrally matched control individuals were also found to harbour this variant, one of whom carried this change as a homozygous variant in both alleles (4/186 alleles, 2.2%, X^2=0.25).

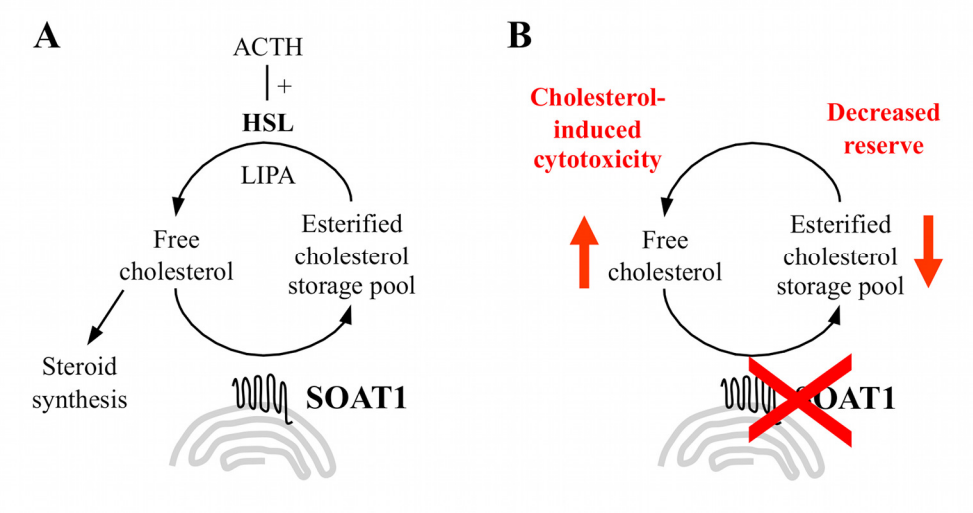

Figure 5.7. SOAT1 activity in the human adrenal cortex.

A, Cartoon representation of the actions of SOAT1 in adrenocortical cells. B, Hypothesised effects of dysfunctional SOAT1. ACTH, adrenocorticotropin; HSL, hormone-sensitive lipase; LIPA, lipase A.

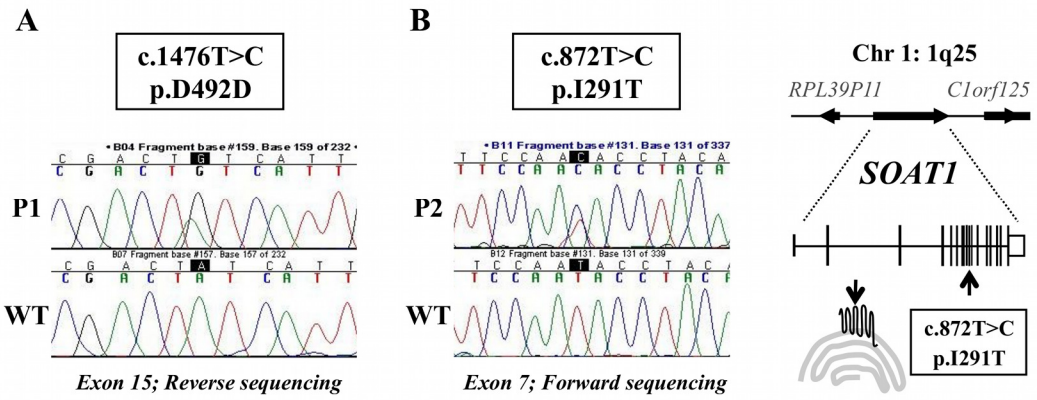

Figure 5.8. Novel variants identified by mutational analysis of *SOAT1* in 43 patients with unexplained adrenal insufficiency.

A, A synonymous heterozygous c.1476T>C variant in exon 15 of *SOAT1* was identified in one patient (P1). WT, wild type sequence. Reverse sequencing electropherograms are shown. B, A non-synonymous heterozygous c.872T>C (p.I291T) variant in exon 9 of SOAT1 was identified in 4 patients, one of whom is shown (P2) (forward sequencing electropherograms). The *SOAT1* locus at 1q25 is depicted in the cartoon showing the location of this allelic variant.

Table 5.11. *SOAT1* variants identified in 43 individuals with unexplained adrenal failure

Exon	cDNA	Protein	WT/WT (n)	WT/Var (n)	Var/Var (n)	Identifier (source)
Previously reported variants						
7	c.579G>A	p.L193L	42	1	0	YRI:1:177576867 (1000 Genomes)
7	c.597C>T	p.P199P	28	12	3	rs11576517 (dbSNP)
7	c.648G>A	p.P216P	42	1	0	YRI:1:177576936 (1000 Genomes)
7	c.774C>T	p.F258F	30	10	3	rs7547733 (dbSNP)
10	c.969C>T	p.V323V	26	16	1	rs10753191 (dbSNP)
14	c.1425C>G	p.L475L	31	11	1	rs3753526 (dbSNP)
15	c.1577A>G	**p.Q526R**	31	11	1	rs13306731 (dbSNP)
Novel synonymous variant						
15	c.1476T>C	p.D492D	42	1	0	
Novel non-synonymous variant						
9	c.872T>C	**p.I291T**	39	4	0	

WT, wild type; Var, variant. Human genetic variation information was obtained using the 1000 Genomes browser at http://browser.1000genomes.org; dbSNP indicates the Single Nucleotide Polymorphism database (NCBI, USA). Non-synonymous changes are shown in bold.

5.4. Discussion

Transient overexpression of wild type SF-1 in NCI-H295R adrenocortical cells resulted in differential expression of 1058 genes in comparison to overexpression of mutant G35E SF-1. The naturally occurring G35E change is associated with the most severe phenotype of human SF-1 deficiency *in vivo* (Achermann et al., 1999) and has been shown to fail to activate a variety of SF-1 target promoters *in vitro* (Ito et al., 2000; Lin et al., 2007). Indeed, quantitative RT-PCR and microarray gene expression analysis performed here show that overexpression of G35E was a *bona fide* experimental control as several well-established SF-1 target genes in the adrenal cortex were appropriately differentially expressed, such as *STAR*, *CYP11A1*, *HSD3B2* and *CYP17A1*. Nevertheless, reported sequence-specific differences in G35E SF-1-binding and transactivation of target promoters (Ito et al., 2000) might constitute a potential limitation of this experimental design. Still, the ability to selectively analyse gene expression in cells overexpressing SF-1 through GFP co-expression and cell sorting constitutes a major advantage of this protocol, and has led to the identification of a broad range of differentially expressed transcripts.

Functional enrichment analysis provided some insight into the biological processes resulting from SF-1 overexpression in this cell line. Genes up-regulated by SF-1 seemed to be involved with steroidogenesis and hormonal homeostasis, whereas those down-regulated by SF-1 were chiefly involved in cytoskeletal functions and apoptotic processes, indicating that SF-1's main role in this system may resemble its *in vivo* activity in promoting steroidogenesis and stimulating cell proliferation. However, identifying which of the several newly identified SF-1 target genes were more likely to have important biological roles proved to be challenging given the

size of the data set and limitations of purely bioinformatic approaches. We therefore hypothesised that genes differentially expressed following bidirectional manipulation of SF-1 would be more likely biologically relevant and combined the results of overexpression analysis with another experimental data set resulting from gene expression analysis following SF-1 knockdown with small hairpin RNA in NCI-H295R cells. Our strategy for SF-1 overexpression or knockdown appeared robust at detecting positively-regulated SF-1 targets, as *CYP11A1* and *STAR* were two of seven genes identified in the overlapping data set. The five novel putative targets of SF-1 identified were: visinin-like 1 (*VSNL1*); zinc finger, imprinted 2 (*ZIM2*); paternally expressed 3 (*PEG3*); metastasis suppressor 1 (*MTSS1*), and, interestingly, sterol O-acyltransferase 1 (*SOAT1*). As noted previously, this subset of genes is more likely to represent targets dynamically regulated by SF-1 over a matter of hours in response to acute stress or stimulation. In this regard, the identification of *CYP11A1* and *STAR* within this group makes biological and methodological sense.

Despite substantial progress in our understanding of the molecular basis of human adrenal development and function in recent years, a significant proportion of cases of primary adrenal failure currently remain unexplained (Lin et al., 2006). As several targets of SF-1 have been shown to cause adrenal dysfunction in humans, novel SF-1 targets unravelled by this gene discovery strategy based on the bidirectional manipulation of SF-1 in human adrenal cells could potentially be promising candidates for adrenal disorders.

Subsequent studies focussed on SOAT1 (MIM 102642), a regulator of cholesteryl ester formation, since ACTH-induced mobilisation of stored ester pools via hormone-sensitive lipase is an important mechanism to generate free cholesterol for adrenal steroidogenesis (Kraemer, 2007; Chang et al., 2009). Furthermore, SOAT1 is

essential for intracellular cholesterol homeostasis, maintaining appropriate levels of unesterified cholesterol within cells for membrane stability (Warner et al., 1995). The studies reported here show that *SOAT1* is under SF-1 regulation in adrenal cells *in vitro* and that *SOAT1* expression *in vivo* coincides spatially and chronologically with active steroidogenesis in the human fetal adrenal cortex.

Naturally occurring (*ald*, *AKR*, *Soat1*^{ald}) or targeted disruption of *Soat1* in mice leads to marked lipid depletion in the adrenal cortex, and variable abnormalities of cholesterol esterification and corticosterone synthesis (Meiner et al., 1996; Meiner et al., 1998). Furthermore, substantial interspecies differences exist in the mechanisms of cholesterol generation as well as in the expression and activity of this enzyme (Gwynne and Strauss, 1982; Lee et al., 2000), as recently demonstrated by differences in anti-atherogenic effects elicited by SOAT1 inhibitors between species (Nissen et al., 2006). It was, therefore, hypothesised that impaired SOAT1 activity could result in adrenal insufficiency in humans, either through reduced cholesteryl ester reserves or through toxic destruction of the adrenal cells during development. Several polymorphic and allelic variants were found in the *SOAT1* gene, but no likely disease-associated changes were identified. Although *SOAT1* changes were not a common cause of adrenal dysfunction in this heterogeneous cohort of patients studied, it is possible that *SOAT1* allelic variants may explain less severe cases of adrenal dysfunction or may have more prominent effects in systems more susceptible to subtle changes in steroidogenic output such as the developing testis.

It is also possible that alterations in several of the other potential SF-1 targets identified through bidirectional manipulation or within the SF-1 overexpression data set could be important mechanisms of human adrenal (and gonadal) dysfunction. Mutational analysis of additional genes has been beyond the scope of the work

presented in this thesis but, as higher throughput technologies become available to sequence large regions or multiexon genes more rapidly, these could provide useful candidates for analysis. In addition, whole exome sequencing is already providing large data sets of potential rare allelic variants in patients with rare or orphan diseases where the genetic basis is unknown. Biologically relevant functional data sets, such as the one provided here, should be a useful resource in helping to focus on which potential genes may be relevant from large sets of rare allelic variants obtained through high-throughput sequencing of patients with adrenal failure.

In conclusion, this "reverse discovery" approach based on the bidirectional manipulation of SF-1 in adrenal cells led to the identification of novel SF-1-targets in this system and defined SOAT1 as an important factor in human adrenal steroidogenesis. SF-1-dependent up-regulation of *SOAT1* may therefore be important for maintaining readily-releasable pools of cholesterol esters needed at times of active steroidogenesis or during episodes of recurrent stress.

CHAPTER 6

GENERAL DISCUSSION

It has now been nearly 20 years since the nuclear receptor steroidogenic factor-1 was identified. From its initial characterisation as a transcriptional regulator of genes encoding the enzymatic machinery involved in steroidogenesis, SF-1 has emerged as a major regulator of several aspects of adrenal and gonadal development and function. The work presented in this thesis considerably broadens our understanding of the regulatory spectrum of SF-1 in human adrenocortical cells by identifying that:

1. SF-1 binds to and activates the promoter of the transcriptional cofactor CITED2;
2. SF-1 and the related orphan nuclear receptor DAX1 synergistically activate the promoter of the transcription factor PBX1;
3. SF-1 binds to an extended promoter region of approximately 450 genes, including factors involved in angiogenic processes;
4. SF-1 binds to and activates the promoter of angiopoietin 2 (Ang2, *ANGPT2*), suggesting that regulation of angiogenesis might be an important additional action of SF-1 during adrenal development and tumorigenesis;
5. Overexpression of SF-1 leads to differential expression of approximately 1100 transcripts, many of which are involved in steroidogenesis, lipid metabolism and cell proliferation;
6. Genes positively regulated by bidirectional manipulation of SF-1 include well-established targets such as *STAR* and *CYP11A1* and the novel target *SOAT1*, a regulator of cholesterol esterification.

Notably, most of this work was performed *in vitro* using the human adrenocortical carcinoma NCI-H295R cell line and therefore speculation about the biological relevance of these findings must be taken with some degree of caution. Nevertheless,

these cells are arguably the best model of human adrenocortical cells available, and have been extensively studied by several groups over several years. NCI-H295R cells express steroidogenic regulatory and enzymatic machinery and secrete a range of steroids in basal conditions, resembling the pluripotent steroidogenic profile of human fetal adrenal cells (Rainey et al., 1994; Staels et al., 1993; Rainey et al., 2004). Moreover, they have innate proliferative and tumorigenic potential retained from the original hypersecretive adrenocortical carcinoma from which this line derives (Gazdar et al., 1990; Fassnacht et al., 2003; Doghman et al., 2007). Therefore, NCI-H295R cells provide a practical human-based system to explore novel targets of steroidogenic factor-1. Unfortunately it was not possible to obtain a sufficient supply of primary adrenal cells to work with during the time course of these studies. However, wherever relevant an attempt has been made to validate the findings in a more natural and *in vivo* setting, such as the analyses of gene and protein expression in human fetal adrenal tissues at critical early stages of development.

The link between developmental processes and tumorigenesis has been increasingly reported in the endocrine and genetic literature. In some cases, loss of function changes in key transcriptional regulators or signalling pathways result in hypoplasia of developing glands and hormone deficiency syndromes. Conversely, overactivity or increased expression of these factors or pathways has been associated with tumorigenesis. This is the case for the thyroid transcription factor-1 (TTF-1, encoded by *NKX2-1*) (Krude et al., 2002; Gudmundsson et al., 2009) and the thyrotropin receptor (TSHR) (Sunthornthepvarakui et al., 1995; Parma et al., 1993) in the thyroid, and for the luteinizing hormone/choriogonadotropin receptor (LHCGR) in the testis (Kremer et al., 1995; Liu et al., 1999). In light of the extensive evidence for

a key role of SF-1 in adrenal development and the emerging data on overactivity of SF-1 in adrenocortical tumours, it seems likely that this is the case for SF-1 as well. Consequently, the analysis of SF-1 targets in adrenocortical carcinoma cells may indeed give clues to its developmental and/or physiological actions.

6.1. SF-1 and candidate targets *CITED2* and *PBX1*

Taken together, data from reporter gene assays (Chapter 3) and ChIP-on-chip (Chapter 4) show that SF-1 binds to distal elements in the *CITED2* promoter, around 3.0 kb upstream of the transcriptional start, resulting in transcriptional activation. Interestingly, initial studies of the *CITED2* promoter linked to luciferase have shown greater activity in human osteosarcoma U2-OS cells when similarly large fragments of the promoter were analysed (Leung et al., 1999). Whilst it is not known whether SF-1 is basally expressed in these cells, SF-1 is expressed in human fetal osteoblasts (ArrayExpress, ID E-MEXP-1216) and in several non-steroidogenic cell lines (Ramayya et al., 1997) therefore a contribution of SF-1 to the extended promoter activity observed in U2-OS cells can be speculated.

Much of the interest in CITED2 as a transcriptional regulator in adrenal development has arisen from studies in mice, where disruption of *Cited2* leads to adrenal agenesis. Recent studies in mice implicate Cited2 as an important regulator of Sf-1 dosage, hence it would be interesting to study if CITED2 in turn can also regulate SF-1 in human systems in the future. Notwithstanding, the present data on *CITED2* expression at early developmental stages in the human fetal adrenal and its regulation by SF-1 *in vitro* support a place for CITED2 within the transcriptional machinery of human adrenal development.

Along similar lines, *PBX1* is shown here to be expressed in the developing human fetal adrenal. *In vitro* activation of a *PBX1* minimal promoter by SF-1, however, seems to be weak at maximal doses, and, surprisingly, a dose-dependent *synergistic activation* by SF-1 and DAX1 is seen. Mutations in both DAX1 and SF-1 lead to adrenal insufficiency, however several studies have shown that DAX1 paradoxically acts as a *repressor* of SF-1-mediated transactivation (Zazopoulos et al., 1997; Iyer and McCabe, 2004; Lalli and Alonso, 2010). This present result adds to a limited but increasing number of recent reports that have shown that SF-1 and DAX1 can synergistically up-regulate genes involved in adrenal development and function (Verrijn Stuart et al., 2007; Xu et al., 2009), as well as in the hypothalamic-pituitary-gonadal axis (Li et al., 2010).

Interestingly, the synergistic effects of DAX1 and SF-1 in the *PBX1* promoter were attenuated when naturally occurring severe and partial DAX1 mutants were studied, suggesting this mechanism could contribute to the impaired definitive zone development in patients with X-linked adrenal hypoplasia congenita (AHC). Findings of normal adrenal development in the *Dax1* (*Nr0b1*) exon 2 deleted mouse contrast with the many reported cases of AHC due to DAX1 mutations in humans, and might indicate that the balance between activating/repressing function of this atypical nuclear receptor might be different amongst species. Therefore, the suggestion that DAX1 may also have an *activating* role during certain stages of human development, in a promoter- or cell-specific fashion is exciting and certainly warrants further studies, although the experimental design to address this in terms of human biology may be challenging.

6.2. Genome-wide SF-1-binding and transcriptomic effects of SF-1 overexpression

The advent of high-throughput functional genomic technologies presents an exciting opportunity to explore novel SF-1 targets *in vitro* beyond pre-conceived functional or expression-based hypothetical associations. The present results indicate that, in NCI-H295R cells, SF-1 natively binds to an extended promoter region (from 10 kb upstream to 3 kb downstream of the transcriptional start, in general) of 445 genes as shown by ChIP-on-chip and that forced overexpression of wild type SF-1 leads to differential expression of 1058 genes.

Notably, a large overlap between these data sets was not seen (Appendix 9). This may be attributable to the differences in nature and purpose of these experiments: while ChIP-on-chip analysis potentially identifies DNA-binding sites of SF-1 in basal conditions (i.e., 'promoters to which SF-1 is naturally bound to in these cells'), gene expression analysis following SF-1 overexpression is likely to identify transcripts that SF-1 is capable of regulating in a cell equipped with appropriate transcriptional machinery under forcedly magnified conditions (i.e., 'what effects a boost of SF-1 elicits in the transcriptional output of adrenal cells'). It would be a simplification of a complex biological process such as transcriptional regulation to expect that every instance of DNA-binding represents an active regulatory event. Indeed, emerging reports of ChIP-on-chip and ChIP-Seq have revealed a majority of binding sites located far removed from transcriptional start sites and at the moment the significance of this binding is not clear (Carroll et al., 2005; Jothi et al., 2008; Welboren et al., 2009). It is hoped, however, that as these technologies become more available and are applied in a variety of experimental settings, patterns will be recognised and more robust biological meaning will be drawn. On the other hand,

and in light of what is currently known about the action of SF-1 as a transcriptional regulator, it could be plausible to expect that a significant proportion of those transcripts being up-regulated by SF-1 overexpression are direct SF-1 targets and that regulation took effect through DNA-binding and transactivation. Therefore, the scant overlap between these experimental data sets could reflect different actions of SF-1 in different developmental or physiological scenarios.

The majority of the targets identified through ChIP-on-chip or overexpression had not been associated with SF-1 before. Whether they may represent biologically relevant factors can only be determined by exhaustive individual experimental analysis. Certainly, the bioinformatics approach employed here, making use of functional enrichment and network analysis and additional public experimental data sets, helped to focus the analysis on *ANGPT2* and *SOAT1* as potentially relevant novel SF-1 target genes. Nevertheless, these large experimental data sets will be made available to the scientific community and may be useful as additional pieces of the jigsaw puzzle for ongoing and future exploration of the actions of SF-1 in the adrenal gland.

6.3. SF-1, angiopoietin 2 and angiogenesis

ChIP-on-chip analysis has shown that SF-1 is bound to several gene loci associated with angiogenic and vascular remodelling processes, amongst which is *ANGPT2*. The SF-1-binding region identified in the *ANGPT2* promoter is 1.1-kb long and is located 3.0 kb upstream of the transcriptional start. Strikingly, *in silico* analysis predicted 18 SF-1 binding motifs to be located in this highly repetitive region and dose-dependent activation by wild type SF-1 is seen in reporter gene assays when a 4.5-kb *ANGPT2* promoter construct is studied, but not when shorter promoter

fragments are analysed. Whilst this is *in vitro* evidence, these findings strongly suggest that SF-1 may regulate angiopoietin 2 *in vivo*. Indeed, immunohistochemical studies show that expression of SF-1 and Ang2 coincides in areas of the definitive zone of the human fetal adrenal cortex at critical developmental stages.

Although novel, the concept that angiopoietin 2 and angiogenic factors may be under SF-1 regulation is biologically plausible. The developing human adrenal glands are highly vascularised and vascular abnormalities were seen in the adrenal cortex of Sf-1 (*Nr5a1*) haploinsufficient mice (Bland et al., 2000). Additionally, angiopoietin 2 expression is a hallmark of neoplastic vascular remodelling and high levels of *ANGPT2* mRNA have been consistently documented in independent reports of adrenocortical carcinoma gene expression profiling (West et al., 2007; Giordano et al., 2009; Soon et al., 2009). Considering that SF-1 is a master regulator of adrenal development and that several lines of evidence point towards its contribution to adrenocortical tumorigenesis, regulation of angiogenesis in these settings may well be under the control of SF-1.

Given the potential implications in terms of adjuvant adrenal cancer treatment, future work will require validation of these observations *in vivo*. In particular, analysis of *Angpt2* expression in *Nr5a1* haploinsufficient mice might be informative, as well as studies of anti-Ang2 immunotherapy in animal models of adrenocortical cancer with or without Sf-1 inverse agonists. Exploration beyond the adrenal might be warranted as well, since target networks mediating the reduction in size and architectural abnormalities in the spleen of Sf-1 null mice have not yet been clarified and recent data have shown direct involvement of Ang2 in lymphangiogenesis (Gordon et al., 2010). Lastly, although Ang2 was the focus of this work, other angiogenic factors identified as putative SF-1-binding targets will require validation and further

investigation in the future. Indeed, data on CITED2 co-activation of angiogenic signalling cascades (Tien et al., 2004; Withington et al., 2006) and on the involvement of NGFI-B in many aspects of vascular biology (Zhao and Bruemmer, 2010) suggest that nuclear receptors and transcriptional co-activators might play a broader role in these regulatory networks.

6.4. Bidirectional manipulation of SF-1 as a gene discovery strategy

Hypothesising that genes with significant changes in expression in response to both increased and decreased SF-1 dosage were more likely to be important SF-1 targets in this system, results from overexpression studies were combined with those from SF-1 knockdown with small hairpin RNA (shRNA). Notably, these data sets differed in size, with significant differential expression of approximately 13 times more transcripts following SF-1 overexpression than following SF-1 knockdown (Figure 6.1). This probably reflects the difference in magnitude of experimentally induced increase or reduction in SF-1 expression levels, as 14-fold increase in SF-1 protein level resulted from SF-1 overexpression while 0.5-fold reduction resulted from SF-1 knockdown. Still, an overlap was detected and led to the identification of seven genes positively regulated by SF-1 in NCI-H295R cells. Remarkably, amongst these were the well-established SF-1 targets *STAR* and *CYP11A1*, which are crucial for adrenocortical steroidogenesis and for normal adrenal development and function (Takayama et al., 1994; Sugawara et al., 1996; Bose et al., 1996; Kim et al., 2008). Considering SF-1's role as a master regulator of adrenal development, and that defects in several other SF-1 target genes have also been associated with human adrenal disorders, bidirectional manipulation of SF-1 seemed to be a valid gene discovery strategy for novel candidates for human adrenal disorders.

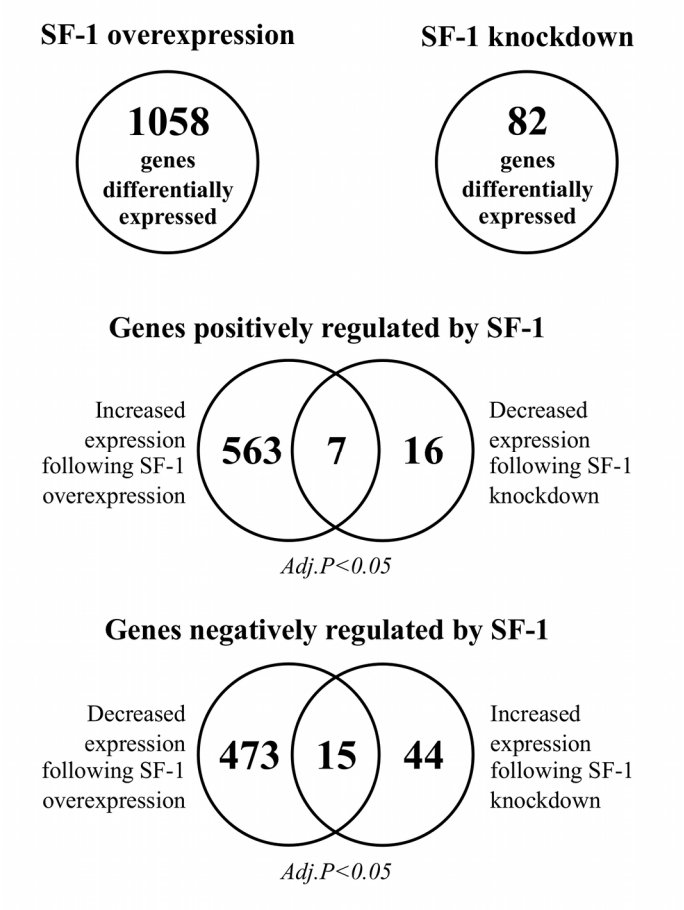

Figure 6.1. Characteristics and overlap between SF-1 overexpression and knockdown experimental data sets. Adj.P, Benjamini-Hochberg-corrected P-value

Five novel putative positively regulated SF-1 target genes were identified using this approach: *VSNL1*, *ZIM2*, *PEG3*, *SOAT1* and *MTSS1*. Visinin-like 1 (VILIP-1, *VSNL1*) is a neuronal calcium sensor protein that modulates various cellular signal transduction pathways (e.g., G-protein coupled receptors, MAPK signalling) and has been shown to act as a tumour suppressor (Braunewell and Klein-Szanto, 2009; Fu et al., 2009). Although mainly expressed in the brain, *VSNL1* expression has also been

detected in testes, adrenals and in the endocrine pancreas. Zinc finger, imprinted 2 (*ZIM2*) and paternally expressed 3 (*PEG3*) share the same *loci* at 19q13.4 and are represented by a single transcript cluster in the microarray platform used. In humans, *ZIM2* and *PEG3* share a set of 5' exons, have a common promoter and are both paternally expressed (Kim et al., 2000; Kim et al., 2004). Notably, both genes are strongly expressed in testes and adrenals and are proposed to act as zinc finger transcription regulators. Metastasis suppressor 1 (missing-in-metastasis, MIM, *MTSS1*) is an actin regulatory protein involved in sonic hedgehog signalling and Gli-regulated transcription (Bershteyn et al., 2010), pathways known to be important for murine adrenal development (Ching and Vilain, 2009). Therefore, whilst the present work has focussed on *SOAT1* given its established role in adrenal cholesterol utilisation, it is clear that these remaining novel putative SF-1 targets warrant further investigation in the future.

Similarly, the identification of 15 *negatively* regulated SF-1 targets by SF-1 bidirectional manipulation in NCI-H295R cells presents a compelling opportunity to explore SF-1 activity as a *repressor* of gene expression. To date, SF-1 has not been shown to directly repress gene expression in any instance, and these might constitute indirect targets or secondary effects of SF-1 overexpression or knockdown. Nevertheless, considering that an activating role for DAX1 is emerging, it could be that SF-1 will transpire to be an occasional repressor in the future.

6.5. SOAT1 as a candidate gene for adrenal disorders

Sterol O-acyltransferase 1 (acyl-Coenzyme A:cholesterol acyltransferase 1, ACAT, *SOAT1*) is an important regulator of cholesterol metabolism in the adrenal cortex, esterifying free cholesterol for intracellular storage. These stored pools of esterified

cholesterol can be readily liberated for steroidogenesis following ACTH stimulation, and protect cells from the potentially damaging effects of free cholesterol. Present results show that *SOAT1* is up-regulated by overexpression of wild type SF-1 and down-regulated by SF-1 knockdown with shRNA in NCI-H295R cells, where an extended *SOAT1* promoter is activated by wild type SF-1. Supported by strong expression of SOAT1 in the developing human fetal adrenal as seen by immunohistochemical analysis, defects in *SOAT1* were hypothesised to lead to adrenal insufficiency due to reduced cholesteryl ester reserves or through toxic destruction of adrenal cells during development. Indeed, such a model of cellular destruction due to free cholesterol excess is a recognised disease-causing mechanism in lipoid congenital adrenal hyperplasia due to *STAR* mutations (Bose et al., 1996). Therefore, mutational analysis of *SOAT1* was performed in 43 cases of adrenal insufficiency where a molecular diagnosis had not been achieved.

No mutations were identified, indicating that defects in *SOAT1* are not a cause of adrenal failure in this cohort. It is possible that this analysis was limited by numbers or by the heterogeneity of the cases studied, and hence analysis of *SOAT1* in larger cohorts may be warranted. It is also possible, however, that *SOAT1* allelic variants may have a bigger impact in systems more susceptible to subtle changes in steroidogenic output such as the developing testis, where slight changes in testosterone production at critical stages of male sex development can determine a more obvious phenotype (e.g., hypospadias). Alternatively, defects in SOAT1 could result in an altered adrenocortical stress response as effects may only be apparent at times when cholesterol ester storage is challenged. Therefore, future work could include mutational analysis of *SOAT1* in other cohorts, such as 46,XY disorders of sex development without clinically manifest adrenal insufficiency.

6.6. Conclusion

The present investigation of novel targets of steroidogenic factor-1 has expanded our understanding of the many roles performed by this developmental and functional regulator. The use of high-throughput technologies has contributed to identify novel mechanisms involving SF-1 in human adrenal cells and has also resulted in several new interesting questions arising. Indeed, angiogenesis seems to be yet another process under the control of SF-1 in the adrenal, and the novel SF-1 targets identified through a "reverse-discovery" strategy may be promising candidates for human adrenal disorders. Overall, the studies presented in this thesis hopefully help to convey the message that SF-1 has come a long way from being purely a *steroidogenic* factor in its 20-year history.

References

Achermann JC, Ito M, Ito M, Hindmarsh PC, Jameson JL 1999. A mutation in the gene encoding steroidogenic factor-1 causes XY sex reversal and adrenal failure in humans. Nat Genet 22(2): 125-6.

Achermann JC, Ito M, Silverman BL, Habiby RL, Pang S, Rosler A, Jameson JL 2001. Missense mutations cluster within the carboxyl-terminal region of DAX-1 and impair transcriptional repression. J Clin Endocrinol Metab 86(7): 3171-5.

Achermann JC, Ozisik G, Ito M, Orun UA, Harmanci K, Gurakan B, Jameson JL 2002. Gonadal determination and adrenal development are regulated by the orphan nuclear receptor steroidogenic factor-1, in a dose-dependent manner. J Clin Endocrinol Metab 87(4): 1829-33.

Ahmad I, Paterson WF, Lin L, Adlard P, Duncan P, Tolmie J, Achermann JC, Donaldson MD 2007. A novel missense mutation in DAX-1 with an unusual presentation of X-linked adrenal hypoplasia congenita. Horm Res 68(1): 32-7.

Aigueperse C, Val P, Pacot C, Darne C, Lalli E, Sassone-Corsi P, Veyssiere G, Jean C, Martinez A 2001. SF-1 (steroidogenic factor-1), C/EBPbeta (CCAAT/enhancer binding protein), and ubiquitous transcription factors NF1 (nuclear factor 1) and Sp1 (selective promoter factor 1) are required for regulation of the mouse aldose reductase-like gene (AKR1B7) expression in adrenocortical cells. Mol Endocrinol 15(1): 93-111.

Almeida MQ, Soares IC, Ribeiro TC, Fragoso MC, Marins LV, Wakamatsu A, Ressio RA, Nishi MY, Jorge AA, Lerario AM and others 2010. Steroidogenic factor 1 overexpression and gene amplification are more frequent in adrenocortical tumors from children than from adults. J Clin Endocrinol Metab 95(3): 1458-62.

Baba T, Mimura J, Nakamura N, Harada N, Yamamoto M, Morohashi K, Fujii-Kuriyama Y 2005. Intrinsic function of the aryl hydrocarbon (dioxin) receptor as a key factor in female reproduction. Mol Cell Biol 25(22): 10040-51.

Babu PS, Bavers DL, Beuschlein F, Shah S, Jeffs B, Jameson JL, Hammer GD 2002. Interaction between Dax-1 and steroidogenic factor-1 in vivo: increased adrenal responsiveness to ACTH in the absence of Dax-1. Endocrinology 143(2): 665-73.

Bach F, Uddin FJ, Burke D 2007. Angiopoietins in malignancy. Eur J Surg Oncol 33(1): 7-15.

Baker BY, Lin L, Kim CJ, Raza J, Smith CP, Miller WL, Achermann JC 2006. Nonclassic congenital lipoid adrenal hyperplasia: a new disorder of the steroidogenic acute regulatory protein with very late presentation and normal male genitalia. J Clin Endocrinol Metab 91(12): 4781-5.

Bamforth SD, Braganca J, Eloranta JJ, Murdoch JN, Marques FI, Kranc KR, Farza H, Henderson DJ, Hurst HC, Bhattacharya S 2001. Cardiac malformations, adrenal agenesis, neural crest defects and exencephaly in mice lacking Cited2, a new Tfap2 co-activator. Nat Genet 29(4): 469-74.

Bardoni B, Zanaria E, Guioli S, Floridia G, Worley KC, Tonini G, Ferrante E, Chiumello G, McCabe ER, Fraccaro M and others 1994. A dosage sensitive locus at chromosome Xp21 is involved in male to female sex reversal. Nat Genet 7(4): 497-501.

Bashamboo A, Ferraz-de-Souza B, Lourenco D, Lin L, Sebire NJ, Montjean D, Bignon-Topalovic J, Mandelbaum J, Siffroi JP, Christin-Maitre S and others 2010. Human male infertility associated with mutations in NR5A1 encoding steroidogenic factor 1. Am J Hum Genet 87(4): 505-12.

Benjamini Y, Hochberg Y 1995. Controlling the False Discovery Rate: A Practical and Powerful Approach to Multiple Testing. J R Statist Soc B 57(1): 289-300.

Bergada I, Del Rey G, Lapunzina P, Bergada C, Fellous M, Copelli S 2005. Familial occurrence of the IMAGe association: additional clinical variants and a proposed mode of inheritance. J Clin Endocrinol Metab 90(6): 3186-90.

Bernard P, Drogat J, Maure JF, Dheur S, Vaur S, Genier S, Javerzat JP 2006. A screen for cohesion mutants uncovers Ssl3, the fission yeast counterpart of the cohesin loading factor Scc4. Curr Biol 16(9): 875-81.

Bershteyn M, Atwood SX, Woo WM, Li M, Oro AE 2010. MIM and cortactin antagonism regulates ciliogenesis and hedgehog signaling. Dev Cell 19(2): 270-83.

Beuschlein F, Mutch C, Bavers DL, Ulrich-Lai YM, Engeland WC, Keegan C, Hammer GD 2002. Steroidogenic factor-1 is essential for compensatory adrenal growth following unilateral adrenalectomy. Endocrinology 143(8): 3122-35.

Bhattacharya S, Michels CL, Leung MK, Arany ZP, Kung AL, Livingston DM 1999. Functional role of p35srj, a novel p300/CBP binding protein, during transactivation by HIF-1. Genes Dev 13(1): 64-75.

Biason-Lauber A, Schoenle EJ 2000. Apparently normal ovarian differentiation in a prepubertal girl with transcriptionally inactive steroidogenic factor 1 (NR5A1/SF-1) and adrenocortical insufficiency. Am J Hum Genet 67(6): 1563-8.

Biason-Lauber A, Konrad D, Navratil F, Schoenle EJ 2004. A WNT4 mutation associated with Mullerian-duct regression and virilization in a 46,XX woman. N Engl J Med 351(8): 792-8.

Bischof LJ, Kagawa N, Moskow JJ, Takahashi Y, Iwamatsu A, Buchberg AM, Waterman MR 1998. Members of the meis1 and pbx homeodomain protein families cooperatively bind a cAMP-responsive sequence (CRS1) from bovine CYP17. J Biol Chem 273(14): 7941-8.

Blais A, Dynlacht BD 2005. Devising transcriptional regulatory networks operating during the cell cycle and differentiation using ChIP-on-chip. Chromosome Res 13(3): 275-88.

Bland ML, Jamieson CA, Akana SF, Bornstein SR, Eisenhofer G, Dallman MF, Ingraham HA 2000. Haploinsufficiency of steroidogenic factor-1 in mice disrupts adrenal development leading to an impaired stress response. Proc Natl Acad Sci U S A 97(26): 14488-93.

Bland ML, Fowkes RC, Ingraham HA 2004. Differential requirement for steroidogenic factor-1 gene dosage in adrenal development versus endocrine function. Mol Endocrinol 18(4): 941-52.

Bose HS, Sugawara T, Strauss JF, 3rd, Miller WL 1996. The pathophysiology and genetics of congenital lipoid adrenal hyperplasia. N Engl J Med 335(25): 1870-8.

Bose J, Grotewold L, Ruther U 2002. Pallister-Hall syndrome phenotype in mice mutant for Gli3. Hum Mol Genet 11(9): 1129-35.

Bradford MM 1976. A rapid and sensitive method for the quantitation of microgram quantities of protein utilizing the principle of protein-dye binding. Anal Biochem 72: 248-54.

Braunewell KH, Klein-Szanto AJ 2009. Visinin-like proteins (VSNLs): interaction partners and emerging functions in signal transduction of a subfamily of neuronal Ca2+ -sensor proteins. Cell Tissue Res 335(2): 301-16.

British Standards Institution 1995. Water for analytical laboratory use - Specification and test methods BS EN ISO 3696:1995.

Bulun SE, Utsunomiya H, Lin Z, Yin P, Cheng YH, Pavone ME, Tokunaga H, Trukhacheva E, Attar E, Gurates B and others 2009. Steroidogenic factor-1 and endometriosis. Mol Cell Endocrinol 300(1-2): 104-8.

Campbell LA, Faivre EJ, Show MD, Ingraham JG, Flinders J, Gross JD, Ingraham HA 2008. Decreased recognition of SUMO-sensitive target genes following modification of SF-1 (NR5A1). Mol Cell Biol 28(24): 7476-86.

Cao G, Garcia CK, Wyne KL, Schultz RA, Parker KL, Hobbs HH 1997. Structure and localization of the human gene encoding SR-BI/CLA-1. Evidence for transcriptional control by steroidogenic factor 1. J Biol Chem 272(52): 33068-76.

Capel B 2000. The battle of the sexes. Mech Dev 92(1): 89-103.

Carbon S, Ireland A, Mungall CJ, Shu S, Marshall B, Lewis S 2009. AmiGO: online access to ontology and annotation data. Bioinformatics 25(2): 288-9.

Carroll JS, Liu XS, Brodsky AS, Li W, Meyer CA, Szary AJ, Eeckhoute J, Shao W, Hestermann EV, Geistlinger TR and others 2005. Chromosome-wide mapping of estrogen receptor binding reveals long-range regulation requiring the forkhead protein FoxA1. Cell 122(1): 33-43.

Carroll JS, Meyer CA, Song J, Li W, Geistlinger TR, Eeckhoute J, Brodsky AS, Keeton EK, Fertuck KC, Hall GF and others 2006. Genome-wide analysis of estrogen receptor binding sites. Nat Genet 38(11): 1289-97.

Cartharius K, Frech K, Grote K, Klocke B, Haltmeier M, Klingenhoff A, Frisch M, Bayerlein M, Werner T 2005. MatInspector and beyond: promoter analysis based on transcription factor binding sites. Bioinformatics 21(13): 2933-42.

Casal AJ, Sinclair VJ, Capponi AM, Nicod J, Huynh-Do U, Ferrari P 2006. A novel mutation in the steroidogenic acute regulatory protein gene promoter leading to reduced promoter activity. J Mol Endocrinol 37(1): 71-80.

Castillo AG, Mellone BG, Partridge JF, Richardson W, Hamilton GL, Allshire RC, Pidoux AL 2007. Plasticity of fission yeast CENP-A chromatin driven by relative levels of histone H3 and H4. PLoS Genet 3(7): e121.

Chang TY, Li BL, Chang CC, Urano Y 2009. Acyl-coenzyme A:cholesterol acyltransferases. Am J Physiol Endocrinol Metab 297(1): E1-9.

Chen WY, Lee WC, Hsu NC, Huang F, Chung BC 2004. SUMO modification of repression domains modulates function of nuclear receptor 5A1 (steroidogenic factor-1). J Biol Chem 279(37): 38730-5.

Chen WY, Juan LJ, Chung BC 2005. SF-1 (nuclear receptor 5A1) activity is activated by cyclic AMP via p300-mediated recruitment to active foci, acetylation, and increased DNA binding. Mol Cell Biol 25(23): 10442-53.

Ching S, Vilain E 2009. Targeted disruption of Sonic Hedgehog in the mouse adrenal leads to adrenocortical hypoplasia. Genesis 47(9): 628-37.

Chomczynski P, Sacchi N 1987. Single-step method of RNA isolation by acid guanidinium thiocyanate-phenol-chloroform extraction. Anal Biochem 162(1): 156-9.

Christenson LK, McAllister JM, Martin KO, Javitt NB, Osborne TF, Strauss JF, 3rd 1998. Oxysterol regulation of steroidogenic acute regulatory protein gene expression. Structural specificity and transcriptional and posttranscriptional actions. J Biol Chem 273(46): 30729-35.

Clark AJ, McLoughlin L, Grossman A 1993. Familial glucocorticoid deficiency associated with point mutation in the adrenocorticotropin receptor. Lancet 341(8843): 461-2.

Clark AJ, Weber A 1998. Adrenocorticotropin insensitivity syndromes. Endocr Rev 19(6): 828-43.

Cooray SN, Chan L, Metherell L, Storr H, Clark AJ 2008. Adrenocorticotropin resistance syndromes. Endocr Dev 13: 99-116.

Correa RV, Domenice S, Bingham NC, Billerbeck AE, Rainey WE, Parker KL, Mendonca BB 2004. A microdeletion in the ligand binding domain of human steroidogenic factor 1 causes XY sex reversal without adrenal insufficiency. J Clin Endocrinol Metab 89(4): 1767-72.

Coutant R, Mallet D, Lahlou N, Bouhours-Nouet N, Guichet A, Coupris L, Croue A, Morel Y 2007. Heterozygous mutation of steroidogenic factor-1 in 46,XY subjects may mimic partial androgen insensitivity syndrome. J Clin Endocrinol Metab 92(8): 2868-73.

Crawford PA, Sadovsky Y, Milbrandt J 1997. Nuclear receptor steroidogenic factor 1 directs embryonic stem cells toward the steroidogenic lineage. Mol Cell Biol 17(7): 3997-4006.

Curtin D, Ferris HA, Hakli M, Gibson M, Janne OA, Palvimo JJ, Shupnik MA 2004. Small nuclear RING finger protein stimulates the rat luteinizing hormone-beta promoter by interacting with Sp1 and steroidogenic factor-1 and protects from androgen suppression. Mol Endocrinol 18(5): 1263-76.

Dammer EB, Leon A, Sewer MB 2007. Coregulator exchange and sphingosine-sensitive cooperativity of steroidogenic factor-1, general control nonderepressed 5, p54, and p160 coactivators regulate cyclic adenosine 3',5'-monophosphate-dependent cytochrome P450c17 transcription rate. Mol Endocrinol 21(2): 415-38.

Davies D 2007. Cell sorting by flow cytometry. In: Macey MG ed. Flow cytometry: principles and applications. Totowa, Humana Press Inc. Pp. 257-76.

Del Tredici AL, Andersen CB, Currier EA, Ohrmund SR, Fairbain LC, Lund BW, Nash N, Olsson R, Piu F 2008. Identification of the first synthetic steroidogenic factor 1 inverse agonists: pharmacological modulation of steroidogenic enzymes. Mol Pharmacol 73(3): 900-8.

Dennis G, Jr., Sherman BT, Hosack DA, Yang J, Gao W, Lane HC, Lempicki RA 2003. DAVID: Database for Annotation, Visualization, and Integrated Discovery. Genome Biol 4(5): P3.

de-Souza BF, Lin L, Achermann JC 2006. Steroidogenic factor-1 (SF-1) and its relevance to pediatric endocrinology. Pediatr Endocrinol Rev 3(4): 359-64.

Doghman M, Karpova T, Rodrigues GA, Arhatte M, De Moura J, Cavalli LR, Virolle V, Barbry P, Zambetti GP, Figueiredo BC and others 2007. Increased steroidogenic factor-1 dosage triggers adrenocortical cell proliferation and cancer. Mol Endocrinol 21(12): 2968-87.

Doghman M, Cazareth J, Douguet D, Madoux F, Hodder P, Lalli E 2009. Inhibition of adrenocortical carcinoma cell proliferation by steroidogenic factor-1 inverse agonists. J Clin Endocrinol Metab 94(6): 2178-83.

Domenice S, Latronico AC, Brito VN, Arnhold IJ, Kok F, Mendonca BB 2001. Adrenocorticotropin-dependent precocious puberty of testicular origin in a boy with X-linked adrenal hypoplasia congenita due to a novel mutation in the DAX1 gene. J Clin Endocrinol Metab 86(9): 4068-71.

Ehrhart-Bornstein M, Hinson JP, Bornstein SR, Scherbaum WA, Vinson GP 1998. Intraadrenal interactions in the regulation of adrenocortical steroidogenesis. Endocr Rev 19(2): 101-43.

Ehrlund A, Anthonisen EH, Gustafsson N, Venteclef N, Robertson Remen K, Damdimopoulos AE, Galeeva A, Pelto-Huikko M, Lalli E, Steffensen KR and others 2009. E3 ubiquitin ligase RNF31 cooperates with DAX-1 in transcriptional repression of steroidogenesis. Mol Cell Biol 29(8): 2230-42.

Else T, Hammer GD 2005. Genetic analysis of adrenal absence: agenesis and aplasia. Trends Endocrinol Metab 16(10): 458-68.

Evans RM 1988. The steroid and thyroid hormone receptor superfamily. Science 240(4854): 889-95.

Fairbrother WG, Yeh RF, Sharp PA, Burge CB 2002. Predictive identification of exonic splicing enhancers in human genes. Science 297(5583): 1007-13.

Fan W, Yanase T, Morinaga H, Gondo S, Okabe T, Nomura M, Komatsu T, Morohashi K, Hayes TB, Takayanagi R and others 2007. Atrazine-induced aromatase expression is SF-1 dependent: implications for endocrine disruption in wildlife and reproductive cancers in humans. Environ Health Perspect 115(5): 720-7.

Fassnacht M, Hahner S, Hansen IA, Kreutzberger T, Zink M, Adermann K, Jakob F, Troppmair J, Allolio B 2003. N-terminal proopiomelanocortin acts as a mitogen in adrenocortical tumor cells and decreases adrenal steroidogenesis. J Clin Endocrinol Metab 88(5): 2171-9.

Fatchiyah, Zubair M, Shima Y, Oka S, Ishihara S, Fukui-Katoh Y, Morohashi K 2006. Differential gene dosage effects of Ad4BP/SF-1 on target tissue development. Biochem Biophys Res Commun 341(4): 1036-45.

Ferrara N, Kerbel RS 2005. Angiogenesis as a therapeutic target. Nature 438(7070): 967-74.

Ferraz-de-Souza B, Achermann JC 2008. Disorders of adrenal development. Endocr Dev 13: 19-32.

Ferraz-de-Souza B, Martin F, Mallet D, Hudson-Davies RE, Cogram P, Lin L, Gerrelli D, Beuschlein F, Morel Y, Huebner A, Achermann JC 2009. CBP/p300-interacting transactivator, with Glu/Asp-rich C-terminal domain, 2, and pre-B-cell leukemia transcription factor 1 in human adrenal development and disease. J Clin Endocrinol Metab 94(2): 678-83.

Ferraz-de-Souza B, Lin L, Achermann JC 2010a. Steroidogenic factor-1 (SF-1, NR5A1) and human disease. [E-pub ahead of print] Mol Cell Endocrinol. doi: 10.1016/j.mce.2010.11.006

Ferraz-de-Souza B, Lin L, Shah S, Jina N, Hubank M, Dattani MT, Achermann JC 2010b. ChIP-on-chip analysis reveals angiopoietin 2 (Ang2, ANGPT2) as a novel target of steroidogenic factor-1 (SF-1, NR5A1) in the human adrenal gland. FASEB J *in press*. doi: 10.1096/fj.10-170522

Ferraz-de-Souza B, Hudson-Davies RE, Lin L, Parnaik R, Hubank M, Dattani MT, Achermann JC 2011. Sterol O-acyltransferase 1 (SOAT1, ACAT) is a novel target of steroidogenic factor-1 (SF-1, NR5A1, Ad4BP) in the human adrenal. J Clin Endocrinol Metab *in press*. doi: 10.1210/jc.2010-2021

Figueiredo BC, Cavalli LR, Pianovski MA, Lalli E, Sandrini R, Ribeiro RC, Zambetti G, DeLacerda L, Rodrigues GA, Haddad BR 2005. Amplification of the steroidogenic factor 1 gene in childhood adrenocortical tumors. J Clin Endocrinol Metab 90(2): 615-9.

Fu J, Zhang J, Jin F, Patchefsky J, Braunewell KH, Klein-Szanto AJ 2009. Promoter regulation of the visinin-like subfamily of neuronal calcium sensor proteins by nuclear respiratory factor-1. J Biol Chem 284(40): 27577-86.

Garcia-Pineres AJ, Hildesheim A, Williams M, Trivett M, Strobl S, Pinto LA 2006. DNAse treatment following thawing of cryopreserved PBMC is a procedure suitable for lymphocyte functional studies. J Immunol Methods 313(1-2): 209-13.

Gazdar AF, Oie HK, Shackleton CH, Chen TR, Triche TJ, Myers CE, Chrousos GP, Brennan MF, Stein CA, La Rocca RV 1990. Establishment and characterization of a human adrenocortical carcinoma cell line that expresses multiple pathways of steroid biosynthesis. Cancer Res 50(17): 5488-96.

Gevry NY, Lalli E, Sassone-Corsi P, Murphy BD 2003. Regulation of niemann-pick c1 gene expression by the 3'5'-cyclic adenosine monophosphate pathway in steroidogenic cells. Mol Endocrinol 17(4): 704-15.

Giordano TJ, Kuick R, Else T, Gauger PG, Vinco M, Bauersfeld J, Sanders D, Thomas DG, Doherty G, Hammer G 2009. Molecular classification and prognostication of adrenocortical tumors by transcriptome profiling. Clin Cancer Res 15(2): 668-76.

Gizard F, Lavallee B, DeWitte F, Teissier E, Staels B, Hum DW 2002. The transcriptional regulating protein of 132 kDa (TReP-132) enhances P450scc gene transcription through interaction with steroidogenic factor-1 in human adrenal cells. J Biol Chem 277(42): 39144-55.

Gordon EJ, Rao S, Pollard JW, Nutt SL, Lang RA, Harvey NL 2010. Macrophages define dermal lymphatic vessel calibre during development by regulating lymphatic endothelial cell proliferation. Development 137(22): 3899-910.

Goto M, Piper Hanley K, Marcos J, Wood PJ, Wright S, Postle AD, Cameron IT, Mason JI, Wilson DI, Hanley NA 2006. In humans, early cortisol biosynthesis provides a mechanism to safeguard female sexual development. J Clin Invest 116(4): 953-60.

Graham FL, Smiley J, Russell WC, Nairn R 1977. Characteristics of a human cell line transformed by DNA from human adenovirus type 5. J Gen Virol 36(1): 59-74.

Griffin BD, Moynagh PN 2006. Persistent interleukin-1beta signaling causes long term activation of NFkappaB in a promoter-specific manner in human glial cells. J Biol Chem 281(15): 10316-26.

Gruber F, Hufnagl P, Hofer-Warbinek R, Schmid JA, Breuss JM, Huber-Beckmann R, Lucerna M, Papac N, Harant H, Lindley I and others 2003. Direct binding of Nur77/NAK-1 to the plasminogen activator inhibitor 1 (PAI-1) promoter regulates TNF alpha -induced PAI-1 expression. Blood 101(8): 3042-8.

Gu P, Goodwin B, Chung AC, Xu X, Wheeler DA, Price RR, Galardi C, Peng L, Latour AM, Koller BH and others 2005. Orphan nuclear receptor LRH-1 is required to maintain Oct4 expression at the epiblast stage of embryonic development. Mol Cell Biol 25(9): 3492-505.

Guclu M, Lin L, Erturk E, Achermann JC, Cangul H 2010. Puberty, stress, and sudden death. Lancet 376(9751): 1512.

Gudmundsson J, Sulem P, Gudbjartsson DF, Jonasson JG, Sigurdsson A, Bergthorsson JT, He H, Blondal T, Geller F, Jakobsdottir M and others 2009. Common variants on 9q22.33 and 14q13.3 predispose to thyroid cancer in European populations. Nat Genet 41(4): 460-4.

Gummow BM, Scheys JO, Cancelli VR, Hammer GD 2006. Reciprocal regulation of a glucocorticoid receptor-steroidogenic factor-1 transcription complex on the Dax-1

promoter by glucocorticoids and adrenocorticotropic hormone in the adrenal cortex. Mol Endocrinol 20(11): 2711-23.

Guo W, Burris TP, McCabe ER 1995. Expression of DAX-1, the gene responsible for X-linked adrenal hypoplasia congenita and hypogonadotropic hypogonadism, in the hypothalamic-pituitary-adrenal/gonadal axis. Biochem Mol Med 56(1): 8-13.

Guo IC, Shih MC, Lan HC, Hsu NC, Hu MC, Chung BC 2007. Transcriptional regulation of human CYP11A1 in gonads and adrenals. J Biomed Sci 14(4): 509-15.

Gwynne JT, Strauss JF, 3rd 1982. The role of lipoproteins in steroidogenesis and cholesterol metabolism in steroidogenic glands. Endocr Rev 3(3): 299-329.

Haase M, Schott M, Bornstein SR, Malendowicz LK, Scherbaum WA, Willenberg HS 2007. CITED2 is expressed in human adrenocortical cells and regulated by basic fibroblast growth factor. J Endocrinol 192(2): 459-65.

Hall JG, Pallister PD, Clarren SK, Beckwith JB, Wiglesworth FW, Fraser FC, Cho S, Benke PJ, Reed SD 1980. Congenital hypothalamic hamartoblastoma, hypopituitarism, imperforate anus and postaxial polydactyly--a new syndrome? Part I: clinical, causal, and pathogenetic considerations. Am J Med Genet 7(1): 47-74.

Hammer GD, Krylova I, Zhang Y, Darimont BD, Simpson K, Weigel NL, Ingraham HA 1999. Phosphorylation of the nuclear receptor SF-1 modulates cofactor recruitment: integration of hormone signaling in reproduction and stress. Mol Cell 3(4): 521-6.

Hammer GD, Parker KL, Schimmer BP 2005. Minireview: transcriptional regulation of adrenocortical development. Endocrinology 146(3): 1018-24.

Hanley NA, Ball SG, Clement-Jones M, Hagan DM, Strachan T, Lindsay S, Robson S, Ostrer H, Parker KL, Wilson DI 1999. Expression of steroidogenic factor 1 and Wilms' tumour 1 during early human gonadal development and sex determination. Mech Dev 87(1-2): 175-80.

Hanley NA, Rainey WE, Wilson DI, Ball SG, Parker KL 2001. Expression profiles of SF-1, DAX1, and CYP17 in the human fetal adrenal gland: potential interactions in gene regulation. Mol Endocrinol 15(1): 57-68.

Hasegawa T, Fukami M, Sato N, Katsumata N, Sasaki G, Fukutani K, Morohashi K, Ogata T 2004. Testicular dysgenesis without adrenal insufficiency in a 46,XY patient with a heterozygous inactive mutation of steroidogenic factor-1. J Clin Endocrinol Metab 89(12): 5930-5.

Hiroi H, Christenson LK, Chang L, Sammel MD, Berger SL, Strauss JF, 3rd 2004. Temporal and spatial changes in transcription factor binding and histone modifications at the steroidogenic acute regulatory protein (stAR) locus associated with stAR transcription. Mol Endocrinol 18(4): 791-806.

Hoivik EA, Lewis AE, Aumo L, Bakke M 2010. Molecular aspects of steroidogenic factor 1 (SF-1). Mol Cell Endocrinol 315(1-2): 27-39.

Honda S, Morohashi K, Nomura M, Takeya H, Kitajima M, Omura T 1993. Ad4BP regulating steroidogenic P-450 gene is a member of steroid hormone receptor superfamily. J Biol Chem 268(10): 7494-502.

Hong CY, Park JH, Ahn RS, Im SY, Choi HS, Soh J, Mellon SH, Lee K 2004. Molecular mechanism of suppression of testicular steroidogenesis by proinflammatory cytokine tumor necrosis factor alpha. Mol Cell Biol 24(7): 2593-604.

Houtz M, Trotter J, Sasaki D 2004. Tips on cell preparation for flow cytometric analysis and sorting. BD FACService Technotes/Customer Focused Solutions 9(4): 1-4.

Hu MC, Hsu NC, Pai CI, Wang CK, Chung B 2001. Functions of the upstream and proximal steroidogenic factor 1 (SF-1)-binding sites in the CYP11A1 promoter in basal transcription and hormonal response. Mol Endocrinol 15(5): 812-8.

Huang da W, Sherman BT, Lempicki RA 2009. Systematic and integrative analysis of large gene lists using DAVID bioinformatics resources. Nat Protoc 4(1): 44-57.

Hutz JE, Krause AS, Achermann JC, Vilain E, Tauber M, Lecointre C, McCabe ER, Hammer GD, Keegan CE 2006. IMAGe association and congenital adrenal hypoplasia: no disease-causing mutations found in the ACD gene. Mol Genet Metab 88(1): 66-70.

Ikeda Y, Shen WH, Ingraham HA, Parker KL 1994. Developmental expression of mouse steroidogenic factor-1, an essential regulator of the steroid hydroxylases. Mol Endocrinol 8(5): 654-62.

Ingham PW, McMahon AP 2001. Hedgehog signaling in animal development: paradigms and principles. Genes Dev 15(23): 3059-87.

Ishimoto H, Ginzinger DG, Jaffe RB 2006. Adrenocorticotropin preferentially up-regulates angiopoietin 2 in the human fetal adrenal gland: implications for coordinated adrenal organ growth and angiogenesis. J Clin Endocrinol Metab 91(5): 1909-15.

Ishimoto H, Minegishi K, Higuchi T, Furuya M, Asai S, Kim SH, Tanaka M, Yoshimura Y, Jaffe RB 2008. The periphery of the human fetal adrenal gland is a site of angiogenesis: zonal differential expression and regulation of angiogenic factors. J Clin Endocrinol Metab 93(6): 2402-8.

Ito M, Yu R, Jameson JL 1997. DAX-1 inhibits SF-1-mediated transactivation via a carboxy-terminal domain that is deleted in adrenal hypoplasia congenita. Mol Cell Biol 17(3): 1476-83.

Ito M, Yu RN, Jameson JL 1998. Steroidogenic factor-1 contains a carboxy-terminal transcriptional activation domain that interacts with steroid receptor coactivator-1. Mol Endocrinol 12(2): 290-301.

Ito M, Achermann JC, Jameson JL 2000. A naturally occurring steroidogenic factor-1 mutation exhibits differential binding and activation of target genes. J Biol Chem 275(41): 31708-14.

Iyer VR, Horak CE, Scafe CS, Botstein D, Snyder M, Brown PO 2001. Genomic binding sites of the yeast cell-cycle transcription factors SBF and MBF. Nature 409(6819): 533-8.

Iyer AK, McCabe ER 2004. Molecular mechanisms of DAX1 action. Mol Genet Metab 83(1-2): 60-73.

Jackson RJ, Howell MT, Kaminski A 1990. The novel mechanism of initiation of picornavirus RNA translation. Trends Biochem Sci 15(12): 477-83.

Jackson RS, Creemers JW, Ohagi S, Raffin-Sanson ML, Sanders L, Montague CT, Hutton JC, O'Rahilly S 1997. Obesity and impaired prohormone processing associated with mutations in the human prohormone convertase 1 gene. Nat Genet 16(3): 303-6.

Jackson RS, Creemers JW, Farooqi IS, Raffin-Sanson ML, Varro A, Dockray GJ, Holst JJ, Brubaker PL, Corvol P, Polonsky KS and others 2003. Small-intestinal dysfunction accompanies the complex endocrinopathy of human proprotein convertase 1 deficiency. J Clin Invest 112(10): 1550-60.

Jacob AL, Lund J, Martinez P, Hedin L 2001. Acetylation of steroidogenic factor 1 protein regulates its transcriptional activity and recruits the coactivator GCN5. J Biol Chem 276(40): 37659-64.

Jang SK, Krausslich HG, Nicklin MJ, Duke GM, Palmenberg AC, Wimmer E 1988. A segment of the 5' nontranslated region of encephalomyocarditis virus RNA directs internal entry of ribosomes during in vitro translation. J Virol 62(8): 2636-43.

Ji H, Wong WH 2005. TileMap: create chromosomal map of tiling array hybridizations. Bioinformatics 21(18): 3629-36.

Ji H, Vokes SA, Wong WH 2006. A comparative analysis of genome-wide chromatin immunoprecipitation data for mammalian transcription factors. Nucleic Acids Res 34(21): e146.

Ji H, Jiang H, Ma W, Johnson DS, Myers RM, Wong WH 2008. An integrated software system for analyzing ChIP-chip and ChIP-seq data. Nat Biotechnol 26(11): 1293-300.

Johnson DS, Mortazavi A, Myers RM, Wold B 2007. Genome-wide mapping of in vivo protein-DNA interactions. Science 316(5830): 1497-502.

Johnson DS, Li W, Gordon DB, Bhattacharjee A, Curry B, Ghosh J, Brizuela L, Carroll JS, Brown M, Flicek P and others 2008. Systematic evaluation of variability in ChIP-chip experiments using predefined DNA targets. Genome Res 18(3): 393-403.

Johnston JJ, Olivos-Glander I, Killoran C, Elson E, Turner JT, Peters KF, Abbott MH, Aughton DJ, Aylsworth AS, Bamshad MJ and others 2005. Molecular and clinical analyses of Greig cephalopolysyndactyly and Pallister-Hall syndromes: robust phenotype prediction from the type and position of GLI3 mutations. Am J Hum Genet 76(4): 609-22.

Johnston JJ, Sapp JC, Turner JT, Amor D, Aftimos S, Aleck KA, Bocian M, Bodurtha JN, Cox GF, Curry CJ and others 2010. Molecular analysis expands the spectrum of phenotypes associated with GLI3 mutations. Hum Mutat 31(10): 1142-54.

Jothi R, Cuddapah S, Barski A, Cui K, Zhao K 2008. Genome-wide identification of in vivo protein-DNA binding sites from ChIP-Seq data. Nucleic Acids Res 36(16): 5221-31.

Kagawa N, Ogo A, Takahashi Y, Iwamatsu A, Waterman MR 1994. A cAMP-regulatory sequence (CRS1) of CYP17 is a cellular target for the homeodomain protein Pbx1. J Biol Chem 269(29): 18716-9.

Kamps MP, Murre C, Sun XH, Baltimore D 1990. A new homeobox gene contributes the DNA binding domain of the t(1;19) translocation protein in pre-B ALL. Cell 60(4): 547-55.

Kang S, Graham JM, Jr., Olney AH, Biesecker LG 1997. GLI3 frameshift mutations cause autosomal dominant Pallister-Hall syndrome. Nat Genet 15(3): 266-8.

Katoh-Fukui Y, Owaki A, Toyama Y, Kusaka M, Shinohara Y, Maekawa M, Toshimori K, Morohashi K 2005. Mouse Polycomb M33 is required for splenic vascular and adrenal gland formation through regulating Ad4BP/SF1 expression. Blood 106(5): 1612-20.

Keegan CE, Hutz JE, Krause AS, Koehler K, Metherell LA, Boikos S, Stergiopoulos S, Clark AJ, Stratakis CA, Huebner A and others 2007. Novel polymorphisms and lack of mutations in the ACD gene in patients with ACTH resistance syndromes. Clin Endocrinol (Oxf) 67(2): 168-74.

Kelberman D, Dattani MT 2006. The role of transcription factors implicated in anterior pituitary development in the aetiology of congenital hypopituitarism. Ann Med 38(8): 560-77.

Kelberman D, Rizzoti K, Lovell-Badge R, Robinson IC, Dattani MT 2009. Genetic regulation of pituitary gland development in human and mouse. Endocr Rev 30(7): 790-829.

Kelso J, Visagie J, Theiler G, Christoffels A, Bardien S, Smedley D, Otgaar D, Greyling G, Jongeneel CV, McCarthy MI and others 2003. eVOC: a controlled vocabulary for unifying gene expression data. Genome Res 13(6A): 1222-30.

Kim J, Bergmann A, Stubbs L 2000. Exon sharing of a novel human zinc-finger gene, ZIM2, and paternally expressed gene 3 (PEG3). Genomics 64(1): 114-8.

Kim J, Bergmann A, Lucas S, Stone R, Stubbs L 2004. Lineage-specific imprinting and evolution of the zinc-finger gene ZIM2. Genomics 84(1): 47-58.

Kim TH, Ren B 2006. Genome-wide analysis of protein-DNA interactions. Annu Rev Genomics Hum Genet 7: 81-102.

Kim AC, Hammer GD 2007. Adrenocortical cells with stem/progenitor cell properties: recent advances. Mol Cell Endocrinol 265-266: 10-6.

Kim Y, Bingham N, Sekido R, Parker KL, Lovell-Badge R, Capel B 2007. Fibroblast growth factor receptor 2 regulates proliferation and Sertoli differentiation during male sex determination. Proc Natl Acad Sci U S A 104(42): 16558-63.

Kim CJ, Lin L, Huang N, Quigley CA, AvRuskin TW, Achermann JC, Miller WL 2008. Severe combined adrenal and gonadal deficiency caused by novel mutations in the cholesterol side chain cleavage enzyme, P450scc. J Clin Endocrinol Metab 93(3): 696-702.

Kim AC, Barlaskar FM, Heaton JH, Else T, Kelly VR, Krill KT, Scheys JO, Simon DP, Trovato A, Yang WH and others 2009. In search of adrenocortical stem and progenitor cells. Endocr Rev 30(3): 241-63.

King PJ, Guasti L, Laufer E 2008. Hedgehog signalling in endocrine development and disease. J Endocrinol 198(3): 439-50.

King P, Paul A, Laufer E 2009. Shh signaling regulates adrenocortical development and identifies progenitors of steroidogenic lineages. Proc Natl Acad Sci U S A 106(50): 21185-90.

Kohler B, Lin L, Ferraz-de-Souza B, Wieacker P, Heidemann P, Schroder V, Biebermann H, Schnabel D, Gruters A, Achermann JC 2008. Five novel mutations in steroidogenic factor 1 (SF1, NR5A1) in 46,XY patients with severe underandrogenization but without adrenal insufficiency. Hum Mutat 29(1): 59-64.

Kohler B, Lin L, Mazen I, Cetindag C, Biebermann H, Akkurt I, Rossi R, Hiort O, Gruters A, Achermann JC 2009. The spectrum of phenotypes associated with mutations in steroidogenic factor 1 (SF-1, NR5A1, Ad4BP) includes severe penoscrotal hypospadias in 46,XY males without adrenal insufficiency. Eur J Endocrinol 161(2): 237-42.

Kohler B, Achermann JC 2010. Update--steroidogenic factor 1 (SF-1, NR5A1). Minerva Endocrinol 35(2): 73-86.

Komatsu T, Mizusaki H, Mukai T, Ogawa H, Baba D, Shirakawa M, Hatakeyama S, Nakayama KI, Yamamoto H, Kikuchi A and others 2004. Small ubiquitin-like modifier 1 (SUMO-1) modification of the synergy control motif of Ad4 binding protein/steroidogenic factor 1 (Ad4BP/SF-1) regulates synergistic transcription between Ad4BP/SF-1 and Sox9. Mol Endocrinol 18(10): 2451-62.

Kraemer FB 2007. Adrenal cholesterol utilization. Mol Cell Endocrinol 265-266: 42-5.

Kreidberg JA, Sariola H, Loring JM, Maeda M, Pelletier J, Housman D, Jaenisch R 1993. WT-1 is required for early kidney development. Cell 74(4): 679-91.

Kremer H, Kraaij R, Toledo SP, Post M, Fridman JB, Hayashida CY, van Reen M, Milgrom E, Ropers HH, Mariman E and others 1995. Male pseudohermaphroditism due to a

homozygous missense mutation of the luteinizing hormone receptor gene. Nat Genet 9(2): 160-4.

Krude H, Biebermann H, Luck W, Horn R, Brabant G, Gruters A 1998. Severe early-onset obesity, adrenal insufficiency and red hair pigmentation caused by POMC mutations in humans. Nat Genet 19(2): 155-7.

Krude H, Schutz B, Biebermann H, von Moers A, Schnabel D, Neitzel H, Tonnies H, Weise D, Lafferty A, Schwarz S and others 2002. Choreoathetosis, hypothyroidism, and pulmonary alterations due to human NKX2-1 haploinsufficiency. J Clin Invest 109(4): 475-80.

Krude H, Biebermann H, Schnabel D, Tansek MZ, Theunissen P, Mullis PE, Gruters A 2003. Obesity due to proopiomelanocortin deficiency: three new cases and treatment trials with thyroid hormone and ACTH4-10. J Clin Endocrinol Metab 88(10): 4633-40.

Krylova IN, Sablin EP, Moore J, Xu RX, Waitt GM, MacKay JA, Juzumiene D, Bynum JM, Madauss K, Montana V and others 2005. Structural analyses reveal phosphatidyl inositols as ligands for the NR5 orphan receptors SF-1 and LRH-1. Cell 120(3): 343-55.

Lala DS, Rice DA, Parker KL 1992. Steroidogenic factor I, a key regulator of steroidogenic enzyme expression, is the mouse homolog of fushi tarazu-factor I. Mol Endocrinol 6(8): 1249-58.

Lala DS, Syka PM, Lazarchik SB, Mangelsdorf DJ, Parker KL, Heyman RA 1997. Activation of the orphan nuclear receptor steroidogenic factor 1 by oxysterols. Proc Natl Acad Sci U S A 94(10): 4895-900.

Lalli E, Sassone-Corsi P 2003. DAX-1, an unusual orphan receptor at the crossroads of steroidogenic function and sexual differentiation. Mol Endocrinol 17(8): 1445-53.

Lalli E 2010. Adrenocortical development and cancer: focus on SF-1. J Mol Endocrinol 44(6): 301-7.

Lalli E, Alonso J 2010. Targeting DAX-1 in embryonic stem cells and cancer. Expert Opin Ther Targets 14(2): 169-77.

Lamolet B, Pulichino AM, Lamonerie T, Gauthier Y, Brue T, Enjalbert A, Drouin J 2001. A pituitary cell-restricted T box factor, Tpit, activates POMC transcription in cooperation with Pitx homeoproteins. Cell 104(6): 849-59.

Laverty CR, Fortune DW, Beischer NA 1973. Congenital idiopathic adrenal hypoplasia. Obstet Gynecol 41(5): 655-64.

Lee RG, Willingham MC, Davis MA, Skinner KA, Rudel LL 2000. Differential expression of ACAT1 and ACAT2 among cells within liver, intestine, kidney, and adrenal of nonhuman primates. J Lipid Res 41(12): 1991-2001.

Lee SB, Haber DA 2001. Wilms tumor and the WT1 gene. Exp Cell Res 264(1): 74-99.

Lee TI, Johnstone SE, Young RA 2006. Chromatin immunoprecipitation and microarray-based analysis of protein location. Nat Protoc 1(2): 729-48.

Lehmann SG, Wurtz JM, Renaud JP, Sassone-Corsi P, Lalli E 2003. Structure-function analysis reveals the molecular determinants of the impaired biological function of DAX-1 mutants in AHC patients. Hum Mol Genet 12(9): 1063-72.

Leung MK, Jones T, Michels CL, Livingston DM, Bhattacharya S 1999. Molecular cloning and chromosomal localization of the human CITED2 gene encoding p35srj/Mrg1. Genomics 61(3): 307-13.

Lewis AE, Rusten M, Hoivik EA, Vikse EL, Hansson ML, Wallberg AE, Bakke M 2008. Phosphorylation of steroidogenic factor 1 is mediated by cyclin-dependent kinase 7. Mol Endocrinol 22(1): 91-104.

Li Y, Choi M, Cavey G, Daugherty J, Suino K, Kovach A, Bingham NC, Kliewer SA, Xu HE 2005. Crystallographic identification and functional characterization of phospholipids as ligands for the orphan nuclear receptor steroidogenic factor-1. Mol Cell 17(4): 491-502.

Li D, Urs AN, Allegood J, Leon A, Merrill AH, Jr., Sewer MB 2007. Cyclic AMP-stimulated interaction between steroidogenic factor 1 and diacylglycerol kinase theta facilitates induction of CYP17. Mol Cell Biol 27(19): 6669-85.

Li N, Liu R, Zhang H, Yang J, Sun S, Zhang M, Liu Y, Lu Y, Wang W, Mu Y and others 2010. Seven novel DAX1 mutations with loss of function identified in Chinese patients with congenital adrenal hypoplasia. J Clin Endocrinol Metab 95(9): E104-11.

Lichtenauer UD, Duchniewicz M, Kolanczyk M, Hoeflich A, Hahner S, Else T, Bicknell AB, Zemojtel T, Stallings NR, Schulte DM and others 2007. Pre-B-cell transcription factor 1 and steroidogenic factor 1 synergistically regulate adrenocortical growth and steroidogenesis. Endocrinology 148(2): 693-704.

Lin L, Achermann JC 2004. Inherited adrenal hypoplasia: not just for kids! Clin Endocrinol (Oxf) 60(5): 529-37.

Lin L, Gu WX, Ozisik G, To WS, Owen CJ, Jameson JL, Achermann JC 2006. Analysis of DAX1 (NR0B1) and steroidogenic factor-1 (NR5A1) in children and adults with primary adrenal failure: ten years' experience. J Clin Endocrinol Metab 91(8): 3048-54.

Lin L, Philibert P, Ferraz-de-Souza B, Kelberman D, Homfray T, Albanese A, Molini V, Sebire NJ, Einaudi S, Conway GS and others 2007. Heterozygous missense mutations in steroidogenic factor 1 (SF1/Ad4BP, NR5A1) are associated with 46,XY disorders of sex development with normal adrenal function. J Clin Endocrinol Metab 92(3): 991-9.

Lin BC, Suzawa M, Blind RD, Tobias SC, Bulun SE, Scanlan TS, Ingraham HA 2009. Stimulating the GPR30 estrogen receptor with a novel tamoxifen analogue activates SF-1 and promotes endometrial cell proliferation. Cancer Res 69(13): 5415-23.

Little TH, Zhang Y, Matulis CK, Weck J, Zhang Z, Ramachandran A, Mayo KE, Radhakrishnan I 2006. Sequence-specific deoxyribonucleic acid (DNA) recognition by steroidogenic factor 1: a helix at the carboxy terminus of the DNA binding domain is necessary for complex stability. Mol Endocrinol 20(4): 831-43.

Liu G, Duranteau L, Carel JC, Monroe J, Doyle DA, Shenker A 1999. Leydig-cell tumors caused by an activating mutation of the gene encoding the luteinizing hormone receptor. N Engl J Med 341(23): 1731-6.

Livak KJ, Schmittgen TD 2001. Analysis of relative gene expression data using real-time quantitative PCR and the 2(-Delta Delta C(T)) Method. Methods 25(4): 402-8.

Lopez D, Shea-Eaton W, McLean MP 2001. Characterization of a steroidogenic factor-1-binding site found in promoter of sterol carrier protein-2 gene. Endocrine 14(2): 253-61.

Lourenco D, Brauner R, Lin L, De Perdigo A, Weryha G, Muresan M, Boudjenah R, Guerra-Junior G, Maciel-Guerra AT, Achermann JC and others 2009. Mutations in NR5A1 associated with ovarian insufficiency. N Engl J Med 360(12): 1200-10.

Luo X, Ikeda Y, Parker KL 1994. A cell-specific nuclear receptor is essential for adrenal and gonadal development and sexual differentiation. Cell 77(4): 481-90.

Majdic G, Young M, Gomez-Sanchez E, Anderson P, Szczepaniak LS, Dobbins RL, McGarry JD, Parker KL 2002. Knockout mice lacking steroidogenic factor 1 are a novel genetic model of hypothalamic obesity. Endocrinology 143(2): 607-14.

Mallet D, Bretones P, Michel-Calemard L, Dijoud F, David M, Morel Y 2004. Gonadal dysgenesis without adrenal insufficiency in a 46, XY patient heterozygous for the nonsense C16X mutation: a case of SF1 haploinsufficiency. J Clin Endocrinol Metab 89(10): 4829-32.

Mandel H, Shemer R, Borochowitz ZU, Okopnik M, Knopf C, Indelman M, Drugan A, Tiosano D, Gershoni-Baruch R, Choder M and others 2008. SERKAL syndrome: an autosomal-recessive disorder caused by a loss-of-function mutation in WNT4. Am J Hum Genet 82(1): 39-47.

Mantovani G, Ozisik G, Achermann JC, Romoli R, Borretta G, Persani L, Spada A, Jameson JL, Beck-Peccoz P 2002. Hypogonadotropic hypogonadism as a presenting feature of late-onset X-linked adrenal hypoplasia congenita. J Clin Endocrinol Metab 87(1): 44-8.

Mascaro C, Nadal A, Hegardt FG, Marrero PF, Haro D 2000. Contribution of steroidogenic factor 1 to the regulation of cholesterol synthesis. Biochem J 350 Pt 3: 785-90.

Matthews JC, Hori K, Cormier MJ 1977. Purification and properties of Renilla reniformis luciferase. Biochemistry 16(1): 85-91.

Meiner VL, Cases S, Myers HM, Sande ER, Bellosta S, Schambelan M, Pitas RE, McGuire J, Herz J, Farese RV, Jr. 1996. Disruption of the acyl-CoA:cholesterol acyltransferase gene in mice: evidence suggesting multiple cholesterol esterification enzymes in mammals. Proc Natl Acad Sci U S A 93(24): 14041-6.

Meiner VL, Welch CL, Cases S, Myers HM, Sande E, Lusis AJ, Farese RV, Jr. 1998. Adrenocortical lipid depletion gene (ald) in AKR mice is associated with an acyl-CoA:cholesterol acyltransferase (ACAT) mutation. J Biol Chem 273(2): 1064-9.

Mellgren G, Borud B, Hoang T, Yri OE, Fladeby C, Lien EA, Lund J 2003. Characterization of receptor-interacting protein RIP140 in the regulation of SF-1 responsive target genes. Mol Cell Endocrinol 203(1-2): 91-103.

Mellon SH, Bair SR 1998. 25-Hydroxycholesterol is not a ligand for the orphan nuclear receptor steroidogenic factor-1 (SF-1). Endocrinology 139(6): 3026-9.

Mesiano S, Jaffe RB 1997. Developmental and functional biology of the primate fetal adrenal cortex. Endocr Rev 18(3): 378-403.

Metherell LA, Chapple JP, Cooray S, David A, Becker C, Ruschendorf F, Naville D, Begeot M, Khoo B, Nurnberg P and others 2005. Mutations in MRAP, encoding a new interacting partner of the ACTH receptor, cause familial glucocorticoid deficiency type 2. Nat Genet 37(2): 166-70.

Metherell LA, Naville D, Halaby G, Begeot M, Huebner A, Nurnberg G, Nurnberg P, Green J, Tomlinson JW, Krone NP and others 2009. Nonclassic lipoid congenital adrenal hyperplasia masquerading as familial glucocorticoid deficiency. J Clin Endocrinol Metab 94(10): 3865-71.

Miller WL, Achermann JC, Fluck CE 2008. The adrenal cortex and its disorders. In: Sperling MA ed. Pediatric endocrinology. 3rd ed. Philadelphia, Saunders Elservier. Pp. 444-511.

Miller WL 2009. Androgen synthesis in adrenarche. Rev Endocr Metab Disord 10(1): 3-17.

Mita AC, Takimoto CH, Mita M, Tolcher A, Sankhala K, Sarantopoulos J, Valdivieso M, Wood L, Rasmussen E, Sun YN and others 2010. Phase 1 study of AMG 386, a selective angiopoietin 1/2-neutralizing peptibody, in combination with chemotherapy in adults with advanced solid tumors. Clin Cancer Res 16(11): 3044-56.

Moens CB, Selleri L 2006. Hox cofactors in vertebrate development. Dev Biol 291(2): 193-206.

Moerman P, Fryns JP, Goddeeris P, Lauweryns JM 1983. Multiple ankyloses, facial anomalies, and pulmonary hypoplasia associated with severe antenatal spinal muscular atrophy. J Pediatr 103(2): 238-41.

Morohashi K, Honda S, Inomata Y, Handa H, Omura T 1992. A common trans-acting factor, Ad4-binding protein, to the promoters of steroidogenic P-450s. J Biol Chem 267(25): 17913-9.

Morohashi K, Zanger UM, Honda S, Hara M, Waterman MR, Omura T 1993. Activation of CYP11A and CYP11B gene promoters by the steroidogenic cell-specific transcription factor, Ad4BP. Mol Endocrinol 7(9): 1196-204.

Morohashi K, Tsuboi-Asai H, Matsushita S, Suda M, Nakashima M, Sasano H, Hataba Y, Li CL, Fukata J, Irie J and others 1999. Structural and functional abnormalities in the spleen of an mFtz-F1 gene-disrupted mouse. Blood 93(5): 1586-94.

Mouillet JF, Sonnenberg-Hirche C, Yan X, Sadovsky Y 2004. p300 regulates the synergy of steroidogenic factor-1 and early growth response-1 in activating luteinizing hormone-beta subunit gene. J Biol Chem 279(9): 7832-9.

Muscatelli F, Strom TM, Walker AP, Zanaria E, Recan D, Meindl A, Bardoni B, Guioli S, Zehetner G, Rabl W and others 1994. Mutations in the DAX-1 gene give rise to both X-linked adrenal hypoplasia congenita and hypogonadotropic hypogonadism. Nature 372(6507): 672-6.

Naughton C, MacLeod K, Kuske B, Clarke R, Cameron DA, Langdon SP 2007. Progressive loss of estrogen receptor alpha cofactor recruitment in endocrine resistance. Mol Endocrinol 21(11): 2615-26.

Naville D, Penhoat A, Durand P, Begeot M 1999. Three steroidogenic factor-1 binding elements are required for constitutive and cAMP-regulated expression of the human adrenocorticotropin receptor gene. Biochem Biophys Res Commun 255(1): 28-33.

Niakan KK, McCabe ER 2005. DAX1 origin, function, and novel role. Mol Genet Metab 86(1-2): 70-83.

Nicol JW, Helt GA, Blanchard SG, Jr., Raja A, Loraine AE 2009. The Integrated Genome Browser: free software for distribution and exploration of genome-scale datasets. Bioinformatics 25(20): 2730-1.

Nissen SE, Tuzcu EM, Brewer HB, Sipahi I, Nicholls SJ, Ganz P, Schoenhagen P, Waters DD, Pepine CJ, Crowe TD and others 2006. Effect of ACAT inhibition on the progression of coronary atherosclerosis. N Engl J Med 354(12): 1253-63.

Nourse J, Mellentin JD, Galili N, Wilkinson J, Stanbridge E, Smith SD, Cleary ML 1990. Chromosomal translocation t(1;19) results in synthesis of a homeobox fusion mRNA that codes for a potential chimeric transcription factor. Cell 60(4): 535-45.

Oba K, Yanase T, Nomura M, Morohashi K, Takayanagi R, Nawata H 1996. Structural characterization of human Ad4bp (SF-1) gene. Biochem Biophys Res Commun 226(1): 261-7.

Oberley MJ, Tsao J, Yau P, Farnham PJ 2004. High-throughput screening of chromatin immunoprecipitates using CpG-island microarrays. Methods Enzymol 376: 315-34.

Ogo A, Waterman MR, McAllister JM, Kagawa N 1997. The homeodomain protein Pbx1 is involved in cAMP-dependent transcription of human CYP17. Arch Biochem Biophys 348(1): 226-31.

Ou Q, Mouillet JF, Yan X, Dorn C, Crawford PA, Sadovsky Y 2001. The DEAD box protein DP103 is a regulator of steroidogenic factor-1. Mol Endocrinol 15(1): 69-79.

Papetti M, Herman IM 2002. Mechanisms of normal and tumor-derived angiogenesis. Am J Physiol Cell Physiol 282(5): C947-70.

Parakh TN, Hernandez JA, Grammer JC, Weck J, Hunzicker-Dunn M, Zeleznik AJ, Nilson JH 2006. Follicle-stimulating hormone/cAMP regulation of aromatase gene expression requires beta-catenin. Proc Natl Acad Sci U S A 103(33): 12435-40.

Park YY, Park KC, Shong M, Lee SJ, Lee YH, Choi HS 2007. EID-1 interacts with orphan nuclear receptor SF-1 and represses its transactivation. Mol Cells 24(3): 372-7.

Parker KL, Schimmer BP 1997. Steroidogenic factor 1: a key determinant of endocrine development and function. Endocr Rev 18(3): 361-77.

Parma J, Duprez L, Van Sande J, Cochaux P, Gervy C, Mockel J, Dumont J, Vassart G 1993. Somatic mutations in the thyrotropin receptor gene cause hyperfunctioning thyroid adenomas. Nature 365(6447): 649-51.

Pedreira CC, Savarirayan R, Zacharin MR 2004. IMAGe syndrome: a complex disorder affecting growth, adrenal and gonadal function, and skeletal development. J Pediatr 144(2): 274-7.

Perry R, Kecha O, Paquette J, Huot C, Van Vliet G, Deal C 2005. Primary adrenal insufficiency in children: twenty years experience at the Sainte-Justine Hospital, Montreal. J Clin Endocrinol Metab 90(6): 3243-50.

Phelan JK, McCabe ER 2001. Mutations in NR0B1 (DAX1) and NR5A1 (SF1) responsible for adrenal hypoplasia congenita. Hum Mutat 18(6): 472-87.

Pulichino AM, Vallette-Kasic S, Couture C, Gauthier Y, Brue T, David M, Malpuech G, Deal C, Van Vliet G, De Vroede M and others 2003. Human and mouse TPIT gene mutations cause early onset pituitary ACTH deficiency. Genes Dev 17(6): 711-6.

Rainey WE, Bird IM, Mason JI 1994. The NCI-H295 cell line: a pluripotent model for human adrenocortical studies. Mol Cell Endocrinol 100(1-2): 45-50.

Rainey WE, Saner K, Schimmer BP 2004. Adrenocortical cell lines. Mol Cell Endocrinol 228(1-2): 23-38.

Ramayya MS, Zhou J, Kino T, Segars JH, Bondy CA, Chrousos GP 1997. Steroidogenic factor 1 messenger ribonucleic acid expression in steroidogenic and nonsteroidogenic human tissues: Northern blot and in situ hybridization studies. J Clin Endocrinol Metab 82(6): 1799-806.

Ren B, Robert F, Wyrick JJ, Aparicio O, Jennings EG, Simon I, Zeitlinger J, Schreiber J, Hannett N, Kanin E and others 2000. Genome-wide location and function of DNA binding proteins. Science 290(5500): 2306-9.

Ren B, Dynlacht BD 2004. Use of chromatin immunoprecipitation assays in genome-wide location analysis of mammalian transcription factors. Methods Enzymol 376: 304-15.

Reutens AT, Achermann JC, Ito M, Gu WX, Habiby RL, Donohoue PA, Pang S, Hindmarsh PC, Jameson JL 1999. Clinical and functional effects of mutations in the DAX-1 gene in patients with adrenal hypoplasia congenita. J Clin Endocrinol Metab 84(2): 504-11.

Reuter AL, Goji K, Bingham NC, Matsuo M, Parker KL 2007. A novel mutation in the accessory DNA-binding domain of human steroidogenic factor 1 causes XY gonadal dysgenesis without adrenal insufficiency. Eur J Endocrinol 157(2): 233-8.

Rice DA, Mouw AR, Bogerd AM, Parker KL 1991. A shared promoter element regulates the expression of three steroidogenic enzymes. Mol Endocrinol 5(10): 1552-61.

Romero DG, Welsh BL, Gomez-Sanchez EP, Yanes LL, Rilli S, Gomez-Sanchez CE 2006. Angiotensin II-mediated protein kinase D activation stimulates aldosterone and cortisol secretion in H295R human adrenocortical cells. Endocrinology 147(12): 6046-55.

Romero DG, Yanes LL, de Rodriguez AF, Plonczynski MW, Welsh BL, Reckelhoff JF, Gomez-Sanchez EP, Gomez-Sanchez CE 2007. Disabled-2 is expressed in adrenal zona glomerulosa and is involved in aldosterone secretion. Endocrinology 148(6): 2644-52.

Sablin EP, Blind RD, Krylova IN, Ingraham JG, Cai F, Williams JD, Fletterick RJ, Ingraham HA 2009. Structure of SF-1 bound by different phospholipids: evidence for regulatory ligands. Mol Endocrinol 23(1): 25-34.

Sadovsky Y, Crawford PA, Woodson KG, Polish JA, Clements MA, Tourtellotte LM, Simburger K, Milbrandt J 1995. Mice deficient in the orphan receptor steroidogenic factor 1 lack adrenal glands and gonads but express P450 side-chain-cleavage enzyme in the placenta and have normal embryonic serum levels of corticosteroids. Proc Natl Acad Sci U S A 92(24): 10939-43.

Samandari E, Kempna P, Nuoffer JM, Hofer G, Mullis PE, Fluck CE 2007. Human adrenal corticocarcinoma NCI-H295R cells produce more androgens than NCI-H295A cells and differ in 3beta-hydroxysteroid dehydrogenase type 2 and 17,20 lyase activities. J Endocrinol 195(3): 459-72.

Sambrook J, Russell DW 2001. In vitro amplification of DNA by the polymerase chain reaction. In: Sambrook J, Russell DW ed. Molecular cloning: a laboratory manual. 3rd ed, Cold Spring Harbor Laboratory Press. Pp. 8.13-8.15.

Sanger F, Nicklen S, Coulson AR 1977. DNA sequencing with chain-terminating inhibitors. Proc Natl Acad Sci U S A 74(12): 5463-7.

Sbiera S, Schmull S, Assie G, Voelker HU, Kraus L, Beyer M, Ragazzon B, Beuschlein F, Willenberg HS, Hahner S and others 2010. High diagnostic and prognostic value of steroidogenic factor-1 expression in adrenal tumors. J Clin Endocrinol Metab 95(10): E161-71.

Schimmer BP, White PC 2010. Minireview: steroidogenic factor 1: its roles in differentiation, development, and disease. Mol Endocrinol 24(7): 1322-37.

Schnabel CA, Selleri L, Cleary ML 2003. Pbx1 is essential for adrenal development and urogenital differentiation. Genesis 37(3): 123-30.

Schroeder A, Mueller O, Stocker S, Salowsky R, Leiber M, Gassmann M, Lightfoot S, Menzel W, Granzow M, Ragg T 2006. The RIN: an RNA integrity number for assigning integrity values to RNA measurements. BMC Mol Biol 7: 3.

Seed B 1987. An LFA-3 cDNA encodes a phospholipid-linked membrane protein homologous to its receptor CD2. Nature 329(6142): 840-2.

Sewer MB, Waterman MR 2003. CAMP-dependent protein kinase enhances CYP17 transcription via MKP-1 activation in H295R human adrenocortical cells. J Biol Chem 278(10): 8106-11.

Sewer MB, Dammer EB, Jagarlapudi S 2007. Transcriptional regulation of adrenocortical steroidogenic gene expression. Drug Metab Rev 39(2-3): 371-88.

Shaikh MG, Boyes L, Kingston H, Collins R, Besley GT, Padmakumar B, Ismayl O, Hughes I, Hall CM, Hellerud C and others 2008. Skewed X inactivation is associated with phenotype in a female with adrenal hypoplasia congenita. J Med Genet 45(9): e1.

Shapiro HM 2003. Practical flow cytometry. 4th ed. Hoboken, John Wiley & Sons, Inc.

Shinoda K, Lei H, Yoshii H, Nomura M, Nagano M, Shiba H, Sasaki H, Osawa Y, Ninomiya Y, Niwa O and others 1995. Developmental defects of the ventromedial hypothalamic nucleus and pituitary gonadotroph in the Ftz-F1 disrupted mice. Dev Dyn 204(1): 22-9.

Shioda T, Fenner MH, Isselbacher KJ 1997. MSG1 and its related protein MRG1 share a transcription activating domain. Gene 204(1-2): 235-41.

Song KH, Park YY, Kee HJ, Hong CY, Lee YS, Ahn SW, Kim HJ, Lee K, Kook H, Lee IK and others 2006. Orphan nuclear receptor Nur77 induces zinc finger protein GIOT-1 gene expression, and GIOT-1 acts as a novel corepressor of orphan nuclear receptor SF-1 via recruitment of HDAC2. J Biol Chem 281(23): 15605-14.

Soon PS, Gill AJ, Benn DE, Clarkson A, Robinson BG, McDonald KL, Sidhu SB 2009. Microarray gene expression and immunohistochemistry analyses of adrenocortical tumors identify IGF2 and Ki-67 as useful in differentiating carcinomas from adenomas. Endocr Relat Cancer 16(2): 573-83.

Staels B, Hum DW, Miller WL 1993. Regulation of steroidogenesis in NCI-H295 cells: a cellular model of the human fetal adrenal. Mol Endocrinol 7(3): 423-33.

Stewart PM 2008. The adrenal cortex. In: Kronenberg HM, Melmed S, Polonsky KS, Larsen PR ed. Williams textbook of endocrinology. 11th ed. Philadelphia, Saunders Elservier. Pp. 445-503.

Storr HL, Kind B, Parfitt DA, Chapple JP, Lorenz M, Koehler K, Huebner A, Clark AJ 2009. Deficiency of ferritin heavy-chain nuclear import in triple a syndrome implies nuclear oxidative damage as the primary disease mechanism. Mol Endocrinol 23(12): 2086-94.

Su AI, Cooke MP, Ching KA, Hakak Y, Walker JR, Wiltshire T, Orth AP, Vega RG, Sapinoso LM, Moqrich A and others 2002. Large-scale analysis of the human and mouse transcriptomes. Proc Natl Acad Sci U S A 99(7): 4465-70.

Sucheston ME, Cannon MS 1968. Development of zonular patterns in the human adrenal gland. J Morphol 126(4): 477-91.

Sugawara T, Holt JA, Kiriakidou M, Strauss JF, 3rd 1996. Steroidogenic factor 1-dependent promoter activity of the human steroidogenic acute regulatory protein (StAR) gene. Biochemistry 35(28): 9052-9.

Sun HB, Zhu YX, Yin T, Sledge G, Yang YC 1998. MRG1, the product of a melanocyte-specific gene related gene, is a cytokine-inducible transcription factor with transformation activity. Proc Natl Acad Sci U S A 95(23): 13555-60.

Sunthornthepvarakui T, Gottschalk ME, Hayashi Y, Refetoff S 1995. Brief report: resistance to thyrotropin caused by mutations in the thyrotropin-receptor gene. N Engl J Med 332(3): 155-60.

Suzuki T, Kasahara M, Yoshioka H, Morohashi K, Umesono K 2003. LXXLL-related motifs in Dax-1 have target specificity for the orphan nuclear receptors Ad4BP/SF-1 and LRH-1. Mol Cell Biol 23(1): 238-49.

Tabarin A, Achermann JC, Recan D, Bex V, Bertagna X, Christin-Maitre S, Ito M, Jameson JL, Bouchard P 2000. A novel mutation in DAX1 causes delayed-onset adrenal insufficiency and incomplete hypogonadotropic hypogonadism. J Clin Invest 105(3): 321-8.

Tajima T, Fujieda K, Kouda N, Nakae J, Miller WL 2001. Heterozygous mutation in the cholesterol side chain cleavage enzyme (p450scc) gene in a patient with 46,XY sex reversal and adrenal insufficiency. J Clin Endocrinol Metab 86(8): 3820-5.

Takayama K, Morohashi K, Honda S, Hara N, Omura T 1994. Contribution of Ad4BP, a steroidogenic cell-specific transcription factor, to regulation of the human CYP11A and bovine CYP11B genes through their distal promoters. J Biochem 116(1): 193-203.

Taketo M, Parker KL, Howard TA, Tsukiyama T, Wong M, Niwa O, Morton CC, Miron PM, Seldin MF 1995. Homologs of Drosophila Fushi-Tarazu factor 1 map to mouse chromosome 2 and human chromosome 9q33. Genomics 25(2): 565-7.

Tamura M, Kanno Y, Chuma S, Saito T, Nakatsuji N 2001. Pod-1/Capsulin shows a sex- and stage-dependent expression pattern in the mouse gonad development and represses expression of Ad4BP/SF-1. Mech Dev 102(1-2): 135-44.

Tan TY, Jameson JL, Campbell PE, Ekert PG, Zacharin M, Savarirayan R 2006. Two sisters with IMAGe syndrome: cytomegalic adrenal histopathology, support for autosomal recessive inheritance and literature review. Am J Med Genet A 140(16): 1778-84.

Tanaka T, Gondo S, Okabe T, Ohe K, Shirohzu H, Morinaga H, Nomura M, Tani K, Takayanagi R, Nawata H and others 2007. Steroidogenic factor 1/adrenal 4 binding protein transforms human bone marrow mesenchymal cells into steroidogenic cells. J Mol Endocrinol 39(5): 343-50.

Taylor BA, Meier H 1975. Mapping the adrenal lipid depletion gene of the AKR/J mouse strain. Genet Res 26(3): 307-12.

Tien ES, Davis JW, Vanden Heuvel JP 2004. Identification of the CREB-binding protein/p300-interacting protein CITED2 as a peroxisome proliferator-activated receptor alpha coregulator. J Biol Chem 279(23): 24053-63.

Tremblay JJ, Viger RS 2003. A mutated form of steroidogenic factor 1 (SF-1 G35E) that causes sex reversal in humans fails to synergize with transcription factor GATA-4. J Biol Chem 278(43): 42637-42.

Tullio-Pelet A, Salomon R, Hadj-Rabia S, Mugnier C, de Laet MH, Chaouachi B, Bakiri F, Brottier P, Cattolico L, Penet C and others 2000. Mutant WD-repeat protein in triple-A syndrome. Nat Genet 26(3): 332-5.

Ueda H, Sun GC, Murata T, Hirose S 1992. A novel DNA-binding motif abuts the zinc finger domain of insect nuclear hormone receptor FTZ-F1 and mouse embryonal long terminal repeat-binding protein. Mol Cell Biol 12(12): 5667-72.

Umesono K, Evans RM 1989. Determinants of target gene specificity for steroid/thyroid hormone receptors. Cell 57(7): 1139-46.

Umesono K, Murakami KK, Thompson CC, Evans RM 1991. Direct repeats as selective response elements for the thyroid hormone, retinoic acid, and vitamin D3 receptors. Cell 65(7): 1255-66.

Untergasser A, Nijveen H, Rao X, Bisseling T, Geurts R, Leunissen JA 2007. Primer3Plus, an enhanced web interface to Primer3. Nucleic Acids Res 35(Web Server issue): W71-4.

Utsunomiya H, Cheng YH, Lin Z, Reierstad S, Yin P, Attar E, Xue Q, Imir G, Thung S, Trukhacheva E and others 2008. Upstream stimulatory factor-2 regulates steroidogenic factor-1 expression in endometriosis. Mol Endocrinol 22(4): 904-14.

Val P, Martinez-Barbera JP, Swain A 2007. Adrenal development is initiated by Cited2 and Wt1 through modulation of Sf-1 dosage. Development 134(12): 2349-58.

Val P, Swain A 2010. Gene dosage effects and transcriptional regulation of early mammalian adrenal cortex development. Mol Cell Endocrinol 323(1): 105-14.

Vallette-Kasic S, Brue T, Pulichino AM, Gueydan M, Barlier A, David M, Nicolino M, Malpuech G, Dechelotte P, Deal C and others 2005. Congenital isolated adrenocorticotropin deficiency: an underestimated cause of neonatal death, explained by TPIT gene mutations. J Clin Endocrinol Metab 90(3): 1323-31.

Varshochi R, Halim F, Sunters A, Alao JP, Madureira PA, Hart SM, Ali S, Vigushin DM, Coombes RC, Lam EW 2005. ICI182,780 induces p21Waf1 gene transcription through releasing histone deacetylase 1 and estrogen receptor alpha from Sp1 sites to induce cell cycle arrest in MCF-7 breast cancer cell line. J Biol Chem 280(5): 3185-96.

Verrijn Stuart AA, Ozisik G, de Vroede MA, Giltay JC, Sinke RJ, Peterson TJ, Harris RM, Weiss J, Jameson JL 2007. An amino-terminal DAX1 (NROB1) missense mutation associated with isolated mineralocorticoid deficiency. J Clin Endocrinol Metab 92(3): 755-61.

Vilain E, Guo W, Zhang YH, McCabe ER 1997. DAX1 gene expression upregulated by steroidogenic factor 1 in an adrenocortical carcinoma cell line. Biochem Mol Med 61(1): 1-8.

Vilain E, Le Merrer M, Lecointre C, Desangles F, Kay MA, Maroteaux P, McCabe ER 1999. IMAGe, a new clinical association of intrauterine growth retardation, metaphyseal dysplasia, adrenal hypoplasia congenita, and genital anomalies. J Clin Endocrinol Metab 84(12): 4335-40.

Wada Y, Okada M, Hasegawa T, Ogata T 2005. Association of severe micropenis with Gly146Ala polymorphism in the gene for steroidogenic factor-1. Endocr J 52(4): 445-8.

Wada Y, Okada M, Fukami M, Sasagawa I, Ogata T 2006. Association of cryptorchidism with Gly146Ala polymorphism in the gene for steroidogenic factor-1. Fertil Steril 85(3): 787-90.

Walker AP, Chelly J, Love DR, Brush YI, Recan D, Chaussain JL, Oley CA, Connor JM, Yates J, Price DA and others 1992. A YAC contig in Xp21 containing the adrenal hypoplasia congenita and glycerol kinase deficiency genes. Hum Mol Genet 1(8): 579-85.

Warner GJ, Stoudt G, Bamberger M, Johnson WJ, Rothblat GH 1995. Cell toxicity induced by inhibition of acyl coenzyme A:cholesterol acyltransferase and accumulation of unesterified cholesterol. J Biol Chem 270(11): 5772-8.

Waterman MR 1994. Biochemical diversity of cAMP-dependent transcription of steroid hydroxylase genes in the adrenal cortex. J Biol Chem 269(45): 27783-6.

Weck J, Mayo KE 2006. Switching of NR5A proteins associated with the inhibin alpha-subunit gene promoter after activation of the gene in granulosa cells. Mol Endocrinol 20(5): 1090-103.

Weinmann AS, Yan PS, Oberley MJ, Huang TH, Farnham PJ 2002. Isolating human transcription factor targets by coupling chromatin immunoprecipitation and CpG island microarray analysis. Genes Dev 16(2): 235-44.

Welboren WJ, van Driel MA, Janssen-Megens EM, van Heeringen SJ, Sweep FC, Span PN, Stunnenberg HG 2009. ChIP-Seq of ERalpha and RNA polymerase II defines genes differentially responding to ligands. EMBO J 28(10): 1418-28.

West AN, Neale GA, Pounds S, Figueredo BC, Rodriguez Galindo C, Pianovski MA, Oliveira Filho AG, Malkin D, Lalli E, Ribeiro R and others 2007. Gene expression profiling of childhood adrenocortical tumors. Cancer Res 67(2): 600-8.

Whitby RJ, Dixon S, Maloney PR, Delerive P, Goodwin BJ, Parks DJ, Willson TM 2006. Identification of small molecule agonists of the orphan nuclear receptors liver receptor homolog-1 and steroidogenic factor-1. J Med Chem 49(23): 6652-5.

White PC 2006. Ontogeny of adrenal steroid biosynthesis: why girls will be girls. J Clin Invest 116(4): 872-4.

Wilhelm D, Englert C 2002. The Wilms tumor suppressor WT1 regulates early gonad development by activation of Sf1. Genes Dev 16(14): 1839-51.

Wilson TE, Fahrner TJ, Milbrandt J 1993. The orphan receptors NGFI-B and steroidogenic factor 1 establish monomer binding as a third paradigm of nuclear receptor-DNA interaction. Mol Cell Biol 13(9): 5794-804.

Wiltshire E, Couper J, Rodda C, Jameson JL, Achermann JC 2001. Variable presentation of X-linked adrenal hypoplasia congenita. J Pediatr Endocrinol Metab 14(8): 1093-6.

Winnay JN, Hammer GD 2006. Adrenocorticotropic hormone-mediated signaling cascades coordinate a cyclic pattern of steroidogenic factor 1-dependent transcriptional activation. Mol Endocrinol 20(1): 147-66.

Withington SL, Scott AN, Saunders DN, Lopes Floro K, Preis JI, Michalicek J, Maclean K, Sparrow DB, Barbera JP, Dunwoodie SL 2006. Loss of Cited2 affects trophoblast formation and vascularization of the mouse placenta. Dev Biol 294(1): 67-82.

Wong M, Ramayya MS, Chrousos GP, Driggers PH, Parker KL 1996. Cloning and sequence analysis of the human gene encoding steroidogenic factor 1. J Mol Endocrinol 17(2): 139-47.

Wood KV, de Wet JR, Dewji N, DeLuca M 1984. Synthesis of active firefly luciferase by in vitro translation of RNA obtained from adult lanterns. Biochem Biophys Res Commun 124(2): 592-6.

Xu B, Yang WH, Gerin I, Hu CD, Hammer GD, Koenig RJ 2009. Dax-1 and steroid receptor RNA activator (SRA) function as transcriptional coactivators for steroidogenic factor 1 in steroidogenesis. Mol Cell Biol 29(7): 1719-34.

Xue Q, Lin Z, Yin P, Milad MP, Cheng YH, Confino E, Reierstad S, Bulun SE 2007. Transcriptional activation of steroidogenic factor-1 by hypomethylation of the 5' CpG island in endometriosis. J Clin Endocrinol Metab 92(8): 3261-7.

Yancopoulos GD, Davis S, Gale NW, Rudge JS, Wiegand SJ, Holash J 2000. Vascular-specific growth factors and blood vessel formation. Nature 407(6801): 242-8.

Yang WH, Heaton JH, Brevig H, Mukherjee S, Iniguez-Lluhi JA, Hammer GD 2009. SUMOylation inhibits SF-1 activity by reducing CDK7-mediated serine 203 phosphorylation. Mol Cell Biol 29(3): 613-25.

Yu RN, Ito M, Saunders TL, Camper SA, Jameson JL 1998a. Role of Ahch in gonadal development and gametogenesis. Nat Genet 20(4): 353-7.

Yu RN, Ito M, Jameson JL 1998b. The murine Dax-1 promoter is stimulated by SF-1 (steroidogenic factor-1) and inhibited by COUP-TF (chicken ovalbumin upstream promoter-transcription factor) via a composite nuclear receptor-regulatory element. Mol Endocrinol 12(7): 1010-22.

Zanaria E, Muscatelli F, Bardoni B, Strom TM, Guioli S, Guo W, Lalli E, Moser C, Walker AP, McCabe ER and others 1994. An unusual member of the nuclear hormone

receptor superfamily responsible for X-linked adrenal hypoplasia congenita. Nature 372(6507): 635-41.

Zazopoulos E, Lalli E, Stocco DM, Sassone-Corsi P 1997. DNA binding and transcriptional repression by DAX-1 blocks steroidogenesis. Nature 390(6657): 311-5.

Zeng H, Qin L, Zhao D, Tan X, Manseau EJ, Van Hoang M, Senger DR, Brown LF, Nagy JA, Dvorak HF 2006. Orphan nuclear receptor TR3/Nur77 regulates VEGF-A-induced angiogenesis through its transcriptional activity. J Exp Med 203(3): 719-29.

Zhang H, Thomsen JS, Johansson L, Gustafsson JA, Treuter E 2000. DAX-1 functions as an LXXLL-containing corepressor for activated estrogen receptors. J Biol Chem 275(51): 39855-9.

Zhao Y, Bruemmer D 2010. NR4A orphan nuclear receptors: transcriptional regulators of gene expression in metabolism and vascular biology. Arterioscler Thromb Vasc Biol 30(8): 1535-41.

Zubair M, Ishihara S, Oka S, Okumura K, Morohashi K 2006. Two-step regulation of Ad4BP/SF-1 gene transcription during fetal adrenal development: initiation by a Hox-Pbx1-Prep1 complex and maintenance via autoregulation by Ad4BP/SF-1. Mol Cell Biol 26(11): 4111-21.

Zubair M, Parker KL, Morohashi K 2008. Developmental links between the fetal and adult zones of the adrenal cortex revealed by lineage tracing. Mol Cell Biol 28(23): 7030-40.

Appendices

Appendix 1: List of laboratory equipment used

Benchtop centrifuge: Sorvall Legend RT (swinging buckets rotor 7500 6445), Sorvall, Germany.

Benchtop microcentrifuge: Heraeus Pico 17, Thermo Fisher Scientific, UK.

Cell culture incubator: Heraeus Heracell CO_2 incubator, Thermo Fisher Scientific.

Cell culture microscope: Nikon TMS-F, Nikon, Japan.

ChemiDoc system: Bio-Rad Laboratories Ltd., UK.

Class II biological safety cabinet: HeraSafe HS12, Thermo Fisher Scientific.

Cold room (4°C): Stancold, UK.

Combined incubator & shaker: Orbital incubator S150, Stuart Scientific/Bibby, UK.

Drying cabinet: Unitemp, LTE Scientific, UK.

Electronic multichannel pipettes (0.5-10 µl; 5-100 µl): Research pro, Eppendorf AG, Germany.

Electronic pipette filler: Easypet, Eppendorf.

Electrophoresis power supply: PowerPac 300, Bio-Rad.

Electrophoresis system: Sub-Cell GT, Bio-Rad.

Freezer (-20°C): ISU57, Lec, UK.

Freezer (-80°C): Ultra Low model U57085, New Brunswick Scientific, UK.

High performance stand alone centrifuge: Sorval RC 5C Plus (rotor SA-600), Sorvall.

Ice flake machine: KF75, Porkka, UK.

Incubator: Economy incubator size 2, Sanyo Gallenkamp, UK.

Laboratory glasswasher: Mielabor G7783, Miele, Germany.

Luminescence/fluorescence plate reader: FLUOstar OPTIMA, BMG Labtech Ltd., UK.

Microbiological incubator: Heraeus Kelvitron T, Thermo Fisher Scientific.

Microwave oven: Proline, UK

Orbital platform shaker: R100 Rotatest shaker, Luckham, UK.

Precision micropipettes (0.5-10 µl; 2-20 µl; 20-200 µl; 100-1000 µl): Discovery precision variable volume single pipettes, PZ HTL S.A., Poland.

Refrigerated benchtop microcentrifuge: Accuspin Micro R, Thermo Fisher Scientific.

Scale: BL 150S, Sartorius, UK.

Spectrophotometers: NanoDrop 1000, Thermo Fisher Scientific, and Eppendorf BioPhotometer, Eppendorf.

Thermal cycler: Mastercycler gradient, Eppendorf.

Tube rotator: Blood tube rotator SB1, Stuart Scientific/Bibby.

UV Transilluminator: Chromato-Vue cabinet, UVP Inc., USA.

Vibrating platform shaker: Titramax 100, Heidolph, Germany.

Vortex: Vortex-Genie 2, Scientific Industries Inc., USA.

Waterbath: Grant W14, Grant Instruments (Cambridge) Ltd., UK.

Appendix 2: Vector maps

pCMX expression vector

Constructed at the Evans Laboratory/Salk Institute for Biological Studies, USA, and used with permission of Dr Ronald M. Evans.

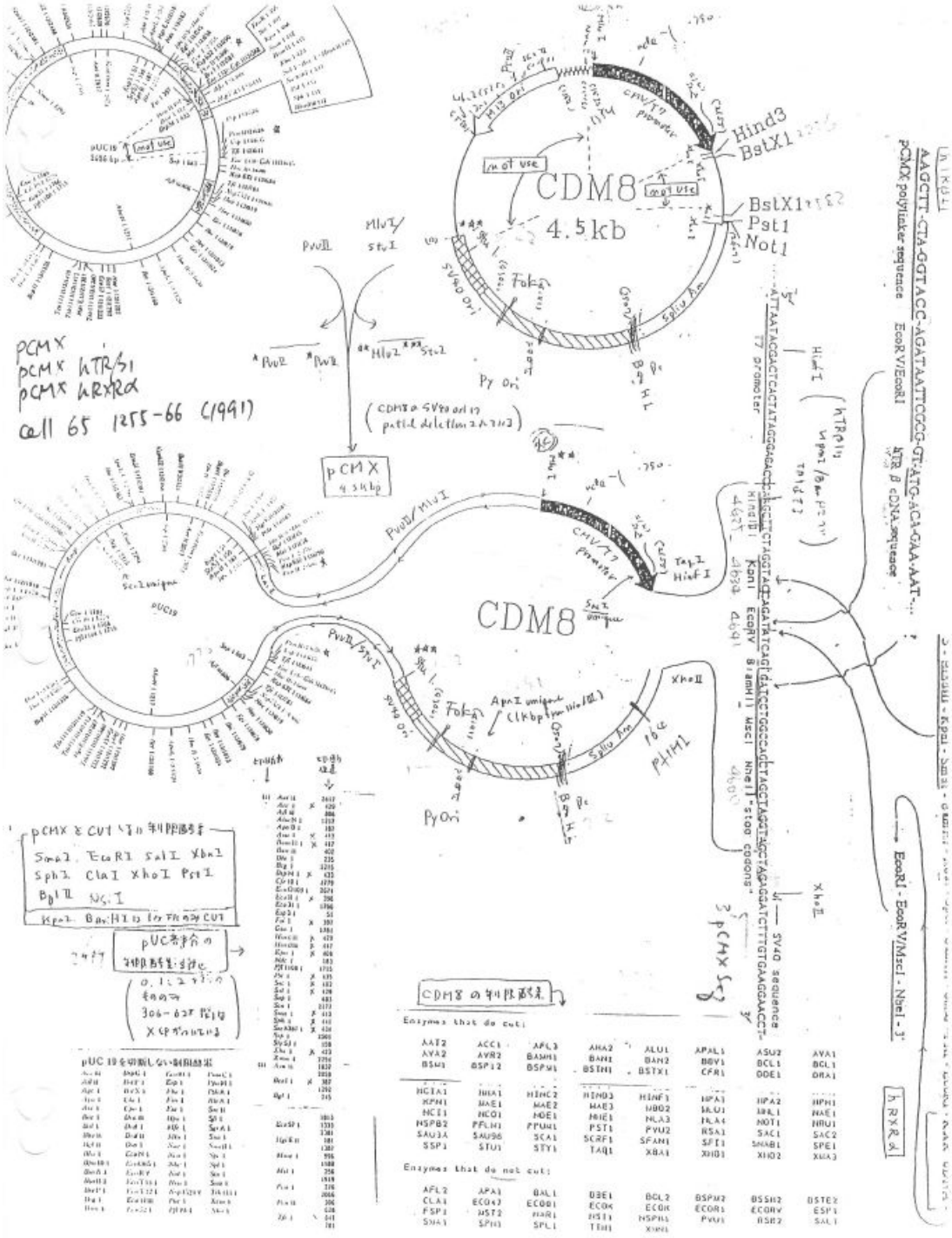

pGL4.10[luc2] luciferase reporter vector

Obtained from Promega, UK.

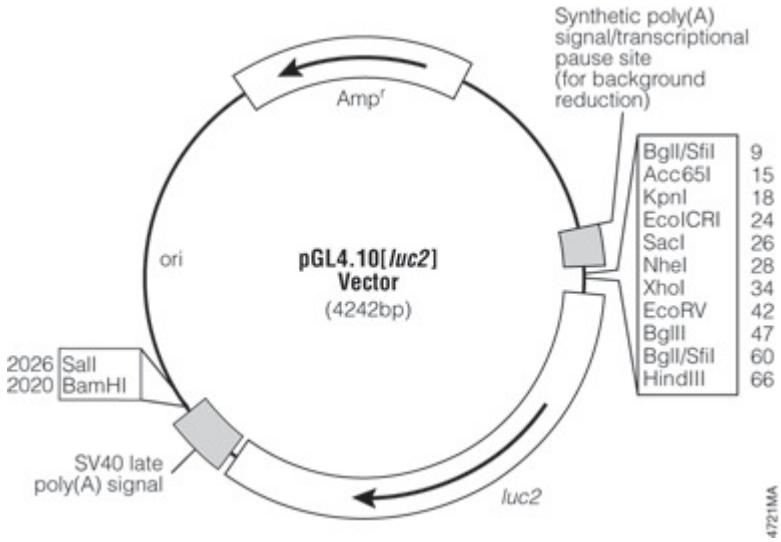

pRL-SV40 Renilla luciferase reporter vector

Obtained from Promega, UK.

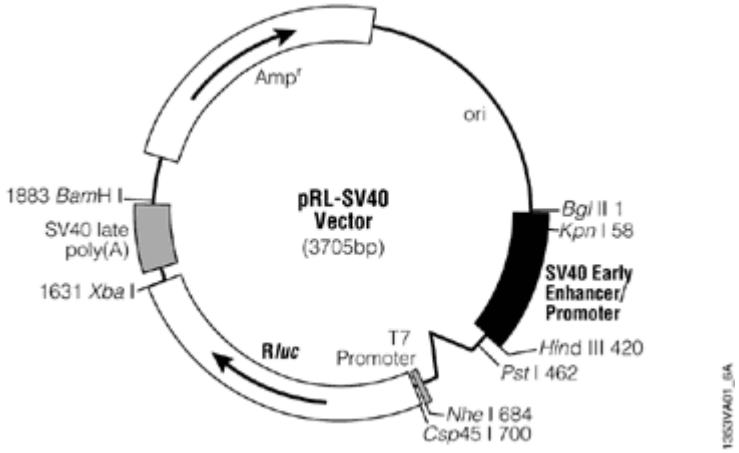

pCR-XL-TOPO

Obtained from Invitrogen, UK, as part of the TOPO XL PCR cloning kit.

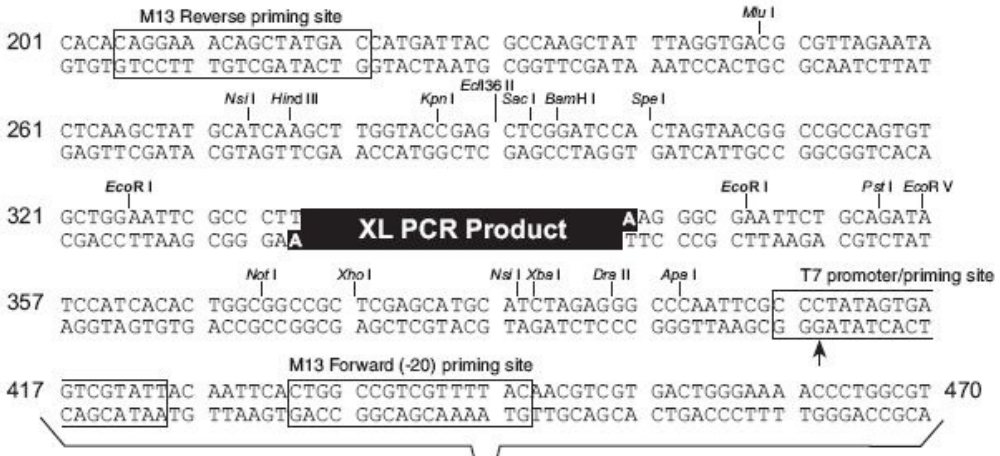

Comments for pCR®-XL-TOPO®
3519 nucleotides

Lac promoter/operator region: bases 95-216
M13 Reverse priming site: bases 205-221
Lac Za ORF: bases 217-576
Multiple Cloning Site: bases 248-399
TOPO® Cloning site: bases 336-337
T7 promoter priming site: bases 406-425
M13 Forward (-20) priming site: bases 433-448
Fusion joint: bases 577-585
*ccd*B lethal gene ORF: bases 586-888
Kanamycin resistance ORF: bases 1237-2031
Zeocin resistance ORF: bases 2238-2612
pUC origin: bases 2680-3393

pIRES2-AcGFP1-Nuc bicistronic expression vector

Obtained from Clontech-Takara Bio Europe, France.

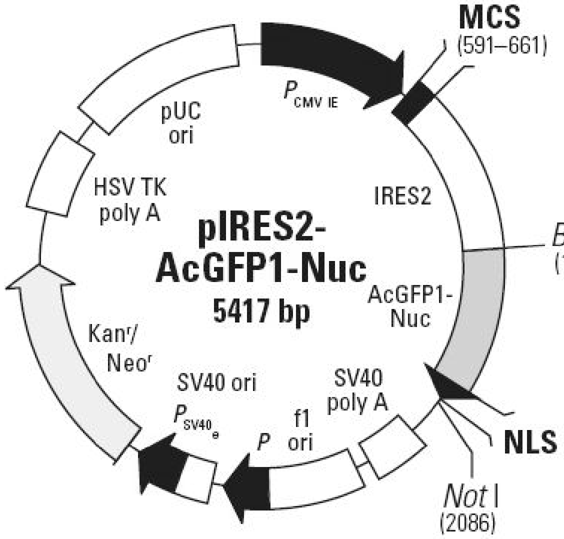


```
                                                                    PstI
                                                                       AccI
     NheI                          SacI            EcoRI               SalI
1    TCCGCTAGCG CTACCGGACT CAGATCTCGA GCTCAAGCTT CGAATTCTGC AGTCGACGGT
     AGGCGATCGC GATGGCCTGA GTCTAGAGCT CGAGTTCGAA GCTTAAGACG TCAGCTGCCA

                 XmaI
     SacII       SmaI
61   ACCGCGGGCC CGGGAT
     TGGCGCCCGG GCCCTA
```

Appendix 3: Literature review of sonication parameters

Published reports (until April 2008) using the Sanyo Soniprep 150 sonicator for chromatin sonication for chromatin immunoprecipitation assays.

Report	**Cell type**	**Number of cells**	**Number of pulses x duration - amplitude**
Varshochi et al., 2005	MCF-7 human breast carcinoma cells	n/a	4 x 15 s – "maximum settings" (30μm)
Bernard et al., 2006	Yeast	2×10^8	3 x 10 s – 16μm
Griffin & Moynagh, 2006	1321N1 human astrocytoma cells	n/a	7 x 10 s – "one third of total amplitude" (10μm)
Castillo et al., 2007	Yeast	n/a	3 x 17 s – "maximum amplitude" (30μm)
Naughton et al., 2007	MCF-7 human breast carcinoma cells	2×10^6	12 x 20 s – 2μm

n/a, information not available. The amplitude range in the Sanyo Soniprep 150 sonicator is from 0 to 30 μm.

Appendix 4: Quality control of ChIP-on-chip microarray data

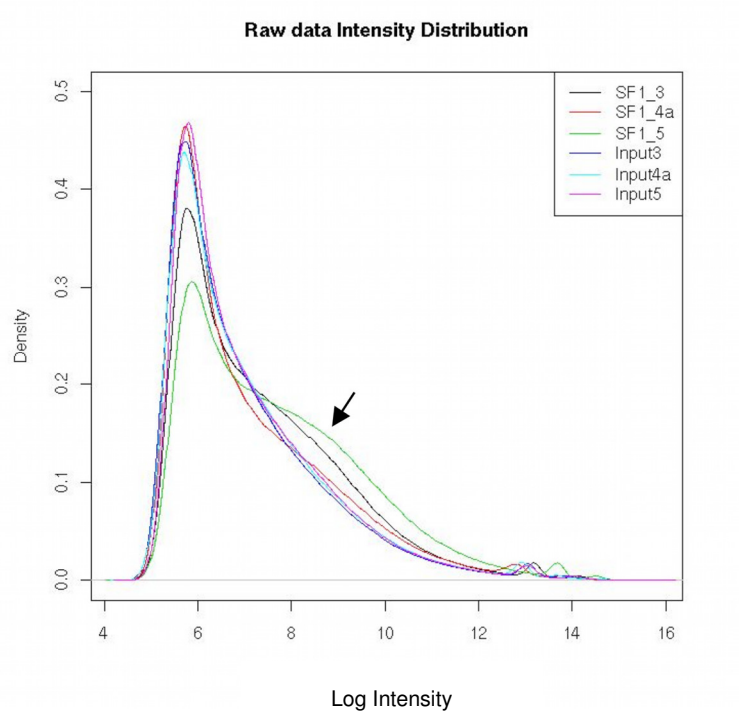

Histogram of raw microarray data intensity distribution. The log intensity of signal from individual probes in the array is plotted on the x axis, while probe density is plotted on the y axis. In experiments 3 and 5 (SF1_3, SF1_5), differential distribution of a subset of high-intensity probes (indicated by the arrow) is seen in comparison to respective input control arrays (Input3, Input5), confirming enrichment by immunoprecipitation. No such difference was detected for experiment 4 (SF1_4a vs. Input4a), indicating poor enrichment. Quality control of microarray data was performed by Dr Sonia Shah at the Bloomsbury Centre for Bioinformatics using R/Bioconductor.

Appendix 5: Complete results of SF-1 ChIP-on-chip analysis

SF-1-binding regions identified by ChIP-on-chip (738 peaks) annotated to 445 neighbouring gene loci where the binding region was located from 10 kb upstream to 3 kb downstream of a transcriptional start. Regions are ranked according to statistical significance (MA Z-score, CisGenome), and chromosomal coordinates are based on NCBIv36. Region length and distance to transcriptional start site (TSS) are stated in base pairs (bp). For peaks located upstream of TSSs, distance value is negative.

Peak	MA Z-score	Chr	Start	End	Region length	Distance to TSS	Gene symbol
1	8.015228	chr19	61052876	61053237	362	-2142	NLRP4
3	7.263901	chr4	606174	606996	823	-2787	PDE6B
4	7.215482	chr3	8671294	8671558	265	-2690	C3orf32
5	7.14255	chr13	113199316	113199973	658	-6621	DCUN1D2
7	6.809306	chr9	99502264	99502676	413	-3011	XPA
8	6.509813	chr15	20377626	20377881	256	-7189	TUBGCP5
12	6.172289	chr13	113367394	113368774	1381	-7583	ATP4B
12	6.172289	chr13	113367394	113368774	1381	-1513	GRK1
13	6.124405	chr3	8672091	8672356	266	-3487	C3orf32
18	5.84227	chr14	92455627	92456518	892	-3172	CHGA
20	5.77975	chr19	3123496	3123904	409	-6065	S1PR4
22	5.612978	chr8	6411196	6412323	1128	-3588	ANGPT2
26	5.489602	chr13	113149179	113149920	742	1908	ADPRHL1
27	5.488133	chr19	40729390	40729965	576	1293	TMEM147
32	5.362761	chr2	183644509	183645199	691	-6877	DUSP19
34	5.295386	chr7	43878032	43878592	561	-2643	MRPS24
37	5.243781	chr9	110664647	110665656	1010	-7121	ACTL7B
37	5.243781	chr9	110664647	110665656	1010	728	ACTL7A
39	5.20512	chr22	22563867	22564131	265	-2565	MIF
40	5.190733	chr21	44030889	44031745	857	-2541	RRP1
43	5.135087	chr9	130885372	130885644	273	2282	DOLPP1
44	5.116028	chr7	43881830	43882948	1119	-6720	MRPS24
46	5.07807	chr2	121263371	121263617	247	-2832	GLI2
47	5.075489	chr3	12804229	12804769	541	-8671	CAND2
49	5.068231	chr3	48450915	48451316	402	-9370	PLXNB1
49	5.068231	chr3	48450915	48451316	402	-5574	CCDC72
50	5.066161	chr9	139889204	139889711	508	-2604	CACNA1B
51	5.060924	chr15	38971991	38972237	247	-1805	VPS18
52	5.045175	chr15	73417958	73418364	407	-8301	NEIL1
52	5.045175	chr15	73417958	73418364	407	2735	COMMD4
53	5.04365	chr7	43924834	43926219	1386	-7045	UBE2D4
55	4.980009	chr15	82938284	82938637	354	-6792	ZSCAN2
56	4.960408	chr15	20384158	20384443	286	-642	TUBGCP5
59	4.93756	chr10	134104255	134104469	215	-4341	C10orf91
60	4.926209	chr9	139888430	139888657	228	-3518	CACNA1B
62	4.851348	chr22	19647683	19648220	538	-1482	AIFM3
64	4.848373	chr7	44756247	44757153	907	1646	ZMIZ2
65	4.844168	chr12	46882744	46883107	364	416	OR10AD1
67	4.826022	chr5	493697	493911	215	-2529	EXOC3
68	4.803632	chr7	44985779	44986174	396	-784	MYO1G
69	4.796889	chr19	51318905	51319375	471	630	IGFL3
70	4.78761	chr9	137571535	137572343	809	-5866	OBP2A
71	4.786212	chr12	55911720	55912224	505	2154	SHMT2
72	4.775732	chr4	41679151	41679629	479	-7889	SLC30A9
72	4.775732	chr4	41679151	41679629	479	858	DCAF4L1
73	4.775485	chr6	116885315	116886296	982	-3443	FAM26F
74	4.76586	chr12	119226110	119226293	184	1656	SIRT4
80	4.717554	chr5	910679	911563	885	-7021	ZDHHC11
81	4.716923	chr3	158363382	158364043	662	-2537	CCNL1
88	4.677037	chr9	129933326	129934401	1076	-3569	PTGES2
91	4.636873	chr21	42309531	42309838	308	-6166	ZNF295

94	4.620342	chrX	149484496	149484652	157	-3152	MTM1
95	4.613583	chr7	47545808	47546908	1101	-635	TNS3
96	4.587711	chr2	132197264	132197608	345	903	C2orf27A
97	4.58604	chr15	38544640	38545265	626	-5552	CHST14
98	4.581953	chr7	44199086	44199682	597	-7718	YKT6
98	4.581953	chr7	44199086	44199682	597	-3822	GCK
99	4.577531	chr3	52805428	52805746	319	1734	ITIH3
101	4.559715	chr13	113151583	113152145	563	-407	ADPRHL1
102	4.559699	chr7	44144836	44145092	257	2476	MYL7
105	4.550741	chr1	163682216	163682464	249	-1287	RXRG
110	4.528661	chr8	20162272	20162432	161	-5270	LZTS1
111	4.522822	chr7	44760221	44761389	1169	-1506	ZMIZ2
112	4.522124	chr7	44195300	44195749	450	38	GCK
114	4.508037	chr3	46997005	46997529	525	-4025	CCDC12
115	4.502563	chrX	152523205	152523703	499	-5680	FAM58A
120	4.483624	chr20	23913754	23914127	374	1571	GGTLC1
122	4.479429	chr9	135206983	135207267	285	-6123	SURF2
122	4.479429	chr9	135206983	135207267	285	-2333	MED22
122	4.479429	chr9	135206983	135207267	285	2236	RPL7A
126	4.474116	chr12	46486131	46486276	146	-7014	HDAC7
127	4.47259	chr14	94303735	94304029	295	2369	GSC
128	4.465217	chr15	20379527	20380187	661	-5085	TUBGCP5
130	4.462032	chr8	88954474	88954904	431	722	DCAF4L2
131	4.45955	chr5	63292645	63292889	245	534	HTR1A
135	4.447345	chr7	45888398	45888890	493	-5839	IGFBP1
136	4.445727	chr3	49701177	49701389	213	-710	RNF123
136	4.445727	chr3	49701177	49701389	213	-185	MST1
137	4.443639	chr6	139739907	139740330	424	-2641	CITED2
138	4.442299	chr5	132021528	132022239	712	120	IL13
139	4.437616	chr20	23924106	23924428	323	-6852	GGTLC1
141	4.435696	chr12	8269042	8269336	295	2274	FAM90A1
144	4.429069	chr7	45574721	45575779	1059	-5395	ADCY1
148	4.414691	chr12	46455243	46455459	217	2094	SLC48A1
150	4.409676	chr3	198244571	198244840	270	-3667	MFI2
151	4.40955	chr22	20345623	20346217	595	-4355	PPIL2
153	4.406404	chr15	72682411	72682871	461	-5124	CLK3
154	4.403355	chr3	49134002	49134332	331	-951	USP19
162	4.373758	chr9	129508595	129509039	445	-9361	TTC16
162	4.373758	chr9	129508595	129509039	445	-3981	C9orf117
165	4.364384	chr19	56006434	56007473	1040	-7168	C19orf48
166	4.361236	chr15	66285466	66285961	496	-212	CALML4
167	4.359157	chr3	185088196	185088662	467	-3043	PARL
168	4.355254	chr1	45247483	45247935	453	-2707	UROD
168	4.355254	chr1	45247483	45247935	453	1677	HECTD3
169	4.349874	chr13	112917118	112918240	1123	-6696	PCID2
171	4.338375	chr17	23927038	23927548	511	-4639	PIGS
171	4.338375	chr17	23927038	23927548	511	784	ALDOC
172	4.335957	chr3	50370010	50370448	439	-6740	TUSC4
172	4.335957	chr3	50370010	50370448	439	1713	TMEM115
173	4.334534	chr7	45887119	45887841	723	-7003	IGFBP1
174	4.332266	chr12	52062467	52062648	182	2312	SP1
176	4.327346	chr22	20425921	20426343	423	-6062	YPEL1
181	4.31358	chr2	27657805	27658487	683	-1250	ZNF512
184	4.303182	chr17	58950288	58950624	337	-3970	KCNH6
185	4.299245	chr7	45123526	45123813	288	-5828	TBRG4
188	4.293737	chr7	44086280	44087020	741	1956	POLM
189	4.293468	chr10	71809866	71810123	258	1425	LRRC20
190	4.291876	chrX	153433050	153433296	247	-4193	G6PD
193	4.283765	chr16	30037231	30037507	277	-5011	GDPD3
195	4.272373	chr7	44155770	44156100	331	-8495	MYL7
197	4.269127	chr17	25909357	25910087	731	-987	TBC1D29
200	4.258121	chr19	46047785	46048443	659	65	CYP2A6
203	4.255374	chr19	36459841	36460361	521	1913	TSHZ3
205	4.251882	chr7	100018271	100018660	390	-3426	FBXO24
211	4.240032	chr22	18385115	18385378	264	-3384	C22orf25
211	4.240032	chr22	18385115	18385378	264	-938	ARVCF
212	4.236902	chr3	38322783	38323034	252	478	SLC22A14
215	4.230017	chr15	72250849	72251379	531	-2025	ISLR
220	4.20051	chr15	81180925	81181321	397	-5435	AP3B2
221	4.195445	chr3	49036997	49037532	536	-3794	DALRD3
222	4.195404	chr15	41445908	41446094	187	-4603	TUBGCP4

225	4.180069	chr9	114950827	114951175	349	-2057	SLC31A2
227	4.175215	chr19	54349668	54350169	502	-2945	TRPM4
227	4.175215	chr19	54349668	54350169	502	574	HRC
228	4.174565	chr19	44020522	44021027	506	-6438	ECH1
229	4.171363	chr12	6529258	6529462	205	-826	IFFO1
230	4.168067	chr21	46436038	46436190	153	-7386	C21orf56
231	4.167076	chr17	75811516	75811752	237	-2916	SGSH
231	4.167076	chr17	75811516	75811752	237	2803	SLC26A11
234	4.157963	chr13	97972848	97973581	734	-873	STK24
235	4.157113	chr15	67376934	67377193	260	-1284	PAQR5
237	4.15384	chr15	47051742	47052028	287	-8953	SHC4
239	4.151241	chr13	113162831	113163178	348	-7165	ADPRHL1
240	4.150568	chr19	45594175	45594526	352	-6417	HIPK4
241	4.145963	chr13	40665622	40665951	330	915	KBTBD7
242	4.145479	chr9	115175827	115176146	320	2175	HDHD3
243	4.145194	chr17	62387050	62387277	228	-4311	CACNG4
246	4.140381	chr12	51072980	51073152	173	-7383	KRT84
252	4.120863	chr5	134810429	134810985	557	229	C5orf20
253	4.12029	chr9	100744571	100744994	424	-1176	COL15A1
255	4.113177	chr7	47549757	47549973	217	-4142	TNS3
256	4.111693	chr22	21740501	21741046	546	-1895	GNAZ
260	4.099116	chr15	64778033	64778476	444	-3433	SMAD6
262	4.095217	chr14	93450903	93451034	132	-4042	FAM181A
264	4.091799	chr20	23917521	23918391	871	-541	GGTLC1
265	4.084833	chr3	53862489	53862680	192	-7369	CHDH
268	4.077457	chr19	46000759	46001112	354	2915	EGLN2
269	4.07666	chr7	149194362	149194922	561	-6347	ATP6V0E2
270	4.074702	chr3	52415140	52416462	1323	-3765	PHF7
272	4.074114	chr15	99849087	99849403	317	-1536	PCSK6
277	4.067316	chr9	36159937	36160779	843	968	CCIN
279	4.065802	chr7	6371614	6371869	256	-8909	RAC1
282	4.062705	chr7	44134270	44134483	214	-4722	POLD2
284	4.059432	chr1	170686075	170686298	224	-6334	PIGC
285	4.054601	chrX	148579651	148579839	189	921	MAGEA11
286	4.047627	chr18	72857520	72857815	296	375	MBP
288	4.039282	chr7	49778102	49778894	793	-5304	VWC2
293	4.036869	chr19	51936497	51936759	263	-4514	FKRP
295	4.034387	chr13	112906366	112906680	315	-4563	CUL4A
297	4.032113	chr7	44335798	44336222	425	-4262	CAMK2B
300	4.026517	chr1	181195422	181195972	551	-6522	C1orf14
301	4.025576	chr7	50312446	50313056	611	-2172	IKZF1
304	4.018816	chr19	42879810	42880028	219	-4928	ZNF781
305	4.016359	chr7	44090262	44090596	335	-1823	POLM
306	4.014527	chr7	49779153	49779281	129	-4585	VWC2
308	4.014353	chr19	8023710	8023961	252	-98	CCL25
310	4.011081	chr7	119702543	119702753	211	1691	KCND2
312	4.006463	chr15	20382416	20382694	279	-2387	TUBGCP5
314	4.004635	chr9	138491483	138491764	282	-6144	C9orf163
315	4.003577	chr7	142850641	142850847	207	77	TAS2R60
322	3.992534	chr15	73418770	73419194	425	-7480	NEIL1
327	3.97955	chr1	148746972	148747224	253	-108	ECM1
328	3.979118	chr16	1662968	1663188	221	-5200	HN1L
329	3.975924	chr2	73723187	73723698	512	-398	NAT8
333	3.970275	chr5	151056121	151056641	521	-9672	SPARC
334	3.967338	chr1	109823120	109823424	305	-4811	ATXN7L2
336	3.965409	chr1	150819153	150819536	384	259	LCE3D
337	3.964724	chr9	115299346	115299794	449	-3957	RGS3
339	3.957641	chr1	111847251	111847515	265	249	ADORA3
340	3.955359	chr3	49029209	49029572	364	-4687	NDUFAF3
340	3.955359	chr3	49029209	49029572	364	1630	DALRD3
343	3.952578	chr5	31834647	31835073	427	73	PDZD2
344	3.952078	chr15	64645064	64645251	188	-269	LCTL
345	3.949712	chr19	54692621	54692831	211	1281	RPS11
349	3.942845	chr15	40239660	40239917	258	-3687	PLA2G4F
350	3.941872	chr7	44545027	44545399	373	2225	NPC1L1
352	3.939366	chr22	22455867	22456217	351	-3107	SMARCB1
353	3.938968	chr12	50721660	50721800	141	-9727	NR4A1
354	3.938683	chr2	102394225	102394363	139	-7391	IL18RAP
355	3.935046	chr15	73034113	73034356	244	2593	RPP25
358	3.929106	chr7	44548639	44549132	494	-1447	NPC1L1
359	3.927484	chr19	40448847	40449154	308	-2735	USF2

361	3.925935	chr5	131659276	131660376	1101	1783	SLC22A4
362	3.92325	chr19	52051611	52051922	312	-5724	AP2S1
368	3.917381	chr13	114009514	114009876	363	-8780	CDC16
369	3.916933	chr3	52787371	52787787	417	-7601	NEK4
369	3.916933	chr3	52787371	52787787	417	932	ITIH1
374	3.906105	chr19	51215711	51215958	248	2328	PGLYRP1
375	3.906042	chr7	44983580	44983891	312	1457	MYO1G
376	3.904772	chr12	2027684	2027974	291	-4895	CACNA1C
377	3.904351	chr1	158436101	158436449	349	-5475	PEA15
379	3.902776	chr3	38001933	38002189	257	-8020	VILL
380	3.901805	chr22	18331614	18332361	748	1918	COMT
381	3.898462	chr16	55453113	55453574	462	-3299	SLC12A3
382	3.895863	chr12	6947601	6947884	284	-2511	EMG1
382	3.895863	chr12	6947601	6947884	284	2409	PHB2
383	3.893321	chr19	48399492	48399893	402	1937	PSG4
384	3.889716	chr7	44072867	44073129	263	-1311	PGAM2
385	3.889227	chr21	46850219	46850558	340	-926	S100B
386	3.888929	chr9	35801362	35801691	330	732	SPAG8
387	3.886664	chr22	22564940	22565155	216	-1517	MIF
389	3.88112	chr13	114093380	114093983	604	-4435	ZNF828
390	3.880803	chr3	8744345	8744657	313	-5994	CAV3
391	3.880755	chr9	131447114	131447348	235	-2967	ASB6
393	3.876845	chr3	49143291	49143908	618	2003	LAMB2
394	3.876771	chr4	686826	687005	180	-2657	PCGF3
396	3.8758	chr5	140748094	140748273	180	-9695	PCDHGB5
396	3.8758	chr5	140748094	140748273	180	-3483	PCDHGA8
396	3.8758	chr5	140748094	140748273	180	548	PCDHGB4
397	3.87542	chr9	91401680	91401916	237	-7949	GADD45G
399	3.873898	chr9	115886054	115886223	170	-5603	AMBP
400	3.872272	chr17	75691408	75691623	216	1639	GAA
402	3.871379	chr15	79263395	79263646	252	1266	IL16
405	3.869737	chr22	19125119	19125440	322	-3134	SCARF2
407	3.866451	chr12	56294054	56294242	189	-5811	SLC26A10
407	3.866451	chr12	56294054	56294242	189	2664	GEFT
409	3.862207	chr10	13436733	13436987	255	-6575	SEPHS1
412	3.857637	chr9	124836182	124836411	230	-370	GPR21
413	3.857244	chr22	19693339	19693633	295	-7083	THAP7
413	3.857244	chr22	19693339	19693633	295	-5962	P2RX6
414	3.854759	chr15	66517305	66517640	336	-5927	ITGA11
415	3.85222	chr4	9385569	9385805	237	-7013	DRD5
416	3.851434	chr15	76312771	76313017	247	1059	ACSBG1
417	3.850231	chr6	41411979	41412561	583	766	NCR2
418	3.850075	chr5	131616136	131616470	335	-4982	PDLIM4
420	3.847479	chr7	55396709	55396884	176	-3838	LANCL2
423	3.839801	chr7	44200627	44201009	383	-6284	YKT6
423	3.839801	chr7	44200627	44201009	383	-5256	GCK
425	3.837919	chr21	34805232	34805446	215	1103	KCNE1
427	3.834346	chr3	161769187	161769702	516	-3375	KPNA4
428	3.832983	chr1	224176389	224176639	251	2073	PYCR2
429	3.827998	chr7	127009437	127009793	357	-6137	ARF5
431	3.823915	chr17	7166650	7166983	334	-7435	GPS2
432	3.823119	chr8	41648208	41648522	315	-6125	ANK1
433	3.822924	chr7	44156977	44157313	337	-9705	MYL7
435	3.820158	chr12	103894634	103894989	356	-9416	C12orf45
437	3.818129	chr12	46413388	46413612	225	-7884	ENDOU
438	3.816969	chr12	54316893	54317158	266	83	OR10P1
441	3.808962	chr3	140743220	140743582	363	-2222	RBP1
445	3.803331	chr3	38048136	38048468	333	-7397	DLEC1
445	3.803331	chr3	38048136	38048468	333	-2166	PLCD1
447	3.802121	chr12	55684149	55684586	438	2129	ZBTB39
453	3.790951	chr9	131124529	131124717	189	1508	C9orf106
455	3.790423	chr16	66250023	66250178	156	-8119	C16orf86
455	3.790423	chr16	66250023	66250178	156	-2251	PARD6A
455	3.790423	chr16	66250023	66250178	156	2113	ACD
456	3.789123	chr9	129606144	129606426	283	957	FPGS
457	3.788506	chr12	51731608	51731955	348	1680	TENC1
459	3.785187	chr17	44327982	44328185	204	2937	ATP5G1
460	3.784406	chr22	34264870	34265113	244	-2306	RASD2
462	3.783676	chr14	46190175	46190543	369	418	RPL10L
463	3.781678	chr19	60108991	60109323	333	-180	NCR1
464	3.777012	chr17	18160165	18160537	373	-1306	TOP3A

464	3.777012	chr17	18160165	18160537	373	911	SMCR8
465	3.776313	chr7	44128007	44128402	396	1450	POLD2
466	3.775941	chr19	59989365	59989868	504	12	KIR3DL1
468	3.768851	chr5	56813169	56813376	208	1120	ACTBL2
471	3.766168	chr3	42105325	42105499	175	-2337	TRAK1
472	3.765971	chr15	72398514	72398926	413	768	CCDC33
473	3.765393	chr9	129509618	129510228	611	-8255	TTC16
473	3.765393	chr9	129509618	129510228	611	-2875	C9orf117
474	3.765092	chr15	67375065	67375317	253	-3156	PAQR5
475	3.764703	chr11	44837705	44837834	130	-683	TSPAN18
476	3.762913	chr3	10827242	10828098	857	-5246	SLC6A11
479	3.761619	chr9	116133548	116133760	213	1765	ORM2
480	3.75801	chr22	20643275	20644126	852	-6484	PPM1F
481	3.757751	chr5	176009337	176009542	206	2446	TSPAN17
482	3.756619	chr9	135228772	135228950	179	-4243	C9orf96
484	3.754765	chr4	2791836	2792193	358	1676	SH3BP2
486	3.751831	chr3	185227471	185227902	432	-9266	ABCC5
486	3.751831	chr3	185227471	185227902	432	-4339	HTR3D
487	3.751322	chr1	159398481	159398754	274	-4200	PPOX
487	3.751322	chr1	159398481	159398754	274	2740	USP21
488	3.751285	chr2	96892892	96893140	249	-5542	ANKRD39
489	3.750335	chr19	49695086	49695416	331	1143	ZNF180
492	3.744702	chr5	1399823	1400074	252	-1947	CLPTM1L
493	3.743832	chr5	141315981	141316358	378	2641	PCDH12
495	3.741835	chr3	9759823	9760255	433	-5665	OGG1
496	3.741761	chr9	130878607	130878774	168	-4536	DOLPP1
497	3.740755	chr9	139596960	139597126	167	-3836	WDR85
498	3.7396	chr9	115675384	115675640	257	-2870	ZNF618
499	3.738981	chr5	1500930	1501265	336	-2555	SLC6A3
500	3.736551	chr22	18087748	18088073	326	-3155	GP1BB
504	3.735144	chr9	130748175	130748443	269	-1488	NUP188
504	3.735144	chr9	130748175	130748443	269	1523	DOLK
505	3.73373	chr3	12184983	12185127	145	-9409	TIMP4
509	3.728535	chr9	132698848	132699165	318	-1645	ABL1
510	3.727856	chr15	68938512	68938900	389	-5155	LARP6
511	3.72692	chr7	44166534	44166677	144	-1194	GCK
512	3.726725	chr14	54662000	54662252	253	-3498	LGALS3
514	3.725575	chr6	8010873	8011055	183	-1319	MUTED
517	3.721253	chr3	195832899	195833449	551	2227	TMEM44
523	3.712925	chr6	155581508	155581660	153	1796	TIAM2
526	3.712043	chr9	33392378	33393110	733	-228	AQP7
527	3.710105	chr1	154096111	154096359	249	-2640	GON4L
527	3.710105	chr1	154096111	154096359	249	312	SYT11
530	3.708143	chr4	660454	660736	283	-2474	ATP5I
530	3.708143	chr4	660454	660736	283	-1115	MYL5
533	3.704917	chr9	130686954	130687129	176	-2867	CCBL1
533	3.704917	chr9	130686954	130687129	176	2774	LRRC8A
534	3.704317	chr15	40235582	40235863	282	379	PLA2G4F
539	3.700536	chr1	159464792	159465108	317	-4909	APOA2
539	3.700536	chr1	159464792	159465108	317	2494	TOMM40L
541	3.699978	chr9	34637420	34637671	252	-9778	SIGMAR1
541	3.699978	chr9	34637420	34637671	252	-6386	IL11RA
541	3.699978	chr9	34637420	34637671	252	911	GALT
542	3.699342	chr8	124482363	124482810	448	-4719	ATAD2
544	3.697968	chrX	151909255	151909467	213	2052	PNMA5
547	3.694365	chr21	44598237	44598524	288	469	TRPM2
550	3.691844	chr1	152433139	152433375	237	-2025	TPM3
556	3.679796	chr1	153273565	153273846	282	-825	DCST2
556	3.679796	chr1	153273565	153273846	282	782	DCST1
557	3.67944	chr11	64561578	64561928	351	-3227	SAC3D1
559	3.676646	chr7	28414495	28414663	169	-4089	CREB5
564	3.670568	chr17	31075926	31076062	137	-6876	RASL10B
566	3.667987	chr1	151498719	151498894	176	4	LOR
567	3.667571	chr17	23724216	23724360	145	-2789	VTN
567	3.667571	chr17	23724216	23724360	145	1036	SARM1
568	3.666297	chr11	67110127	67110271	145	2338	GSTP1
569	3.666085	chr22	22362347	22362832	486	-458	RGL4
570	3.665133	chr19	46903377	46903635	259	-863	CEACAM5
571	3.663311	chr11	69305637	69306006	370	-6470	FGF4
572	3.66331	chr2	136589275	136589485	211	902	CXCR4
573	3.6621	chr17	35332420	35332736	317	-4150	GSDMB

577	3.655969	chr11	63028767	63029126	360	-1185	LGALS12
578	3.654927	chr9	134747829	134748000	172	-3896	C9orf98
580	3.653775	chr22	48700344	48700607	264	-2366	ALG12
580	3.653775	chr22	48700344	48700607	264	2128	CRELD2
581	3.653443	chr5	112797638	112797958	321	766	TSSK1B
583	3.652241	chr15	83000880	83001142	263	-2487	WDR73
583	3.652241	chr15	83000880	83001142	263	1794	NMB
584	3.651297	chr22	22364853	22365207	355	1983	RGL4
589	3.649309	chr3	49886146	49886694	549	-4048	CAMKV
592	3.645952	chr5	140004335	140004620	286	-3090	IK
592	3.645952	chr5	140004335	140004620	286	2946	NDUFA2
593	3.645018	chr15	32453389	32453738	350	-6877	LPCAT4
599	3.629519	chr1	151698732	151698909	178	940	S100A7
600	3.627657	chr6	43700129	43700715	587	-4834	MAD2L1BP
601	3.627505	chr9	126582553	126582792	240	-9276	NR6A1
602	3.627385	chr15	88448568	88448742	175	-1944	IDH2
603	3.62657	chr22	22441735	22441890	156	-3223	MMP11
603	3.62657	chr22	22441735	22441890	156	-1672	CHCHD10
604	3.625996	chr22	22425105	22425464	360	-9923	C22orf15
604	3.625996	chr22	22425105	22425464	360	-2006	ZNF70
604	3.625996	chr22	22425105	22425464	360	1307	VPREB3
605	3.625961	chr12	1898017	1898203	187	20	CACNA2D4
606	3.625661	chr19	62646360	62646646	287	-86	ZNF749
608	3.624192	chr9	138428274	138428650	377	-3588	SDCCAG3
609	3.624183	chr14	94149746	94150025	280	1419	SERPINA3
610	3.623697	chr17	59261976	59262563	588	-4082	FTSJ3
611	3.623614	chr22	22446651	22446922	272	-6646	CHCHD10
611	3.623614	chr22	22446651	22446922	272	1751	MMP11
612	3.622429	chr20	43954671	43955206	536	-5294	C20orf165
612	3.622429	chr20	43954671	43955206	536	-1631	NEURL2
612	3.622429	chr20	43954671	43955206	536	1326	CTSA
613	3.620274	chr19	40730262	40730437	176	1965	TMEM147
615	3.619443	chr22	22568768	22569050	283	2345	MIF
616	3.618752	chr15	66651592	66651803	212	-6931	CORO2B
617	3.618615	chr1	177824079	177824441	363	-3387	TDRD5
620	3.613801	chr1	31859409	31859659	251	2307	HCRTR1
621	3.610916	chr3	50312644	50312928	285	-7864	IFRD2
621	3.610916	chr3	50312644	50312928	285	-1071	NAT6
621	3.610916	chr3	50312644	50312928	285	-884	HYAL3
625	3.608902	chr17	40184047	40184231	185	-7954	ADAM11
626	3.608511	chr1	43660207	43660463	257	-1048	KIAA0467
628	3.607275	chr9	116126781	116126957	177	-5020	ORM2
628	3.607275	chr9	116126781	116126957	177	1713	ORM1
632	3.604365	chr9	89688260	89688463	204	770	C9orf79
633	3.603861	chr19	40935140	40935382	243	-7086	U2AF1L4
633	3.603861	chr19	40935140	40935382	243	-5622	C19orf55
635	3.601895	chr20	31084515	31084815	301	1551	BPIL3
636	3.601072	chr22	20320366	20320723	358	-6205	YDJC
636	3.601072	chr22	20320366	20320723	358	-5997	SDF2L1
638	3.600586	chr22	22360984	22361272	289	-1919	RGL4
639	3.598948	chr16	66423308	66423573	266	1860	CENPT
640	3.598032	chr15	73038164	73038577	414	-1543	RPP25
641	3.59509	chr3	50337182	50337446	265	-2169	HYAL2
643	3.592704	chr15	89250392	89250571	180	2058	MAN2A2
646	3.591513	chr11	61320328	61320466	139	-3737	C11orf10
648	3.588553	chr9	37031138	37031401	264	-6794	PAX5
649	3.587995	chr9	35803288	35803505	218	-1138	SPAG8
649	3.587995	chr9	35803288	35803505	218	1645	HINT2
651	3.585123	chr19	16099757	16100047	291	-5935	HSH2D
652	3.584083	chr3	9756083	9756412	330	-9457	OGG1
656	3.58102	chr3	185508281	185508526	246	-7384	EIF4G1
657	3.580913	chr10	135024724	135024949	226	-3318	C10orf125
662	3.57896	chr22	20669168	20669485	318	-2180	TOP3B
663	3.578408	chr3	12857252	12857540	289	-448	RPL32
667	3.574413	chr17	9748826	9749109	284	441	RCVRN
668	3.573931	chr3	49805092	49805634	543	-6387	IP6K1
671	3.568338	chr19	58495673	58495965	293	-9133	BIRC8
672	3.567291	chr1	207996657	207996804	148	584	TRAF3IP3
673	3.567104	chr17	49255762	49256120	359	681	KIF2B
677	3.563304	chr9	34699406	34699698	293	594	CCL21
678	3.563177	chr1	157442248	157442415	168	1198	DARC

679	3.56306	chr9	37406946	37407300	355	-5583	GRHPR
682	3.561089	chr7	143378547	143378851	305	272	OR2A5
685	3.56009	chr17	7062557	7062742	186	-1227	ACADVL
685	3.56009	chr17	7062557	7062742	186	1095	DLG4
686	3.559854	chr15	67372575	67373198	624	-5461	PAQR5
688	3.557474	chr21	44899886	44900213	328	-2227	KRTAP12-3
688	3.557474	chr21	44899886	44900213	328	-1046	KRTAP12-4
689	3.55736	chr19	53244328	53244494	167	-5296	CABP5
692	3.555666	chr19	41041468	41041711	244	-9651	APLP1
692	3.555666	chr19	41041468	41041711	244	-7011	NPHS1
692	3.555666	chr19	41041468	41041711	244	1926	KIRREL2
693	3.55143	chr16	28762873	28763164	292	2125	TUFM
694	3.55128	chr1	43598875	43599289	415	1868	CDC20
700	3.544536	chr9	137535639	137535910	272	-4193	C9orf116
702	3.542528	chr7	99794495	99794634	140	1003	PILRB
704	3.541493	chr2	26057042	26057344	303	1713	KIF3C
705	3.541148	chr22	22355582	22356054	473	-7229	RGL4
708	3.53711	chr12	47777388	47777650	263	-2651	DHH
710	3.532764	chr3	45955806	45956016	211	-4065	CXCR6
711	3.532646	chr22	22304367	22304767	401	-81	C22orf43
712	3.530184	chr12	51914803	51915107	305	-2653	RARG
713	3.528339	chr11	118538031	118538256	226	-6506	NLRX1
715	3.525275	chrX	153323201	153323383	183	-2409	FAM50A
717	3.522255	chr5	195844	196057	214	2578	PLEKHG4B
718	3.52158	chr7	44147600	44148217	618	-468	MYL7
720	3.519182	chr2	119323046	119323221	176	-905	EN1
722	3.517028	chr11	125648257	125648598	342	-9764	TIRAP
722	3.517028	chr11	125648257	125648598	342	-4468	SRPR
723	3.515631	chr22	21744232	21744570	339	1733	GNAZ
724	3.515559	chr7	44196260	44196589	330	-862	GCK
729	3.512034	chr3	50360958	50361232	275	-7725	RASSF1
729	3.512034	chr3	50360958	50361232	275	-2936	ZMYND10
729	3.512034	chr3	50360958	50361232	275	-2205	CYB561D2
729	3.512034	chr3	50360958	50361232	275	2394	TUSC4
732	3.509612	chr19	40632850	40633033	184	485	FFAR2
735	3.506203	chr19	44572048	44572325	278	-1616	MED29
735	3.506203	chr19	44572048	44572325	278	1332	PAF1
736	3.50585	chr15	88247662	88247916	255	-9584	AP3S2
738	3.500047	chr11	67125002	67125144	143	-5909	NDUFV1

Appendix 6: Gene loci with multiple SF-1-binding regions (ChIP-on-chip)

Peak	MA Z-score	Chr	Start	End	Distance to TSS	Gene symbol
Gene loci where two SF-1-binding regions were identified						
4	7.22	chr3	8671294	8671558	-2690	C3orf32
13	6.12	chr3	8672091	8672356	-3487	
162	4.37	chr9	129508595	129509039	-3981	C9orf117
473	3.77	chr9	129509618	129510228	-2875	
50	5.07	chr9	139889204	139889711	-2604	CACNA1B
60	4.93	chr9	139888430	139888657	-3518	
603	3.63	chr22	22441735	22441890	-1672	CHCHD10
611	3.62	chr22	22446651	22446922	-6646	
221	4.20	chr3	49036997	49037532	-3794	DALRD3
340	3.96	chr3	49029209	49029572	1630	
43	5.14	chr9	130885372	130885644	2282	DOLPP1
496	3.74	chr9	130878607	130878774	-4536	
256	4.11	chr22	21740501	21741046	-1895	GNAZ
723	3.52	chr22	21744232	21744570	1733	
135	4.45	chr7	45888398	45888890	-5839	IGFBP1
173	4.33	chr7	45887119	45887841	-7003	
603	3.63	chr22	22441735	22441890	-3223	MMP11
611	3.62	chr22	22446651	22446922	1751	
34	5.30	chr7	43878032	43878592	-2643	MRPS24
44	5.12	chr7	43881830	43882948	-6720	
68	4.80	chr7	44985779	44986174	-784	MYO1G
375	3.91	chr7	44983580	44983891	1457	
52	5.05	chr15	73417958	73418364	-8301	NEIL1
322	3.99	chr15	73418770	73419194	-7480	
350	3.94	chr7	44545027	44545399	2225	NPC1L1
358	3.94	chr7	44548639	44549132	-1447	
495	3.74	chr3	9759823	9760255	-5665	OGG1
652	3.58	chr3	9756083	9756412	-9457	
479	3.76	chr9	116133548	116133760	1765	ORM2
628	3.61	chr9	116126781	116126957	-5020	
349	3.94	chr15	40239660	40239917	-3687	PLA2G4F
534	3.70	chr15	40235582	40235863	379	
282	4.06	chr7	44134270	44134483	-4722	POLD2
465	3.78	chr7	44128007	44128402	1450	
188	4.29	chr7	44086280	44087020	1956	POLM
305	4.02	chr7	44090262	44090596	-1823	
355	3.94	chr15	73034113	73034356	2593	RPP25
640	3.60	chr15	73038164	73038577	-1543	
386	3.89	chr9	35801362	35801691	732	SPAG8
649	3.59	chr9	35803288	35803505	-1138	

Peak	MA Z-score	Chr	Start	End	Distance to TSS	Gene symbol
27	5.49	chr19	40729390	40729965	1293	TMEM147
613	3.62	chr19	40730262	40730437	1965	
95	4.61	chr7	47545808	47546908	-635	TNS3
255	4.11	chr7	47549757	47549973	-4142	
162	4.37	chr9	129508595	129509039	-9361	TTC16
473	3.77	chr9	129509618	129510228	-8255	
172	4.34	chr3	50370010	50370448	-6740	TUSC4
729	3.51	chr3	50360958	50361232	2394	
288	4.04	chr7	49778102	49778894	-5304	VWC2
306	4.01	chr7	49779153	49779281	-4585	
98	4.58	chr7	44199086	44199682	-7718	YKT6
423	3.84	chr7	44200627	44201009	-6284	
64	4.85	chr7	44756247	44757153	1646	ZMIZ2
111	4.52	chr7	44760221	44761389	-1506	
Gene loci where three SF-1-binding regions were identified						
26	5.49	chr13	113149179	113149920	1908	ADPRHL1
101	4.56	chr13	113151583	113152145	-407	
239	4.15	chr13	113162831	113163178	-7165	
120	4.48	chr20	23913754	23914127	1571	GGTLC1
139	4.44	chr20	23924106	23924428	-6852	
264	4.09	chr20	23917521	23918391	-541	
39	5.21	chr22	22563867	22564131	-2565	MIF
387	3.89	chr22	22564940	22565155	-1517	
615	3.62	chr22	22568768	22569050	2345	
235	4.16	chr15	67376934	67377193	-1284	PAQR5
474	3.77	chr15	67375065	67375317	-3156	
686	3.56	chr15	67372575	67373198	-5461	
Gene loci where four SF-1-binding regions were identified						
102	4.56	chr7	44144836	44145092	2476	MYL7
195	4.27	chr7	44155770	44156100	-8495	
433	3.82	chr7	44156977	44157313	-9705	
718	3.52	chr7	44147600	44148217	-468	
569	3.67	chr22	22362347	22362832	-458	RGL4
584	3.65	chr22	22364853	22365207	1983	
638	3.60	chr22	22360984	22361272	-1919	
705	3.54	chr22	22355582	22356054	-7229	
8	6.51	chr15	20377626	20377881	-7189	TUBGCP5
56	4.96	chr15	20384158	20384443	-642	
128	4.47	chr15	20379527	20380187	-5085	
312	4.01	chr15	20382416	20382694	-2387	
Gene locus where five SF-1-binding regions were identified						
98	4.58	chr7	44199086	44199682	-3822	GCK
112	4.52	chr7	44195300	44195749	38	
423	3.84	chr7	44200627	44201009	-5256	
511	3.73	chr7	44166534	44166677	-1194	
724	3.52	chr7	44196260	44196589	-862	

Peak refers to SF-1-binding region identified by CisGenome. Only peaks located from 10 kb upstream to 3 kb downstream of a transcriptional start are included. Chr, chromosome; TSS, transcriptional start site.

Appendix 7: Fluorescence-activated cell sorting reports (SF-1 overexpression)

Two representative FACS reports are shown, corresponding to experiment 4, SF-1 overexpression (WT; M4A) and control (mutant G35E; M4B), respectively.

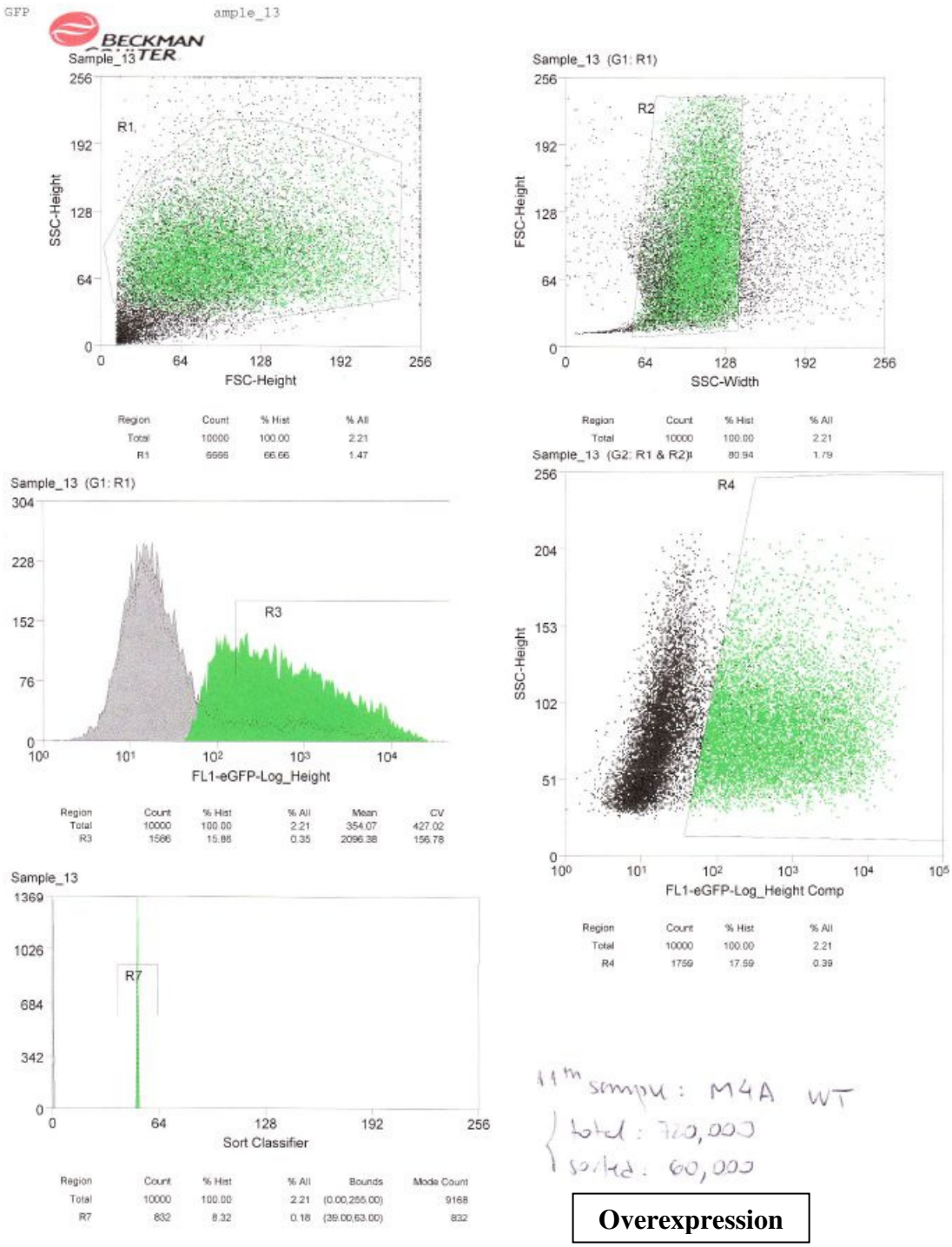

GFP ample_14

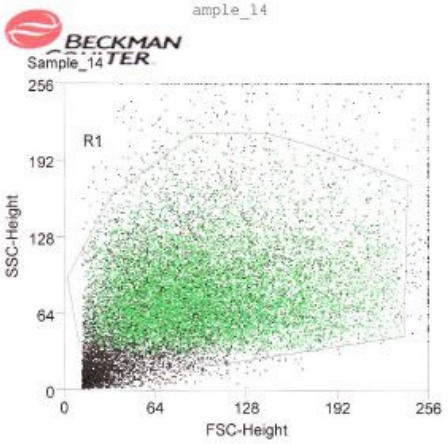

Region	Count	% Hist	% All
Total	10000	100.00	7.71
R1	6512	65.12	5.02

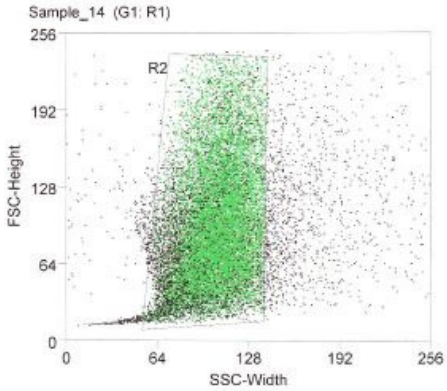

Region	Count	% Hist	% All
Total	10000	100.00	7.71
R2	8534	85.34	6.58

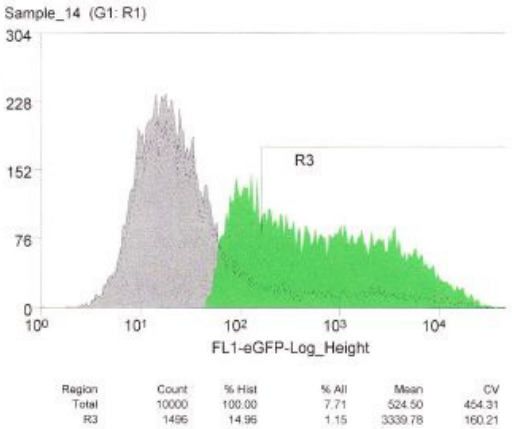

Region	Count	% Hist	% All	Mean	CV
Total	10000	100.00	7.71	524.50	454.31
R3	1496	14.96	1.15	3339.78	160.21

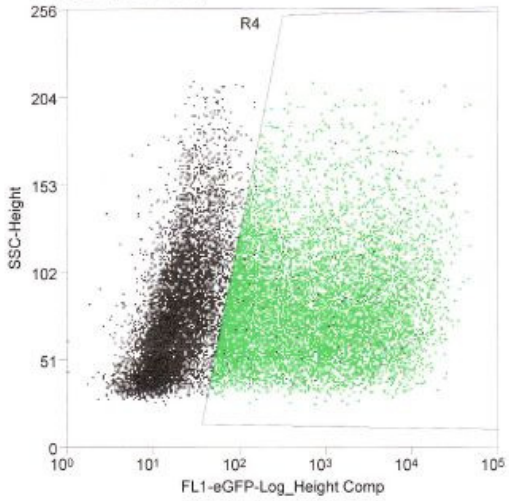

Region	Count	% Hist	% All
Total	10000	100.00	7.71
R4	1894	18.94	1.46

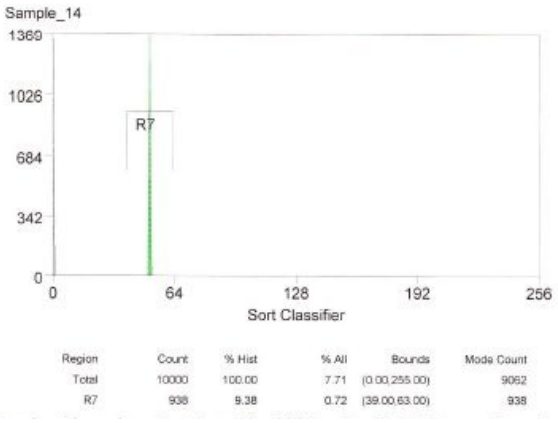

Region	Count	% Hist	% All	Bounds	Mode Count
Total	10000	100.00	7.71	(0.00,255.00)	9062
R7	938	9.38	0.72	(39.00,63.00)	938

12th sample : M4B Mutant

{ total : 793,000
{ sorted : 72,000

Control

Appendix 8: Complete results of gene expression analysis following SF-1 overexpression

Transcripts are ordered by fold change (FC) in expression levels following SF-1 overexpression in NCI-H295R cells. Transcript Cluster ID, Affymetrix Human Gene 1.0 ST array Transcript Cluster ID; Adj.P-Val, Benjamini-Hochberg-corrected P-value.

Transcript Cluster ID	FC	Adj.P-Val	Gene symbol
7972946	12.4	0.00000751	RASA3
7935116	12.3	0.00000751	RBP4
8039353	9	0.00000978	TNNI3
8071642	6.36	0.00000751	IGLV6-57
8095110	6.15	0.000903	KIT
8141737	5.35	0.0000978	MYL10
8114249	5.17	0.000656	CXCL14
8056113	4.38	0.000128	CD302
8056113	4.38	0.000128	LY75
7920285	4.29	0.000402	S100A2
8116653	4.06	0.000073	BPHL
8116649	4.06	0.000073	TUBB2A
8116649	4.06	0.000073	TUBB2B
8036079	3.61	0.0000974	DMKN
7991323	3.61	0.000329	PEX11A
7934993	3.56	0.000903	NUDT9P1
8069508	3.53	0.0171	C21orf81
8069508	3.53	0.0171	LOC375010
8103951	3.51	0.00121	ACSL1
8087691	3.51	0.000168	CACNA2D2
7951662	3.41	0.000588	CRYAB
8066214	3.36	0.00028	TGM2
8158671	3.29	0.00316	ASS1
8104930	3.16	0.000888	SLC1A3
7920278	3.14	0.00278	S100A3
8158995	3.03	0.0272	LCN1
8101828	3.03	0.00354	TSPAN5
8123407	3.01	0.000244	MLLT4
8053741	2.97	0.000423	ANKRD20A1
8053741	2.97	0.000423	ANKRD20A2
8053741	2.97	0.000423	ANKRD20A3
8053741	2.97	0.000423	ANKRD20A4
8053741	2.97	0.000423	ANKRD20B
8080184	2.93	0.000306	ALAS1
8155591	2.89	0.00255	CCDC29
8155591	2.89	0.00255	RP11-195B21.3
8155414	2.81	0.00455	LOC100289454
8160531	2.69	0.00544	C9orf72
8037053	2.69	0.000959	CEACAM7
7942064	2.68	0.00917	GAL
8171653	2.66	0.000588	MAP3K15
8171653	2.66	0.000588	PDHA1
7904408	2.6	0.00808	HSD3B2
8161415	2.6	0.00598	LOC100289026
8123246	2.58	0.00647	SLC22A3
8058238	2.53	0.00171	ALS2CR11
8172043	2.53	0.000423	SRPX
7970381	2.5	0.00164	LOC100287836
7970381	2.5	0.00164	LOC643166
7970381	2.5	0.00164	LOC728897
8033233	2.5	0.00207	TUBB4
7902883	2.48	0.000631	LRRC8D
7990333	2.46	0.00598	CYP11A1
8079588	2.46	0.0249	NDUFB1P1
8022420	2.46	0.00026	ZNF519
7972487	2.45	0.00115	DOCK9
7914342	2.43	0.00593	FABP3
8162652	2.41	0.00188	CTSL2
8097335	2.41	0.00138	HSPA4L
8018038	2.39	0.00219	ABCA5
8080487	2.39	0.00138	PRKCD
8155602	2.38	0.00133	ANKRD20A5
8155602	2.38	0.00133	LOC100290156
7908940	2.35	0.000888	ATP2B4
8164293	2.33	0.000765	AK1
7952526	2.33	0.000746	CDON
7990774	2.33	0.00138	RASGRF1
8155665	2.31	0.0031	PGM5
7970763	2.3	0.00864	FLT1
8169580	2.3	0.00546	IL13RA1
8070538	2.27	0.000656	C2CD2
7930025	2.27	0.00339	ELOVL3
8075838	2.27	0.0105	PVALB
8069505	2.23	0.00237	C21orf15
8041781	2.23	0.00125	EPAS1
7952805	2.23	0.0108	LOC283174
7932584	2.23	0.00662	PRTFDC1
8066590	2.22	0.0047	TNNC2
8040430	2.2	0.00401	VSNL1
7913237	2.19	0.000888	CAMK2N1
8010978	2.17	0.0124	LOC100130876
8039977	2.17	0.00128	SNTG2
7933437	2.16	0.00532	PTPN20A
7933437	2.16	0.00532	PTPN20B
8164967	2.16	0.00158	VAV2
8097435	2.14	0.0307	C4orf33
8054513	2.14	0.0047	LOC151009
8054513	2.14	0.0047	LOC440894
8069565	2.08	0.00128	BTG3
7979269	2.07	0.00663	GCH1
7950883	2.07	0.0293	OR7E13P
7933442	2.07	0.00788	PTPN20C
7905147	2.06	0.0208	C1orf54
8151101	2.06	0.00439	MYBL1
8147548	2.06	0.00784	POP1
7928046	2.06	0.00092	TSPAN15
8164235	2.04	0.00231	C9orf117
7926105	2.04	0.0031	GATA3
8164235	2.04	0.00231	PTRH1
8164235	2.04	0.00231	TTC16
8079407	2.03	0.00689	CCRL2
8020339	2.03	0.00383	MC5R
8150253	2.03	0.00491	STAR
8150691	2.01	0.00948	EFCAB1
7976451	2.01	0.0118	PPP4R4
8017843	2.01	0.0497	SLC16A6

8069178	2	0.00249	ADARB1
7974737	2	0.0272	LRRC9
8108873	1.99	0.00451	ARHGAP26
8083415	1.98	0.00689	AADAC
8170513	1.97	0.00272	FATE1
7947270	1.97	0.0202	KCNA4
8023259	1.95	0.0249	SNORD58A
8143054	1.94	0.00662	AKR1B1
8147132	1.94	0.0416	CA2
8174891	1.93	0.00384	MIR220A
8020955	1.93	0.00128	MOCOS
7909586	1.93	0.0113	PPP2R5A
7928308	1.92	0.00504	DDIT4
8019046	1.92	0.00291	EIF4A3
8008237	1.92	0.0108	ITGA3
7905548	1.92	0.0245	SPRR3
8075239	1.92	0.00228	THOC5
7986446	1.91	0.00788	ALDH1A3
7917912	1.91	0.00188	DPYD
8109194	1.88	0.00575	SLC26A2
7985213	1.87	0.0118	CHRNA5
7947599	1.87	0.00555	CHST1
8112649	1.87	0.00632	FAM169A
7934852	1.87	0.00403	GLUD1
7934852	1.87	0.00403	GLUD2
8147439	1.87	0.00569	PLEKHF2
8139118	1.87	0.0157	TRGV5P
8071671	1.86	0.00558	GNAZ
8160637	1.84	0.00567	B4GALT1
7984298	1.84	0.00751	DIS3L
7927363	1.84	0.00294	FAM25A
7927363	1.84	0.00294	FAM25B
7927363	1.84	0.00294	FAM25C
7927363	1.84	0.00294	FAM25G
8021187	1.84	0.0372	SKA1
8020702	1.84	0.00451	TAF4B
8107307	1.83	0.0204	CAMK4
7964997	1.83	0.0352	CAPS2
8068383	1.83	0.0121	CLIC6
7930304	1.83	0.002	GSTO1
8143341	1.83	0.0108	JHDM1D
8044212	1.83	0.00302	SULT1C2
8145954	1.83	0.00138	TACC1
8137709	1.83	0.0241	ZFAND2A
8053744	1.82	0.00344	FLJ43315
7967727	1.82	0.00662	GALNT9
8088285	1.82	0.0453	HESX1
7981750	1.82	0.00221	LOC400968
7981427	1.81	0.00555	CKB
8061013	1.81	0.00384	ISM1
7989146	1.81	0.0146	MNS1
8020814	1.81	0.0122	RNF138
8037079	1.8	0.00458	ATP1A3
8133770	1.79	0.0066	CCDC146
7911096	1.79	0.0164	EFCAB2
8099246	1.79	0.00378	GRPEL1
8164848	1.79	0.0323	LCN1L1
8163535	1.78	0.0146	AMBP
8026971	1.78	0.0219	IFI30
8070557	1.78	0.00221	ZNF295
8166184	1.77	0.007	CA5B
8096744	1.77	0.00234	CYP2U1
7905220	1.77	0.00455	ECM1
7919642	1.77	0.0479	HIST2H2AB
7912994	1.76	0.0422	IFFO2
8156848	1.76	0.0242	NR4A3
8146717	1.75	0.0205	C8orf44
8164607	1.75	0.00932	FNBP1
8039607	1.75	0.0045	PEG3
8076998	1.75	0.00576	PLXNB2
8146717	1.75	0.0205	SGK3

8144786	1.75	0.0397	SLC7A2
8127987	1.75	0.0187	SNORD50A
8013771	1.75	0.0465	TLCD1
8039607	1.75	0.0045	ZIM2
8086880	1.74	0.00615	CDC25A
8008706	1.74	0.0232	DYNLL2
8107164	1.74	0.0216	HISPPD1
8146649	1.74	0.0402	MTFR1
8084717	1.74	0.00517	ST6GAL1
7959312	1.74	0.0125	TMEM120B
8105456	1.73	0.00583	C5orf35
8041487	1.73	0.00451	CCDC75
8047854	1.73	0.0183	CCNYL1
7993776	1.73	0.00215	LOC81691
7909866	1.73	0.0117	MOSC2
7900540	1.73	0.0111	RIMKLA
7930714	1.72	0.00244	ATRNL1
8044700	1.72	0.043	DPP10
8047127	1.72	0.0338	MYO1B
8112033	1.71	0.00948	ARL15
7939341	1.71	0.00932	CD44
7949916	1.71	0.00727	CHKA
8034315	1.71	0.0314	ZNF823
7940147	1.7	0.00237	FAM111B
7991577	1.7	0.0498	LOC440313
7986214	1.7	0.00583	SLCO3A1
8156706	1.7	0.017	TMOD1
8034379	1.7	0.0108	ZNF442
8101228	1.69	0.00294	CNOT6L
8083272	1.69	0.00959	GYG1
7924888	1.69	0.0251	HIST3H2A
7929388	1.69	0.00656	PLCE1
7909877	1.68	0.00645	MOSC1
7956658	1.68	0.0157	SLC16A7
8046340	1.67	0.0161	DYNC1I2
7917707	1.67	0.0491	EVI5
8155268	1.67	0.00588	POLR1E
8150138	1.67	0.0149	TEX15
8113577	1.67	0.0086	TRIM36
8035847	1.67	0.0286	ZNF675
8091629	1.66	0.0309	C3orf33
8070730	1.66	0.0197	DNMT3L
8096361	1.66	0.0246	HERC5
8095303	1.66	0.00821	LPHN3
8092177	1.66	0.00529	NCEH1
8127989	1.66	0.0247	SNORD50B
7944667	1.66	0.0108	SORL1
8065089	1.65	0.0277	KIF16B
7936559	1.65	0.00756	PDZD8
7971723	1.65	0.044	RP11-327P2.4
8157144	1.64	0.00675	C9orf6
7916356	1.64	0.00756	HSPB11
8157144	1.64	0.00675	IKBKAP
7914878	1.64	0.0164	LOC100289612
8039545	1.64	0.0275	NLRP11
8173825	1.64	0.0395	RPS6KA6
8019877	1.64	0.0103	SMCHD1
8088106	1.64	0.00756	TKT
8066461	1.64	0.00662	TOMM34
8104234	1.64	0.0228	TRIP13
8080511	1.63	0.0063	CACNA1D
8153939	1.63	0.0302	DGAT1
8044111	1.63	0.0432	MRPS9
8011407	1.63	0.0379	TAX1BP3
7955063	1.63	0.00576	TMEM106C
7928558	1.63	0.00591	ZMIZ1
7970428	1.63	0.0193	ZMYM5
7995976	1.62	0.00738	CPNE2
8006736	1.62	0.0181	DUSP14
8094609	1.62	0.00854	FAM114A1
8133540	1.62	0.0299	GATS

8133540	1.62	0.0299	GATSL1
8133540	1.62	0.0299	GATSL2
8043981	1.62	0.0314	IL1R2
7970577	1.62	0.0117	MIPEP
7985662	1.62	0.00848	PDE8A
8107563	1.62	0.0244	PRR16
8113938	1.61	0.0235	ACSL6
8054702	1.61	0.0464	CKAP2L
8113938	1.61	0.0235	LOC728637
7909529	1.61	0.0279	RCOR3
8078014	1.61	0.00891	SLC6A6
7907702	1.61	0.0114	SOAT1
7951207	1.61	0.00828	TMEM123
8115261	1.6	0.0222	CCDC69
8109528	1.6	0.0255	CYFIP2
7972912	1.6	0.012	DCUN1D2
8071063	1.6	0.00451	psiTPTE22
8158998	1.6	0.00625	RPL7A
8158998	1.6	0.00625	SNORD36A
8158998	1.6	0.00625	SNORD36C
8039340	1.6	0.0372	TNNT1
8140752	1.59	0.0236	ABCB4
8058258	1.59	0.0203	ALS2CR4
7974653	1.59	0.0272	KIAA0586
7921882	1.59	0.0398	OLFML2B
8105778	1.59	0.00654	PIK3R1
8147796	1.59	0.0212	RIMS2
8017582	1.59	0.00893	TEX2
8020973	1.58	0.0193	FHOD3
7956271	1.58	0.0495	HSD17B6
8159441	1.58	0.00593	PHPT1
8135734	1.57	0.0318	C7orf58
7924450	1.57	0.0101	DUSP10
8155630	1.57	0.0464	LOC100133920
8155630	1.57	0.0464	LOC286297
8070961	1.57	0.0101	LSS
8155630	1.57	0.0464	MTHFD1L
8111892	1.57	0.00756	OXCT1
7903203	1.57	0.0246	SNX7
7903239	1.56	0.0145	AGL
8155327	1.56	0.0108	ALDH1B1
8034837	1.56	0.021	DNAJB1
8081676	1.56	0.0337	GTPBP8
7929282	1.56	0.0236	HHEX
8050537	1.56	0.00946	MATN3
7933010	1.56	0.036	PARD3
7929132	1.56	0.0303	PCGF5
7933619	1.56	0.0149	SGMS1
8047174	1.56	0.00985	SLC39A10
7943297	1.55	0.0236	CEP57
8068593	1.55	0.0105	ETS2
8057045	1.55	0.0147	FKBP7
8070720	1.55	0.0449	ICOSLG
8043431	1.55	0.0496	IGKC
8043431	1.55	0.0496	IGKV1-33
8043431	1.55	0.0496	IGKV1D-33
8043431	1.55	0.0496	LOC100291464
8043431	1.55	0.0496	LOC652694
8013068	1.55	0.00948	PLD6
8158059	1.55	0.0372	STXBP1
7979611	1.55	0.0218	ZBTB25
7964460	1.54	0.0118	DDIT3
7954185	1.54	0.0216	DERA
8109912	1.54	0.0269	KCNIP1
7960730	1.54	0.0123	LPCAT3
8175256	1.54	0.0145	MGC16121
8126860	1.54	0.0293	MUT
7936050	1.53	0.0164	CYP17A1
8127787	1.53	0.0221	IBTK
7943376	1.53	0.0487	KIAA1377
7981460	1.53	0.0301	PPP1R13B
7991283	1.53	0.0255	RHCG
7929816	1.53	0.0255	SCD
8107920	1.53	0.00583	SLC22A5
8162086	1.52	0.0285	AGTPBP1
8022380	1.52	0.0221	CEP76
8001564	1.52	0.0194	DOK4
7972336	1.52	0.0264	DZIP1
8105121	1.52	0.0254	GHR
8157727	1.52	0.044	GPR21
7958158	1.52	0.0128	HCFC2
7931479	1.52	0.0213	INPP5A
8112331	1.52	0.0203	ISCA1
8112331	1.52	0.0203	ISCA1L
7931728	1.52	0.0416	LARP4B
8034762	1.52	0.0139	PRKACA
7924092	1.52	0.0106	SLC30A1
8052861	1.52	0.0302	SNRPG
7979698	1.51	0.0146	ATP6V1D
8071649	1.51	0.00738	BMS1
8131583	1.51	0.0173	BZW2
7955107	1.51	0.02	C12orf68
7971950	1.51	0.0335	DACH1
7919591	1.51	0.0241	FAM72A
7919591	1.51	0.0241	FAM72B
7919591	1.51	0.0241	FAM72C
7919591	1.51	0.0241	FAM72D
8148448	1.51	0.025	KHDRBS3
8071649	1.51	0.00738	LOC96610
7983228	1.51	0.015	MAP1A
8013908	1.51	0.0132	NUFIP2
7989759	1.51	0.0289	PARP16
8093398	1.51	0.0276	PCGF3
8082314	1.51	0.02	PLXNA1
8066275	1.51	0.0411	PRO0628
8001748	1.51	0.0286	SNORA50
7962358	1.51	0.0484	YAF2
8069131	1.5	0.0134	C21orf30
8114425	1.5	0.0251	CDC25C
8081997	1.5	0.0246	FBXO40
7944769	1.5	0.0148	GRAMD1B
8098985	1.5	0.0118	HAUS3
8042283	1.5	0.0488	HSPC159
8080911	1.5	0.0338	KBTBD8
8103646	1.5	0.0208	NEK1
7903227	1.5	0.0243	PALMD
8098985	1.5	0.0118	POLN
8135323	1.5	0.0372	RINT1
8082797	1.5	0.042	TF
7985134	1.49	0.0323	ACSBG1
8081645	1.49	0.0291	C3orf52
8024566	1.49	0.0411	GNA11
8056837	1.49	0.0132	GPR155
7985134	1.49	0.0323	IDH3A
8060736	1.49	0.0144	MIR103-2
8060736	1.49	0.0144	MIR103-2AS
8033069	1.49	0.0079	NDUFA11
8060736	1.49	0.0144	PANK2
8113881	1.49	0.0103	RAPGEF6
7918622	1.49	0.0108	SLC16A1
7923824	1.49	0.0284	SLC41A1
8093993	1.49	0.0203	TADA2B
7987892	1.49	0.0305	ZFP106
8065032	1.48	0.00919	ESF1
7974166	1.48	0.0359	FANCM
8050719	1.48	0.00875	ITSN2
8164698	1.48	0.0234	MED27
7978628	1.48	0.0211	PPP2R3C
7932420	1.48	0.0347	PTPLA
8169365	1.48	0.00854	TMEM164
8157947	1.48	0.0193	ZBTB34
7942858	1.47	0.0145	ANKRD42

7991581	1.47	0.0204	CHSY1
8144669	1.47	0.0125	FDFT1
8162777	1.47	0.0168	GABBR2
8068866	1.47	0.0204	NDUFV3
8068866	1.47	0.0204	PKNOX1
8069711	1.47	0.0348	RNF160
7914202	1.47	0.0213	SNHG12
8175023	1.47	0.0126	ZDHHC9
7996012	1.46	0.0124	ARL2BP
8147424	1.46	0.0314	C8orf38
8165046	1.46	0.02	CAMSAP1
8172708	1.46	0.0432	NUDT11
7952785	1.46	0.0182	OPCML
8059996	1.46	0.0142	PER2
7944302	1.46	0.0123	PHLDB1
7977003	1.46	0.0146	RCOR1
8066513	1.46	0.0212	SDC4
8172280	1.46	0.0407	SLC9A7
8019842	1.46	0.0124	TYMS
7931168	1.45	0.0468	ACADSB
8164200	1.45	0.0299	ANGPTL2
8044375	1.45	0.0333	BCL2L11
7954132	1.45	0.0468	C12orf60
7969096	1.45	0.0106	CDADC1
8148728	1.45	0.0158	CYC1
8067864	1.45	0.0151	hCG_2042718
7987642	1.45	0.0162	NDUFAF1
8123936	1.45	0.0348	NEDD9
8046804	1.45	0.0144	NUP35
7953218	1.45	0.031	RAD51AP1
7929116	1.45	0.0109	RPP30
8108099	1.45	0.0266	SEC24A
7915472	1.45	0.0231	SLC2A1
7965769	1.45	0.0365	SLC5A8
8157381	1.45	0.031	ZNF618
8089527	1.44	0.0224	ATG3
8137874	1.44	0.0442	CARD11
7942123	1.44	0.0425	CCND1
8152582	1.44	0.036	DSCC1
7976698	1.44	0.0213	EML1
8010050	1.44	0.0276	FAM100B
8095907	1.44	0.0133	FRAS1
7944603	1.44	0.0445	GRIK4
7960177	1.44	0.0208	SLC6A12
7953508	1.44	0.0224	TPI1
8128977	1.44	0.0393	TUBE1
8162940	1.43	0.0179	ABCA1
7973850	1.43	0.0458	AKAP6
8019357	1.43	0.0397	DCXR
7949995	1.43	0.015	MRPL21
8071676	1.43	0.02	RAB36
8130151	1.43	0.0233	RAET1E
8148966	1.43	0.04	RPL23AP53
8094301	1.43	0.0224	SLIT2
8132097	1.42	0.043	AQP1
8168958	1.42	0.0372	ARMCX5
8047265	1.42	0.0417	C2orf47
8047265	1.42	0.0417	C2orf60
8132097	1.42	0.043	FAM188B
8026541	1.42	0.0229	FAM32A
8001764	1.42	0.0346	GOT2
8132097	1.42	0.043	INMT
7978846	1.42	0.0463	POLE2
8008754	1.42	0.0264	RAD51C
8121794	1.42	0.0262	SMPDL3A
7978570	1.42	0.0176	SNX6
8035808	1.42	0.0318	ZNF100
8175076	1.42	0.0457	ZNF280C
7922095	1.41	0.0193	BRP44
7977058	1.41	0.032	EIF5
8018793	1.41	0.0359	JMJD6
8040340	1.41	0.0302	LPIN1
8093086	1.41	0.0242	PCYT1A
8145136	1.41	0.0311	PPP3CC
8081786	1.41	0.0487	QTRTD1
7933999	1.41	0.0322	RUFY2
8061075	1.41	0.0213	SNRPB2
8175039	1.4	0.0203	ELF4
8024485	1.4	0.0249	GADD45B
7963438	1.4	0.0215	KRT71
7954591	1.4	0.0262	MRPS35
7965048	1.4	0.0382	NAP1L1
8001082	1.4	0.0236	SLC6A10P
8001082	1.4	0.0236	SLC6A8
7927981	1.4	0.0213	SUPV3L1
8100231	1.4	0.0483	TEC
8142912	1.4	0.0359	TMEM209
8025998	1.4	0.0439	ZNF136
7974587	1.39	0.0429	ACTR10
7991516	1.39	0.0325	ADAMTS17
7986350	1.39	0.0419	ARRDC4
8097373	1.39	0.0335	C4orf29
8158418	1.39	0.0483	C9orf114
8005661	1.39	0.0239	CYTSB
8158418	1.39	0.0483	ENDOG
8098021	1.39	0.02	GRIA2
7930208	1.39	0.047	INA
7971620	1.39	0.0213	KPNA3
7939767	1.39	0.0411	MADD
8168215	1.39	0.0323	MED12
8072328	1.39	0.0377	MTP18
8113981	1.39	0.0309	P4HA2
8155673	1.39	0.0462	PIP5K1B
8153223	1.39	0.0278	PTK2
8013616	1.39	0.0262	SARM1
8072328	1.39	0.0377	SEC14L2
8013616	1.39	0.0262	SLC46A1
8154059	1.39	0.0291	SMARCA2
7937465	1.39	0.0398	TALDO1
8013616	1.39	0.0262	TMEM199
7903803	1.38	0.0393	AHCYL1
8161829	1.38	0.0495	C9orf41
7972936	1.38	0.0491	FAM70B
7983890	1.38	0.0329	GCOM1
8115410	1.38	0.0363	GEMIN5
7983890	1.38	0.0329	GRINL1A
8045349	1.38	0.042	MGAT5
7973314	1.38	0.0197	OXA1L
8107100	1.38	0.0215	RGMB
8020508	1.38	0.0372	RIOK3
8101366	1.38	0.0386	SCD5
8136039	1.37	0.0292	ATP6V1F
7936706	1.37	0.0363	C10orf119
8006123	1.37	0.0307	CPD
8164535	1.37	0.0201	CRAT
8135114	1.37	0.0286	CUX1
7983350	1.37	0.0402	EIF3J
7948612	1.37	0.0379	FADS1
8096753	1.37	0.046	HADH
8057719	1.37	0.0317	HIBCH
7897561	1.37	0.0363	KIF1B
8037913	1.37	0.0491	NAPA
7932094	1.37	0.0389	PHYH
8060418	1.37	0.0284	SIRPA
8029219	1.37	0.0356	TMEM145
8090772	1.37	0.0214	TOPBP1
8089234	1.37	0.0236	ZBTB11
7930380	1.36	0.0243	ADD3
8152668	1.36	0.0487	ATAD2
7967127	1.36	0.0349	CAMKK2
8098500	1.36	0.0355	CDKN2AIP
8086028	1.36	0.0424	GLB1

7951589	1.36	0.0456	LOC120364
7990620	1.36	0.0432	TSPAN3
7954701	1.35	0.0483	C12orf72
8082846	1.35	0.037	EPHB1
8164343	1.35	0.0397	FAM102A
7957126	1.35	0.0432	KCNMB4
8152764	1.35	0.0362	MTSS1
7900201	1.35	0.0261	UTP11L
8074780	1.35	0.042	YPEL1
8130732	1.34	0.0406	BRP44L
7978923	1.34	0.0366	C14orf138
8074939	1.34	0.0299	CHCHD10
8015835	1.34	0.0425	DUSP3
8138857	1.34	0.0352	GGCT
7931393	1.34	0.0445	GLRX3
8096385	1.34	0.0495	HERC3
8111677	1.34	0.0397	LIFR
8106098	1.34	0.0416	MAP1B
8152597	1.34	0.0443	MRPL13
7939087	1.33	0.0388	C11orf46
7942783	1.33	0.036	C11orf67
7930682	1.33	0.037	FAM160B1
7942783	1.33	0.036	INTS4
8074791	1.33	0.0319	MAPK1
8050591	1.33	0.0335	NDUFAF2
8018652	1.33	0.0489	RNF157
8146550	1.33	0.0382	SDCBP
7912928	1.33	0.0397	SDHB
8061114	1.32	0.0432	DSTN
7992987	1.32	0.0416	HMOX2
8150225	1.32	0.047	RAB11FIP1
7951077	1.32	0.0474	SESN3
7971644	1.31	0.0401	C13orf1
8046408	1.31	0.0397	PDK1
8097570	1.31	0.0394	USP38
7998886	1.3	0.0488	PKMYT1
7934196	1.3	0.0443	PSAP
8157933	1.3	0.0443	ZBTB43
8029437	-1.3	0.0491	PVR
7965723	-1.3	0.0447	PXK
7965723	-1.3	0.0447	UHRF1BP1L
7918749	-1.31	0.0497	DENND2C
7990151	-1.31	0.0459	PKM2
8079869	-1.31	0.0498	RBM5
8079869	-1.31	0.0498	RBM6
8102619	-1.32	0.047	ANXA5
8154934	-1.32	0.036	IL11RA
7923453	-1.32	0.0467	KDM5B
7932495	-1.33	0.0438	C10orf114
8167234	-1.33	0.0359	RBM3
8001373	-1.33	0.0491	SNX20
8132245	-1.34	0.047	FLJ20712
8171229	-1.34	0.0396	PNPLA4
7985695	-1.35	0.0358	AKAP13
7919825	-1.35	0.0475	ARNT
7935660	-1.35	0.0487	DNMBP
8164165	-1.35	0.0327	HSPA5
7900228	-1.35	0.0359	NDUFS5
8055404	-1.35	0.0422	UBXN4
7942342	-1.36	0.0293	INPPL1
7962000	-1.36	0.0498	PTHLH
8039013	-1.36	0.0386	ZNF321
7927747	-1.36	0.0328	ZNF365
8116983	-1.37	0.0319	CD83
7955376	-1.37	0.0427	DIP2B
8132860	-1.37	0.0405	EGFR
8027521	-1.37	0.0364	GPATCH1
7985248	-1.37	0.0342	KIAA1024
7906954	-1.37	0.0346	PBX1
8074817	-1.37	0.0462	PI4KA
8019939	-1.37	0.0329	TGIF1

8161701	-1.37	0.0299	TMEM2
8074817	-1.37	0.0462	TOP3B
8146024	-1.38	0.0363	ADAM32
8156610	-1.38	0.0382	CDC14B
8156610	-1.38	0.0382	HABP4
8142232	-1.38	0.0307	LAMB4
8040927	-1.38	0.0249	NRBP1
7920725	-1.38	0.0372	SCAMP3
8013741	-1.38	0.0272	SDF2
8029969	-1.38	0.0327	SEPW1
8167185	-1.38	0.0468	TIMP1
8136067	-1.38	0.0446	TSPAN33
7990054	-1.38	0.0227	UACA
8112746	-1.38	0.0229	WDR41
7981273	-1.39	0.0416	CCDC85C
7933877	-1.39	0.0416	JMJD1C
7995806	-1.39	0.0226	MT1A
8132387	-1.39	0.0432	POU6F2
8166402	-1.39	0.0432	SMS
8157216	-1.39	0.0438	UGCG
7946635	-1.39	0.0359	ZBED5
8131815	-1.4	0.0272	KLHL7
7991602	-1.4	0.0255	PCSK6
7955078	-1.4	0.0454	PFKM
8163402	-1.4	0.047	ROD1
7970975	-1.4	0.048	SOHLH2
7963713	-1.41	0.0416	ATP5G2
8170247	-1.41	0.0396	CXorf18
8152491	-1.41	0.0422	EXT1
8041995	-1.41	0.0234	SPTBN1
8043100	-1.41	0.0254	TMSB10
7944803	-1.41	0.0166	VWA5A
8056060	-1.42	0.0233	BAZ2B
8163599	-1.42	0.0411	DFNB31
8044933	-1.42	0.0247	GLI2
8077376	-1.42	0.02	ITPR1
7995813	-1.42	0.0204	MT1DP
8023481	-1.42	0.0243	NARS
7961540	-1.42	0.0207	RERG
8018558	-1.43	0.0216	ACOX1
8122827	-1.43	0.0347	C6orf97
8116998	-1.43	0.0247	JARID2
8018209	-1.43	0.0259	NAT9
7943892	-1.43	0.0496	NCAM1
8160857	-1.43	0.0201	SIGMAR1
8096301	-1.43	0.0456	SPP1
8020630	-1.43	0.0181	TTC39C
8167069	-1.43	0.032	UBA1
8100870	-1.44	0.0236	ADAMTS3
8177560	-1.44	0.015	BDP1
8115543	-1.44	0.0144	EBF1
7904303	-1.44	0.0272	IGSF2
8122013	-1.44	0.0361	L3MBTL3
7984704	-1.44	0.0326	NEO1
8150276	-1.44	0.0363	PPAPDC1B
8064808	-1.44	0.0286	SLC23A2
7962537	-1.44	0.0286	SLC38A2
8045933	-1.44	0.0375	TANK
8096675	-1.44	0.0211	TET2
8174893	-1.44	0.0221	THOC2
8122336	-1.45	0.0246	C6orf115
8012931	-1.45	0.0318	CDRT1
8134699	-1.45	0.0445	COPS6
8012931	-1.45	0.0318	FBXW10
8062041	-1.46	0.0481	ACSS2
8081431	-1.46	0.0401	ALCAM
7961964	-1.46	0.0126	C12orf11
8083223	-1.46	0.0118	C3orf58
8047381	-1.46	0.0219	CFLAR
7972750	-1.46	0.0145	COL4A1
7980680	-1.46	0.0394	FOXN3

8106769	-1.46	0.0203	LOC645181
8007828	-1.46	0.0216	MAPT
7958884	-1.46	0.048	OAS1
8104788	-1.46	0.021	RAI14
7984364	-1.46	0.0135	SMAD3
7927964	-1.46	0.0299	SRGN
8121838	-1.46	0.0297	TPD52L1
8038792	-1.47	0.0126	ETFB
8142194	-1.47	0.0132	LAMB1
8139534	-1.47	0.0244	PKD1L1
8141688	-1.47	0.0302	PLOD3
8016994	-1.47	0.0363	RNF43
8109001	-1.47	0.0427	SPINK5
8022356	-1.47	0.0227	SPIRE1
8056583	-1.48	0.0491	ABCB11
8150988	-1.48	0.0222	ASPH
8032863	-1.48	0.0215	C19orf10
7917885	-1.48	0.0123	CNN3
8114920	-1.48	0.0235	DPYSL3
8040725	-1.48	0.0432	DPYSL5
7986293	-1.48	0.02	MCTP2
8107722	-1.48	0.0146	MEGF10
8161056	-1.48	0.0146	TLN1
7921970	-1.49	0.00819	ALDH9A1
8108478	-1.49	0.0236	C5orf32
8174527	-1.49	0.0498	CAPN6
7969060	-1.49	0.0117	FNDC3A
7955873	-1.49	0.0132	HOXC4
7955873	-1.49	0.0132	HOXC5
7955873	-1.49	0.0132	HOXC6
7922268	-1.49	0.0447	KIFAP3
7901140	-1.49	0.0352	MAST2
7921121	-1.49	0.0324	MRPL24
8100298	-1.49	0.0211	OCIAD2
7977615	-1.49	0.029	RNASE1
8095545	-1.49	0.0098	RUFY3
7990632	-1.49	0.0331	SGK269
8057056	-1.49	0.0286	TTN
8101260	-1.5	0.0139	ANTXR2
7904254	-1.5	0.00959	ATP1A1
7920737	-1.5	0.0116	CLK2
8155096	-1.5	0.00939	CREB3
7928354	-1.5	0.0498	FAM149B1
7984524	-1.5	0.0359	PAQR5
7906564	-1.5	0.0148	PEA15
7907611	-1.5	0.02	RASAL2
8162264	-1.51	0.0114	AUH
7980390	-1.51	0.0249	C14orf148
7923596	-1.51	0.0173	ETNK2
8101449	-1.51	0.0128	HPSE
7989365	-1.51	0.0354	RORA
8113666	-1.51	0.047	SEMA6A
8072160	-1.51	0.0171	ZNRF3
8069676	-1.52	0.0206	ADAMTS1
8171493	-1.52	0.0468	CTPS2
7939365	-1.52	0.0133	FJX1
7972055	-1.52	0.0171	KCTD12
8102232	-1.52	0.0138	LEF1
8049530	-1.52	0.031	LRRFIP1
8044133	-1.52	0.0123	NCK2
8054227	-1.52	0.00848	REV1
7944011	-1.52	0.0109	REXO2
8103630	-1.52	0.0197	SH3RF1
8085486	-1.52	0.0426	XPC
7932243	-1.53	0.0151	FAM171A1
8027778	-1.53	0.00808	FXYD5
7969003	-1.53	0.00959	ITM2B
7930533	-1.53	0.0236	LOC143188
8087447	-1.53	0.048	MST1
8039389	-1.53	0.0299	PTPRH
8037505	-1.53	0.0379	TRAPPC6A

8008609	-1.54	0.00765	ANKFN1
7907370	-1.54	0.0178	DNM3
8106354	-1.54	0.00808	IQGAP2
7990457	-1.54	0.0439	MAN2C1
8047228	-1.54	0.0349	MOBKL3
8164077	-1.54	0.00766	NR5A1
7979615	-1.54	0.0121	SPTB
8073081	-1.55	0.0112	APOBEC3F
7951807	-1.55	0.0125	CADM1
7916045	-1.55	0.00848	EPS15
8015806	-1.55	0.0357	ETV4
8089596	-1.55	0.0164	WDR52
7907861	-1.55	0.00622	XPR1
7927732	-1.56	0.00997	ARID5B
8141150	-1.56	0.0115	ASNS
8038126	-1.56	0.0416	CA11
8170166	-1.56	0.00662	HTATSF1
8054281	-1.56	0.011	LONRF2
8102800	-1.56	0.0119	SLC7A11
7924508	-1.56	0.0225	SUSD4
8102904	-1.56	0.00689	UCP1
7969204	-1.56	0.037	WDFY2
7969438	-1.57	0.0491	LMO7
8041383	-1.57	0.011	LTBP1
8156043	-1.57	0.0108	PSAT1
7897877	-1.57	0.0133	TNFRSF1B
8092970	-1.58	0.00756	APOD
8102263	-1.58	0.0218	COL25A1
8141328	-1.58	0.0229	CYP3A5
8141328	-1.58	0.0229	CYP3A5P2
7906400	-1.58	0.0118	IFI16
8091255	-1.58	0.02	PAQR9
7938231	-1.58	0.0338	PPFIBP2
8051547	-1.58	0.00662	PRKD3
7950743	-1.58	0.0291	RAB30
8069744	-1.58	0.00549	RWDD2B
8097098	-1.58	0.0112	USP53
8056005	-1.59	0.00762	ACVR1
7979963	-1.59	0.0318	DPF3
8104592	-1.59	0.00435	FBXL7
8127109	-1.59	0.00516	ICK
7951614	-1.59	0.00587	PPP2R1B
8102678	-1.59	0.0106	TRPC3
8005638	-1.6	0.00378	ALDH3A2
7957759	-1.6	0.0148	APAF1
7906900	-1.6	0.0194	DDR2
7995776	-1.6	0.00726	MT3
7984276	-1.6	0.0101	SLC24A1
8023121	-1.6	0.00891	ST8SIA5
7922382	-1.61	0.026	ANKRD45
8004167	-1.61	0.0242	FAM64A
7963187	-1.61	0.0173	LIMA1
8055711	-1.61	0.02	NEB
8087935	-1.61	0.00576	NT5DC2
7981947	-1.61	0.0419	SNORD109A
7981947	-1.61	0.0419	SNORD109B
7979824	-1.62	0.0106	ACTN1
7909332	-1.62	0.00788	CD55
8097753	-1.62	0.042	DCLK2
8149835	-1.62	0.0103	LOC100129717
8170420	-1.62	0.0128	MAMLD1
8106068	-1.62	0.00546	MCCC2
8149835	-1.62	0.0103	NEFL
7909967	-1.63	0.00509	CAPN2
8065758	-1.63	0.0375	FLJ38773
8108251	-1.63	0.0101	NPY6R
7943760	-1.63	0.00604	SIK2
8122464	-1.63	0.0119	UTRN
7916862	-1.64	0.00414	GPR177
8152280	-1.64	0.00759	LRP12
7897953	-1.64	0.0229	SNORA59A

7897953	-1.64	0.0229	SNORA59B
7897953	-1.64	0.0229	VPS13D
8057418	-1.64	0.0347	ZNF385B
7962579	-1.66	0.0249	AMIGO2
7965686	-1.66	0.0481	ANKS1B
7947230	-1.66	0.0279	BDNF
8130553	-1.66	0.0427	FLJ27255
7957298	-1.66	0.0276	NAV3
7962367	-1.66	0.0117	ZCRB1
7907601	-1.67	0.0192	FAM5B
7982299	-1.67	0.0262	LOC390561
8143367	-1.67	0.00403	SLC37A3
8131600	-1.67	0.0395	TSPAN13
8078397	-1.68	0.0277	CMTM8
8121429	-1.68	0.0229	FIG4
7904726	-1.68	0.00854	TXNIP
7985310	-1.69	0.00782	FAM108C1
8166408	-1.69	0.00662	PHEX
7979455	-1.69	0.0146	RTN1
8081219	-1.69	0.0189	ST3GAL6
8134257	-1.7	0.0105	GNG11
8134420	-1.7	0.0386	TAC1
8005475	-1.7	0.0125	TRIM16
8005475	-1.7	0.0125	TRIM16L
8017766	-1.71	0.00451	APOH
7979959	-1.71	0.00615	C14orf57
7956930	-1.71	0.0189	DYRK2
7971197	-1.71	0.00917	ELF1
8083901	-1.71	0.00371	FNDC3B
8130556	-1.71	0.0121	SOD2
8174092	-1.72	0.0086	ARMCX2
7953603	-1.72	0.0132	C1S
8102862	-1.72	0.0098	MAML3
8078330	-1.72	0.00662	RBMS3
8156060	-1.72	0.00782	TLE4
8146000	-1.73	0.0031	ADAM9
8120719	-1.73	0.0194	CD109
8056222	-1.73	0.0109	DPP4
8013319	-1.73	0.0101	GRAP
8063437	-1.73	0.00188	LOC100288461
7905606	-1.73	0.0132	NPR1
8063437	-1.73	0.00188	TSHZ2
7966135	-1.74	0.0083	CORO1C
8139207	-1.74	0.00355	INHBA
8045637	-1.74	0.00673	KIF5C
8148049	-1.74	0.00654	NOV
8051573	-1.75	0.00491	CDC42EP3
7909661	-1.75	0.00357	RPS6KC1
7985317	-1.76	0.015	KIAA1199
8076403	-1.76	0.00276	NAGA
7922756	-1.76	0.0139	NMNAT2
8022747	-1.77	0.0269	B4GALT6
8061211	-1.77	0.00272	DTD1
8154916	-1.77	0.00451	GALT
8114900	-1.77	0.0279	PPP2R2B
7917052	-1.77	0.0113	SLC44A5
8057887	-1.77	0.00433	STK17B
8129458	-1.78	0.00644	ARHGAP18
8055465	-1.78	0.00257	CXCR4
7950804	-1.79	0.0452	CCDC89
8094533	-1.79	0.00505	FLJ16686
7903092	-1.79	0.00756	FNBP1L
7955963	-1.79	0.023	MUCL1
8150537	-1.79	0.0193	SLC20A2
8107594	-1.79	0.0117	SNCAIP
8130211	-1.79	0.00485	SYNE1
8021685	-1.8	0.0135	CCDC102B
7925320	-1.8	0.021	NID1
8151149	-1.81	0.00403	ARFGEF1
7912112	-1.81	0.00561	DNAJC11
7912112	-1.81	0.00561	THAP3
8101971	-1.82	0.00269	PPP3CA
7975482	-1.82	0.00403	RGS6
7917516	-1.83	0.033	GBP1
7917516	-1.83	0.033	GBP3
8151816	-1.83	0.0314	GEM
7918902	-1.84	0.00166	CD58
7943867	-1.85	0.0162	BCO2
8089464	-1.85	0.0207	LOC151760
8173551	-1.85	0.00239	PHKA1
7983527	-1.85	0.00237	SEMA6D
8102415	-1.86	0.0179	CAMK2D
8103415	-1.87	0.0142	C4orf18
8162531	-1.88	0.00237	MT1G
8162531	-1.88	0.00237	MT1P1
8162531	-1.88	0.00237	MT1X
8106019	-1.88	0.0103	PMCHL1
8106019	-1.88	0.0103	PMCHL2
8092726	-1.89	0.00552	CLDN1
8056457	-1.89	0.0122	SCN1A
8004545	-1.9	0.00442	ATP1B2
8142585	-1.9	0.00172	CADPS2
8117054	-1.9	0.00168	CAP2
8051066	-1.9	0.0216	MPV17
7909681	-1.9	0.0156	PROX1
8122634	-1.9	0.00485	SAMD5
8083246	-1.91	0.00234	CPB1
8117243	-1.91	0.00517	LRRC16A
8167965	-1.91	0.00152	MSN
7971150	-1.92	0.0127	LHFP
8095362	-1.92	0.00344	MT2A
7947165	-1.92	0.0098	SLC5A12
8102523	-1.93	0.002	FABP2
8098204	-1.94	0.00624	CPE
7917347	-1.94	0.00228	DDAH1
8169145	-1.94	0.0227	MUM1L1
8107133	-1.94	0.00228	PAM
8168875	-1.95	0.0086	ARMCX3
8029988	-1.95	0.00177	ELSPBP1
8127072	-1.95	0.0021	GSTA1
7983564	-1.95	0.00544	SLC12A1
8148304	-1.95	0.0029	TRIB1
7984517	-1.96	0.00125	GLCE
7925511	-1.96	0.0359	PLD5
8059279	-1.98	0.00245	EPHA4
8168472	-2	0.00414	ATP7A
8089082	-2	0.00116	DCBLD2
8121749	-2	0.000909	GJA1
8122807	-2.01	0.00351	AKAP12
8055911	-2.01	0.00587	LOC100129449
8072735	-2.03	0.00326	APOL1
8174937	-2.03	0.000888	ODZ1
7907893	-2.04	0.000959	MR1
8002303	-2.04	0.00588	NQO1
8102792	-2.04	0.00689	PCDH18
7951351	-2.04	0.00159	PDGFD
8060854	-2.04	0.00219	PLCB1
8009301	-2.04	0.0128	PRKCA
7932254	-2.06	0.00403	ITGA8
8046646	-2.06	0.00171	OSBPL6
7962559	-2.06	0.00689	SLC38A4
7974080	-2.07	0.00149	MIA2
8092959	-2.07	0.00174	PPP1R2
8112865	-2.07	0.00354	SERINC5
8145611	-2.08	0.0327	FZD3
8099524	-2.08	0.0132	LDB2
7932765	-2.08	0.00629	MPP7
8021635	-2.08	0.0108	SERPINB10
8021635	-2.08	0.0108	SERPINB2
7968872	-2.1	0.0236	DNAJC15
7968015	-2.1	0.0118	TNFRSF19
7984569	-2.11	0.00225	LRRC49

7912157	-2.13	0.00171	ERRFI1
8128956	-2.13	0.00284	FYN
8092707	-2.13	0.000888	LEPREL1
8147516	-2.13	0.00504	MATN2
7910611	-2.14	0.00125	KCNK1
8148040	-2.14	0.0121	MAL2
8088247	-2.16	0.00155	ARHGEF3
7995525	-2.16	0.00181	NKD1
8109490	-2.16	0.00283	SGCD
7961083	-2.17	0.00125	CLEC2B
8104901	-2.17	0.00662	IL7R
8161044	-2.17	0.00493	TPM2
7962312	-2.19	0.00919	ABCD2
8103206	-2.19	0.00126	FBXW7
7968417	-2.19	0.0018	FRY
8156923	-2.19	0.000888	RP11-35N6.1
8088560	-2.2	0.00355	ADAMTS9
7942503	-2.2	0.000631	PPME1
8101952	-2.22	0.00155	DDIT4L
7925876	-2.22	0.001	PFKP
8149825	-2.22	0.00932	STC1
8063115	-2.23	0.00383	MMP9
7979044	-2.23	0.000645	NIN
8046124	-2.25	0.00451	DHRS9
8176133	-2.27	0.000694	G6PD
7995843	-2.27	0.000888	NUP93
7961269	-2.27	0.00188	PRB4
7961269	-2.27	0.00188	PRH1
8037283	-2.27	0.00788	PSG1
8037283	-2.27	0.00788	PSG4
8116921	-2.28	0.00238	EDN1
8135218	-2.3	0.0157	LRRC17
7960947	-2.33	0.000903	A2M
8155849	-2.33	0.00614	ANXA1
8174239	-2.33	0.00239	BEX2
8149629	-2.33	0.000631	GFRA2
8119052	-2.33	0.000588	PNPLA1
8060895	-2.33	0.0367	RNU105B
8101762	-2.36	0.00635	SNCA
8045736	-2.38	0.000311	FMNL2
8166784	-2.38	0.00715	TSPAN7
7930194	-2.39	0.000519	CNNM2
8179819	-2.39	0.000888	DDAH2
7963986	-2.39	0.000816	RAB13
8100827	-2.43	0.0108	IGJ
7904361	-2.45	0.000888	FAM46C
8089329	-2.45	0.0014	MYH15
7977933	-2.45	0.00148	SLC7A8
7961142	-2.5	0.0115	OLR1
7979204	-2.51	0.000781	FERMT2
7974090	-2.53	0.00244	CTAGE5
8131666	-2.53	0.00108	ITGB8
7950764	-2.55	0.00504	DLG2
7958253	-2.66	0.000888	C12orf75
8129573	-2.68	0.00221	MOXD1
8138289	-2.69	0.000888	ETV1
7962375	-2.69	0.00115	PRICKLE1
7905544	-2.73	0.00738	SPRR1A
7935058	-2.77	0.000442	MYOF
7954559	-2.81	0.00163	PPFIBP1
7917954	-2.87	0.0049	FRRS1
8112220	-2.87	0.000631	PDE4D
8105302	-2.89	0.00645	FST
7933872	-2.91	0.00026	EGR2
8175492	-2.93	0.000378	ATP11C
7961320	-3.07	0.000253	PRB3
8122222	-3.1	0.000307	PDE7B
7961306	-3.1	0.000222	PRB1
7961306	-3.1	0.000222	PRB2
8154491	-3.12	0.000253	ADAMTSL1
8037949	-3.12	0.00138	SULT2A1
7902687	-3.14	0.000904	CYR61
8088192	-3.14	0.000311	ERC2
8171624	-3.16	0.00587	GPR64
7957140	-3.16	0.000888	LGR5
7956009	-3.16	0.000128	METTL7B
7922474	-3.27	0.000631	KIAA0040
8089011	-3.34	0.000247	PROS1
8168622	-3.39	0.00237	KLHL4
7926545	-3.48	0.000247	PLXDC2
8171297	-3.56	0.000311	MID1
7956759	-3.56	0.000222	SRGAP1
7910022	-3.61	0.00493	CNIH3
8056257	-3.61	0.000888	FAP
7965322	-3.63	0.00205	KITLG
7964834	-3.84	0.000413	CPM
8161884	-3.92	0.000903	PRUNE2
7920123	-3.92	0.00738	S100A10
8121712	-3.94	0.000073	SLC35F1
8122660	-3.97	0.000247	UST
8055688	-4.17	0.00112	RND3
7957966	-4.2	0.00387	MYBPC1
7957570	-4.32	0.000222	PLXNC1
8105040	-4.44	0.000073	OSMR
8077270	-4.5	0.000631	CHL1
8092134	-4.53	0.000247	PLD1
8163637	-5.54	0.0000325	TNC
7909789	-5.82	0.0000265	TGFB2
8166593	-5.86	0.000128	IL1RAPL1
8091243	-7.36	0.0000265	PCOLCE2

Appendix 9: Overlap between SF-1 ChIP-on-chip and overexpression data sets

Gene Symbol	Gene Name	ChIP-on-chip		Overexpression	
		MA Z-score	Distance to TSS	FC	adj.P-Val
*C9orf117**#	Chromosome 9 open reading frame 117	4.37	-3981	2.04	0.00231
		3.77	-2875		
*TTC16**#	Tetratricopeptide repeat domain 16	4.37	-9361	2.04	0.00231
		3.77	-8255		
*GNAZ**	Guanine nucleotide binding protein (G protein), alpha z polypeptide	4.11	-1895	1.86	0.00558
		3.52	1733		
AMBP	Alpha-1-microglobulin/bikunin precursor	3.87	-5603	1.78	0.0146
ZNF295	Zinc finger protein 295	4.64	-6166	1.78	0.00221
ECM1	Extracellular matrix protein 1	3.98	-108	1.77	0.00455
DCUN1D2	DCN1, defective in cullin neddylation 1, domain containing 2 (S. cerevisiae)	7.14	-6621	1.6	0.012
RPL7A	Ribosomal protein L7a	4.48	2236	1.6	0.00625
GPR21	G protein-coupled receptor 21	3.86	-370	1.52	0.044
PCGF3	Polycomb group ring finger 3	3.88	-2657	1.51	0.0276
ACSBG1	Acyl-CoA synthetase bubblegum family member 1	3.85	1059	1.49	0.0323
ZNF618	Zinc finger protein 618	3.74	-2870	1.45	0.031
SARM1	Sterile alpha and TIR motif containing 1	3.67	1036	1.39	0.0262
ATAD2	ATPase family, AAA domain containing 2	3.70	-4719	1.36	0.0487
YPEL1	Yippee-like 1 (Drosophila)	4.33	-6062	1.35	0.042
*CHCHD10**	Coiled-coil-helix-coiled-coil-helix domain containing 10	3.63	-1672	1.34	0.0299
		3.62	-6646		
IL11RA	Interleukin 11 receptor, alpha	3.70	-6386	-1.32	0.036
TOP3B	Topoisomerase (DNA) III beta	3.58	-2180	-1.37	0.0462
PCSK6	Proprotein convertase subtilisin/kexin type 6	4.07	-1536	-1.4	0.0255
GLI2	GLI family zinc finger 2	5.08	-2832	-1.42	0.0247
SIGMAR1	Sigma non-opioid intracellular receptor 1	3.70	-9778	-1.43	0.0201
*PAQR5**	Progestin and adipoQ receptor family member V	4.16	-1284	-1.5	0.0359
		3.77	-3156		
		3.56	-5461		
PEA15	Phosphoprotein enriched in astrocytes 15	3.90	-5475	-1.5	0.0148
MST1	Macrophage stimulating 1 (hepatocyte growth factor-like)	4.45	-185	-1.53	0.048
GALT	Galactose-1-phosphate uridylyltransferase	3.70	911	-1.77	0.00451
CXCR4	Chemokine (C-X-C motif) receptor 4	3.66	902	-1.78	0.00257
G6PD	Glucose-6-phosphate dehydrogenase	4.29	-4193	-2.27	0.000694
PSG4	Pregnancy specific beta-1-glycoprotein 4	3.89	1937	-2.27	0.00788

*Gene loci with more than 1 SF-1-binding region (ChIP-on-chip); #C9orf117 and TTC16 are distinct neighbouring genes located at 9q34.11, represented by the same transcript cluster in GeneChip Human Gene 1.0 ST arrays (overexpression). TSS, transcriptional start site; FC, fold change; adj.P-Val, Benjamini-Hochberg-corrected P-value. Data are ranked by fold change, from positive to negative.

Appendix 10: Publications arising from this thesis

Original research articles

Ferraz-de-Souza B, Martin F, Mallet D, Hudson-Davies RE, Cogram P, Lin L, Gerrelli D, Beuschlein F, Morel Y, Huebner A, Achermann JC 2009. CBP/p300-interacting transactivator, with Glu/Asp-rich C-terminal domain, 2, and pre-B-cell leukemia transcription factor 1 in human adrenal development and disease. J Clin Endocrinol Metab 94(2): 678-83.

Ferraz-de-Souza B, Lin L, Shah S, Jina N, Hubank M, Dattani MT, Achermann JC 2010. ChIP-on-chip analysis reveals angiopoietin 2 (Ang2, ANGPT2) as a novel target of steroidogenic factor-1 (SF-1, NR5A1) in the human adrenal gland. FASEB J *in press*. doi: 10.1096/fj.10-170522.

Ferraz-de-Souza B, Hudson-Davies RE, Lin L, Parnaik R, Hubank M, Dattani MT, Achermann JC 2011. Sterol O-acyltransferase 1 (SOAT1, ACAT) is a novel target of steroidogenic factor-1 (SF-1, NR5A1, Ad4BP) in the human adrenal. J Clin Endocrinol Metab *in press*. doi: 10.1210/jc.2010-2021.

Related original research articles

Lin L, Philibert P, Ferraz-de-Souza B, Kelberman D, Homfray T, Albanese A, Molini V, Sebire NJ, Einaudi S, Conway GS, Hughes IA, Jameson JL, Sultan C, Dattani MT, Achermann JC 2007. Heterozygous missense mutations in steroidogenic factor 1 (SF1/Ad4BP, NR5A1) are associated with 46,XY disorders of sex development with normal adrenal function. J Clin Endocrinol Metab 92(3): 991-9.

Kohler B, Lin L, Ferraz-de-Souza B, Wieacker P, Heidemann P, Schroder V, Biebermann H, Schnabel D, Gruters A, Achermann JC 2008. Five novel mutations in steroidogenic factor 1 (SF1, NR5A1) in 46,XY patients with severe underandrogenization but without adrenal insufficiency. Hum Mutat 29(1): 59-64.

Bashamboo A, Ferraz-de-Souza B, Lourenco D, Lin L, Sebire NJ, Montjean D, Bignon-Topalovic J, Mandelbaum J, Siffroi JP, Christin-Maitre S, Radhakrishna U, Rouba H, Ravel C, Seeler J, Achermann JC, McElreavey K 2010. Human male infertility associated with mutations in NR5A1 encoding steroidogenic factor 1. Am J Hum Genet 87(4): 505-12.

Reviews

de-Souza BF, Lin L, Achermann JC 2006. Steroidogenic factor-1 (SF-1) and its relevance to pediatric endocrinology. Pediatr Endocrinol Rev 3(4): 359-64.

Lin L, Ferraz-de-Souza B, Achermann JC 2007. Genetic disorders involving adrenal development. Endocr Dev 11: 36-46.

Ferraz-de-Souza B, Achermann JC 2008. Disorders of adrenal development. Endocr Dev 13: 19-32.

Ferraz-de-Souza B, Lin L, Achermann JC 2008. Adrenals. In: Carel J-C, Hochberg Z ed. Yearbook of Pediatric Endocrinology 2008. Basel, Karger. Pp. 95-108.

Ferraz-de-Souza B, Lin L, Achermann JC 2009. Adrenals. In: Carel J-C, Hochberg Z ed. Yearbook of Pediatric Endocrinology 2009. Basel, Karger. Pp. 93-110.

Ferraz-de-Souza B, Lin L, Achermann JC 2010. Steroidogenic factor-1 (SF-1, NR5A1) and human disease. Mol Cell Endocrinol *in press*. doi: 10.1016/ j.mce.2010.11.006.

El-Khairi R, Martinez-Aguayo A, Ferraz-de-Souza B, Lin L, Achermann JC 2011. Role of DAX-1 (NR0B1) and steroidogenic factor-1 (NR5A1) in human adrenal function. Endocr Dev 20: 38-46.